THERMOLUMINESCENCE AND FUSION CRUST STUDIES

OF METEORITES

Derek W. Sears

Departments of Astronomy and Geology,

University of Leicester

A thesis submitted for the Ph.D. degree of the

University of Leicester, 1974.

THERMAL HISTORIES AND CRUST STUDIES

Derek W. Beam

Department of Astronomy and Geology,

University of Leicester

A thesis submitted for the Ph.D. degree of the
University of Leicester, 1974.

To

Dad, my most important teacher,

and to

Mum and Hazel

Frontispiece. The electroluminescence of the Allende meteorite.

ACKNOWLEDGEMENTS

ABSTRACT

The thermoluminescence (TL) of meteorites has been examined with apparatus designed with emphasis on linear heating of the sample. The type of TL (i.e. the glow curve) depends on the minerals producing it and on the history of the specimen.

The applications that have been made concern three phases of a meteorite's arrival on Earth; its preatmospheric shape, the temperature gradients produced by heating during atmospheric passage, and the terrestrial age of meteorites for which the fall was not observed. It has been found possible to measure terrestrial ages for some meteorites that have been on the Earth several hundred years. It appears probable that shock considerably increases the rate of decay of TL.

The extent to which high temperatures experienced by the surface of the meteorite during its atmospheric passage have penetrated into the matrix suggests luminous flight times in the order of 10 seconds, but the gradients tend to be 3 - 5 times less than those predicted theoretically. They appear to have the same dependence on the orientation of the meteorite as the temperature gradients determined from the fusion crust; the steepest gradients being experienced at the front of the meteorite. The fusion crust, besides enabling much of the atmospheric behaviour to be determined, provides a useful source of information complementary to TL work. For example, TL gradients produced by atmospheric heating will only be found when the fusion crust contains an innermost zone.

The proatmospheric TL gradients measured in many
meteorites suggest that cosmic ray bombardment produces a
significant amount of TL, and therefore that TL can be used to
measure preatmospheric shape. A comparison with spallogenic
nuclide profiles in meteorites suggests that secondary particles
play an important part in determining TL. Studies of the
Estacado meteorite confirm this expectation and suggest an
elongated preatmospheric shape, approximating to an ellipse of
eccentricity 0.8. From this it is calculated that the pre-
atmospheric mass of Estacado exceeded 8 tons.

CONTENTS

CHAPTER I

INTRODUCTION

I.1   The origins of meteorite luminescence research

Within the last few years luminescence studies on extra-
terrestrial materials have received considerable impetus with the
availability of lunar samples. This has given the subject a
twentieth century character, and the electronic equipment nowadays
associated with thermoluminescence apparatus has also contributed
to this impression. It is true that quantitative studies of the
kind described in this thesis had to wait for the modern photo-
multiplier tube. However, the seeds of the ideas used here date
back to the very origins of the science of meteoritics.

In the late eighteenth century it was ill-advised to be
seen to take meteorites seriously, such was the scepticism towards
superstitious-sounding accounts of 'stones from the sky'. It was
in this climate of opinion that Edward Charles Howard (Figure I.1)
was persuaded by the President of the Royal Society, Sir Joseph
Banks, to perform chemical analyses on four of these stones
(Howard, 1802). A number of discoveries came out of his work
(Sears, 1974b), not the least being the discovery of nickel in
stony meteorites. However, on page 201 of the 1802 volume of the
Philosophical Transactions Howard remarks:

> "I ought not perhaps to suppress, that in endeavouring
> to form an artificial black coating on the interior
> surface of one of the stones from Benares, by sending
> over it the electrical charge of about 37 square feet
> of glass, it was observed to become luminous, in the
> dark, for nearly a quarter of an hour; and that the
> tract of the electrical fluid was rendered black."

Figure I.1 The Hon. Edward Charles Howard (1774 - 1816) who
first observed the luminescence of meteorites.

Howard was well aware that certain materials could be made to luminesce by electricity, but he saw a particular significance in the ability of meteorites to do so, since the mechanism for producing light from a stone (assuming it to be the remnant of a meteor) was a mystery of considerable proportions.

The earliest observations of thermoluminescence are those of Robert Boyle who, in 1663, recorded the fact that diamonds luminesced when held near a hot poker. Hooke and von Liebnitz described the thermoluminescence of fluorite in the early eighteenth century, and were the first of a series of observers who were to lay down the properties of the prominent phenomenon; among these were Dufay, Scheele, Canton, de Dolomeiau and de Saussure (Harvey, 1957). By Howard's time it was known that once a substance had been heated it could not be made to thermoluminesce a second time, except for certain substances which glowed dimly again after prolonged exposure to sunlight. It was also known that there was no weight change, smell or charging associated with the phenomenon.

The mechanism was of course completely unknown. A popular theory was that the substance slowly burned. Another was that light was trapped in the substance until displaced by heat. Throughout the next century numerous compilations of thermoluminescent minerals were made, and it was realised that strongly luminescent minerals tended to be highly coloured. In 1867 Becquerel, in his "La Lumière, ses Causes et ses Effects", stated that luminescence was favoured by the presence of impurities. However, little advance concerning the mechanism of production was to be made until the end of the century.

In 1857 Henry Sorby, making use of his newly devised technique of microscopically examining thin sections, stated that the interior of a meteorite did not appear to have been melted by atmospheric flight. This was contrary to popular belief at the time. However, with the discovery of gases in stony meteorites (Wright, 1875; -Dewar & Ansdell, 1886) it was clear that if the gases were indigenous, the meteorites could not have suffered intense heating. In 1889 it became apparent that the interior of the meteorite could not even have been strongly heated, much less melted, when Professor A.S. Herschel observed the thermoluminescence of the Middlesbrough meteorite:

> "Some fine dust and grains obtained from the interior
> portion of the mass of the Middlesborough aerolite,
> when the meteorite was first being chemically and
> microscopically examined, were found, to my considerable
> surprise, to glow quite distinctly, though not very
> brightly, with yellowish-white light, when sprinkled
> in the usual way for these experiments on a piece of
> nearly red-heated iron in the dark."

After some speculating that the luminescent mineral was feldspar, Herschel continued:

> "To whatever chemical materials in the stone, however,
> the light was really due, it afforded, in all events,
> clear proof that no heat of exceedingly high
> temperature can ever have penetrated to the interior
> of the meteorite, even when it was passing at its
> fall, in a fireball through the atmosphere, since the
> time when it was broken off from some parent rock and
> projected on a celestial course about the sun."

At the time this was written (Herschel, 1889) an understanding of the mechanism responsible for thermoluminescence was becoming possible. Wiedemann (in 1895) and Hoffmann (in 1897) found that cathode rays induced thermoluminescence, and Trowbridge and Burbank (in 1898) found that X-rays did the same. It gradually became clear that thermoluminescence resulted from the storage of

radioactive energy in some way.

I.2 Modern thermoluminescence theory and applications to meteorites

With the discovery of the electron by J.J. Thomson in 1897, and Bragg's use of X-rays to elucidate the atomic structure of crystals (1913 onwards) great strides were made in understanding the mechanism for the production of luminescence. In 1934 D. Curie proposed that the light was emitted when electrons underwent transitions from the conduction band to the valence band in the crystal lattice. When this transition proceeded via an impurity which allowed a transition of the correct energy then the impurity acted as a "luminescence centre". It became generally accepted (e.g. Johnson, 1939) that phosphorescence was the result of the storage of electrons and their subsequent release from 'traps', e.g. imperfections in the lattice, and that in the case of thermoluminescence heat is required to release the electrons. It also seemed that any ionising radiation could excite electrons into the traps (Figure I.2). The importance of imperfections in semi-conductors had been realised a few years earlier.

The first attempt to quantify the thermoluminescent properties of materials came from workers at the University of Birmingham. In 1945 Randall and Wilkins showed that the "glow experiment", measuring the intensity of the emitted light as a function of temperature, could be used to derive the energy of the traps below the conduction band. The traps were found to exist with a Boltzmann distribution about a certain level E, so that the probability of an electron having energy Ξ, at

temperature T is $s \cdot \exp(-E/kT)$, where k is the Boltzmann constant

and s a constant. Heating therefore increases the probability

of an electron leaving the trap and going into the conduction

band. Assuming that decay from the conduction band to the

valence band is first order ($-dn/dt \propto n$), where n is the

number of excited electrons and t is the time) Randall and

Wilkins showed

$$I = n_o \exp\left[- \int^T \frac{1}{\beta} se^{-E/kT} dT\right] se^{-E/kT}$$

where I is the intensity of the luminescence, n_o is the initial

number of trapped electrons, and β is the heating rate.

From the above equation all the properties of the glow curve

(light emitted vs. temperature) can be deduced. They are:

i)   the temperature of the luminescence peak is proportional

      to E (all else being equal) and approximately $25kT_{max}$,

ii)   the temperature of the peak moves to higher temperatures

      if higher heating rates are used, and

iii) higher temperature peaks are less intense and broader,

      but n_o is always equal to the area under the curve.

      In 1948 Garlick and Gibson added

iv)   at low temperatures

$$I = n_o s \exp(-E/kT)$$

An important method for measuring E is therefore to plot

$\log_e I$ vs. $\log_e 1/T$ (measured from the initial part of the glow

curve) the slope of which gives E/k. The initial rise method has

been used throughout this work to measure E. Garlick and Gibson

also reworked Randall and Wilkins' equations assuming second

order decay from the conduction band to the valence band. This

would be the case if the decaying electron had to find a positive

hole, but little agreement with observation was found. Although

there are exceptions, first order decay generally provides

closer agreement with experiment. They interpreted this to mean

a close association between the luminosity centre and the trap.

That the two can actually be identical seems reasonable, for if

one supposes that a manganese ion (of charge 2+ and ionic radius

0.80 $\overset{o}{A}$) substitutes for a calcium ion (charge 2+ and ionic radius

0.99 $\overset{o}{A}$) the manganese outer atomic orbitals allow a visible

transition (Medlin, 1968) and the resulting lattice distortion

may well provide a site which will trap an electron.

In recent years a number of workers (Garlick et al.,

1971) have discovered that in certain materials the electrons

can return to the valence band without undergoing this mechanism.

This 'non-thermal leakage' may place important limitations on the

use of thermoluminescence for absolute age determinations.

In the early nineteen-fifties the applications of thermo-

luminescence began to be investigated (Daniels et al., 1953)

and by the end of the decade Houterman's group in Berne had

started investigating the thermoluminescence of meteorites.

Their early work culminated in a not-too-successful attempt to

relate thermoluminescence intensity to exposure age (Houtermans

and Liener, 1966). Many points emerged from this important

pioneering work and will be discussed later. Liener and Geiss

(1968) tried to find a relationship between thermoluminescence

and fall age, allowing for contributions to the ionising

radiation by cosmic ray bombardment. However, the relationship

was not sufficiently well established to enable thermoluminescence
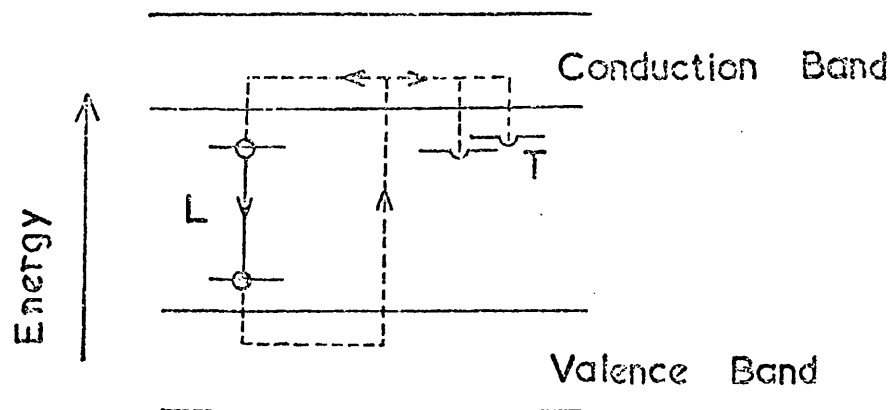
Figure I.2   A theory for the production of thermoluminescence
(after Garlick and Gibson, 1948).   L is the luminescence centre
and T are the electron traps at an energy E below the conduction
band.   The solid line represents a radiative transition (the
visible light observed) and broken lines represent non-radiative
transfers.

to be used to determine reliable ages. The Birmingham group

have also shown an interest in using thermoluminescence to

measure age, but again with very limited success (Durrani and

Christodoulides, 1967; Christodoulides et al., 1970). One of

the major uncertainties is probably the effect of shielding. It

is possible that considerable variation in the intensity of the

thermoluminescence occurs throughout the stone. A group in

France have tried to measure the variation in thermoluminescence

along cores from Saint-Séverin (Lalou et al., 1970) and Vaz

(1971a) has found gradients in Ucera. The subject is very

complicated and will form a major part of this thesis. For

example, the direction of the gradient does not necessarily

indicate the direction towards the centre of the stone because

secondary radiation may build up to give a cascade effect. Vaz

has also made some successful thermoluminescence determinations

of the temperature gradients produced by atmospheric heating in

the Lost City and Ucera meteorites (Vaz, 1971b; 1972).

I.3   This thesis

This thesis is an attempt to explore the extent to which

thermoluminescence can be used to investigate the history of a

meteorite's arrival on Earth. It concerns the determination of

a meteorite's preatmospheric shape, its behaviour in the

atmosphere, and its terrestrial age once on Earth. The thesis

also contains a chapter on the fusion crust of meteorites, since

this is a topic which provides much useful information

complementary to the thermoluminescence studies. In order that

the latter chapter be self-contained a historical introduction

is included therein rather than in this introductory chapter.

The first three chapters are all of an introductory nature, although the third contains mainly original work. Chapter II describes techniques and apparatus; Chapter III the kinds of glow curve, the minerals responsible, and the extent to which the glow curve governs possible applications. The first application considered is the measurement of terrestrial age (Chapter IV) and the implications of the results are discussed in the succeeding chapter. The fusion crust and its use in measuring ablation rates and mass loss constitute Chapter VI. The temperature gradients derived from thermoluminescence fusion crust measurements form Chapter VII. Finally, the variations in thermoluminescence intensity throughout a meteorite are described with a view to discussing the production mechanism and preatmospheric shape (Chapters VIII and IX).

The conclusions and summary (Chapter X) bring together the results and their relevance to an explanation of the meteor flux anomaly discovered by the Prairie camera network (McCrosky and Ceplecha, 1968). It appears that there is an influx of fireballs which considerably exceeds that predicted by meteorite fall statistics and a particular preatmospheric shape may be responsible.

CHAPTER II

APPARATUS AND TECHNIQUE

II.1   Introduction

Apparatus designed to measure thermoluminescence has

frequently been described in the literature (Vaz and Zellov,

1966; Bonfiglioli, 1968; Labeyrie et al., 1968). Even so,

different groups have, until recently, presented different

curves for the same material and it therefore seems desirable to

describe in some detail apparatus used for this work. Even more

important are the techniques for data gathering.

A device is required to heat the meteorite powder in a

vacuum or, better, an inert gas. (Chemiluminescence occurs in

the presence of oxygen (Aitken et al., 1968) and the low thermal

conductivity of the powder militates against heating in a vacuum.)

The light emitted has then to be measured with a photomultiplier

tube (PMT) which responds to continuous low-intensity light.

The PMT signal is amplified and plotted against the temperature

of the powder to produce the "glow curve". A photograph of the

apparatus and a schematic diagram are presented in Figure II.1.

It will be described in detail in the next section.

There has been much debate on the need for a linear

heating rate, some authors claiming that all that is required is

that the heating be reproducible. Houtermans and Liener (1966)

have shown however that the slightest deviation from linearity

gives perfectly reproducible but nevertheless spurious "peaks"

(Figure II.2). In the development of the apparatus used here we

have emphasised the need for an accurate linear heating rate. For

Figure II.1a Photograph of the assembled thermoluminescence apparatus. The photomultiplier tube housing is in the centre resting on the specimen chamber. This is evacuated and filled with an inert gas via the vacuum line on the left. A Dewar flask containing the cold-junctions for the thermocouples stands at the back of the rack which holds the HT unit (top), the control unit, the amplifier and a chart recorder to check the heating rate. At the base of this is the XY recorder and below the bench is a constant-voltage transformer for the control unit
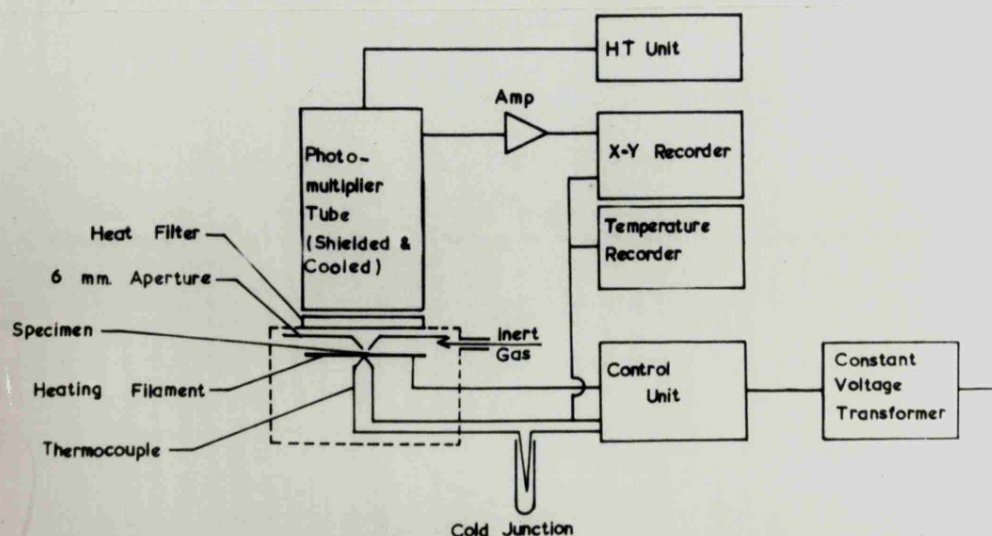
Figure II.1b Schematic diagram of the thermoluminescence apparatus.
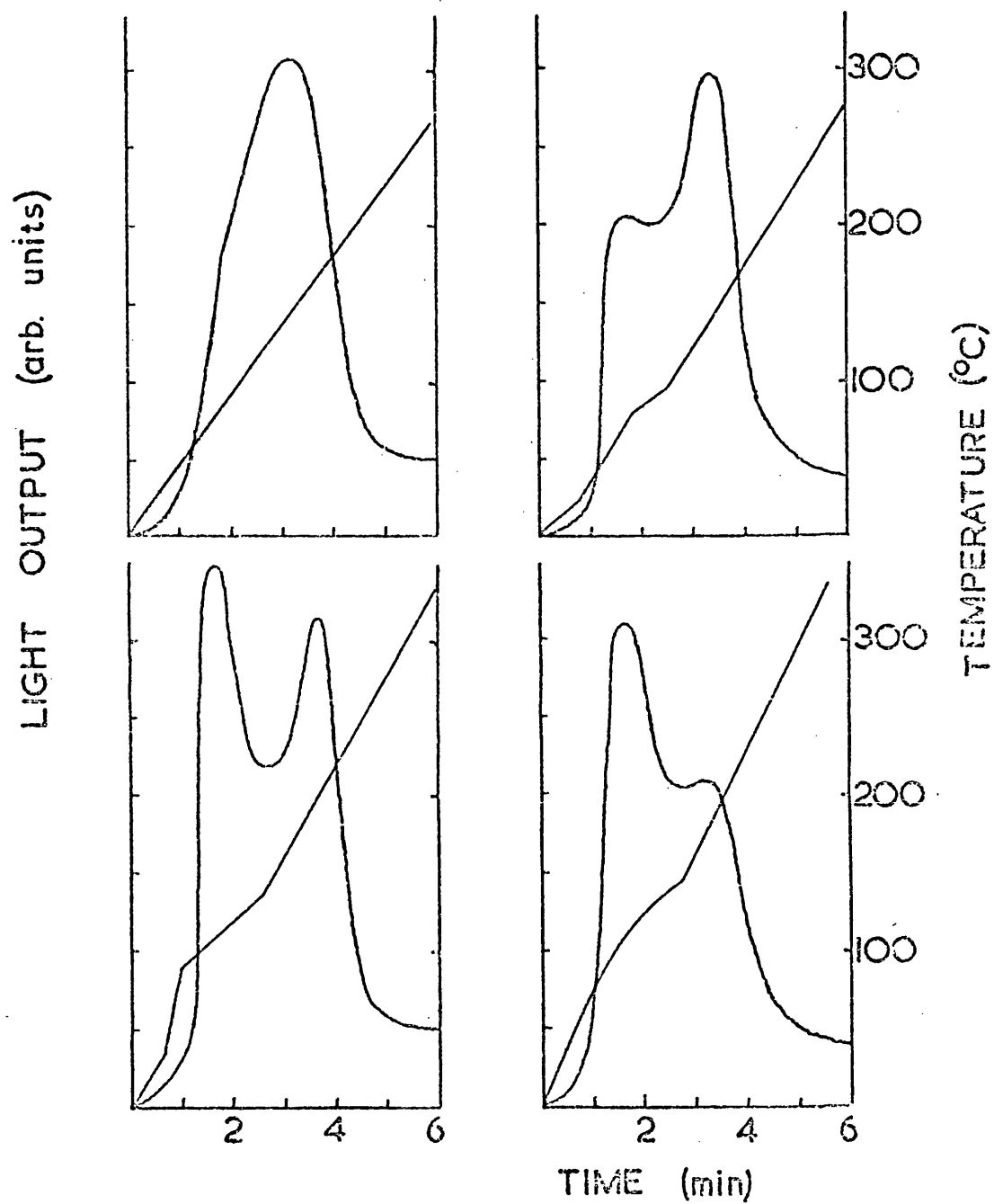
Figure II.2 The effect of irregularities in the heating rate on the shape of part of the glow curve. The diagonal lines give the temperature of the specimen. (After Houtermans and Liener, 1966).

this reason we have used an electronic control unit rather than a simpler man-operated control system. We have also laid much stress on checking the heating rate.

Other desirable qualities embodied in the apparatus are mainly self evident. Accuracy, efficiency (rapid cooling time after use), convenience and adaptability have all been considered. Good repeatability has been obtained. Material from the Ucera meteorite supplied by Dr. E. Vaz (Instituto Venezolano De Investigaciones Cientificas, Venezuela) has been examined with this apparatus and the agreement with his measurements of the same material is excellent.

II.2   Detailed description of the equipment (Figure II.1)

II.2a   The Specimen Chamber (Figure II.3b)

This is a 7.6 x 3.7 cm diameter cylindrical vessel turned from aluminium alloy. Two copper electrodes support a 6 x 1 cm x 0.05" thick molybdenum filament which is replaced every 150 runs (or as soon as it is completely discoloured). Molybdenum was chosen for its electrical and thermal properties. A chromel-alumel thermocouple was employed to measure the temperature of the filament since it produces an electromotive force proportional to temperature over the range concerned. It was spot welded to the underside of the filament. Connections through the specimen chamber wall were made using araldite and araldite plugs made opaque with a black dye produced by the manufacturers. A table supporting an aluminium cone diaphragm with a six millimeter aperture was placed over the filament to screen off I.R. radiation from bare portions of the molybdenum filament. A Chance HA 3 heat

filter was placed in front of the PMT to further reduce the
effect of black body radiation from the filament.

II.2b   Heating Control Unit

The filament was heated by a current of up to 100 amps
at 1 volt. This was supplied by the secondary coil of a heavy-
duty welding transformer, the primary of which was connected to
an electronic control unit. The thermocouple attached to the
filament was also connected to the unit. This control unit was
constructed by the Electronic Control Laboratory of the Engineering
Department, University of Leicester, and is described in detail in
the Appendix. Briefly, it produces a reference voltage which
increases linearly with time at the desired rate, using as its
time base the frequency of the mains. It compares this reference
voltage with the signal from the filament thermocouple. The
control unit compensates for differences between them by adjusting
the power to the heavy-duty transformer. Heating rate and
levelling-off temperature can be pre-set, and the temperature of
the filament can be held indefinitely at any value. The effect
on the glow curve of heating the meteorite powder for a few
seconds at a variety of temperatures could therefore be readily
determined. The unit was found to be sensitive to mains
fluctuations, so it was necessary to connect it via a constant
voltage transformer.

The signal from the filament thermocouple is amplified
(X 56) and presented at the "recorder" output of the control
unit for plotting on the X-axis of the glow curve. Since an
alternating current heats the filament the thermocouple signal

HT INPUT
SIGNAL OUTPUT
GASKET
SILICA GEL
DYNODE RESISTANCE
COOLANT OUT
INSULATION
MU-METAL SHIELD
PHOTOMULTIPLIER TUBE
HEAT FILTER / WINDOW
COOLANT IN
SHUTTER
FILAMENT
THERMOCOUPLE
APERTURE & SUPPORT
FILAMENT ELECTRODES

PHOTOMULTIPLIER TUBE HOUSING

SPECIMEN CHAMBER

AIR OUT / INERT GAS IN
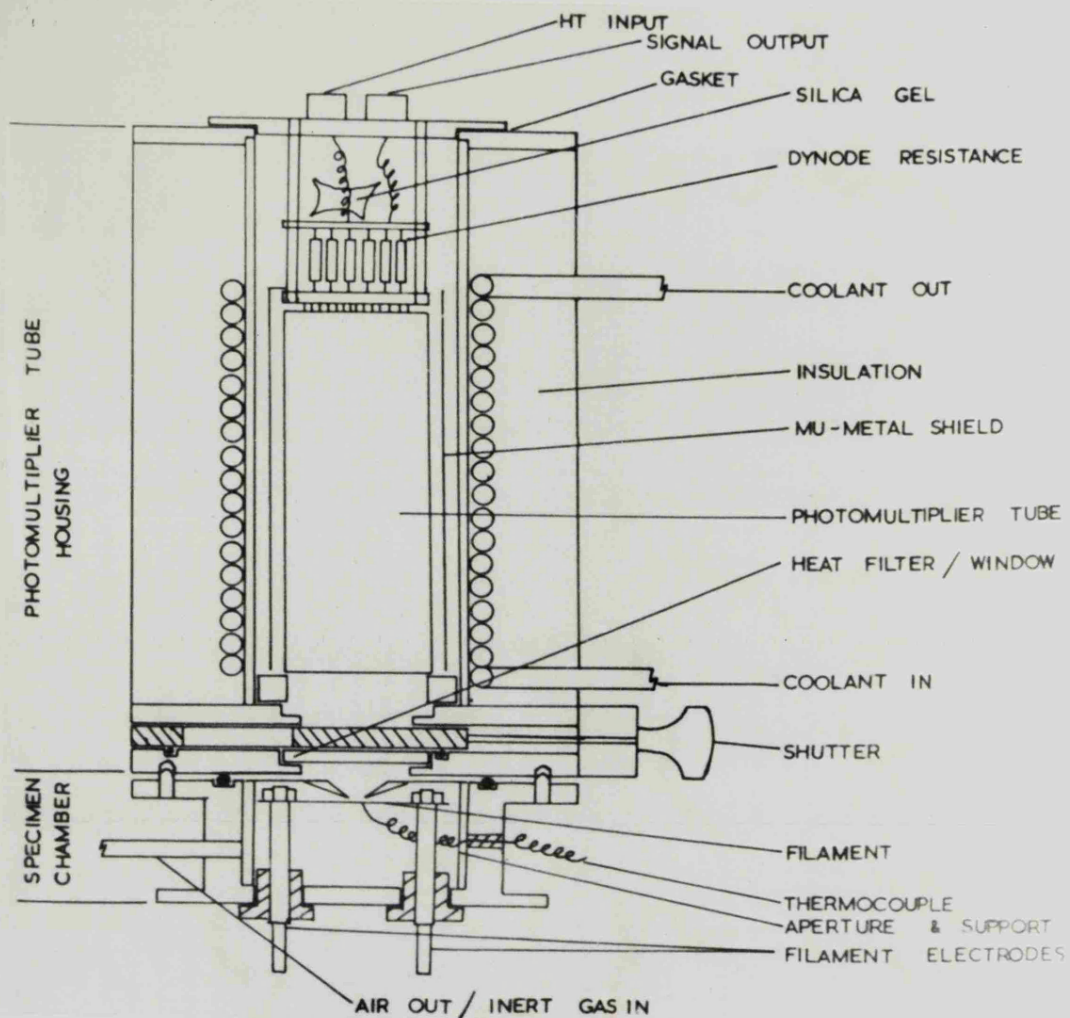
Figure II.3a Scale drawing of the photomultiplier tube housing and the specimen chamber. The whole assembly is $27\frac{1}{2}$ cm high and 15 cm in diameter.
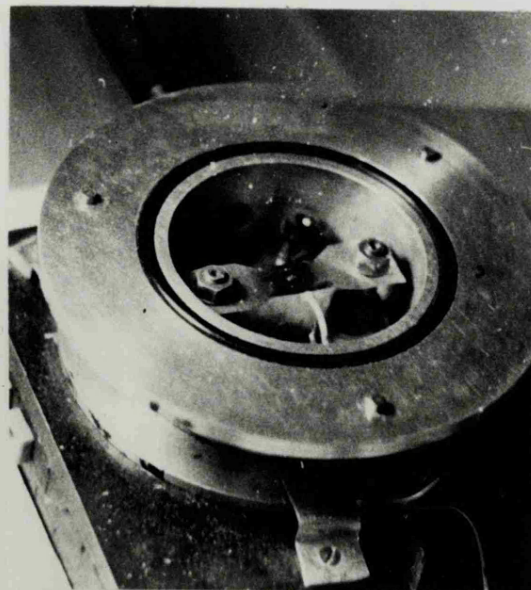
Figure II.3b Photograph of the specimen chamber.

PMT HOUSING

LIGHT TIGHT BOX

APERTURE SLIDE

DIFFUSING DIAPHRAGM

APERTURE

OPAL GLASS

LAMP
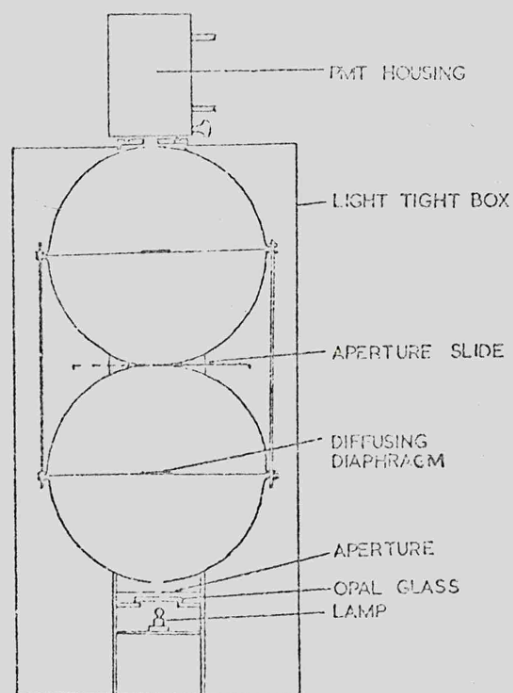
Figure II.4 (Above) Scale drawing of the integrating spheres used to check the linearity of response of the light measuring system. (Below) A graph showing photomultiplier tube response for various aperture settings of the linearity apparatus. The scatter is due to inaccuracies in the diameters of the apertures, the linearity is excellent.
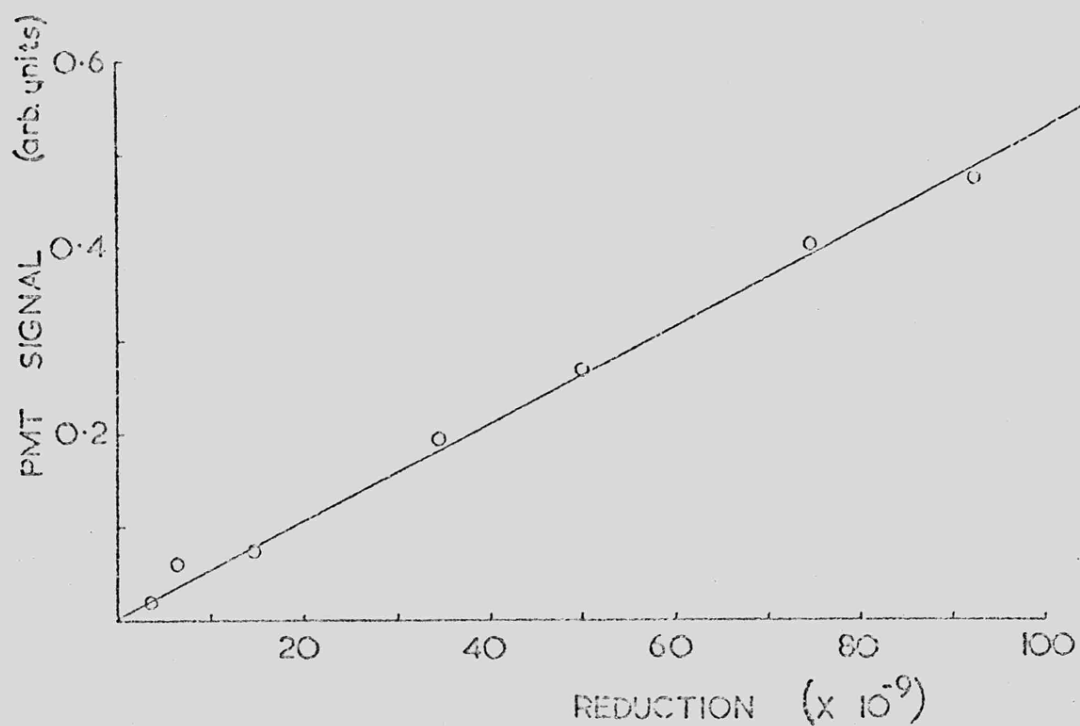
also contains an AC hum which is smoothed out with a simple RC

circuit. The wisdom of plotting temperature on this axis was

challenged by Prachyabrued (1973, personal communication) who

preferred to plot time. His argument was that in the event of

some non-linearity in the heating rate only one axis (the emitted

light) was affected, whereas in using temperature both axes are

affected. Consequently the irregularity is distorted. This

procedure has numerous instrumental difficulties associated with

calibrating the temperature axis and introduces additional errors.

I have therefore continued to use temperature so that it can be

measured directly from the X-axis. So few irregularities have

occurred (see section III.3) that any curves showing them are

discarded.

No attempt was made to zero the meter and the decade

switches controlling the heating rate and levelling-off temperature

in the control unit. It was thought more accurate to prepare

calibration charts, and these are presented in the Appendix.

II.2c   Light Sensing Equipment (Figure II.3a)

The choice of a PMT was governed by the need for high

sensitivity to low level continuous light sources. The PMT

recommended by EMI for thermoluminescence applications (9635B)

was used, the quartz-window version being considered unnecessary

since meteorite TL does not include the UV wavelengths (Sippel,

1973). Most of the meteorites studied here, and all those for

which quantitative results were sought, have blue-green TL. This

is in the region of peak sensitivity for this PMT. The

associated electronics were built according to circuits in the

maker's catalogue to produce a linear response to light. This

required a high negative voltage on the cathode, an earthed

thirteenth dynode resistor and no coupling capacitors. The PMT

was prepared in accordance with the recommendations of James and

Sternberg (1969, page 161). A mu-metal shield, at cathode

potential, provided shielding from both magnetic and electric

fields. The high voltage supply to the PMT (1250 volts) was never

switched off since various workers have claimed that after

switching a tube may take several days to settle down. Instead,

a shutter was fitted to the PMT and closed when the assembly had

to be removed from the sample chamber for loading purposes.

The dark current was measured with various coolants (e.g.

alcohol cooled with solid CO_2) flowing around the PMT assembly,

but the improvement over tap water did not warrant the extra

inconvenience. A typical dark current was 5 nanoamps, whereas

the current from the PMT exposed to low level meteorite TL was

about 10 microamps.

The signal from the PMT was amplified by a Radiospares MOS

FET input operational amplifier. This was chosen because its high

input impedance favoured low input signals. The current-to-

voltage gain was 1000 (20,000 when recording the glow curves of

Allende specimens). The amplified signal was measured on the Y-

axis of an XY recorder with temperature on the X-axis. A glow

curve was thereby obtained directly. The XY recorder used was

manufactured by Bryans (26000 series).

II.3   Checks on equipment

Well over a thousand glow curves were recorded with simultaneous recording of the heating rate. This was achieved by measuring temperature on a separate chart recorder. No deviation from linearity within our ability to determine it was found ($\mp$ 0.05°/sec).

The linearity of response of the light-measuring equipment was checked using a system of integrating spheres (Figure II.4). This apparatus produced a considerable drop in the intensity (say 10^{-10}) of a white-light source without affecting its colour. (Filters always change, sometimes considerably, the colour of the light). The spheres were constructed from four 10" diameter perspex hemispheres (manufactured by Duplex Domes Ltd., Leicester) the insides of which were coated with three coats of white egg-shell finish paint and three coats of photometric integrator paint (Rolls and Co., Edmonton, London). A six volt lamp run off a constant voltage transformer illuminates one sphere which contains a set of diaphragms through which light can enter a second sphere. An aperture in the second sphere acted as a dummy specimen chamber for the PMT housing to rest on. Figure II.4 presents details of the linearity testing procedure. The response to light was checked every few months and no deviation from linearity was observed.

A standard lamp is necessary to check the day-to-day and long-term constancy of the sensitivity of the apparatus. A variety of designs have been constructed but none have been found to be wholly satisfactory. It is thought preferable to rely on duplication of measurements and randomization of errors although

a standard lamp was used as a guide. The lamp that was used for

the bulk of this work was a Saunders-Roe "Betalight" in which a

phosphor is activated by tritium gas (half-life of 12 years).

This was attached to a base which neatly fits on to the filament

so that the light source is in the same position each time. It

was used at the beginning and end of each set of glow curve

determinations. The PMT was left exposed to the standard lamp

for 15 minutes prior to use in order to allow the tube to

saturate at the light levels concerned. Neutral density filters

were used to bring the light level of the standard lamp down to

that of the meteorites being studied.

II.4   Techniques concerning the use of the thermoluminescence

        apparatus

        Where it was impossible to chip material from a specimen

cutting was performed using a Metals Research Ltd. Microslice II

diamond saw and distilled water lubricant. When used in the

annular arrangement an exceptionally thin cut (0.10 mm) could be

achieved. Mounting was performed using adhesive tape and elastic

bands. Samples were lightly crushed and the magnetic portion

removed with a bar magnet. The residue was then ground in a glass

mortar and passed through a 50 micrometer sieve. 10 ± 0.1 mg was

then weighed and placed on a defined area of the filament using

a stencil. The glow curve was recorded in an atmosphere of argon

or oxygen-free nitrogen at a pressure of 10 cm of mercury. In

agreement with numerous other workers we have not been able to

produce triboluminescence by the grinding procedures

(Christodoulides et al., 1970).

Hoyt et al. (1972) and Aitken et al. (1964) have claimed that it is necessary to work in red light when handling samples for TL measurement, since laboratory light drains the TL. We have checked this for meteorites by placing two watch glasses of meteorite powder about three feet from fluorescent laboratory lights. One watch glass was covered with an opaque lid to act as a control. Over 11 hours 8 specimens were taken and their glow curves recorded. No draining of the sample exposed to light was observed and we do not therefore work in red light. The same experiment was performed with powder that had been irradiated.

Irradiation was performed in a Co^{60} bomb manufactured by the Vickers company. It was rated at 18400 Curies of γ-rays when it was delivered to the Chemistry Department, University of Leicester, in May 1970. When used for the work described here it was probably giving a dose of about 700 krad/hour (taking the half-life of Co^{60} as 5.258 yr and assuming 100% absorption of γ-rays). A rack was prepared to hold the specimens in the same position in the bomb during irradiations. The uncertainty in the dose received due to the time during which the specimen was being raised or lowered in the bomb was probably about $\pm$ 2 krad. The error due to less than 100% absorption is unknown. However, since all the measurements used here are relative, and doses are given only to allow comparison with published results, the accuracy given above is probably sufficient. When weighing out specimens the scale pan was carefully wiped when there was any possibility of contamination with irradiated material. Irradiated specimens are allowed to decay at room temperature for about 30 hours to ensure that decay during a series of runs is minimal. Thereafter
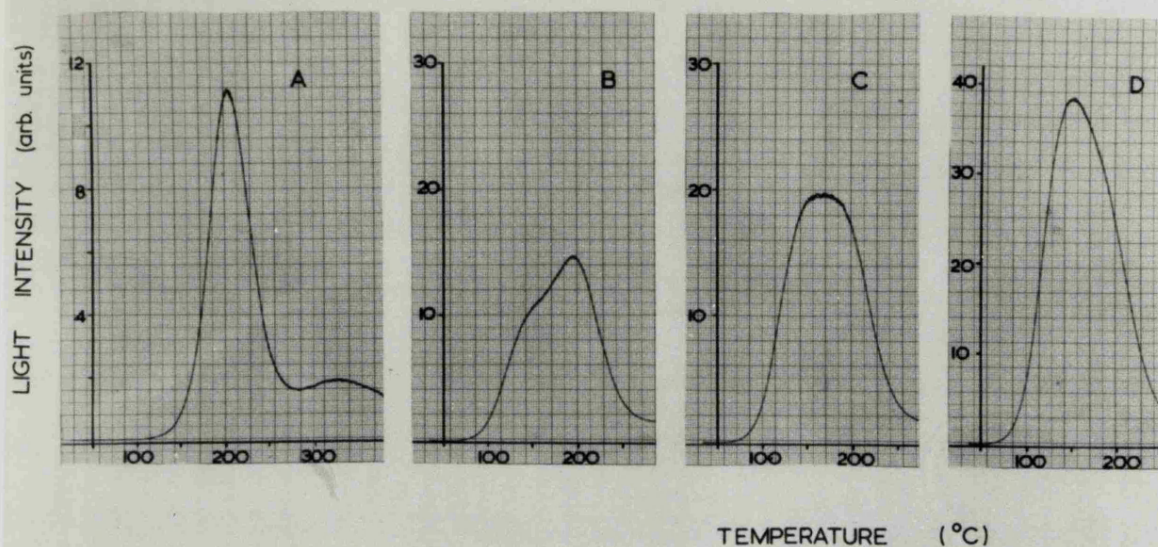
Figure II.5 Part of the glow curve of material from the Tennasilm meteorite. A. natural; B. natural + 23 krad; C. natural + 46 krad; D. natural + 69 krad. Thereafter the thermoluminescence is saturated and the form of the glow curve changes little. The doses are of γ-rays from a Co^{60} source and are accurate to ± 2 krad.
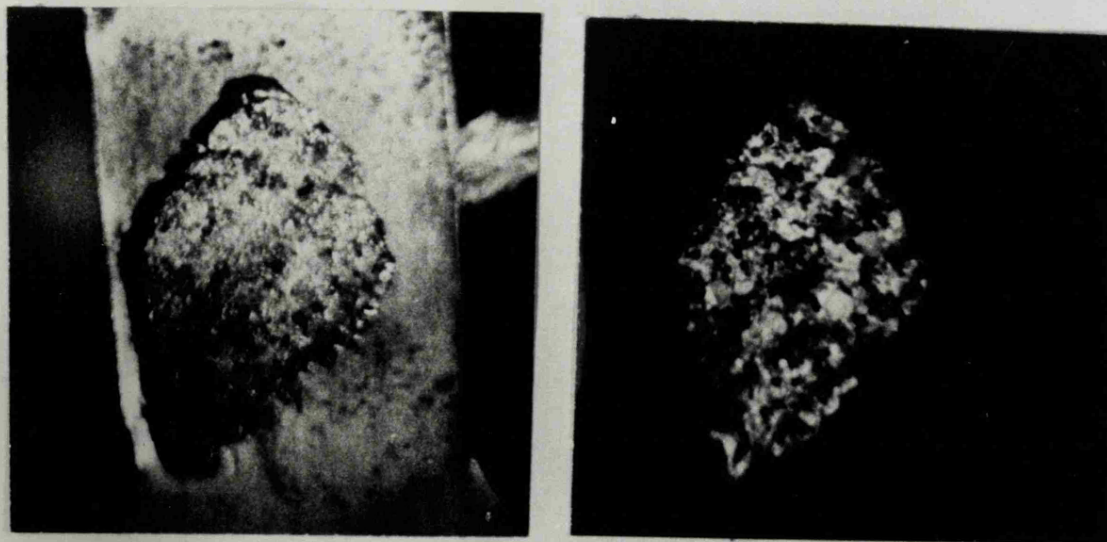
Figure II.6 Photographs of a 1 mm thick slice of the Holbrook meteorite lying on the filament (left) and the slice by the light of its thermoluminescence (right). Good thermal contact was ensured by the use of silicone grease and the sample had been highly irradiated (about 300 krad).

they were stored in a deep freeze at -20°C (Durrani, 1973).

It is important when examining the shape of the glow curve to use small doses. Irradiation preferentially populates the lowest energy levels, and consequently enhances the low temperature peaks until eventually they become so intense that they dominate the glow curve. The optimum dose for our purpose was found to be about 50 krad. Figure II.5 shows the effect of irradiation on part of the glow curve for the Tennasilm meteorite. It can be seen that the two-peak structure soon becomes difficult to see.

Measurements can be taken from glow curves in two ways, depending on the curves and application. As a rule peak height is used. The errors involved in allowing for peaks which overlap make the use of area very difficult, although it is theoretically more meaningful. However, on the occasions when area was thought to be preferable they were measured with an Allbrit planimeter.

II.5   Inspection with naked eye and photography

By covering the specimen chamber with a steel plate in which there was a glass window the thermoluminescence could be observed. Most irradiated meteorite powders produce thermo-luminescence visible to the dark-adapted eye, as do many specimens in their natural state. However, photography is very difficult because of the low light intensities. 400 ASA film (e.g. Kodak Tri-X) readily records the thermoluminescence of irradiated common chondrites, (Figure II.6), but can record the thermoluminescence of natural powder only with great difficulty. No success has been achieved in attempts to photograph the

thermoluminescence of natural and irradiated powders with colour film.

The value of photographing the thermoluminescence of meteorites could be considerable. For example, the distribution of thermoluminescence in a slice could be seen directly, and gradients in any direction could readily be obtained with a microdensitometer. Such ideas and new techniques would no doubt present many foreseen and unforeseen difficulties, and at best cannot readily provide information about the glow curve. The limitations of thermoluminescence to provide some of the information sought are, to a large extent, apparent — the glow curve, a detailed examination of which constitutes the next chapter.

CHAPTER III

THE GLOW CURVE

III.1   Introduction

Most meteorite classes can be expected to produce a
characteristic glow curve depending on the mineral responsible
for the luminescence. The type of curve is important and must be
considered before generalising about the usefulness of thermo-
luminescence for certain applications. For example, there would
be little point in attempting to apply TL to the determination
of the terrestrial age of meteorites which have only a very low
temperature peak in their glow curve. Generally, low temperature
peaks fade very quickly, say within a few years. The pyroxene-
plagioclase achondrites may be an example of this.

The form of the glow curve has been used by Grögler and
Liener (1968) to show that the Shallowater meteorite is not an
aubrite. Although there must be reservations about such a
procedure, in this particular example there are good mineralogical
arguments to substantiate it.

The enstatite achondrites (aubrites) have the most
intense TL, and may be assigned an intensity of 100 arbitrary
units. The next most intense group are the common chondrites with
an intensity of 30. Localised regions in Allende contain a
mineral with TL of about 10, and pyroxene-plagioclase achondrites
and enstatite chondrites show an intensity of about 2. The least
intense meteorite TL found in this study occurred in two other
minerals in Allende, both of which had TL with an intensity of
about 0.05. There is therefore a factor of 2000 difference in the
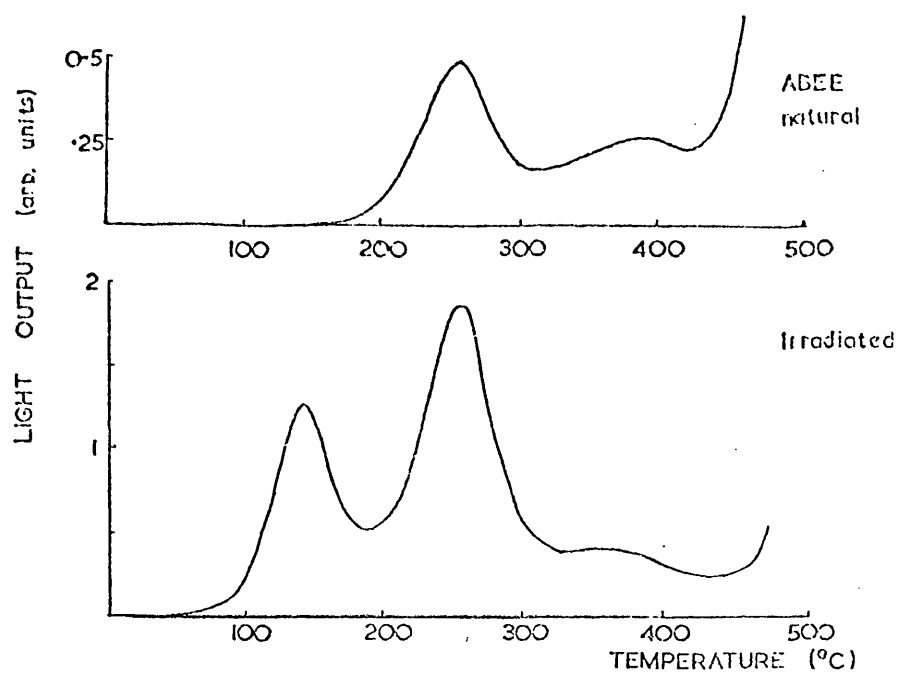
Figure III.1a Glow curves for natural and irradiated powder from the Abee enstatite chondrite.
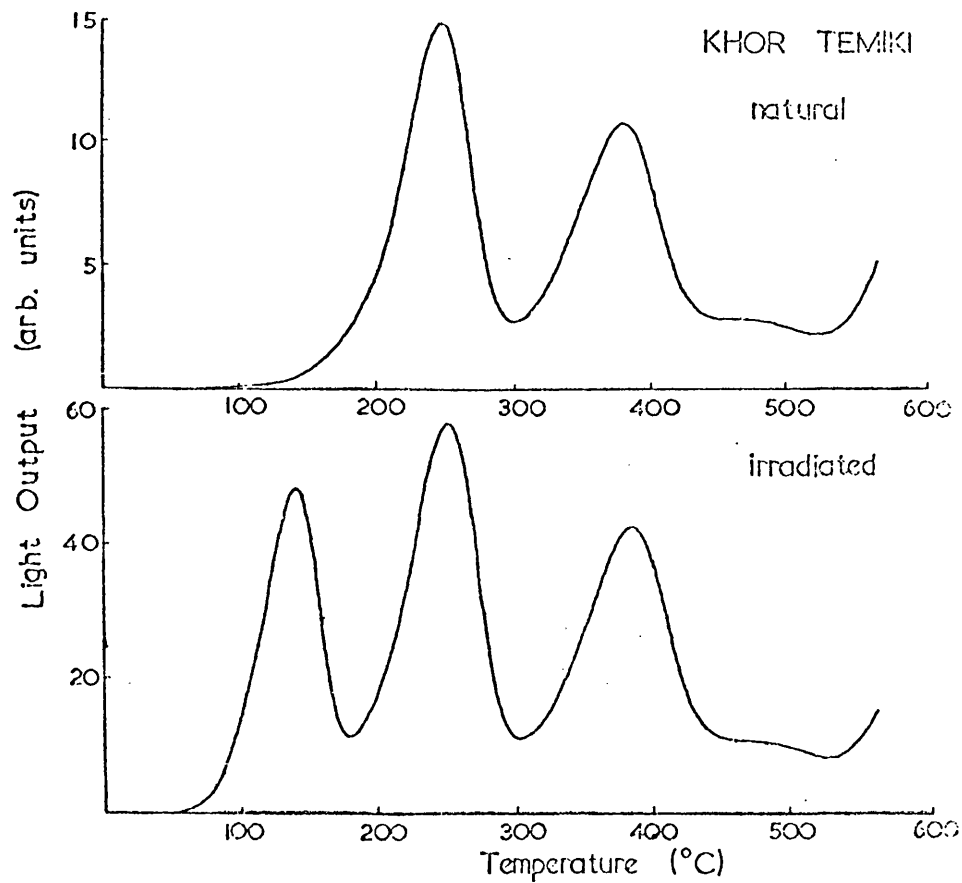
Figure III.1b Glow curves for natural and irradiated powder from the Khor Temiki enstatite achondrite.

range of thermoluminescence exhibited by meteorites.

III.2   Enstatite chondrites and achondrites

The glow curves for these meteorites are presented in
Figure III.1. They are clearly produced by the same mineral —
enstatite achondrites are remarkably pure enstatite. The
intensity difference is considerable, and probably due to
carbonaceous matter present in the chondrites (Mason, 1962).

The TL of the aubrites was discussed by Grögler and Liener
(1968) who gave the peak temperatures as 100, 190, 250 and 400°C
(heating rate 0.75°C/sec). Sun and Gonzales (1966) presented the
glow curves of an aubrite (after electron bombardment) recorded
through blue and red filters in connection with their theory for
the production of transient lunar phenomena. Their glow curves
quantify the fascinating colour changes the meteorite TL exhibits
as the powder is heated. Since the intensity is so high the
luminosity can readily be seen with the dark-adapted eye. The
lower two peaks are different shades of blue and the third is red.
Under electron bombardment high-manganese grains luminesce red
and low-manganese grains luminesce blue (Geake and Walker, 1966;
Reid and Cohen, 1965). However, some caution is necessary when
comparing the luminescence colours obtained by different
instruments, for it was found with the Allende meteorite that
certain minerals have different colours in the electron microprobe
and in an electroluminescence microscope.

III.3   The Allende meteorite

In sharp contrast to the aubrites the intensity of the TL
of the Allende meteorite is very low. Allende is a very
heterogeneous meteorite containing many Ca-Al rich aggregates
which may be expected to contain numerous luminescent minerals
(Marvi., et al., 1971; Kiel and Fuchs, 1971). As a subject for
the study of this phenomenon it is ideal, presenting luminescence
in several colours and associations (frontispiece).

One hundred and six specimens, each about 1 x 4 x 4 mm,
were powdered, sieved, and their glow curves recorded. The
drained powders were then irradiated to about 50 krad by γ-rays
from a Co^{60} source and the glow curves recorded again. It is
therefore possible to describe reasonably well the major TL
properties of this meteorite, although no doubt more remain to be
discovered.

Most of the specimens gave glow curves with peaks at 140
and $200^{\circ}C$. Representative examples are presented in Figure III.2,
in which curves with a strong $140^{\circ}C$ peak are called type 1 and
those with a strong $200^{\circ}C$ peak are called type 5. Combinations
of these constitute types 2, 3 and 4, where 3 has peaks of
comparable intensity. The two peaks are obviously caused by
different minerals since they vary independently over very short
distances. The $140^{\circ}C$ peak is most intense where the specimen
included a chondrule, and since most chondrules in Allende are of
forsterite it seems reasonable that this mineral is responsible
for the peak. This was readily confirmed by recording the X-ray
diffraction pattern of the residues giving the various kinds of
glow curve. The residues were prepared by being placed on a
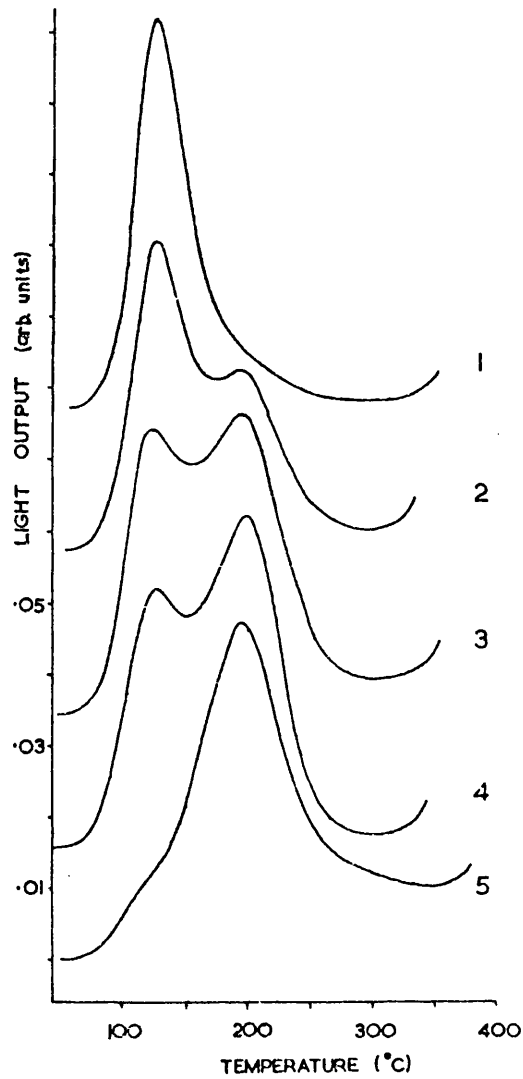
Figure III.2   The glow curves of specimens from the Allende
meteorite. Types 1 and 5 are caused by different minerals
and the others by their combination.
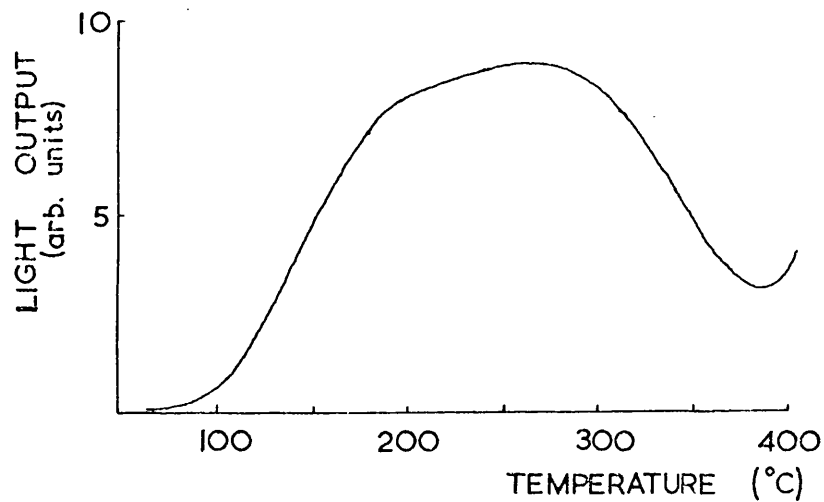
Figure III.3   Glow curve of type 6 produced by material from
the Allende meteorite.

microscope cover slip as a suspension in water. Specimens

giving type 1 glow curves gave an X-ray diffraction pattern

showing both forsteritic and fayalitic olivine peaks, whereas

the material responsible for the other glow curve types produced

only the fayalitic X-ray diffraction peaks.

The discs used for X-ray diffraction measurement were

also placed in an electroluminescence microscope, in which the

luminescence excited by 6 kev electron bombardment could be

observed. Type 1 residues gave red electroluminescence while

type 5 appeared blue. In polished thin section the material

giving red electroluminescence could readily be identified as

olivine, re-affirming our assignment of the $140^{\circ}C$ TL to forsterite.

The polished thin section also contained blue electroluminescent

material as micron or sub-micron grains in the white aggregates.

These were analysed by a Cambridge microscan 5 electron microprobe

operating at 20 kv accelerating voltage, and the results are

presented in Table III.1. The beam was usually wider than the

grain and could not be made smaller as this resulted in the

luminescence being too weak to see. Consequently the calcium

value, which was highly variable, may be due entirely to the beam

extending beyond the grain and on to the Ca-rich matrix of the

aggregate. The average of the analyses most closely resembles

cordierite ($Mg_2Al_4Si_5O_{18}$), (Clarke et al., 1971; Keil and Fuchs,

1971), and we tentatively equate this with the $200^{\circ}C$ peak.

Perhaps the most interesting thermoluminescence in Allende

occurred in certain localised regions of the section. The glow

curve consisted of a single broad band of luminosity between 200

and $300^{\circ}C$ (Figure III.3), about 200 times as intense as types 1

Table III.1

Electron microprobe analyses of the major

thermoluminescent minerals in the Allende meteorite*

	A	B	C	D
CaO	39.2	30.0	10.6(3.1-20.9)	0.5
SiO_2	22.7	37.2	39.7(36.4-41.6)	38.5
Al_2O_3	33.2	30.2	22.5(10.8-30.2)	0.5
FeO	0.2	1.7	6.4(1.5- 7.6)	0.5
MgO	2.4	1.8	20.5(7.0-32.2)	57.4
TiO_2	n.d.	n.d.	n.d.	0.1
Sum	97.7	100.9	99.6	97.5
Number of points	6	3	6	3

* oxides determined by stoichiometry

A Gehlenite

B Luminescent alteration product of gehlenite: responsible for orange-pink electroluminescence and type 6 thermoluminescence

C Blue electroluminescent grains in white aggregates: responsible for the $140^{o}C$ thermoluminescence

D Forsterite: responsible for the $200^{o}C$ thermoluminescence peak and showing red electroluminescence

n.d. not detectable

Analyses for A, B and D are accurate to 10% of the value for the element.
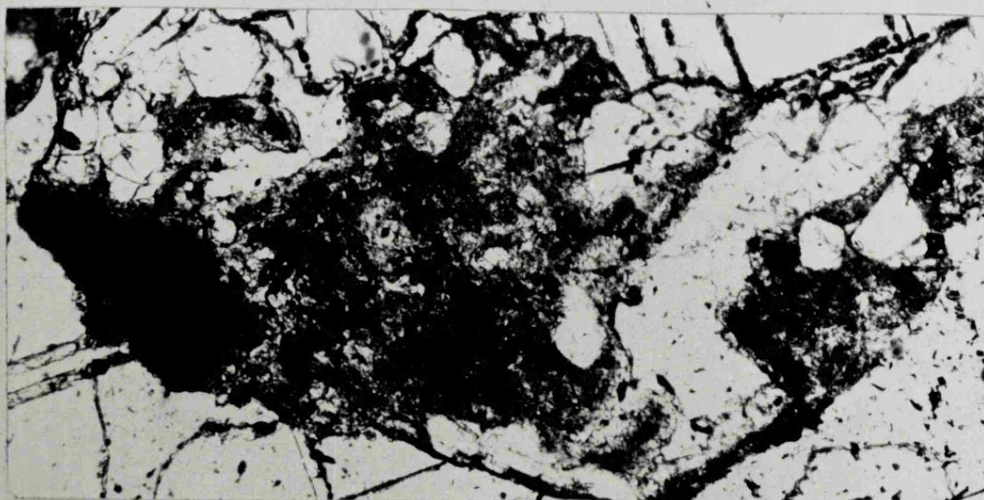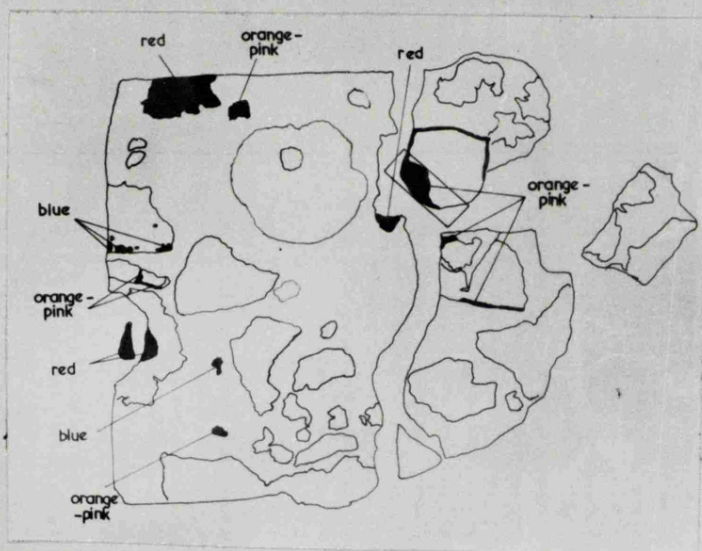
Figure III.4   Top, photograph by transmitted light of a 4 x 4 mm
polished thin section of the Allende meteorite containing type 6
material; middle, sketch giving electroluminescence colours;
bottom, photograph of the boxed region containing type 6 material.

and 5. This is referred to as type 6 and, in the original slice

of meteorite, coincided with a white aggregate in at least one

instance. One of the 1 x 4 x 4 mm sections from a region giving

this kind of glow curve was not powdered, but instead a polished

thin section prepared (Figure III.4) to allow electron microprobe

and electroluminescence investigation. In addition to the red

and blue electroluminescence this section contained an orange-

pink luminescence. It occurred in bands across certain grains,

and around the edges of others. It also appeared to surround a

chondrule which had, unfortunately, been plucked out during

polishing. Under transmitted light the luminous areas were seen

to be disturbed, fuzzy, bands with a slightly brown tinge. In

some instances they resembled shock effects and in others looked

as if they had formed from reaction with the matrix (Figure III.4c).

From electron microprobe analysis (Table III.1) the host grains

are clearly gehlenite $(Ca_2Al_2SiO_7)$. The composition of the

luminous material gives no clue as to the reason for its luminosity,

so presumably it is a structural difference between the luminous

material and the gehlenite which is responsible.

The complex mineralogy of Allende is therefore reflected

in the meteorite having complex TL properties. The most intense

TL is ascribed to an alteration product of gehlenite, the $140^{\circ}C$

peak is caused by forsterite and the $200^{\circ}C$ peak is probably due

to cordierite.

III.4 Pyroxene-plagioclase achondrites

The glow curves of natural pyroxene-plagioclase

achondrites show a little luminosity with a maximum at about

200°C. Irradiated meteorites display a number of peaks, the

strongest being at about 140°C and the others at higher

temperatures. In fact, the glow curve could best be described

as a peak at 140°C sloping off asymmetrically until about 370°C

(Figure III.5).

The luminescent species is undoubtedly feldspar, but

the difference between this and the luminosity caused by the

feldspar in lunar samples (Figure III.6), common chondrites and

terrestrial samples is noteworthy and probably highly significant.

Mason (1967) has noted that the pyroxene-plagioclase achondrites

contain feldspar of bytownite composition.

III.5 Common chondrites

The glow curve of natural common chondritic material is

the simplest of all meteorite glow curves (Figure III.7). It

contains two peaks; a sharp intense peak between 180 and 235°C

(LT) and a broader peak between 300 and 395°C (HT). The exact

temperature of the peak is governed to some extent by overlap but

there clearly is some additional variation (see Table IV.1).

Valladas and Lalou (1973) have made a spectral analysis of the TL

from common chondrites and found LT to have blue-green coloured

luminescence and HT to have blue luminescence. Lalou et al.

(1970) showed by mineral separation that the mineral responsible

for the TL is feldspar. In common chondrites the feldspar has

the oligoclase composition (van Schmus and Ribbe, 1968).
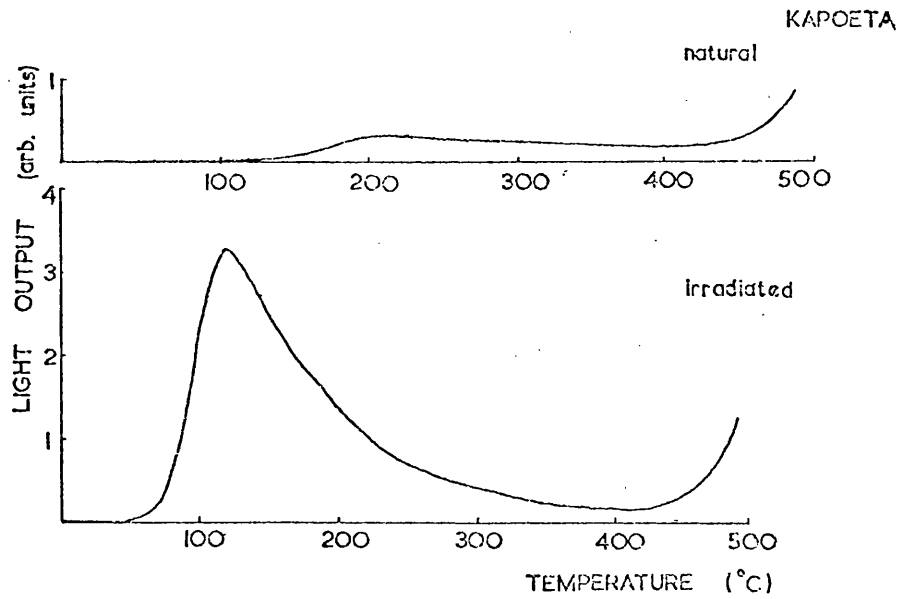
Figure III.5 Glow curves for natural and irradiated powder
from the Kapoeta pyroxene-plagioclase achondrite.
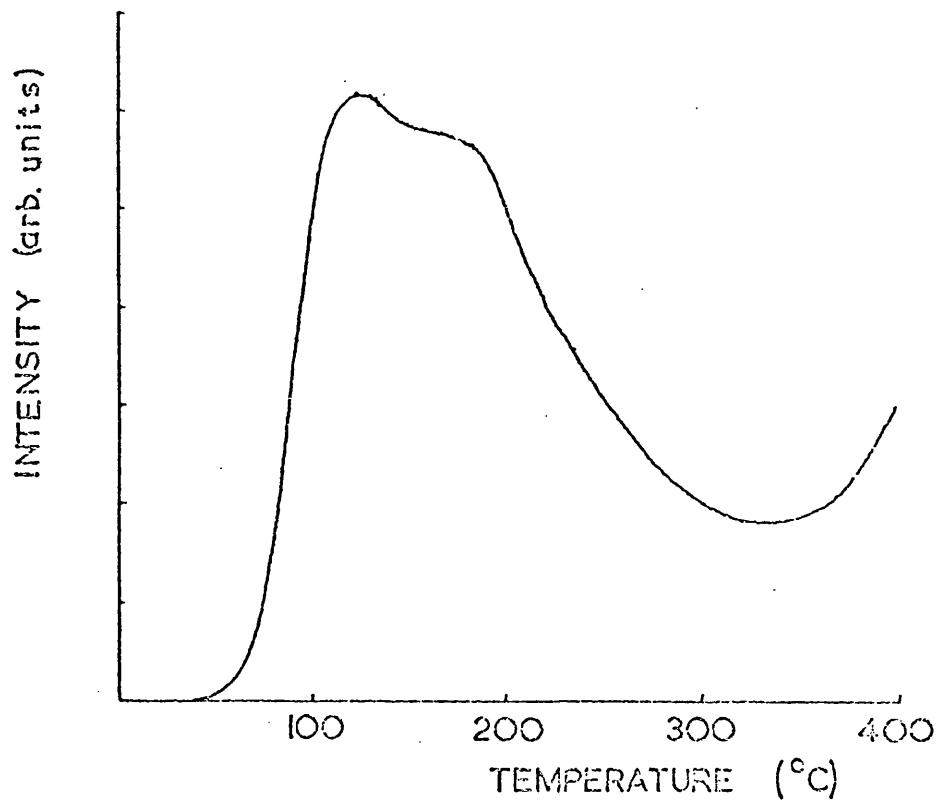
Figure III.6 The glow curve for lunar samples (from Hoyt et al.,
1970).
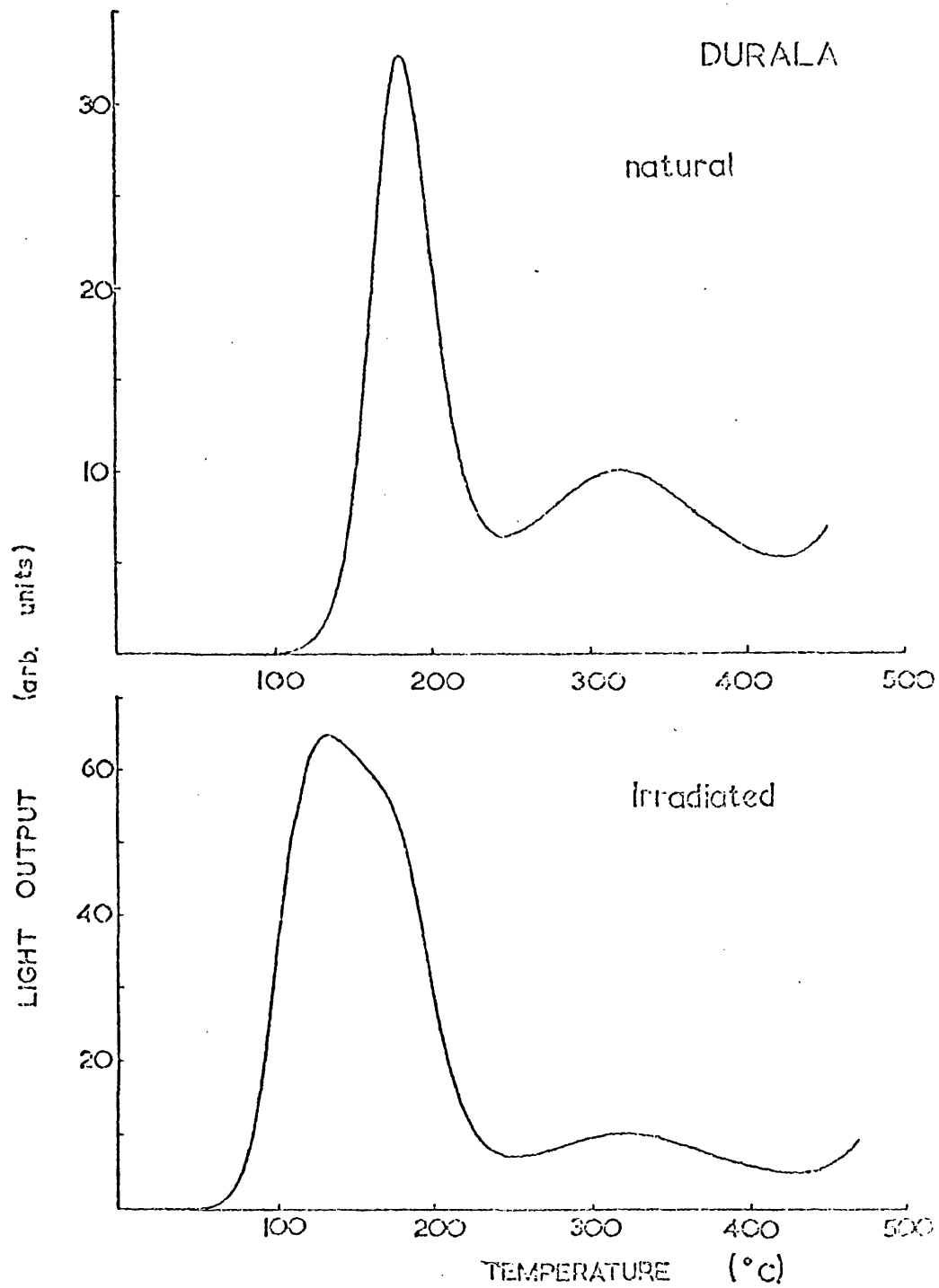
Figure III.7 Glow curves for natural and irradiated powder from the Durala L6 chondrite.

Upon irradiation the peak broadens and moves to lower temperatures (Figure III.7). Without going into details Liener and Geiss (1963) stated that this was due to a difference in the irradiation time of naturally and artificially irradiated material. Three lines of evidence make it clear that the behaviour is due to at least one, and possibly two peaks below 200°C. These will have drained in the natural specimens but are readily re-populated during irradiation. The lines of evidence are:

i) the form of, say, the Tennasilm glow curve (Figure II.6).

ii) the supralinearity of some dose curves (peak height vs. superimposed dose) (Figure IV.6) and,

iii) a displacement in the peak height ratio vs. peak temperature curve (Figure III.8).

This would be monotonic if overlap was occurring between LT and HT only. Hwang (1973) has used completely different evidence to argue for two peaks below 200°C in lunar sample TL.

III.6 **A comparison between the glow curves of materials in which feldspar is the luminescent species**

Pyroxene-plagioclase achondrites, common chondrites and lunar samples are all luminescent by virtue of their feldspar content. The main difference in their glow curves is the extent to which a peak at 250°C is present. In achondrites it is very intense, in lunar samples its presence is indicated by the TL between 200 and 300°C (Figure III.6) and in common chondrites it is exceedingly rare. In fact out of 30 common chondrites only one or two which are highly weathered (e.g. Potter) display a 250°C peak. Lunar samples and achondrites have calcic plagioclase
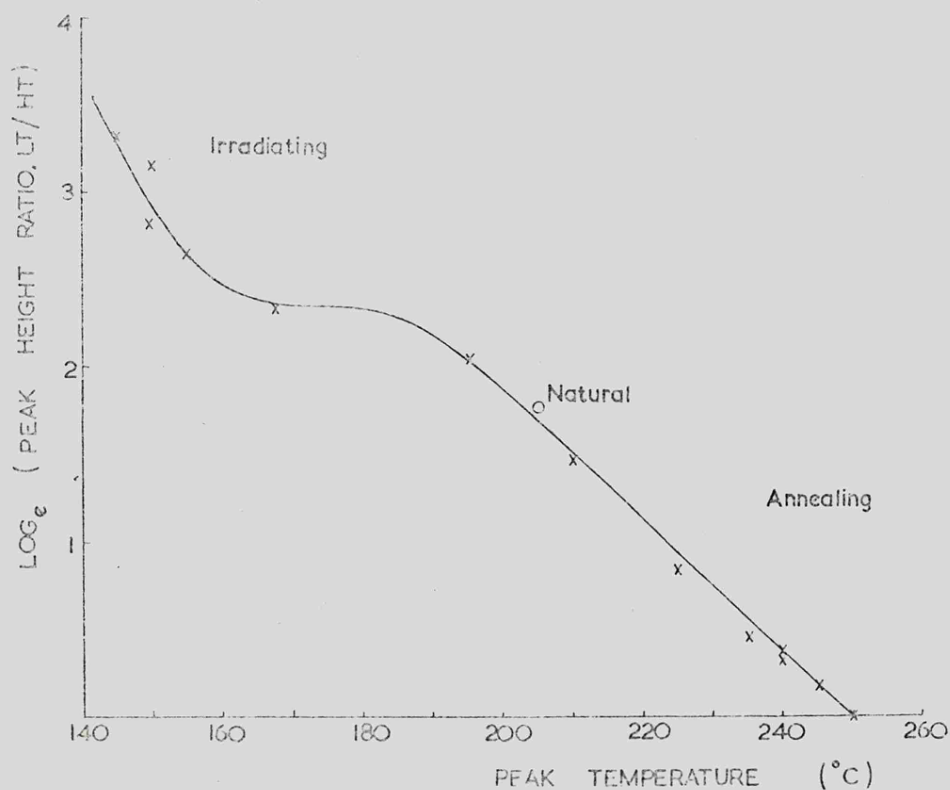
Figure III.8 Variation in the low temperature peak position
with various peak height ratios for material from the Tennasilm
meteorite. The discontinuity suggests that a peak below 200 °C
is present.
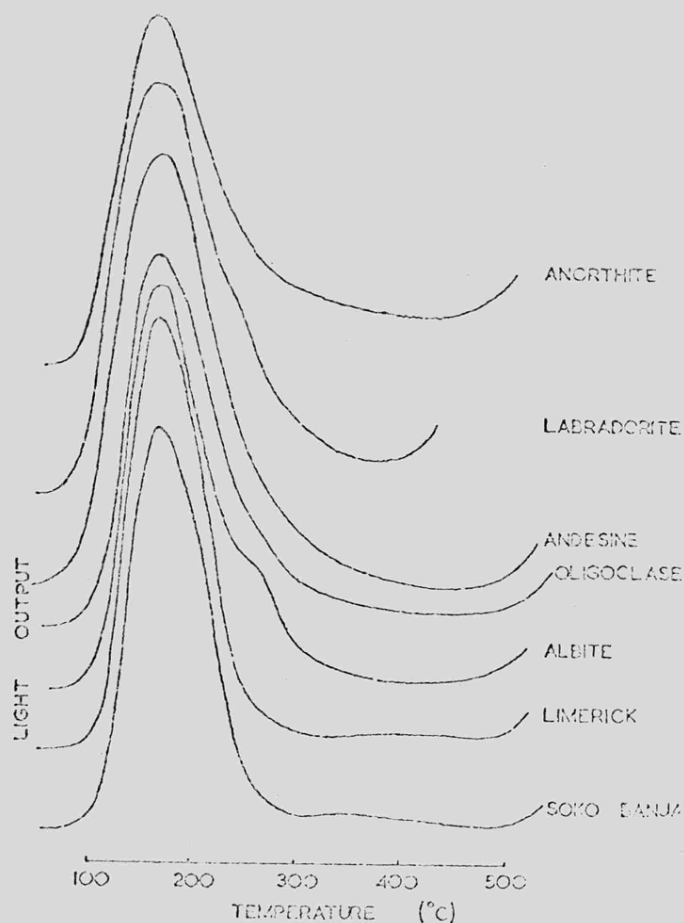
Figure III.9 The glow curves of a variety of terrestrial
feldspars with those of two meteorites for comparison. All had
received the same dose of radiation.

feldspar (Keil et al., 1970; Mason, 1967) whereas common

chondrites have a more sodic feldspar, oligoclase (van Schmus

and Ribbe, 1968). It is therefore tempting to suggest that it is

the nature of the feldspar which governs this peak, and so the

shape of the glow curve. This idea can readily be tested by an

examination of the glow curves of terrestrial feldspars of all

compositions (Figure III.9). Although the 260°C peak is weakly

present in all of them, the expected trend of an increasingly

intense peak as one goes from sodic to calcic feldspar is not

observed. The composition of the feldspar does not therefore

explain the difference in the glow curves.

If the cause of the different glow curves shown by lunar

samples, pyroxene-plagioclase achondrites and common chondrites

is not compositional, then a factor which may be important is the

radiation history of the specimens. Many of the characteristics

of the lunar soil are the result of it being part of the lunar

regolith; e.g. gas implantation by the solar wind (Abell et al.,

1970), and charged particle track measurements (Crozaz et al.,

1970). This fact is clearly an important one in explaining the

properties of the lunar material. There is also some evidence

that the $\overset{\text{Some of}}{\underset{\wedge}{\text{the}}}$ pyroxene-plagioclase achondrites were once part of a

regolith (see Brownlee and Rajan, 1973). It therefore seems not

unlikely that the thermoluminescence in the 250°C region in these

achondrites and in lunar samples is associated with their regolith

origin. Its absence in common chondrites is then explained.

III.7   Summary

It is apparent from the observations made in this chapter
that applications developed for one class of meteorites are not
necessarily applicable to all. There can be considerable
differences between any two classes even when they have a
thermoluminescent mineral in common. In fact the differences in
the glow curves of meteorites may furnish important clues to the
history of the specimen. The thermoluminescence of pyroxene-
plagioclase achondrites may be providing supporting evidence of
their regolith origin. In the next chapter the use of thermo-
luminescence to determine the history of meteorites is carried
further by the discovery that it is probably capable of distinguishing
shocked from unshocked specimens.

The Allende meteorite will be discussed again in detail
later, when an attempt is made to derive quantitative information
for this meteorite. The major problem presented by the Allende
meteorite, and to a lesser extent all meteorites, is heterogeneity.
Studies of the kind described in this chapter may enable this to
be taken into account by considering not just the intensity but
also the structure of the glow curve of the thermoluminescence.

The variety of glow curves presented by meteorites are
described in Table III.2. This includes a list of their relative
intensities and the minerals giving rise to the thermoluminescence.
The simplest glow curves, at least for the natural specimens, appear
to be those of the common chondrites. Since they are also the most
plentiful class of meteorites they are a good choice for study by
thermoluminescence, and the first application to be investigated
is the determination of the terrestrial age of common chondrites.

Table III.2

Thermoluminescence of Meteorites

Meteorite Class	Mineral responsible for TL	Relative intensity of most intense peak *	Temperature of peaks present °C **
Enstatite achondrites	Enstatite	100	130, 250, 380, 470
Enstatite chondrites	Enstatite	2	130, 250, 370
Carbonaceous chondrite type III (Allende)	Gehlenite alteration product	10	200-300 see Figure III.3
	Cordierite***	0.05	200
	Forsterite	0.05	140
Pyroxene-plagioclase achondrites	Feldspar (bytownite)	2	110-300 see Figure III.5
Common chondrites	Feldspar (oligoclase)	30	200, 350

*   assuming enstatite achondrites = 100

**   heating rate 5°/sec.

***   probable.

CHAPTER IV

THE TERRESTRIAL AGE OF METEORITES

IV.1   Introduction

The 'terrestrial age' of a meteorite is that period which

has elapsed since it fell to Earth. The terrestrial ages of

most meteorites are not known directly since the majority in

collections are 'finds' rather than observed 'falls'. The

methods so far used to determine this age (Anders, 1963; Boeckl,

1972; Begemann and Vilcsek, 1969; Chang and Wänke, 1969) employ

the decay of spallation-produced isotopes, and depend on knowing

an original value for the decaying isotope. This is determined

from falls of known age and assumed constant for all meteorites.

It is reasonable to expect that once a meteorite has been

removed from its space environment, where it is being irradiated

at low temperature, its thermoluminescence (TL) will begin to drop

in a time-dependent manner. Christodoulides et al. (1970)

therefore suggested the use of TL for determining terrestrial

age, but no rigorous examination of the possibility was made.

This is the aim of the present chapter, the main results of which

have already been published (Sears and Mills, 1974a; 1974b).

IV.2   Natural thermoluminescence

The glow curves for natural powder from 19 meteorites of

known terrestrial age are shown in Figure IV.1. The expected

tendency of the lower temperature peak (LT) to fade as the

terrestrial age of the meteorite increases is observed. The

higher temperature peak (HT) shows very little change since its
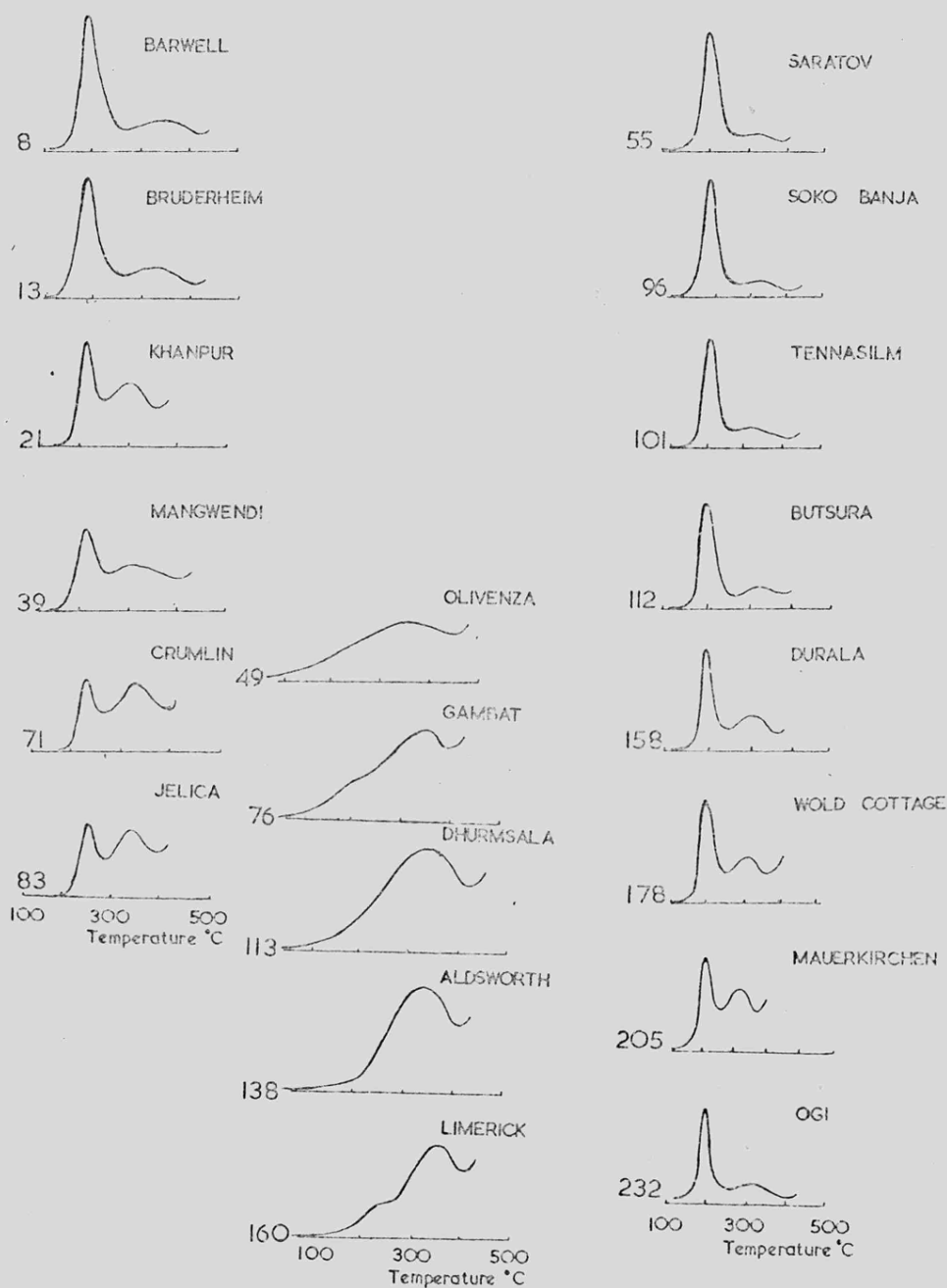
Figure IV.1 Sketches of the glow curves of 19 meteorites of
known terrestrial age. The numbers denote this age in years.
Details of the meteorites, peak positions and intensities are
listed in table VI.1. The vertical axis changes slightly, the
height of HT is approximately constant. The curves turn up at
the right with the onset of black-body radiation.

half-life is much longer, in fact we believe it to be of the
order of 1000 years. Unfortunately, the fading of LT is not of
a simple nature, but two groups are clearly present; one in
which LT fades below HT in about 100 years, and one in which it
takes several hundred years for this to occur. This is perhaps
clearer in a plot of $\log_e$ (peak height ratio LT/HT) vs.
terrestrial age (Figure IV.2). The low retentivity group, in
which LT is fading fastest, shows much scatter from the line but
the high group shows surprisingly little. This suggests that
the meteorites in the high group had a similar peak height ratio
at their time of fall. The cause of the scatter that is present
is probably small initial differences in the TL of the meteorites,
different thermal histories and, in the case of low group
meteorites, varying degrees of shock (see below).

As far as terrestrial age is concerned two points can be
made from these results. Firstly, that there is a relationship
between TL and terrestrial age with the phenomenon appearing to
have the potential to determine terrestrial age and secondly,
that before TL can be used this way a means must be found of
removing the dichotomy or of correctly allocating a meteorite
to its group.

IV.3   The two groups

Details of the 19 meteorites used in Figure IV.1 and of
their TL properties are given in Table IV.1. No difference
(within experimental limits) was apparent in TL position for
high or low retentivity group meteorites, or in the energy of the
peaks as determined by the initial rise method. However, the

laboratory determined mean-lives of the low-temperature peak
were different. Using three meteorites from each group, the
mean-life at 120°C was determined by annealing the powder in the
dark for up to 70 hours in an Abderhalden drying pistol surrounded
by refluxing tetrachloroethylene. The results are presented in
Figure IV.3. It is clear that the two groups are due to
diff...t mean-lives of LT in the luminescent material. The mean-
life ' at room-temperature can be calculated from

$$\tau (300°K) \ = \ \tau (393°K) \ \exp \left[\ \frac{E}{k300} \ - \ \frac{E}{k393} \right]$$

where E, the energy of the peak, can be found by the initial rise
method and k is the Boltzmann Constant (Garlick, 1949). For the
low retentivity group the room-temperature mean-life is 6-8 years,
and for the high group 45-55 years. Laboratory determination of
the mean-life of LT therefore enables a meteorite to be assigned
to its thermoluminescence retentivity group.

We have not been able to determine with certainty the
reason for the two groups, but suspect that it is related to
shock. Both metamorphism and shock change the nature of the
luminescent feldspar; shock producing maskelynite and metamorphism
causing recrystallization. The petrological assignment in van
Schmus and Wood's (1967) classification of chondrites is made on
the extent of metamorphism, and shows no correlation with the
TL groups (Table IV.1). This infers that metamorphism does not
govern TL group membership. However, shock is known to reduce TL
intensity (Houtermans and Liener, 1966) and we believe it also
reduces the mean-life of LT. Most of the low group members have
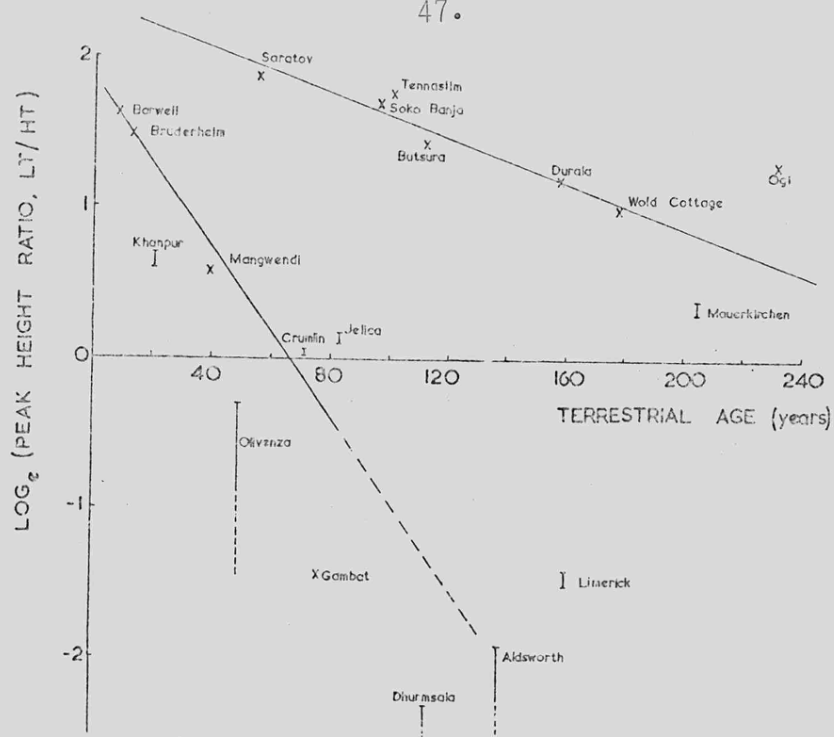
Figure IV.2 Natural logarithm of the peak height ratio (LT/HT) as a function of terrestrial age for the meteorites of known terrestrial age.
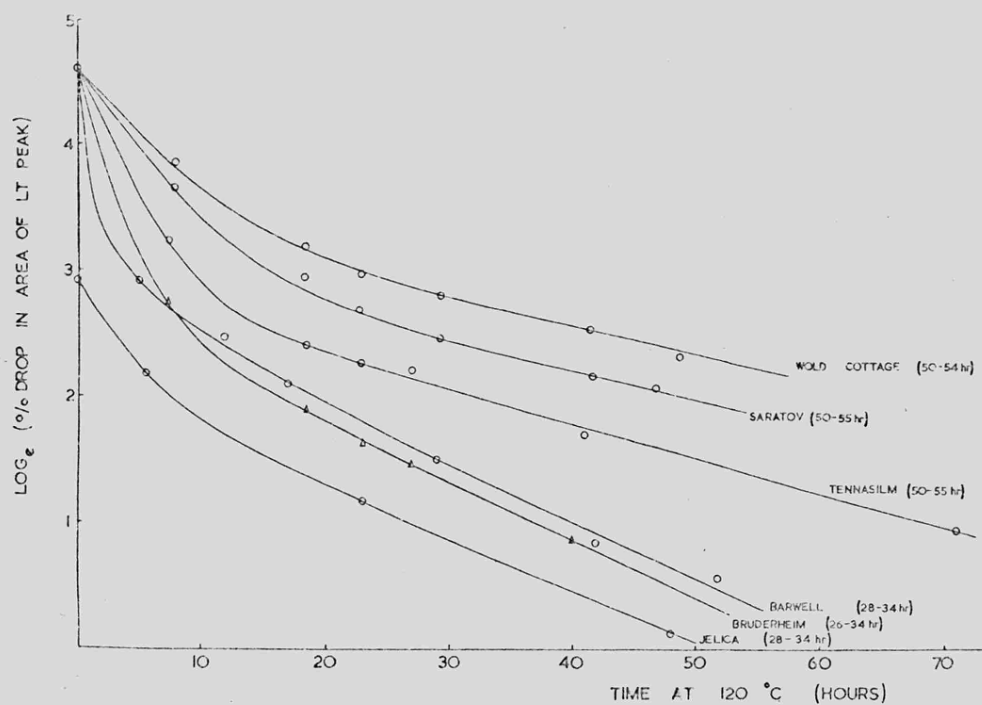
Figure IV.3 Isothermal annealing curves for three high and three low group meteorites. The ordinate is the natural log. of the percentage drop in the area under LT. Overlap with HT has been allowed for where necessary. The curve for Jelica has been displaced downwards for clarity.

PLAINVIEW

DIMMITT

CALLIHAM

BLUFF

SHIELDS

WELLMAN (c)

POTTER

ETTER

100   300   500
Temperature °C
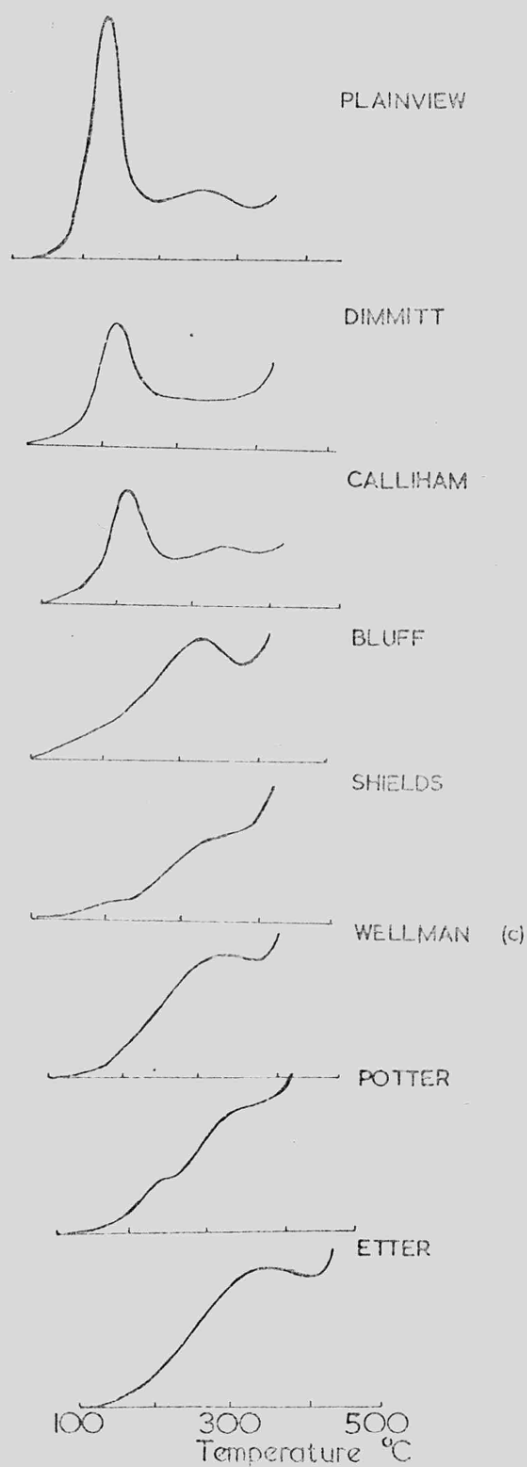
Figure IV.4 Sketches of the glow curves of several finds.
Details of the meteorites, peak positions and intensities are
given in table VI.2. The curves turn up at the right with the
onset of black-body radiation.

Table IV.1

Details of the thermoluminescence of meteorites of known terrestrial age

Group (1)		Terr. Age (years)	Natural Peak Height Ratio	Natural Curve Peak Temperatures (°C) (±5°C) LT	HT	E_{LT} (eV) (2)	Mean-life at 120°C (hr)	Natural equivalent dose (krad)	I_0 (3) (arb. units)
High Retentivity	Saratov	L4	55	6.14	200	320	1.4–1.2 (4)	50–55	46–49	25–28
	Soko Banja	LL4	96	5.5–5.3	190	320	1.13		70–81	80–88
	Tennasilm	L4	101	5.85–5.7	205	330	1.16	50–55	134–145	65–70 sat.(5)
	Butsura	H6	112	4.17	190	235			52–120	45–58 sat.
	Durala	L6	158	3.3–3.26	180	320			81–105	84–86 sat.
	Wold Cottage	L6	178	2.78–2.72	205	345	1.09	50–54	58–250	87–97 sat.
	Mauerkirchen	L6	205	1.37–1.54	220	365	1.06		75–230	96–98 sat.
	Ogi	H6	232	3.67–3.63	200	345			81–105	57–61 sat.
Low Retentivity	Barwell	L6	8	5.12	200	360	1.24	28–34	15–27	40–60
	Bruderheim	L6	13	4.44	190	335	1.18	26–34	70–75	50–56
	Khanpur	LL5	21	2.0–1.8	205	330			105–116	108–112
	Mangwendi	LL6	39	1.78	210	335			116–140	110–130
	Olivenza	LL5	49	<0.74	(225)(6)	375			96–116	102–104 sat.
	Crumlin	L5	71	1.06–1.02	225	350	0.86		145–155	92–95 sat.
	Gambat	L6	76	0.237	220	320			35–46	9–12
	Jelica	LL6	83	1.19–1.12	230	395	1.42	28–34	38–42	75–85
	Dhurmsala	LL6	113	<0.1	(225)	345			52–150	80–130
	Aldsworth	LL5	138	<0.15	(225)	340			170–180	105–115
	Limerick	H5	160	0.26–0.24	235	345			43–49	43–48 sat.

Table IV.2

Details of the thermoluminescence of meteorites of unknown terrestrial age

	Group	Year found	Natural Peak Height Ratio	Natural Curve Peak Temperatures (°C) ($\pm 5°C$) LT	HT	Mean-life at 120°C (hours)	Natural equivalent dose (krad)	I_o (3) (arb. units)
Plainview	H5	1917	3.7	220	365	39-62	55-65	31-52
Calliham	L	1958	2.95-2.35	210	350	40-60	145-155	7.5-8.5
Etter	H	1966	0.25	(225)	330	45-55	20-24	3.2-3.8
Potter	L6	1941	0.48-0.40	250	365	20-28	26-30	6.5-7.7
Bluff	L5	1878	0.05-0.15	(225)	335	22-30	22-26	4.0-5.0
Dimmitt	H3,4	1947	3.5-3.0	220	315-340	45-55	86-100	5.0-6.0
Shields			0.13-0.28	225	345	50-54	36-40	8.0-8.5
Wellman(6)	H	1964	0.43-0.17	(225)	310	40-50	9-20	4.0-9.0

Footnotes:

1. As defined by van Schmus and Wood (1967).

2. As determined by Initial Rise Method.

3. See text for definition.

4. Two determinations using different curves.

5. These meteorites are saturated at the natural equivalent dose, (i.e. additional dose makes no difference to I_o).

6. Where no peak is obvious intensity of LT is measured at 225°C.

been shocked or are breccias (R. Hutchison, private communication).
Olivenza and Barwell are anomalous in this respect, as is Soko
Banja which is in the high group but is a breccia. Shock may
also explain the scatter in the low group line in Figure IV.2,
since it can occur with varying degrees of severity.

IV.4   Terrestrial age from natural thermoluminescence and the
        effect of weathering

By measuring the peak height ratios in their natural glow
curves, and identifying the group by measuring the mean-life, an
approximate age can be determined for 'finds' (at least for the
high group) by using Figure IV.2 as a calibration curve. Some
natural glow curves of finds are presented in Figure IV.4 and
details of their thermoluminescence are given in Table IV.2. It
can be seen from the glow curves that Plainview, Dimmitt and
Calliham are appreciably younger than the others since they have
intense LT. The ages derived by this method are listed in Table IV.3.

The major uncertainty in this approach is that the specimens
show widely differing degrees of weathering. For example Plainview
appears relatively fresh whereas Potter is considerably weathered;
Calliham, with its high LT, is also badly weathered. To investigate
this further we placed a piece of the Barwell meteorite on damp
filter paper for two weeks. After this treatment it had acquired
localised rusting but not an overall brown colouration. This
sample, together with a piece that had been kept dry, were prepared
in the same manner for TL measurement and the glow curves
produced. As expected the TL from the rusted specimen had
dropped (Figure IV.5). Furthermore, the peak height ratio was

clearly different, being 7.7 for rusted specimens compared with

9.2 for fresh specimens. That is, the meteorite that had been

allowed to rust appeared younger on the basis of its peak height

ratio. The obscuration appears to be a selective filtering

effect, varying with the wavelength of the TL peak. Valladas

and Lalou (1973) have recently shown that LT and HT have different

colou. luminescence. Therefore, use of the peak height ratio

to date a meteorite is not considered reliable.

IV.5   Irradiation

  IV.5a   Natural Equivalent Dose

The use of TL to date the firing of ancient pottery is

well established. The radiation dose that is present in the

sample is determined by TL, and if the rate at which that dose

has built up is known, then the time required for the buildup

(i.e. the pot's age) can readily be calculated. In the

determination of the terrestrial age of a meteorite one is

concerned with the rate at which TL is fading, rather than

building up, but the concept of equivalent dose (i.e. the dose

equivalent to a certain TL) may still be useful in overcoming

the weathering problem.

The natural equivalent dose may be determined for HT, and

since HT is fading very slowly this will approximate to the

equivalent dose in the meteorite at its time of fall. If this

dose, therefore, is given to the meteorite sample the height of

LT at the time of fall can be measured. This may then be

compared with the present height of LT and, since its half-life

is known, the terrestrial age of the specimen readily calculated
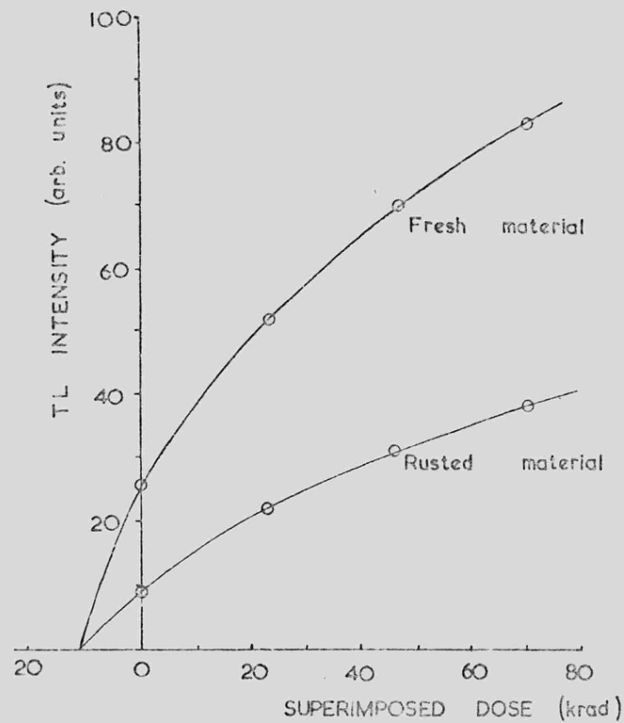
Figure IV.5 The effect of rusting on the dose curve. Both curves are for the Barwell meteorite. The rusted specimen was produced by being left on a wet filter paper for two weeks.
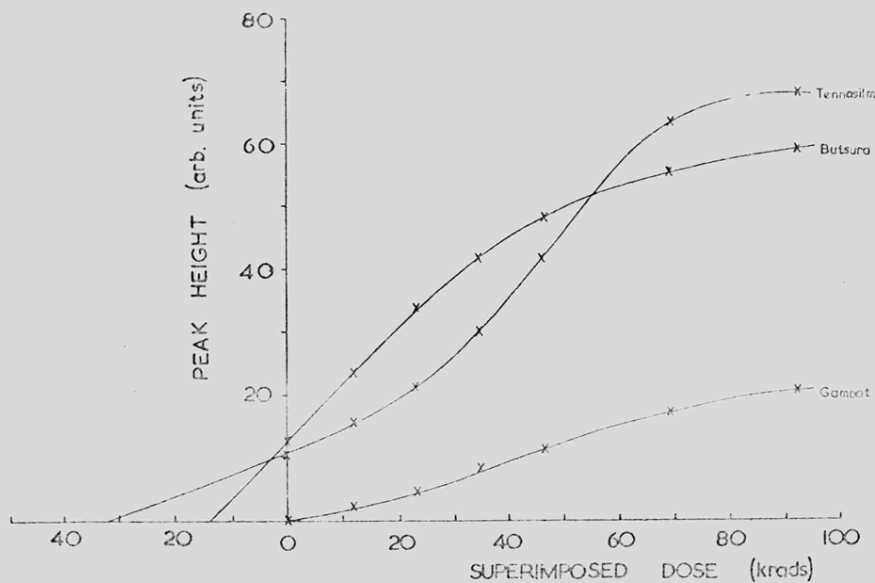
Figure IV.6 Dose curves (peak height vs. superimposed dose) for LT for various meteorites. Tennasilm shows abnormally bad supralinearity like Gambat, but most have curves in which the slope is initially linear like Butsura.

from the formula for first order decay

$$1 = 1_i \exp(-t/\tau')$$

where 1 is the present height, 1_i the initial height, t the
terrestrial age and τ' the mean-life. This method therefore
determines terrestrial age from the decay of LT, using HT to
measr its initial height. The effect of weathering on the
proce ire can be assessed by measuring the natural equivalent
dose of weathered and fresh material from the same meteorite.
This is done by extrapolating to zero TL the peak height vs.
superimposed dose curve (known for simplicity as the dose curve).
Figure IV.5 presents the dose curves for the fresh and rusted
Barwell powders mentioned above. It is clear that despite the
drop in intensity due to obscuration by limonite the same dose
value is obtained. In fact the percentage drop in the intensity
of LT for all doses is very similar (about one third). This
procedure for determining terrestrial age should not be affected
by the extent of weathering.

IV.5b   Saturation

The height of a peak does not increase indefinitely with
increased dose but reaches a plateau. At this dose the TL of the
meteorite is said to be saturated. Valladas and Lalou (1973)
pointed out that the Saint-Séverin meteorite was saturated when
it was in space, since if its natural equivalent dose was given
to LT its peak height would be on the plateau. TL could not
therefore be used to determine the meteorite's cosmic ray
exposure age. We see from Table IV.1 that the same is true for
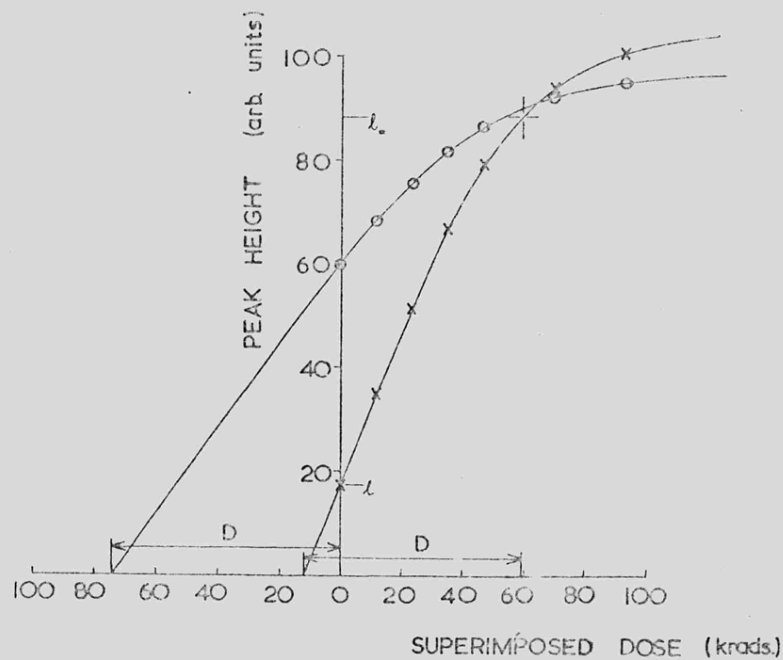
Figure IV.7 Dose curves (peak height vs. superimposed dose) for the Soko Banja meteorite showing the determination of l_o. Crosses denote heights of LT, circles represent heights of HT times twenty.
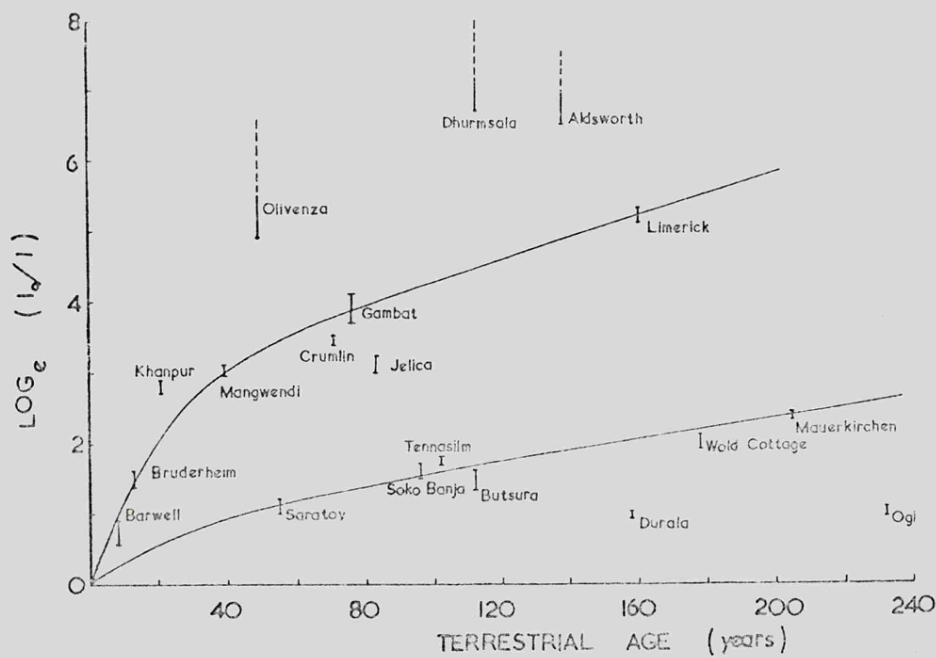
Figure IV.8 Natural log. of l_o/l_{LT} as a function of terrestrial age.

Table IV.3

The Terrestrial ages of stony meteorites in

Table IV.2 as determined by two thermoluminescence methods

Meteorite	Age in Years	
	Peak height ratio	From $\log_e(l_o/l_{it})$
Plainview	135 - 145	225 - 300
Calliham	170 - 210	350 - 400
Etter	300	350
Potter	-	300
Bluff	-	200
Dimmitt	140 - 170	280 - 330
Shields	300	500
Wellman (c)	300	350

Table IV.4

Thermoluminescence ages of stony meteorites compared with radiocarbon ages

Meteorite	TL age (years)	Radiocarbon age (years)	Ref.
Plainview	225 - 300	$\leqslant 2000$	a
		$\leqslant 3800$	b
Calliham	350 - 400	-	
Etter	$\geqslant 350$	-	
Potter	$\geqslant 300$	$\geqslant 20,000$	a
		$\geqslant 21,000$	b
Bluff	$\geqslant 200$	1300 - 6500	c
Dimmitt	280 - 300	0 - 4000	a
		1200 - 6400	c
Shields	$\geqslant 500$	-	
Wellman (c)	$\geqslant 350$		

References:

a.   Suess and Wänke (1962)

b.   Goel and Kohman (1962)

c.   Boeckl (1972)

9 of our meteorites. The fact that only 3 out of 11 meteorites
in the low retentivity class are similarly saturated is consistent
with the mean-lives determined here; the low group meteorites
would drain faster in space and require a higher dose rate to
maintain saturation.

However, for our purposes it is advantageous for the
mete .te to be saturated. The height of LT at the time of fall
can b. more accurately measured since it is less dependent on
dose. This point will be discussed later when accuracy is
considered.

IV.5c   Supralinear Dose Curves and l_o

A few dose curves for the meteorites listed in Table IV.1
were supralinear (Figure IV.6). This is an effect of extra peaks
below $200^{o}C$ in the glow curve. In fact it is not a single peak
that is being measured, but the resultant of overlap between two
or perhaps three curves (see Section III.5). The height obtained
by giving LT the natural equivalent dose is not therefore
necessarily equal to the initial height of LT. The height,
referred to as l_o, is however a measure of this value, and it can
be related to terrestrial age by the use of calibration curves
derived from falls.

IV.6   Terrestrial age by dose curves

The determination of l_o therefore requires measurement of
the natural equivalent dose, and then giving this dose to LT to
restore it to its nominal initial level. However, using the
following technique, these two operations can be performed at the

same time and the need for previously drained material avoided –
since this introduces poorly understood complications. Various
doses of radiation are given *aliquots* to the powdered meteorite sample
and the dose curves drawn for each of the two peaks (Figure IV.7).
By extrapolating back the HT line to zero TL the initial dose may
be found. The height of LT equivalent to this dose (l_o) may then
be determined from the LT line after it too has been extrapolated
back to zero TL.

The values of l_o determined in this way are listed in
Table IV.1 (falls) and Table IV.2 (finds). The calibration
curves, $\log_e(l_o/l)$ vs. terrestrial age, may then be determined
from the falls (Figure IV.8) and the terrestrial ages of the finds
measured from it (Table IV.3).

IV.7   Accuracy and sources of error

The measurement of peak height is complicated by the fact
that many peaks are present and these usually overlap. However,
this should not affect the results because the additional peaks
result from the same mineral as the $120^\circ C$ peak and are present in
both falls and finds.   The curves derived from falls therefore
include any effects from these extra peaks. However, this may
not be true of extra peaks at higher temperatures than LT. In
achondrites (Figure III.5) and in lunar samples (Figure III.6)
there is a peak at $260^\circ C$ which may be confused with LT if it were
to occur in chondrites. Only one of our 28 samples has a peak at
$260^\circ C$; namely Potter, which is also the most highly weathered
meteorite. Overlap may move LT from $200^\circ C$, (e.g. Barwell) to
$235^\circ C$ (e.g. Limerick) as illustrated in Figure III.8. However,

confusion with a possible peak at $260^\circ C$ may be avoided by careful observation of the temperature of LT.

The error bars on the l_o/l_{LT} values in Figure IV.8 were determined from the measurement of l_o and l_{LT}. The error in l_{LT} was determined from duplicate curves where the repeatability was about 5%. l_o usually contains greater error as it is determined from ᵗʰe dose curves, Figure IV.5. It is governed by the accuracy by which lines may be extrapolated to zero height to find the natural equivalent dose. For saturated meteorites, where the natural dose was on the plateau of the peak height vs. dose curve, l_o may be determined very accurately, (say within 10%).

The error bars have been slightly underestimated since there is another source of error which cannot be determined, namely the different terrestrial histories of the meteorites. The major component will be the temperature at which the meteorites have been kept, since the decay is temperature sensitive. The effect is probably less for meteorites in the high group because of their longer mean-lives. Six of the eight high group meteorites fall on or very near the line and we think, therefore, that it is reasonable. Ogi displays anomalously high present TL in both Figure IV.1 and Figure IV.8. Abnormal histories e.g. heating on a hot-plate during cutting procedures, may account for the remaining discrepancies. The scatter of the low group may be caused by additional factors (e.g. shock), but clearly the use of TL to determine accurate terrestrial ages for this group will be difficult. To allow for finds that have suffered appreciably different temperatures we have made a generous allowance for the scatter on the curves in determining the age ranges in our results

(Table IV.3).

IV.8   Discussion and conclusions

The only method for determining the terrestrial age of
stony meteorites, prior to that investigated here, utilises the
decay of carbon-14. It is applicable only to ages exceeding a
few thousand years, because the half-life of carbon-14 is 570
years and the initial value for the abundance of the decaying
isotope is not known directly. TL makes available a method for
the few-hundred-year range for certain meteorites, and enables a
lower limit to be established for others.

Dimmitt, Plainview, Potter and Bluff have been dated by
the carbon-14 method, and the values obtained are compared with
those from TL in Table IV.4. Plainview is an interesting case
since a fireball was seen and a stone recovered in 1902/1903
(Nininger, 1952). However, at least two more finds have been made
in the Plainview area, and it is not certain which belongs to the
observed fireball. Our results suggest that the Plainview stone
we examined (Plainview, 1917) was not associated with the 1902/
1903 fireball.

The carbon-14 method has produced two surprising results
of terrestrial ages in excess of 10,000 years, i.e. Potter and
Woodward County (Goel and Kohman, 1962; Suess and Wänke, 1962).
Boeckl (1972) found the average result for 19 terrestrial age
determinations to be about 5000 years. The results presented here
show that, although terrestrial ages of the order of a few thousand
years may be common, a significant number can also fall in the
few hundred year range.

CHAPTER V

METEORITE FINDS

V.1   Introduction

Terrestrial age determinations have a wide variety of

applications. They enable members of the same fall to be

iden`ified, and when found in old tombs (e.g. the Hopewell M ..)

they ..able an upper estimate to be placed on the age of the ....

One of the more entertaining types of study made on the basis of

terrestrial age determinations correlates meteorite finds with

documented accounts of fireball sightings (e.g. Plainview).

However, the most useful results are those obtained from a

comparison of terrestrial ages with the currently observed influx

rate of meteorites. This will be the topic of Section V.4 of

this chapter. The rest of the chapter reviews the subject of

meteorite finds. This will be done from two aspects: the

terrestrial age results obtained by radioactive and TL methods

(Section V.2), and the geographical distribution of finds (Section

V.3).

V.2   Terrestrial age results

No single age method provides a unique answer for all

meteorites; for example the TL method gives answers for only 3

out of 9 meteorites which have been investigated. It is therefore

necessary to consider in some detail the results obtained by other

methods, and for the sake of completeness we will include irons.

The first terrestrial age results were reviewed by Anders

(1963). The only method suitable for stones, besides TL, utilises

the decay of carbon-14 ($t_{\frac{1}{2}}$ = 5760 years). This has been applied

by Goel and Kohman (1960) and Suess and Wänke (1960), and more

recently by Boeckl (1972). Its obvious drawback is that it is

suitable only for ages between 5000 and about 20,000 years. So

far only one stony meteorite has proved too old, but many are too

young to be successfully dated by this method. The initial iron

results were very disappointing. The first method to be attempted

was the decay of ^{39}Ar ($t_{\frac{1}{2}}$ = 269 years), but very few meteorites

were found to contain the isotope, and only minimum ages were

obtainable. Recently even these have been thrown into doubt with

the realisation that the ^{39}Ar content must vary considerably

during one orbit about the Sun (Begemann,1972). The abundance of

the isotope in the meteorite is therefore governed by the point

at which it intercepted the Earth's orbit, and consequently will

be highly variable from meteorite to meteorite. More recently

^{10}Be decay ($t_{\frac{1}{2}}$ = 2.7 million years) has been applied to the

determination of the terrestrial age of irons with rather more

success. It is applicable to ages between 10^5 and about 5×10^6

years, and a sizeable proportion of irons appear to fall in this

range. The major uncertainty with any radioactive method is the

value for the original abundance of the decaying isotope, which

must be determined from falls. It is known with poor accuracy

since few determinations have been made, and is usually highly

variable because of the unknown effects of shielding. To some

extent this is overcome by expressing the abundance of the

decaying isotope as a ratio to another spallation-produced

isotope, ^{36}Cl.

Results for the terrestrial ages of stones and irons

taken from the literature are given in Table V.1 and in Figure V.1.

Terrestrial ages for iron meteorites determined by the ^{39}Ar

method are included only where there is nothing better. The

values for the terrestrial ages of stony-irons are also very

approximate and those determined from ^{36}Cl "must be regarded with

extreme caution" (Begemann & Vilcsek, 1969).

The terrestrial ages of stony meteorites concentrate

between zero and 10,000 years with a bias towards low values.

Many of the results are not significantly greater than zero.

Boeckl (1972) gave an average of 5000 years, but the errors are

such that this can only indicate an order of magnitude. The

present TL results indicate that although terrestrial ages in the

order of a few thousand years may be common, a significant number

may fall in the few-hundred-year age range. A typical terrestrial

age for stony meteorites may be said to be a few thousand years.

Twenty-nine of thirty-nine iron meteorites fall within the

range of the ^{10}Be method, and show an average age of 0.6 million

years. Three meteorites have ages beyond the range of the method,

and eight have ages insufficient to be measured by ^{10}Be decay

(less than 10^5 years). Unfortunately, the latter are frequently

still too high for the ^{39}Ar method (greater than 10^3 years).

If one assumes an age of 10^4 years for these meteorites the average

becomes 0.4 million years: this value may be considered the

typical terrestrial age of an iron find.
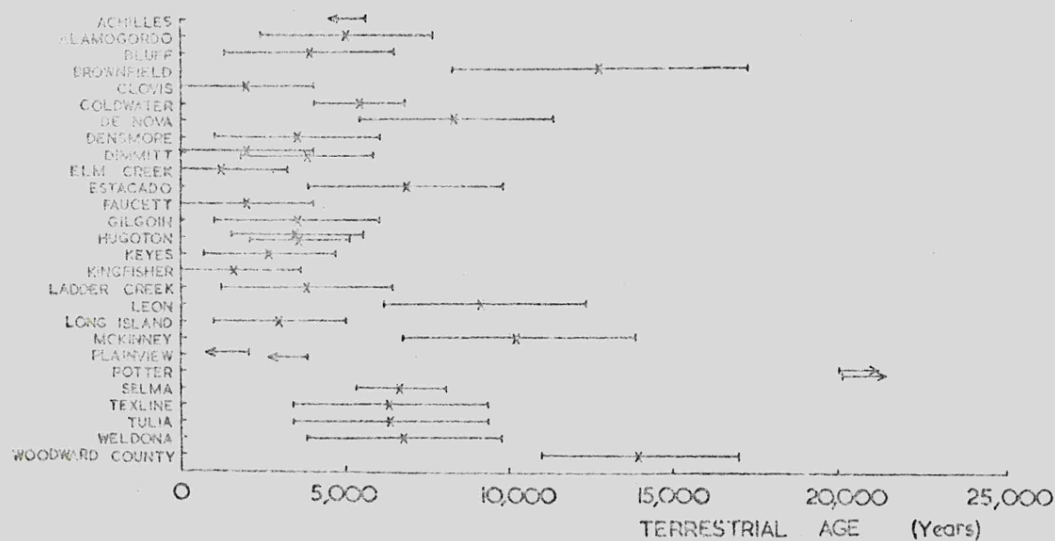
Figure V.1a The terrestrial ages of 27 stony meteorites.
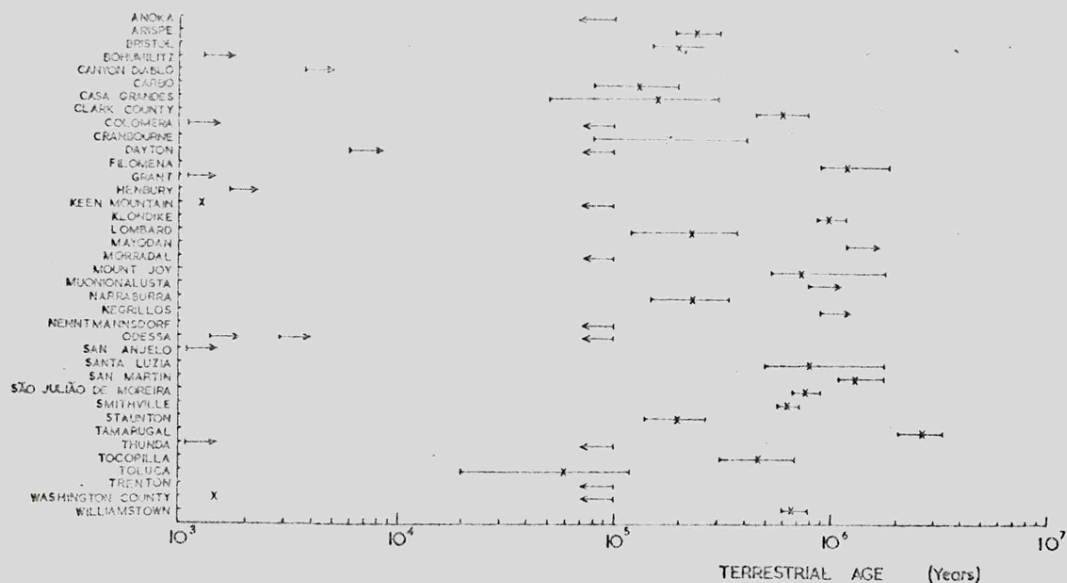
Figure V.1b The terrestrial ages of 38 iron meteorites.
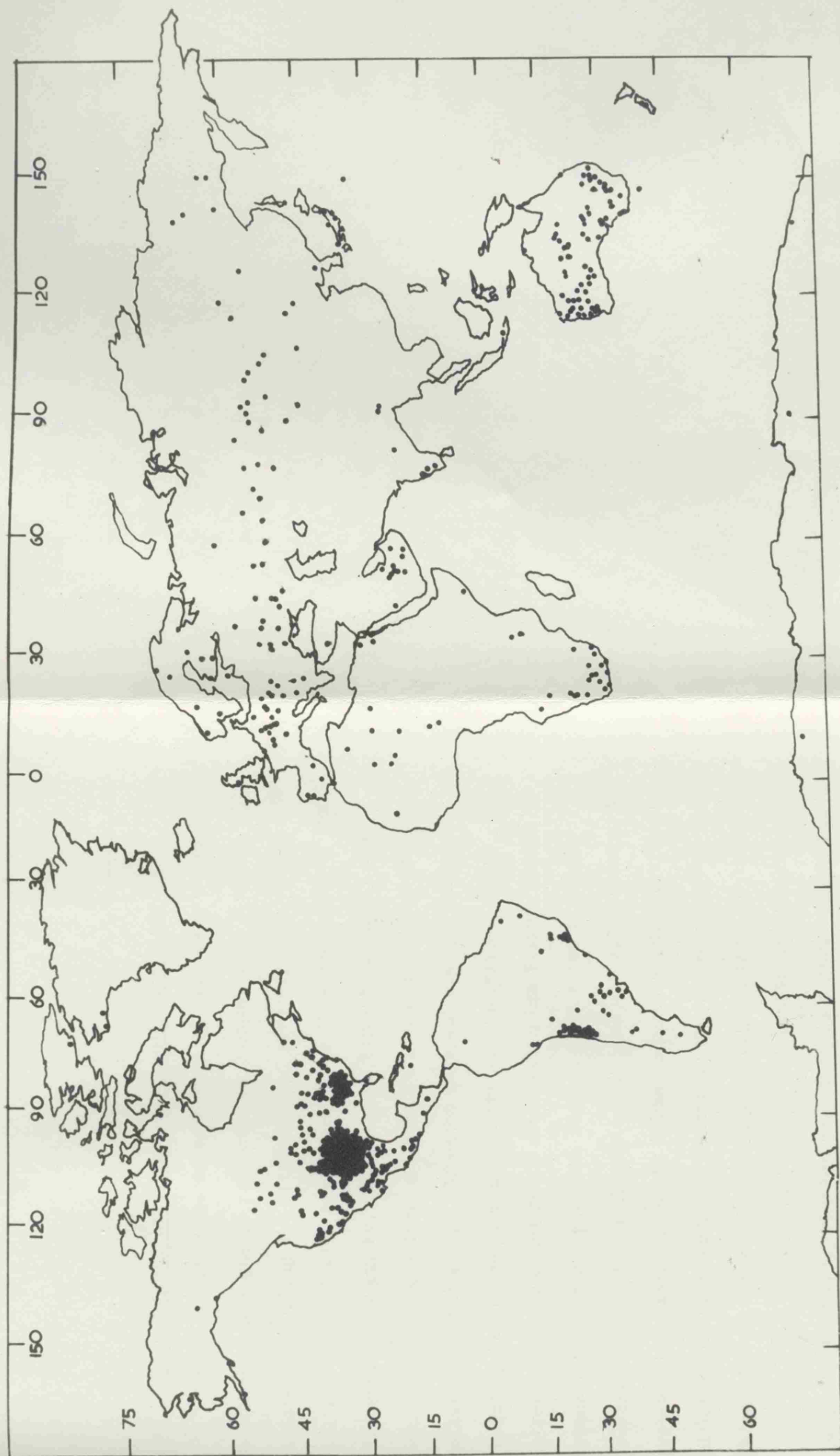
Figure V.2 World-wide distribution of the meteorite finds
listed in the "Catalogue of Meteorites"(Hey, 1966).

V.3   Geographical distribution of meteorite finds

A map showing the distribution of all finds listed in the Hey (1966) catalogue is presented as Figure V.2. A number of factors controlling the efficiency of recovery are evident. They will not be dealt with here however, as they have already been discussed at length by, for example, Farrington (1915) and Krinov (1960). The line of finds following the Trans-Siberian railway is interesting. Of major interest are the number of "high" spots in the surface density of meteorites. Stony meteorites are comparatively abundant in the Prairie states because of the history of the region. Its climate favours preservation and the soil colour and land use aid recovery, but probably the major factor is sudden intensive inhabitation and ploughing after thousands of years as grassland. Another minor "high" for stones is Australia, probably for much the same reason.

A highly localised "high spot" within the Prairie states is Roosevelt County, New Mexico. This is a region which has been intensively searched as it provides conditions which are ideal for meteorite finding. The County is rich in "blowouts" - areas in which the soil has been blown away to expose bedrock. Meteorites therefore tend to concentrate on the exposed bedrock, and Huss chose this area for intensive publicity and searching. Ninety-nine specimens, mainly common chondrites (no irons), of total weight 45.2 kg have been recovered from 2300 acres of Roosevelt County (Huss and Wilson, 1973). This indicates a surface density of meteorite material of 4.8 kg km^{-2} and, assuming the peak meteorite influx for the United States is 1.88×10^{-5} kg/km^2/year (Hawkins, 1960), this would require 2.6×10^5 years to accumulate. This

value is well above typical terrestrial ages for other stony
meteorites from the Prairie states, and indicates either:

    i)   Hawkins' (1960) estimate of the peak influx of

          meteorites is too <u>low</u>.

or,   ii)   Roosevelt County is atypical in the rate at which

          meteorites have fallen. (It would require only one

          really large fall to have occurred in this region to

          upset the statistics).

or,   iii) Meteorites are preserved longer in Roosevelt County

          than in the Prairie states. This is possibly true

          since New Mexico is particularly dry and desert-like.

Finally, and most probably,

    iv)   because the blowouts have concentrated meteorites the

          mean age of meteorites recovered in this region is

          higher than elsewhere in the Prairie states.

Irons have three well-known "highs", and 36% of the
world's finds of iron meteorites come from them (Chang and Wänke,
1969). These are the Arizona desert (for the obvious reason that
finds there are associated with the Barringer Crater), the
Appalachian Mountains and North Chile. At the beginning of the
century it was believed that Mountains physically attracted iron
meteorites (Farrington, 1915), but the explanation that it is
climatic factors which favour preservation of irons rather than
stones sounds more reasonable.

The Chilean iron meteorites, in particular the hexahedrites,
have been the subject of much debate (Fletcher, 1888; Henderson,
1941; Wasson and Goldstein, 1968). Hexahedrites are not
particularly common. Outside Chile 38 have been found and six

seen to fall. It seems remarkable that more than one should have

fallen on the Atacama desert, yet no less than 16 specimens have

been found. Henderson (1941) showed that they have identical

iron, nickel, cobalt and phosphorus content - but that this was

also true for hexahedrites from all over the world. He came to

the conclusion that "most, but perhaps not all, of these are

relat d to a single shower". Wasson and Goldstein (1968) requi

that a minimum of four falls were needed to explain their Ir

content. They went on to show that it was statistically plausible

for this number of hexahedrites to fall in Chile assuming a world-

wide random distribution. Perhaps it is in order to quote from

Fletcher (1888) at this point:

> "Owing to the composite structure of meteorites various
> parts of the same mass present different characters;
> and where the structure is a coarse one there may be a
> difficulty in recognising two fragments as having
> originally belonged to a single specimen. If allowance
> be not made for possible differences in part of a large
> mass, or in the individuals of a meteorite shower, it
> may thus be wrongly inferred that specimens due to a
> single meteor belong to different falls. A good
> illustration of this difficulty is presented by the
> masses which have been named Jewel Hill and Dual Hill
> respectively, the former known since 1854 and the
> latter since 1873. These are placed in two widely
> different groups by Brezina, than whom we can wish for
> no better judge of their structure as revealed by
> etching. Yet it now appears that the difference in
> locality is merely one of spelling, and the two masses
> were found only a mile apart; it is impossible to
> believe that they can have been projected against the
> same part of the same hill at different times; and
> such being the case we can scarcely rely on etching
> figures as a certain method of distinction."

We may add that what is true of metallographic techniques at the

end of the last century may well be true of trace element

techniques now. If brecciation takes no heed of structure, why

should material of varying trace element composition be prevented

from becoming brecciated? Brecciated hexhedrites and octahedrites have been discovered among the Chilean irons. The concentration on the ground of these iron meteorites in north Chile suggests that a few major falls have occurred. The terrestrial ages of Filomena ($12 \pm 5 \times 10^5$ years), Negrillos (greater than 9×10^5 years), San Martin ($13 \pm {}^{5}_{3} \times 10^5$ years) and possibly Tocopilla ($4.7 \pm {}^{2.7}_{1.6} \times 10^5$ years) are not sufficiently different to prove these meteorites to be members of different falls. The octahedrite Tamarugal is the only north Chilean iron whose terrestrial age is known to be appreciably different ($27 \pm {}^{6}_{5} \times 10^5$ years).

V.4   Influx rate and efficiency of recovery

From these results it is possible to estimate the efficiency of recovery of meteorites as finds, assuming that the meteorite influx derived from observed falls is correct (Hawkins, 1960; Brown, 1960). Conversely it is possible, assuming likely efficiencies of recovery, to derive a meteorite influx rate and compare it with the Hawkins/Brown statistics.

The surface density of finds can be calculated from compilations in Hey (1966) or Mason (1962). Hawkins' meteorite flux equation

$$N = N_o - \log m$$

where N is the number of meteorites falling per unit area per unit time of mass equal to or greater than m, and N_o is a constant, can be written

$$\frac{n}{A \, T \, f} = N_o - \log m$$

in which n is the number of finds over an area A with typical

terrestrial age T, and β is the efficiency of recovery. The
latter is dependent on many factors; for example population,
soil use, soil colour, climate and the history of the region.
For the equation to be meaningful a large n is desired: the
value obtained for β must therefore be an optimum one. An
area must therefore be chosen which includes the locations of a
large number of finds of measured terrestrial age.

We will adopt the Prairie states as an area representative
of the optimum conditions for stony meteorite recovery, and the
Appalachian Mountains as the equivalent for iron meteorites. The
expected ages calculated from the equation for various
efficiencies of recovery are listed in Table V.2. These are the
terrestrial ages one would expect for meteorites from the two
localities, assuming the Hawkins/Brown influx statistics are
correct. It can be seen that the typical terrestrial ages
determined experimentally are only in agreement with the influx
statistics if one assumes an extremely low efficiency of recovery
for both irons and stones. It is almost easier to believe that
the influx statistics are wrong than the efficiency of recovery
in the Prairie states is less than $\frac{1}{2}\%$. But this is obviously a
subjective evaluation and some other guide-lines are required.

V.5   Summary and Conclusions

It is possible to calculate expected typical terrestrial
ages knowing the number of meteorites found in a certain area
and the observed rate of fall. The area chosen for such an
exercise must contain a large number of specimens, since this is
essentially a statistical treatment, and it must be an area for

which terrestrial ages are known. It must not be one in which

the number of finds is high because óf one or two really large

falls (e.g. the irons found in Arizona and Chile). It is thought

that representative regions for this purpose are the Prairie

states (stones) and the Appalachian Mountains (irons). Assuming

the meteorite influx statistics of Hawkins (1960), which for our

purposes agree well with those of Brown (1960), the efficiency

with which finds are recovered in these areas appears to be

extremely low (less than $\frac{1}{2}\%$). It is possible, however, that the

efficiency is higher and that the influx rate is lower.

Table V.1

The Terrestrial Ages of Meteorites

Irons

Meteorite	Class	Method	Age in Years	Ref.
ANOKA 1961, Minnesota	Of	^{10}Be	$<10^5$	b
ARISPE 1896, Mexico	Ogg	^{10}Be	$2.4 \, ^{+.6}_{-.5} \times 10^5$	b
BRISTOL 1937, Tennessee	Of	^{10}Be	$2.0 \, ^{+.6}_{-.5} \times 10^5$	b
BOHUMILITZ 1829, Bohemia	Om	^{39}Ar	$\gtrsim 1300$	a
CANYON DIABLO 1891, Arizona	Og	^{39}Ar	$\gtrsim 2700$	a
CARBO 1923, Mexico	Om	^{10}Be	$1.3 \, ^{+.7}_{-.5} \times 10^5$	b
CASA GRANDES 1867, Mexico	Om	^{10}Be	$1.6 \, ^{+1.4}_{-1.1} \times 10^5$	b
CLARK COUNTY pre 1937, Kentucky	Om	^{10}Be	$6.0 \, ^{+2.0}_{-1.5} \times 10^5$	b
COLOMERA 1912, Spain	Om*	^{10}Be	$<10^5$	b
		^{39}Ar	$\gtrsim 1100$	a
CRANBOURNE 1854, Victoria	Og	^{10}Be	$1.8 \, ^{+2.3}_{-1.0} \times 10^5$	b
DAYTON 1892/1893, Ohio	D	^{39}Ar	$<10^5$	b
		^{39}Ar	$\lesssim 1600$	a
FILOMENA pre 1941, Chile	H	^{10}Be	$12 \, ^{+7}_{-3} \times 10^5$	b
GRANT 1929, New Mexico	Of	^{39}Ar	$\gtrsim 1900$	a
HENBURY 1931, Central Australia	Om	^{39}Ar	$\gtrsim 1700$	a
KEEN MOUNTAIN 1950, Virginia	H	^{10}Be	$<10^5$	b
		^{39}Ar	1290	a
KLONDIKE 1901, Canada	D	^{10}Be	$9.8 \, ^{+2.1}_{-1.4} \times 10^5$	

Table V.1 (Continued)

Meteorite	Class	Method	Age in Years	Ref.
LOMBARD 1953, Montana	H	^{10}Be	$2.3 \, ^{+1.5}_{-1.1} \times 10^5$	b
MAYODAN 1920, North Carolina	H	^{10}Be	$>12 \times 10^5$	b
MORRADAL 1892, Norway	D	^{10}Be	$<10^5$	b
MOUNT JOY 1887, Pennsylvania	H	^{10}Be	$7.3 \, ^{+3.5}_{-2.0} \times 10^5$	b
MUONIONALUSTA 1906, Sweden	Of	^{10}Be	$>8 \times 10^5$	b
NARRABURRA 1855, New South Wales	Of	^{10}Be	$2.3 \, ^{+1.1}_{-.8} \times 10^5$	b
NEGRILLOS pre 1936, Chile	H	^{10}Be	9×10^5	b
NENNTMANNSDORF 1872, Germany	H	^{10}Be	$< 10^5$	b
ODESSA (IRON) pre 1922, Texas	Ogg	^{10}Be	$<10^5$	b
		^{39}Ar	> 2900	a
		^{39}Ar	> 1400	a
SAN ANGELO 1897, Texas	Om	^{39}Ar	> 1100	a
SANTA LUZIA 1921, Brazil	Ogg	^{10}Be	$8 \, ^{+10}_{-3} \times 10^5$	b
SAN MARTIN pre 1924, Chile	H	^{10}Be	$13 \, ^{+5}_{-2} \times 10^5$	b
SAO JULIAO DE MOREIRA pre 1883, Portugal	Ogg	^{10}Be	$7.7 \, ^{+1.3}_{-1.0} \times 10^5$	b
SMITHVILLE 1840, Tennessee	Og	^{10}Be	$6.3 \, ^{+.9}_{-.6} \times 10^5$	b
STAUNTON 1858-59, Virginia	Om	^{10}Be	$2.0 \, ^{+.7}_{-.6} \times 10^5$	b
TAMARUGAL 1903, Chile	Om	^{10}Be	$27 \, ^{+6}_{-} \times 10^5$	b
THUNDA 1881, Queensland	Om	^{10}Be	$<10^5$	b
		^{39}Ar	> 1100	a

Table V.1 (Continued)

Meteorite	Class	Method	Age in Years	Ref.
TOCOPILLA 1927, Chile	H	^{10}Be	$4.7 \, ^{+2.1}_{-1.6} \times 10^5$	b
TOLUCA pre 1776, Mexico	Om	^{10}Be	$0.6 \, ^{+.6}_{-.4} \times 10^5$	b
TRENTON 1858, Wisconsin	Om	^{10}Be	$<10^5$	b
WASHINGTON COUNTY 1892, Kentucky	D	^{10}Be	$<10^5$	b
		^{39}Ar	1400	a
WILLIAMSTOWN 1892, Kentucky	Om	^{10}Be	$6.6 \, ^{+1.2}_{-.6} \times 10^5$	b

References:

a.   Anders (1963) and references therein.

b.   Chang and Wänke (1969) assuming $(^{36}Cl/^{10}Be)_{orig.}$

= 4.3 $\pm$ 0.4 (average of 5 falls).

Stony-Irons (Begemann & Vilcsek, 1969)

Meteorite	Class	Method	Age in Years
BENCUBBIN II 1930, Western Australia	M	^{39}Ar	460 $\pm$ 50
CLOVER SPRINGS 1954, Arizona	M	^{39}Ar	800 $\pm$ 300
CRAB ORCHARD 1887, Tennessee	M	^{36}Cl	130,000*
MINCY 1857, Missouri	M	^{36}Cl	90,000*
MORRISTOWN 1887, Tennessee	M	^{39}Ar	750 $\pm$ 250
VACA MEURTA 1861, Chile	M	^{36}Cl	240,000*

*   no argon detectable, assume $^{36}Cl_{orig.}$ = 23.6 dpm/kg,

others assume $(^{39}Ar/^{36}Cl)_{orig.}$ = 1.1 (average of 6 falls).

Table V.1 (Continued)

Stones (All ^{14}C)

Meteorite	Class	Age in Years	Ref.
ACHILLES 1924, Kansas	H	≮5600	a
ALAMAGORDO 1938, New Mexico	H5	5000 ± 2600	b
BLUFF 1878, Texas	L5	3900 ± 2600	b
BROWNFIELD 1937, Texas	H3	12,700 ± 4500	b
CLOVIS 1961, New Mexico	H3 or H6	2000 ± 2000	b
COLDWATER 1924, Kansas	H5	5400 ± 1400	a
DE NOVA 1940, Colorado	L	8300 ± 3000	b
DENSMORE 1879, Kansas	L6	3500 ± 2500	b
DIMMITT 1947, Texas	H3 or 4	2000 ± 2000	c
		3800 ± 2600	b
ELM CREEK 1906, Kansas	H4	1200 ± 2000	b
ESTACADO 1883, Texas	H6	6800 ± 3000	b
FAUCETT 1966, Missouri		2000 ± 2000	b
GILGOIN 1889, New South Wales	H5	3500 ± 2500	b
HUGOTON 1927, Kansas	H5	3500 ± 2000	c
		3600 ± 1500	a
KEYES 1939, Oklahoma	L6	2700 ± 2000	b
KINGFISHER 1950, Oklahoma	L	1600 ± 2000	b
LADDER CREEK 1937, Kansas	L6	3800 ± 2600	b
LEON, Kansas		9200 ± 3100	b
LONG ISLAND 1891, Kansas	L	3000 ± 2000	c
McKINNEY 1870, Texas	L4	10,200 ± 3500	b
PLAINVIEW 1917, Texas	H5	≮2000	c
		≮3800	a

Table V.1 (Continued)

Meteorite	Class	Age in Years	Ref.
POTTER 1941, Nebraska	L6	≽20,000	c
		≽21,000	a
SELMA 1906, Alabama	H4	6700 ± 1400	a
TEXLINE 1937, Texas	H	6400 ± 3000	b
TULIA 1917, Texas	H5	6400 ± 3000	b
WELDONA 1934, Colorado	H	6800 ± 3000	b
WOODWARD COUNTY pre 1933, Oklahoma	H	14,000 ± 3000	c

References:

a. Goel and Kohman (1962) assuming 65 ± 10 dpm/kg (average of 8 falls).

b. Boeckl (1972) assuming 57.3 dpm/kg (average of 4 falls).

c. Suess and Wänke (1960) assuming 48.2 kpm/kg (average of 7 falls).

Table V.2

Terrestrial ages expected from the observed surface

density and fall rate of meteorites

Expected age in years

Percent recovered	Stones (Prairie states)	Irons (Appalachian Mountains)
0.5	2,600	31,400
1	1,320	15,700
2	661	7,850
5	265	3,140
10	105	1,540
15	88.3	1,050
20	53.8	785

CHAPTER VI

THE FUSION CRUST

VI.1   Introduction

The rest of this thesis concerns the application of
thermoluminescence to investigation of the phases of a meteorite's
history immediately preceding its arrival on Earth, i.e. the
temperature gradients produced during atmospheric passage, and
its pre-atmospheric size and shape. These applications are largely
new, and require a cautious approach. A useful check is provided
by studies of the fusion crust, which bears testimony to both the
temperature gradients experienced and, possibly, the amount of
mass removed from the meteoroid by its atmospheric passage. It
therefore forms the subject of this chapter, certain sections of
which have already been published (Sears and Mills, 1973; Sears,
1974a). Study of the fusion crust has yet to become a recognised
subject within meteoritics, it generally being discussed only
in passing, when describing a new meteorite. No extensive review
of the fusion crust has yet appeared, and mention will be made
here of as much of the highly fragmentary literature on this topic
as possible.

Studies on the fusion crust began with Tschermak and
Brezina, who defined the three zones of impregnation, absorption
and fusion (Tschermak, 1885). Borgstrom (1912) observed that the
innermost (impregnation) zone was troilite-rich, a finding we
have confirmed by point counting. Ramdohr (1967) has provided
the most comprehensive description of fusion crust mineralogy, and
numerous papers have appeared in Russia (Iudin, 1955; Iudin et al.,

1968; Kolomensky and Iudin, 1968) confirming the overall

structure and placing on record the existence of many iron

oxides. This has been further discussed by Marvin (1963) who

had a part of a recovered satellite for comparison.

Morphological discussion of the fusion crust began with

Farrington's (1915) book. Nininger (1935a; 1935b; 1936a; 1936b;

1936c) published a series of papers on the surface features, which

he partially reviewed in his book "Out of the Sky" (1952). In

the nineteen-fifties Krinov made a close examination of the

surface structure and devised a system of face type classification

(Krinov, 1960). The use of the fine structure of the fusion crust

was proposed by Huss (1972, personal communication to Dr.

Hutchison) as a means of identifying members of the same fall as

he believed it to be characteristic of individual meteorites.

Chemical studies seem to have progressed at an even slower

rate. In 1802 Howard found that nickel was present in the crust,

as elsewhere in the meteorite. Meurnier (see Farrington, 1915

page 163) and Farrington (1910) performed analyses of the fusion

crust of two iron meteorites. In 1936 Henderson and Davis analysed

the crust of Moore County and, surprisingly, found an alkali.

metal enrichment. More recently Brownlee and Hodge (1973) and

Fechtig and co-workers (Fechtig and Utech, 1964; Elgoresy and

Fechtig, 1965) have applied electron-microprobe techniques to the

crust when evaluating methods for the recognition of cosmic dust.

The fusion crust has the potential to provide two kinds

of information. The surface morphology, when examined more

closely than the gross structures and flowmarks, gives valuable

information on the mode of ablation and the surface temperature.

The ablation rate, which governs the temperature gradient across

the fusion crust, can then be estimated from the dimensions of

the crust. Secondly, the internal structure of the crust may be

used to identify faces that were produced by fragmentation within

the final second of luminous flight. The main drawback of fusion

crust studies is, of course, that the crust we can examine is

that formed only at the end of luminous flight. We estimate that

the period of time involved in freezing the crust, and therefore

amenable to study in this way, is usually about one second.

However, it may be possible, when guided by the light curve, to

make reasonable judgments as to the behaviour of the meteorite at

higher altitudes.

VI.2   Surface morphology of the fusion crust

Mosaics were prepared from scanning electron microscope

photographs of several common chondrites, two of which are shown

as Figure VI.1. They enable an overall impression to be obtained

of the nature of the surface. Although to the naked eye all the

fusion crust specimens had the appearance of frontal surfaces,

at low magnification they were distinctly different. Of course,

the appearance of the surface, even at high magnification, is

governed to some extent by the orientation of the face. However

the similarities are such that it is possible to distinguish

meteorites in accordance with Huss' idea. More important for our

present purposes, though, is that all common chondrites show a

similar mode of crust formation; flow appears to be difficult,

and large irregular globules of molten material form only to be

removed before they can flow into one uniform layer. Sufficiently

Table VI.1

Surface temperatures of the fusion crust of meteorites

Class	Major minerals		Melting point in °C	Assumed surface temperature in °C
Common	Olivine	Mg	1890	
Chondrite		Fe	1481	
		Meteoritic	1680	
	Pyroxene	Mg	1554	1680
		Fe	1100	
Eucrite	Pyroxene	Mg	1554	
		Fe	1100	
		Meteoritic	1350	
		(pigeonite)		1500
	Plagioclase	Ca	1550	
		Na	1118	
		Meteoritic	1500	
Type III	Olivine	Mg	1890	
carbonaceous		Fe	1481	
chondrite	Chondrules		1890	
	(forsterite, 34 v/v %)			1600
	Matrix		1410	
	(50 % Fa, 57 v/v %)			

Sources: Krinov (1960) page 416;   Opik (1959) page 159;

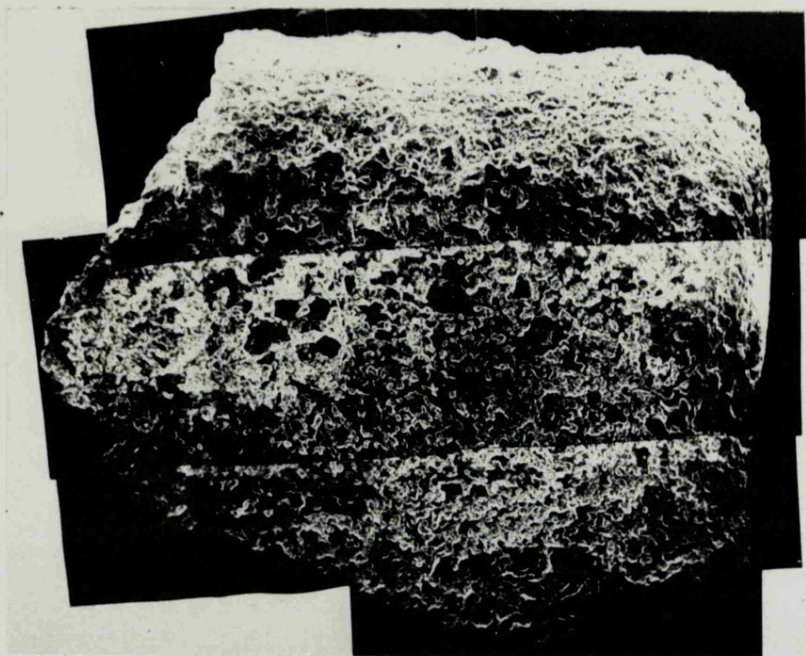Smith (1963) page 202;   Kracek and Clark (1966).

Figure VI.1a Mosaics of scanning electron microscope photographs of the fusion crust of the Holbrook meteorite. The specimen is about 4 mm square.
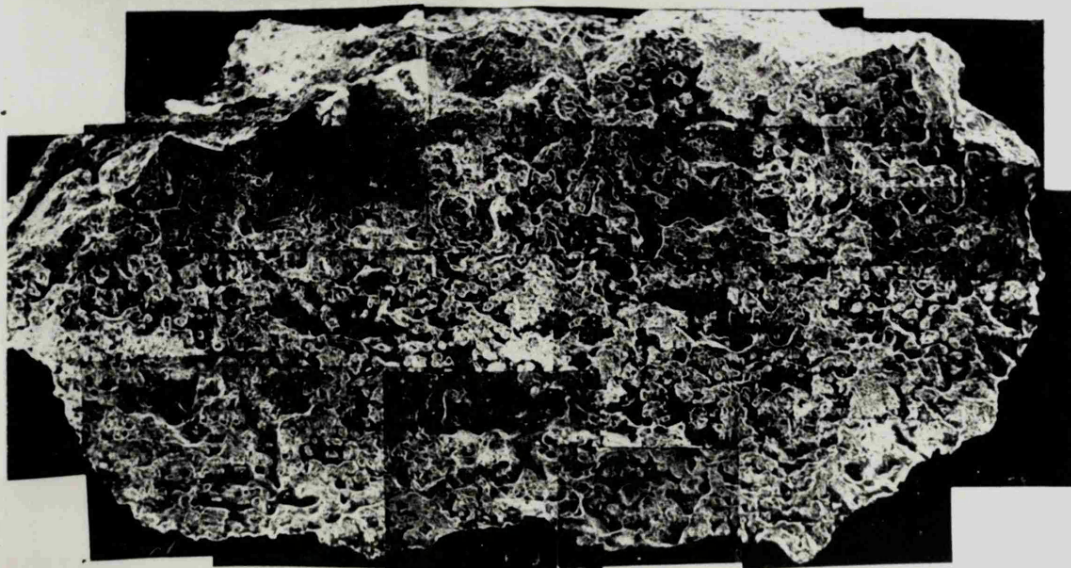

Figure VI.1b The fusion crust of the Limerick meteorite. The specimen is about 4 mm by 8 mm.

high temperatures for low-viscosity flow are not obtained, and

evaporation is the major ablation mechanism. This is in

agreement with the theoretical studies of Baldwin and Sheaffer

(1973) which indicate that stony meteorites of small and moderate

mass ablate mainly by evaporation.

The mode of ablation of the other groups of meteorite

appears to be appreciably different, common chondrites and

eucrites representing two extremes (Figure VI.2). The eucrites

possess a highly characteristic glossy black crust which is seen

in the S.E.M. to be a very smooth, highly uniform, glassy layer.

Bubbles in the crust are numerous and always spherical. In one

photograph, of the edge of the crust, conchoidal fractures are

visible. Liquid run-off was clearly the major ablation mechanism.

The "achondrite"[*] shows an intermediate mode of behaviour; a

uniform layer has just managed to form, but the bubbles in it

are irregular and only partial melting has been achieved. Both

modes of ablation probably occurred on this meteorite. The type

III carbonaceous chondrite might be expected to resemble the

ordinary chondrite since it is predominantly olivine, whereas in

fact the surface resembles a wholly melted tar, tending not to

form a uniform coating. It is a less viscous version of the crust

of the common chondrite.

An interesting additional feature was a cavity on the

fusion crust specimen from Limerick which was found to be lined

---

[*]   This is a meteorite of unknown identity that was acquired
by the Geology Department in 1973 (acq. no. 68057).
It has an anomalous glow curve, most closely resembling
the pyroxene-plagioclase achondrites, and in the hand
specimen no chondrules could be seen. It came therefore
to be known as "the achondrite" although later a
metamorphosed chondrule was found in a thin section.
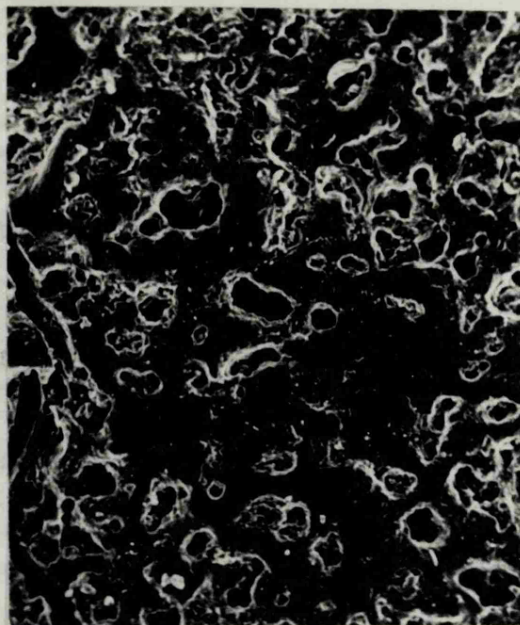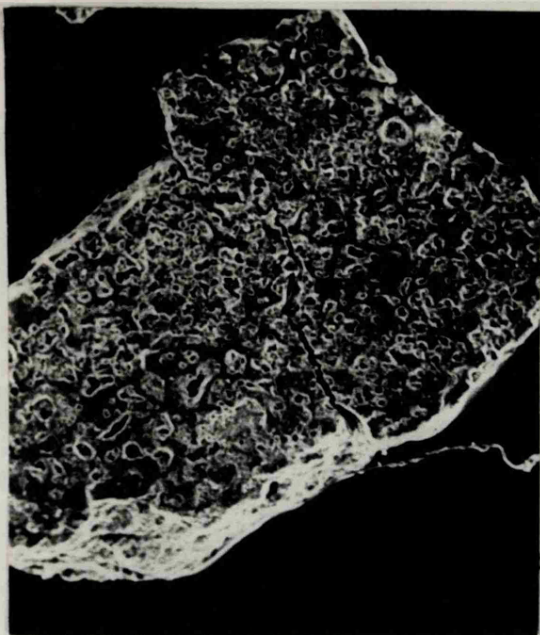
Figure VI.2a (left) Scanning electron microscope picture of the
fusion crust of the achondrite (X21). B (right) Detail at X115.

Figure VI.2c (left) Scanning electron microscope picture of the
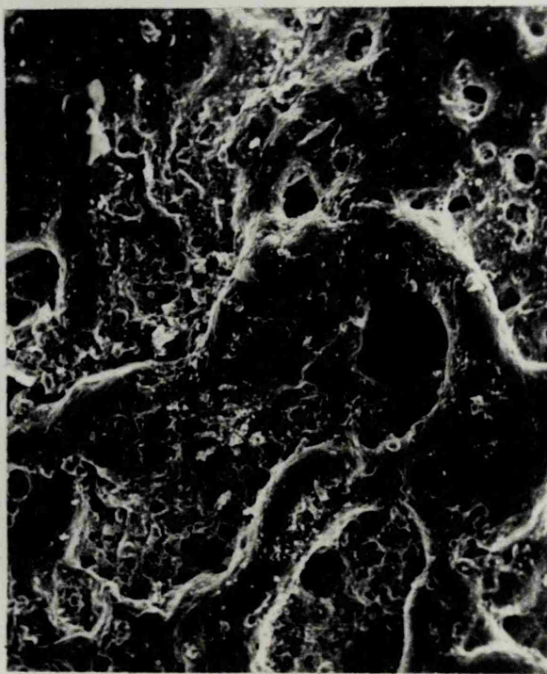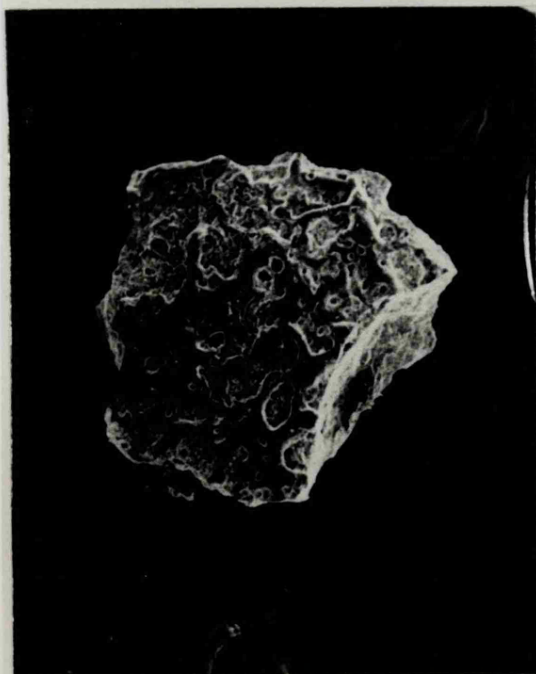Allende type III carbonaceous chondrite fusion crust (X21).
b (right) Detail at X115.
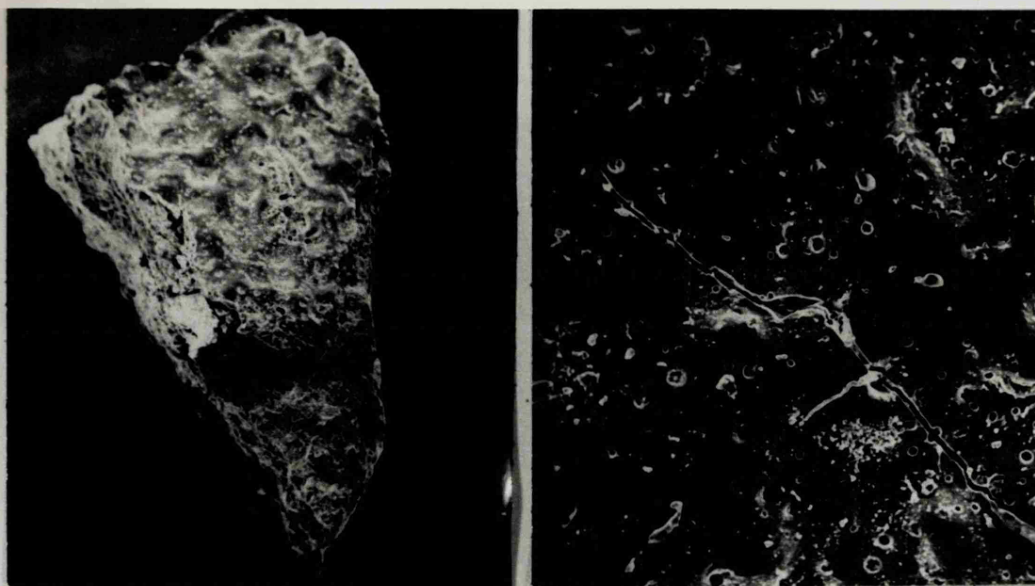
Figure VI.2e (left) Scanning electron microscope picture of
the Stannern eucrite fusion crust (X21). f (right) Detail at X110.

Figure VI.3 A cavity lined with crystallites on the fusion
crust of the Limerick meteorite. (Scanning electron microscope
picture with a magnification of 1200).

with crystallites (Figure VI.3). They were largest at the bottom
of the cavity and became finer near the rim. Such crystallites
can occasionally be seen in thin sections of the fusion crust.

From these considerations it is possible to estimate
surface temperatures of the fusion crust, knowing the melting
points of the major minerals present (Table VI.1). To determine
the temperature gradient across the crust it is obviously
necessary to examine the crust in section, and since opaque
minerals are so much in evidence this usually requires polished
sections.

VI.3   The fusion crust in section

The outermost zone of the fusion crust consists of two
phases; magnetite, occasionally with a wustite nucleus, and
glass (Figure VI.4). This is the zone which actually flowed,
since all flow structures consist of the two phases (Figure VI.4c).
It is also the zone in which degassing occurred, and cavities are
common. Its thickness is arbitrary, being governed by flow, and
is usually thickest on the lateral faces. Pooling may result in
it being several millimeters thick, although a more typical
figure may be a hundred microns. For these reasons the two-phase
zone is of little use in measuring temperature gradients, although
it displays a number of interesting features. For example the
magnetite is skeletal and forms larger structures near the edge
of the meteorite. It is usually concentrated around cavities,
presumably because the reaction

$$FeS \ + \ O_2 \ = \ Fe_3O_4 \ + \ SO_2$$

$$or \ MgFeSiO_4 \ + \ O_2 \ = \ Fe_3O_4 \ + \ (MgSiO_4)_{glass}$$
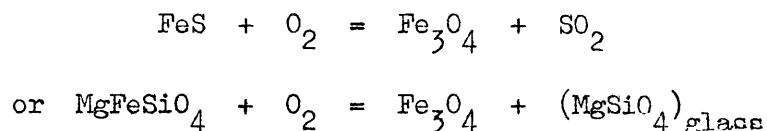
is involved in its production. Frequently the more refractory

crystals produce areas in which no magnetite appears, and in

Figure VI.4e a reaction is occurring in the middle of the crystal

before it has melted.

Beneath this two-phase zone occurs a region in which

crystals have melted around the edges and are surrounded by iron-

rich glass. Near the two-phase region there is a transition zone

in which glass predominates. In transmitted light these zones

appear as a transparent band sandwiched between the outer two-

phase region made opaque by the magnetite, and the third, innermost,

zone (Figure VI.4f).

The innermost zone is one in which troilite and troilite/

nickel-iron eutectics have flowed between the cracks of the

unaltered meteorite matrix. Presumably it is the abundance of

cracks filled with opaques that make this zone opaque. Viens in

the Haverö meteorite have similarly been made opaque by finely

dispersed troilite (Wlotzka, 1972, Figure 2; Ramdohr, 1972). It

is the zone which Borgstrom (1912) said was troilite-rich and

this is clearly so. It is the most meaningful zone for our

purposes and will be discussed at length.

Firstly, it permits a determination of the temperature of

the boundary between the second and third zones. Taking this

together with the value for the surface temperature determined

by the S.E.M. photographs enables calculation of the ablation

rate at the time the crust formed. Bethe and Adams (1959)
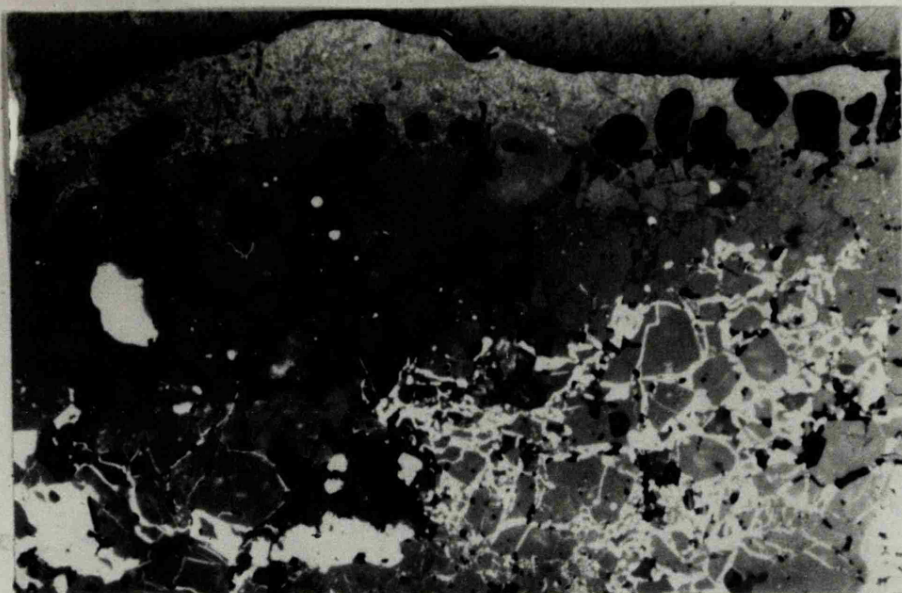
Figure VI.4a A polished section of the fusion crust of the Barwell
meteorite showing all three zones. The outermost is the two-phase
zone, the central zone contains partially melted crystals in a
darker glass and the innermost contains sulphide and metal flows
into unaltered matrix. (Vertical side of the field of view is
about 1 mm.)

Figure VI.4b Detail of the two-phase region. (Vertical side of
the field of view is 200 micrometers.)
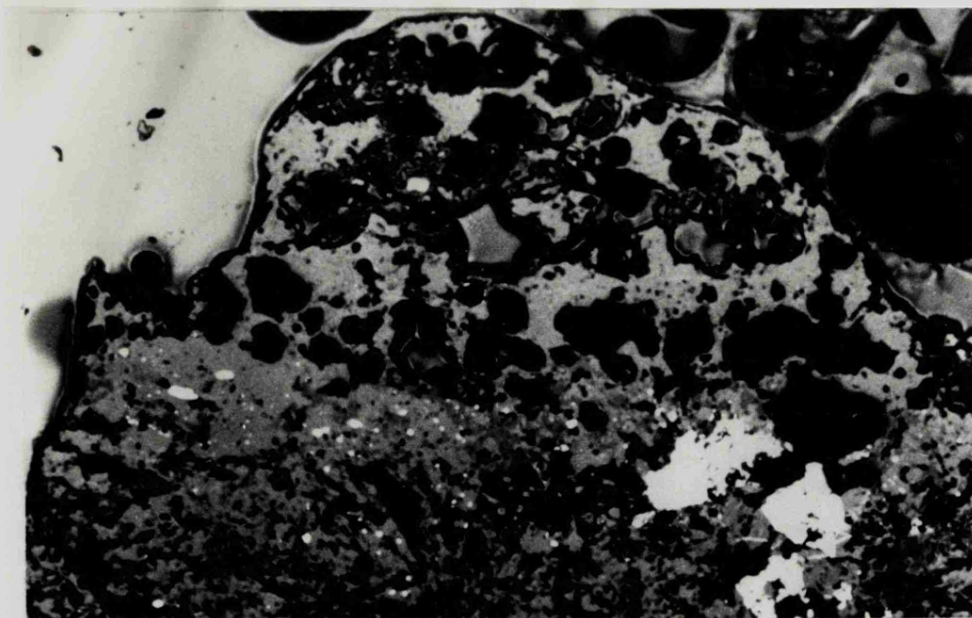
Figure VI.4c Polished section of a globule of viscous crust on
the Barwell meteorite. The globule consists entirely of two-
phase reion material, and the structure of the other zones is
unaffected by it. (Vertical side of the field of view is about 2 mm).
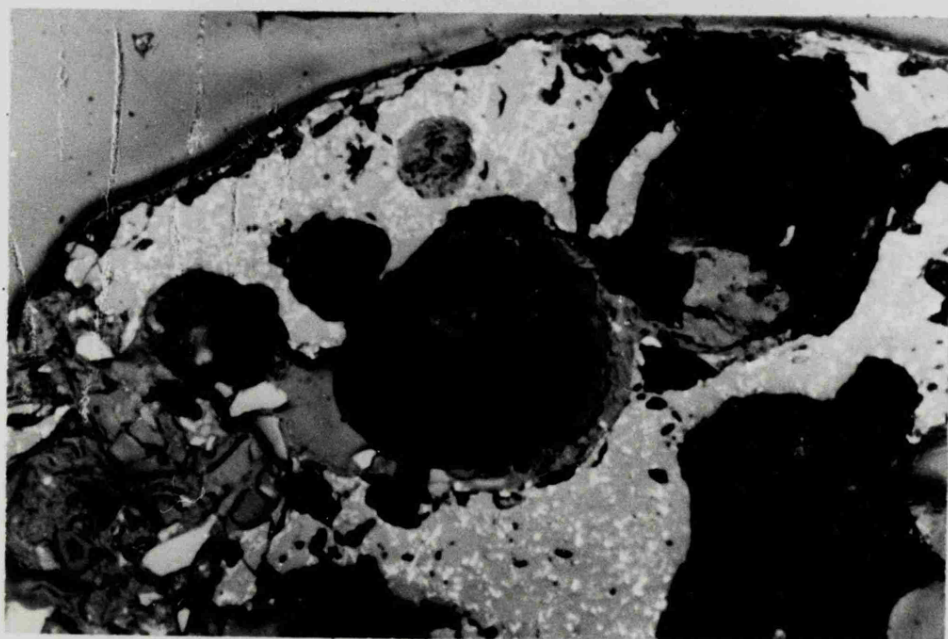
Figure VI.4d Detail of figure VI.4c. (Vertical side of the
field of view is about 150 micrometers.)
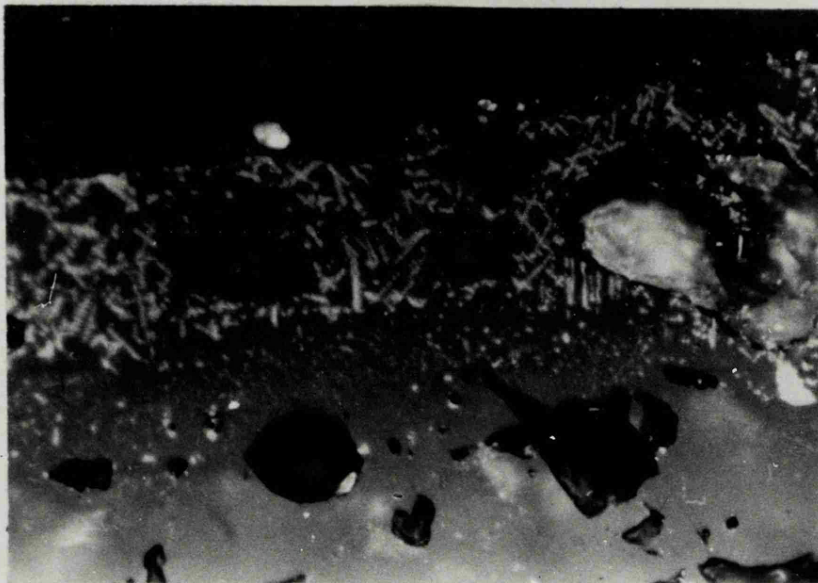
Figure VI.4e Polished section of the fusion crust of the Barwell meteorite showing "ghost" crystals of refractory minerals. Reaction appears to have occured in the middle of these crystals. The size and shape of the magnetite inclusions changes across the zone. (Vertical side of the field of view is about 500 micrometers)
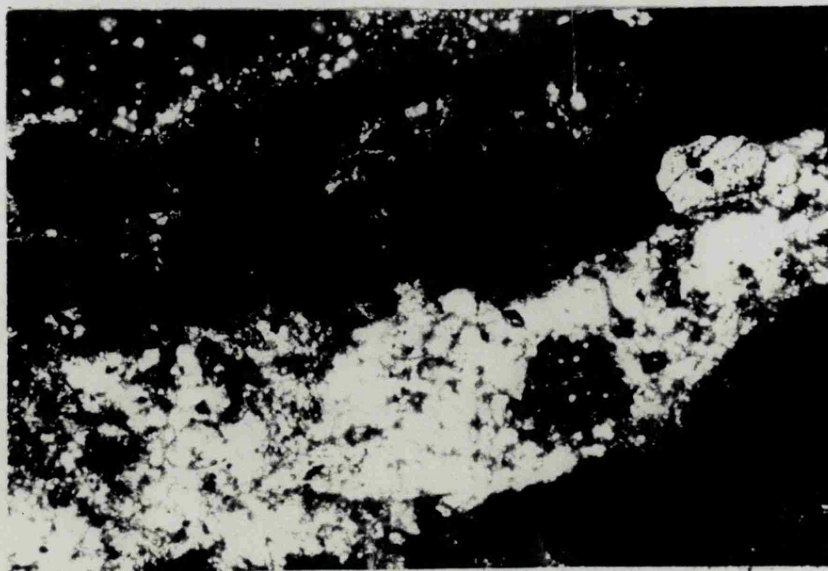
Figure VI.4f The fusion crust of the Barwell meteorite in transmitted light. (Vertical side of the field of view is about 500 micrometers.)

published a theory for the ablation of glassy materials when
spacecraft heat shields were being designed. From this we may
express the terminal ablation rate in terms of the surface
temperature T_o and the temperature T at a boundary y from the
surface as

$$v_w = -\frac{k}{y} \log_e \left(\frac{T}{T_o} \right)$$

where k, the thermal diffusivity, is $K/C_p D$ (in which K is the
thermal conductivity, C_p is the specific heat and D is the
density). $y = 0$ is taken as the boundary between the two-phase
zone and the transparent zone, since the thickness of the former
is arbitrary. The two phase zone is assumed to be isothermal.
Once melted the troilite will no longer be stoichiometric and its
melting point will no longer be $1200^{\circ}C$ (Kellerud and Yoder, 1959).
Departure from stoichiometry is clearly demonstrated by the
electron-microprobe results presented in Table VI.2 Some flows
have appreciable nickel content (from eutectic formation between
nickel iron and troilite). Unfortunately, the Fe-S-Ni phase
diagram is poorly known, but the nickel clearly lowers the melting
point. We have taken $1100^{\circ}C$ as a value likely to be typical of
the boundary between the second and third zones since it is the
temperature of the eutectic in the Fe-S phase diagram, Ramdohr's
(1967) schematic of the fusion crust (Figure VI.5) used this
figure. He also suggested a temperature in the order of $1300^{\circ}C$
for the outer half of the transparent zone, where nearly all the
crystals have vitrified but the two phases had not formed, and
about $900^{\circ}C$ where all the troilite/nickel iron flow material had
solidified.

Some of our measurements are shown in Figure VI.6, which

presents the boundary temperatures of fusion crusts taken from

various faces of the Barwell meteorite. The derived ablation

rates are presented, together with those of the Allende meteorite,

in Table VI.3. They show very well the expected trends, with

frontal faces ablating most and the rear face least. The standard

deviations of the various boundary distance measurements are

75%, 29%, 20% and 22%, for boundaries a, b, c and d respectively.

The value for boundary a is very large because this zone

includes all the surface texture of the crust. The innermost

boundary d is least meaningful as it is governed as much by the

amount of metal and sulphide present as by the temperature. The

other standard deviations reflect the clarity of the boundaries

and the accuracy with which they can be measured. The most

reliable boundary temperature is therefore that of c and it was

used to determine the ablation rates in Table V.3.

The second application one may make of the innermost zone

of the fusion crust involves measuring the amount of troilite/

nickel-iron that has flowed. This was done by point counting,

the volume percent of troilite/nickel-iron in the innermost zone

of four specimens of fusion crust from the Barwell meteorite

being about 25%. The original value is equal to that of the bulk

meteorite. From the rate of flow into the zone, the maximum

being equal to the ablation rate, it is possible to calculate the

time during which troilite/nickel-iron was flowing. This time

may be called the effective heating time since it is the time

required to produce the three zones of the observed fusion crust.

For Barwell it is about one second. Values for this parameter

Table VI.2

Electron-microprobe analyses of flows in the innermost zone

	Frontal face (BM 1966,59)	near face (BM 1966,57)
Fe	63.6	58.9
Ni	7.5	10.0
S	25.4	27.6
Sum	96.5	96.5
Number of points	4	3

Analyses are accurate to 10% of the value.

Table VI.3

Ablation rate determinations from the fusion crust

Specimen	Face type	Ablation rate (cm/sec)
Barwell		
BM 1966,59	Frontal	0.35
BM 1966,65	Front/side	0.27
BM 1966,57	Side	0.22
BM 1966,57	Rear	0.18
Allende		
NMNH 3636	(Front)*	0.39
"	(Rear)*	0.31
Stannern		
43805**	Side	

* Morphology is not conclusive; the assignments are from other criteria.

** Leicester University Geology Department acquisition number.

were given by Krinov (1960, page 282), Nininger (1935) and

Farrington (1915, page 85) all of whom appear to have used

different methods but arrived at much the same value of about 1

second.

VI.4   Chemical studies of the fusion crust and ablation products

The search for cosmic dust has been pursued with most

vigour by melting and filtering polar ice. Much of this surface

collected dust (S.C.D.) must be ablation product, since the

concentration exceeds that predicted by spacecraft measurements

(Hodge and Wright, 1968; 1969). Many studies which have been

made on the fusion crust were, therefore, prompted by its

relevance to S.C.D.

The tendency for nickel-iron to become nickel-rich as

iron preferentially oxidises was observed by Ramdohr (1967) and

its relevance to cosmic dust emphasised by Fechtig and co-workers

(Elgoresy and Fechtig, 1965; Fechtig and Utech, 1964). Nickel

is rarely present in S.C.D. (Ivanov and Florenskii, 1971) but a

few individual analyses show it to be present in very high

concentrations. Trevorite ($Fe_2Ni\ O_4$) has been observed in both

S.C.D. (Ivanov and Florenskii, 1971) and meteorite fusion crusts

(Das Gupta et al., 1969). However, sulphur is absent from the

fusion crusts of two carbonaceous chondrites (Brownlee and Hodge,

1973) but present in large amounts in S.C.D. collected from rock-

salt (Mutch, 1964). The numerous analyses published by Hodge,

Wright and Langway (Hodge and Wright, 1964; Hodge, Wright and

Langway, 1964; 1967; Wright and Hodge, 1965a; 1965b; Wright,

Hodge and Langway, 1963; 1969) provide useful data for comparisons,

for example, with simulated ablation products (Blanchard, 1972;

Hodge and Wright, 1965) and actual ablation products (Carr,

1970). No doubt much of the collected material is contamination

since, as Figure VI.7 illustrates, there is a marked disagreement

in the Al and Fe content of material from two polar collecting

sites, the South Pole and Greenland. Heinzinger et al., (1971)

have considered the use of oxygen isotope ratios to relate the

fusion crust to cosmic spherules.

VI.5   Discussion and conclusions

The innermost zone of the fusion crust provides useful

information on the final phases of a meteorite's atmospheric

descent which is complementary to studies based on morphology or

thermoluminescence. A well-developed fusion crust appears to

require about a second to form. In terms of a meteorite's flight

through the atmosphere this is a very long time. Explosions

frequently occur within the last second of luminous flight as the

meteorite hits the retardation point. This appears to have

happened with our specimen of the Plainview meteorite (BM 1959,805),

in which little or no third zone exists although the specimen does

have a uniform crust. Similarly the secondary crust of a Holbrook

stone has no zone 3, while a primary crust on the same specimen

has a perfectly formed crust with all three zones. Presumably

the fragmentation which produced the secondary face occurred

within the last second of luminous flight.

The ablation rate derived from the fusion crust is clearly

applicable only to the final second of luminous flight. To

obtain more information, especially concerning the pre-atmospheric
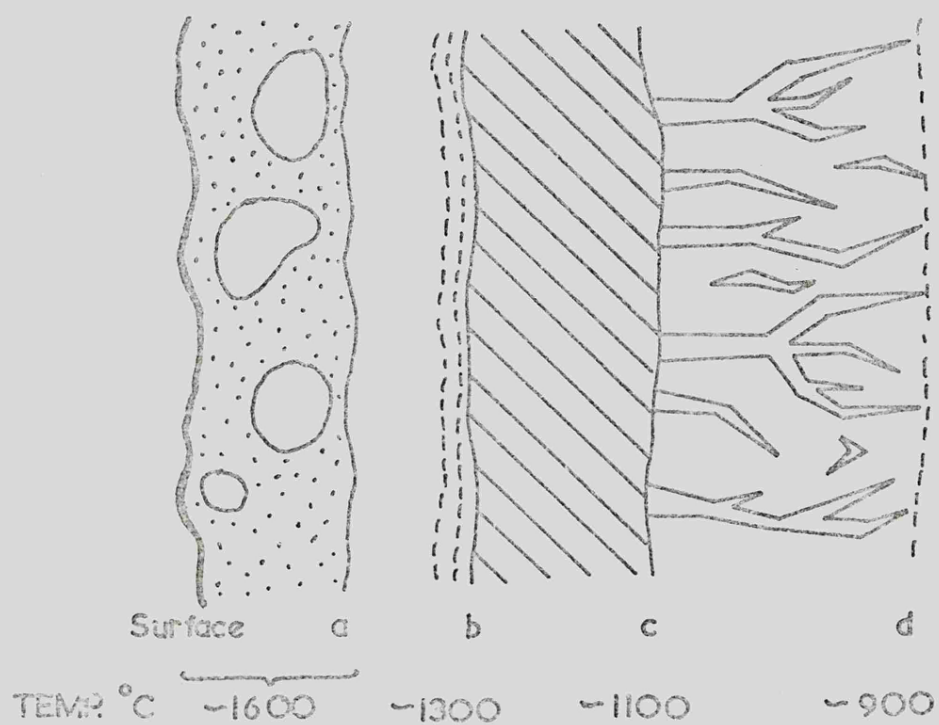
Figure VI.5 Schematic diagram of the fusion crust. (After Ramdohr, 1967).
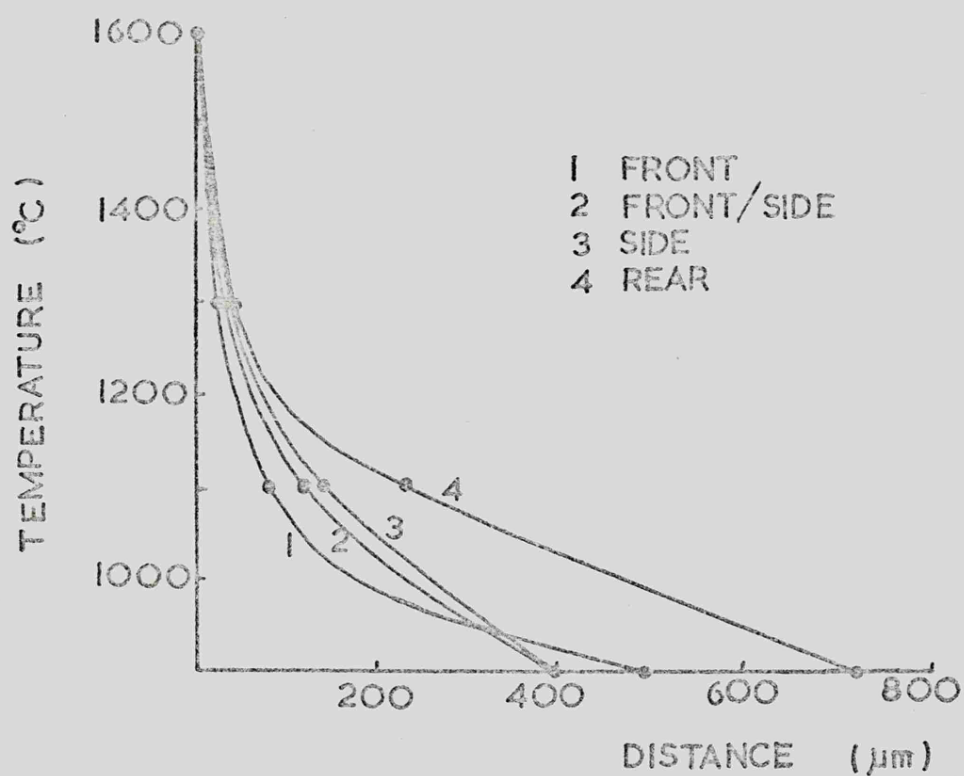
Figure VI.6 Temperature as a function of distance for specimens of the Barwell meteorite taken from various faces.
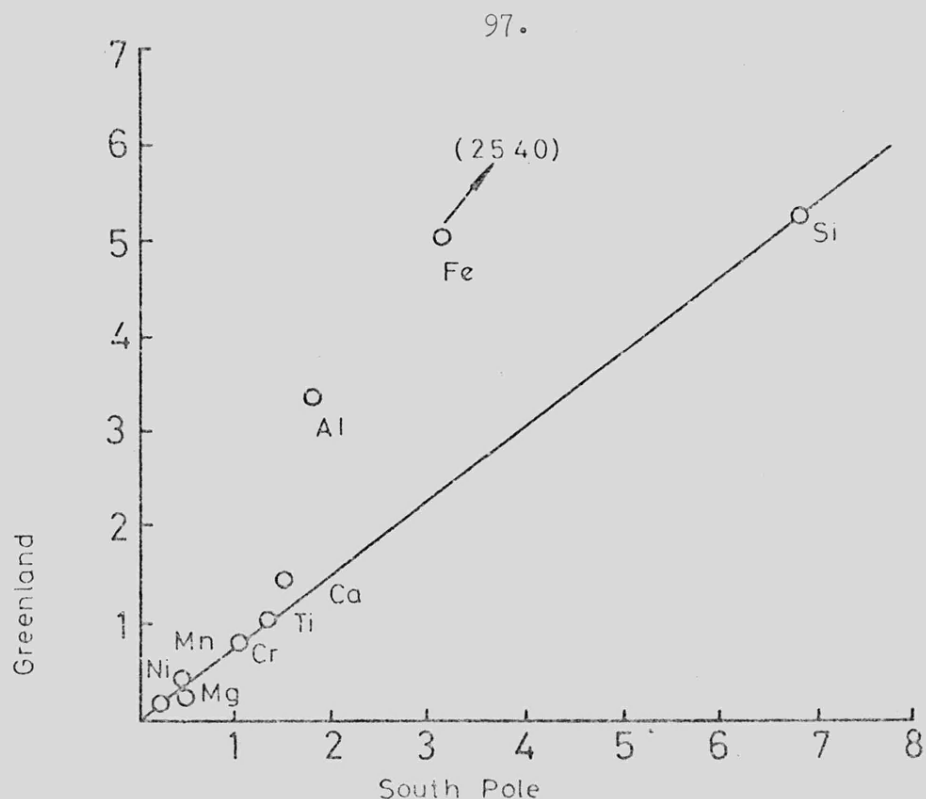
Figure VI.7 A comparison of the composition of 106 spherules separated from ice (% element) collected in Greenland with that of 54 spherules from South Pole ice. There is good agreement for all elements except iron and aluminium.
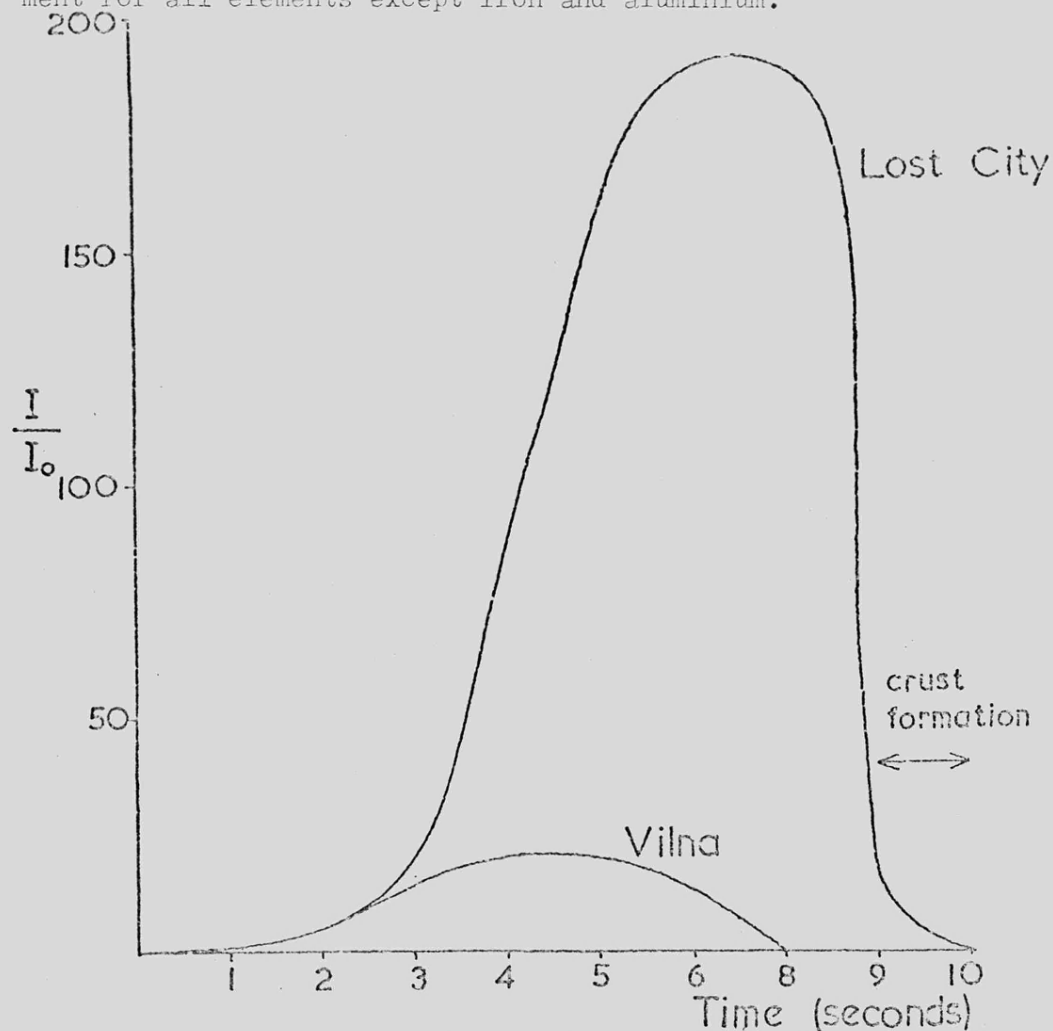
Figure VI.8 Light curves for the Vilna and Lost City meteorites.

mass of the meteorite, more speculative processes are required.

Preatmospheric mass and shape are particularly valuable

parameters because of errors in the exposure age determinations

caused by shielding (Nyquist et al., 1973). An obvious guide to

the ablation rate at any time in the meteorite's luminous flight

is the light curve. The ablative behaviour of the fusion crust

has been related to meteor light curves by Bronshtén et al., (1968)

using high speed cine film and simulated meteorite ablation.

Unfortunately, the light curve is known for very few meteorites.

Two that are known, those for the Vilna meteorite (Folinsbee et

al., 1969) and the Lost City meteorite (McCrosky et al., 1971),

are presented in Figure VI.8. The curves represent meteorites of

vastly different sizes; Lost City was a reasonably sized meteorite

of 17 kg whereas Vilna consisted of two fragments totalling 150 mg.

The curves are presented with light intensity on the ordinate

instead of the more familiar stellar magnitude, so that the curves

reflect the change in ablation rate with time. For meteors whose

flight is in free-molecular flow the ablation rate is directly

proportional to light intensity, but for fireballs the air moves

around the body in conditions of continuum flow and this may not

be strictly true. As a step one better than assuming constant

ablation we will assume that the ablation rate varies as the light

curve, and that one second before the end of luminous flight the

ablation rate is as measured from the fusion crust.

The Vilna data can be fitted reasonably well by a parabola.

The equation can be integrated over the luminous flight time and

the value for the total ablated radius obtained is 0.75 cm. This

indicates a mass loss in excess of 99%.

The Lost City curve can be interpreted as indicating

extreme ablation, say at 10 times the terminal ablation rate, for

about four seconds. The ablated radius is therefore about 10 cm

and the mass loss is 87.5%.

One would expect greater mass loss for smaller meteorites

whose surface area-to-mass ratio is greater. From simple

geometrical arguments, assuming spherical bodies, the mass loss, M,

is related to the post-atmospheric radius, r, by

$$M = \left[1 - \left(1 + \frac{R_0 t_L}{r} \right)^{-3} \right] \times 100$$

where $R_0 t_L$, the ablated radius, could be replaced by the integral

of an equation fitting the light curve.

A large number of pre-atmospheric mass determinations have

recently been published by Begemann and Vilcsek (1965), Marti et

al., (1966) and Eugster et al. (1969) using (n, à) produced

^{36}Cl or ^{80}Kr and by Nyquist et al. (1973) using gas isotope

ratios measured by a variety of authors. These are expressed in

terms of percentage mass-loss in Table VI.4. The mass-loss of

Vilna and Lost City determined here are in agreement with the general

trend in the published values which is that smaller bodies have

ablated most.

In conclusion therefore it may be stated that the fusion

crust contains much information about the final passage of a

meteorite's journey to the Earth, and this can provide useful

auxillary information for studies of atmosphere-induced TL effects.

It is evident from Figure VI.6 that the fusion crust provides a means

of measuring atmosphere induced temperature gradients. These may

also be determined from TL measurements and the results obtained by

these two methods will be discussed in the next Chapter.

Table VI.4

Percentage Mass Loss of stony meteorites

Meteorite	Recovered mass (kg)	Equivalent radius(cm)	Estimated pre-atmospheric mass (kg)	Mass loss	Authors
Abee	107	19.3	170	37	a
		1.5	220	51	b
Akaba	1	14.5	100	99	d
Beenham	44	27.6	200	78	d
Colby, Wisconsin	303	19.2	600	24	d
Dimmitt	105	9.9	400	96.5	c
Finney	10	8.8	200	95	d
Kiel	0.14	0.3	20	80	d
Ladder Creek	35	13.4	600	94.2	d
Leedey	50	15.1	400	87.5	a
Maziba	5	6.8	100	95	d
Mezo Madaras	23	11.7	1400	98.4	b
			1400	94.2	c
Mocs	300	27.4	500	40	d
			1000	70	d
			300	99.7	c
Narellan	0.8	1.3	20	96	d
Ness City	17	10.6	1000	98.3	d
Norton County	1100	44	2500	56	a
Ochansk	500	32.4	400	0	d
			400	0	c
			500	0	d
Parnalee	75	18.0	1500	95	d
			1600	99	c
Pulsora	2	4.3	200	99	d
			200	99	c

Table VI.4 (Continued)

Meteorite	Recovered mass (kg)	Equivalent radius(cm)	Estimated pre-atmospheric mass (kg)	Mass loss	Authors
Ramsdorf	5	6.8	500	99	d
Saline	31	12.9	400	92.2	d
St. Germain	4	6.2	300	87	d
Saint-Séverin	271	26.4	150	0	d
			400	32	d
Texline	26	12.1	600	95.8	d
Tieschitz	28	12.5	200	86	d
Tynes Island	20	11.2	600	96.7	c
Utzenstorf	3.4	3.4	50	93.2	d
Walters	28	12.5	1000	97.2	d
			600	95.3	c
Weston	105	19.0	600	75	d
			800	81	c

References: a   Begemann and Vilcsek (1965)

b   Marti et al. (1966)

c   Eugster et al. (1969)

d   Nyquist et al. (1973)

The estimates by authors b, c and d are minimal.

CHAPTER VII

TEMPERATURE GRADIENTS IN METEORITES PRODUCED

BY HEATING DURING ATMOSPHERIC PASSAGE

VII.1   Introduction

Temperature gradients are produced in a meteorite by

heating during its atmospheric passage. The methods so far

published for its measurement are broadly of two kinds. They are

either petrographic, in which changes in structure and mineralogy

resulting from elevated temperatures are used; or they involve

the use of thermoluminescence. It is necessary with the petro-

graphic methods to use a semi-theoretical approach since the

gradient is not varying linearly, but approximately exponentially.

The observations that have been used tend to be metallurgical,

because of the greater sensitivity of iron meteorite structures

to the range of temperatures involved (Buchwald, 1961; 1967;

Reed, 1972; Lovering et al.,1960; and Marringer and Manning,

1960). Some observations for stony meteorites were made by Clarke

et al. (1971).

Temperature gradients are useful complements to

morphological studies since they reflect the orientation of the

specimen; steeper gradients being experienced at the front of

the stone. They also give a clue to the luminous flight time.

Prachyabrued et al. (1971) employed their results in this way,

while Vaz (1972) used the similarity in the temperature profiles

of Lost City and Ucera to infer similar luminous flight times.

In the work described in this chapter the reduction in thermo-

luminescence near the fusion crust has been examined in several

meteorites. These results are compared with those from an

examination of the fusion crust and with predictions from

theoretical studies.

VII.2   Methods

Ramdohr (1967) pointed out a number of mineralogical

changes that occur in the fusion crust. These were discussed in

the previous Chapter and led to the observed temperature gradients

shown in Figure VI.6. The gradient could be measured roughly by

eye directly from the curves, but since it varies non-linearly

this is impossible to do with any degree of consistency. Instead

one may rearrange the ablation rate equation (Section VI.3) and

differentiate it to show that

$$\frac{\partial T}{\partial y} = \frac{V_w T_i}{k} \exp \left(\frac{-y \, V_w}{k} \right)$$

where the symbols have the same meaning as in the previous chapter.

The temperature gradient can therefore be readily calculated at

any point for which the temperature and distance are known. Our

fusion crust data provides such information.

The alternative method of temperature gradient determination

involves the measurement of thermoluminescence at various depths

below the fusion crust (Vaz, 1971). This results in a curve of

TL vs. depth. A calibration curve may then be prepared showing

the way in which TL drops when the sample is heated to various

temperatures for a short period, and the TL vs. depth curve

expressed as temperature vs. depth.

VII.3   Results

VII.3a   The Barwell Meteorite

A sample of the Barwell meteorite with frontal fusion

crust was used in this investigation (Leicester University Geology

Department acquisition number 43801). The bar taken was at an

angle of about 45° to the surface of the crust and provided

thirty 1 mm thick sections of about $\frac{1}{2}$ cm^2 area. Cutting was

performed with a Metals Research Ltd. Microslice II diamond saw

giving a 0.10 mm wide cut. The specimen was mounted for cutting

with adhesive tape and elastic bands.

The results are presented in Figure VII.1. Figure VII.1a

shows the variation in the height of LT along the bar. The

scatter is removed by expressing the height of LT relative to HT

(Figure VII.1b) or to the height of LT after irradiation of the

drained powder to a standard dose of about 50 krad (Figure VII.1c).

The scatter is due to sample inhomogeneity, presumably variations

in the feldspar content. The peak height ratio produces a curve

with less scatter, but since HT may also vary across the specimen,

could result in the gradient being slightly underestimated. This

is not a serious problem here, however, since compared to LT,

HT is highly insensitive to the temperatures LT is being used to

measure, although it is just as sensitive as LT to sample

inhomogeneity.

Having measured the drop in TL as the specimens approach

the fusion crust, it is necessary to convert the reduction in TL

to the temperature that is responsible for that drop. Powder

from a central portion of the stone was therefore heated for five

seconds at various temperatures and its glow curve was measured.
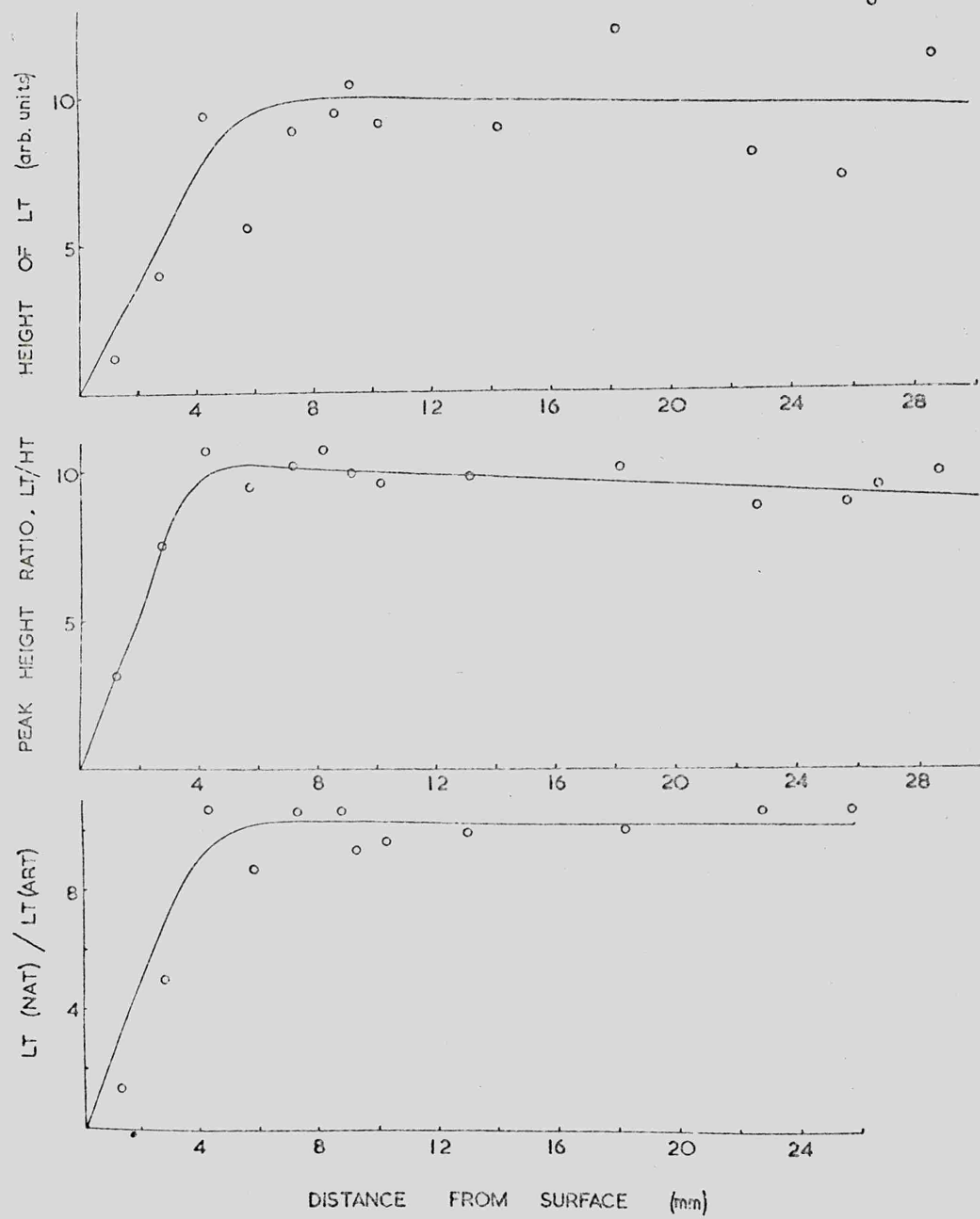
Figure VII.1 Draining of the thermoluminescence by atmospheric heating near the fusion crust in a frontal specimen of the Barwell meteorite.
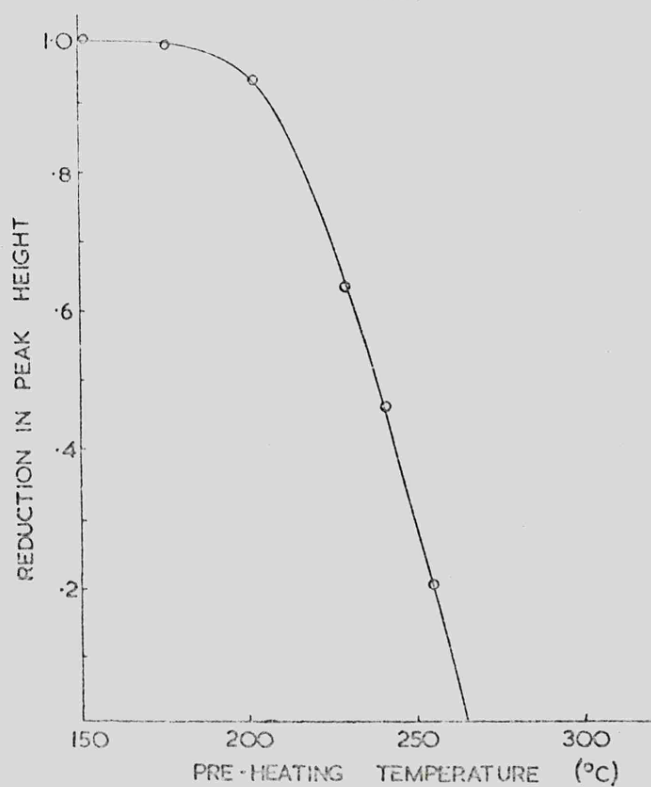
Figure VII.2 The drop in the height of LT caused by heating powder at various pre-heating temperatures for 5 seconds prior to measuring its Th. The powder was taken well from the fusion crust of the Barwell specimen.
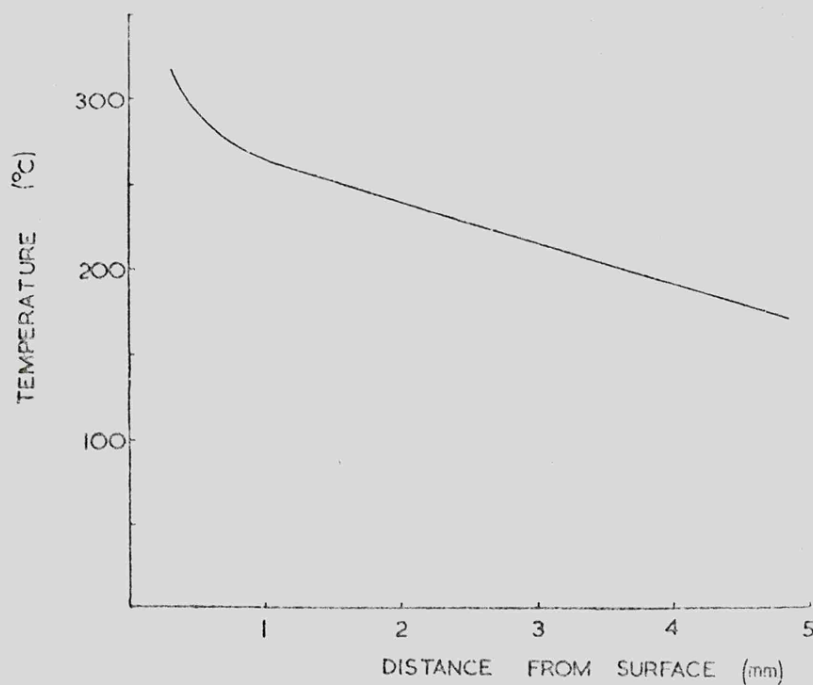
Figure VII.3 The temperature profile for the Barwell meteorite.

Table VII.1

Temperature Gradients and Ablation Rates for the

Barwell Meteorite

Specimen	Face Type	Temperature gradient at boundary c($^{\circ}$C/μm)		Ablation rate (cm/sec)
		From ablation theory	From Figure VI.6	
BM 1966,59	Front,Close	12	5.0	0.35
BM 1966,65	Front Side, Close	7.6	3.9	0.27
BM 1966,57	Lateral, Striated	6.1	3.3	0.22
BM 1966,57	Rear,Warty	3.5	2.3	0.18

The heating was performed by placing the powder on the filament
and using the hold facility of the control unit. The period of
time chosen is clearly very important and is discussed below. A
calibration curve of drop in TL vs. temperature of "pre-heating"
is thereby produced (Figure VII.2) and by converting the y-axis
of the TL vs. depth curve, and correcting for a bar normal to
the surface, the temperature profile can be determined (Figure VII.3).

Temperatures as high as $250^{\circ}C$ have been experienced no
further than 0.5 mm from the present surface, but temperatures
exceeding $150^{\circ}C$ have penetrated to about 5 mm. The mean gradient
at a depth exceeding 1 mm is $15-20^{\circ}C/mm$.

The semi-theoretical results calculated from the fusion
crust measurements are presented in Table VII.1. Since the
troilite/troilite-nickel iron melting boundary is probably the
one most reliably known it is to this boundary that the method
has been applied. For comparison, eye estimates from Figure VI.6
are also given. The results illustrate the strong dependence, at
the shallow depth represented by the fusion crust, of the
temperature gradient on the ablation rate. The gradients from
the fusion crust and TL may be expected to differ because the
fusion crust results apply to a depth of a few hundred micrometers,
while the TL figures apply to depths of many millimeters and, as
we shall see, the temperature drops off approximately exponentially
with depth.

VII.3b   The Allende meteorite

In a study to be discussed in more detail later several
4 x 4 mm bars were taken from a slice of an Allende stone (NMNH

3636). The bars intercepted the fusion crust at 8 locations.
1 mm thick slices were prepared from each of these bars and
atmosphere-induced TL gradients sought. In four cases the
exceptional inhomogeneity shown by Allende obscured the gradients.
However, the remainder had detectable gradients and these are
presented in Figure VII.4. The temperatures are approximate
because of the uncertainty in the average value for the meteorite
(possibly ± 20%) but relatively the accuracy is better. The shape
of the stone suggested an orientation, although not very
convincingly, and the fusion crust supported this; face d has
a temperature gradient of $5^{\circ}C/\mu m$ (for an ablation rate of 0.39 cm/
sec) and face b a value of $4.1^{\circ}C/\mu m$ (for an ablation rate of
0.31 cm/sec). The TL-measured temperature gradients are in
agreement with these trends and support the suggestion that d is
the front and b the rear of the stone.

VII.3c   The Plainview meteorite

Two bars were removed from an approximately rectangular
4 mm thick section of the meteorite (BM 1959,805). They inter-
cepted the crust at four locations, at approximately 90° to each
other. However, a temperature gradient could be detected by TL
for only one of them. In section the fusion crust always shows a
well developed outermost zone, but contains an innermost (FeS/
NiFe-FeS eutectic flow) zone only for the surface at which TL could
detect a temperature gradient. It appears that with the exception
of this one face the stone was not exposed to heat long enough
to produce temperature gradients or an innermost zone, although
it was able to produce a uniform coating of fusion crust (see below).

VII.3d   The Estacado meteorite

Temperature gradients were sought in specimens taken from three fusion-crusted edges of a 17 kg slice of the Estacado meteorite (BM 1906,259). The meteorite was badly weathered, and only HT was present in the glow curves. The fusion crust specimens showed none of the characteristic features; only large bands of limonite and altered meteorite matrix were present. No TL gradients due to atmospheric heating could be detected in this meteorite. (The higher temperatures needed to diminish the HT peak would affect only the outermost millimeter or so.)

Weathering has a complicated effect on the TL of meteorites. In Chapter IV it was stated that it changes the peak height ratio, presumably by filtering the light from one peak more than the other. An additional effect is present in the samples taken from the Estacado meteorite, and this is illustrated in Figure VII.5. Badly weathered meteorites sometimes have a peak at about 250°C and this is true of the glow curves of material from the Estacado meteorite. When HT is very intense the 250°C peak usually appears as an inflexion on its low temperature side. However, near the fusion crust it stands out more clearly, either because it is more intense or because HT is less intense. Either way, being near the surface of the specimen does not appear to reduce the intensity of this peak to the extent that it does HT. There are three possible explanations:

  i)   The 250°C peak is caused by weathering.

  ii) The 250°C is indigenous to the meteorite but can recover from heating during atmospheric descent more quickly than HT and LT.
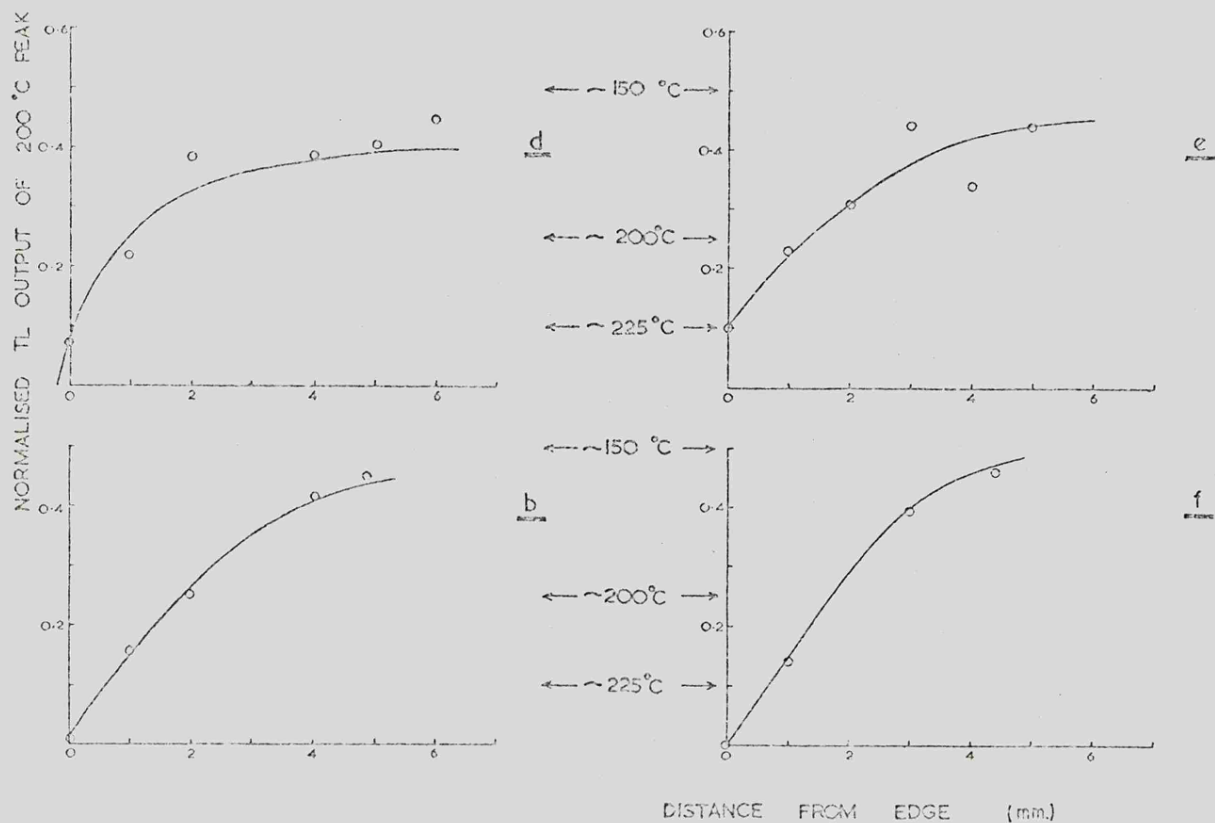
Figure VII.4 The drop in TL near four edges of the Allende
meteorite. The gradients differ in such a way as to infer that
d is the front and b the rear of the stone.
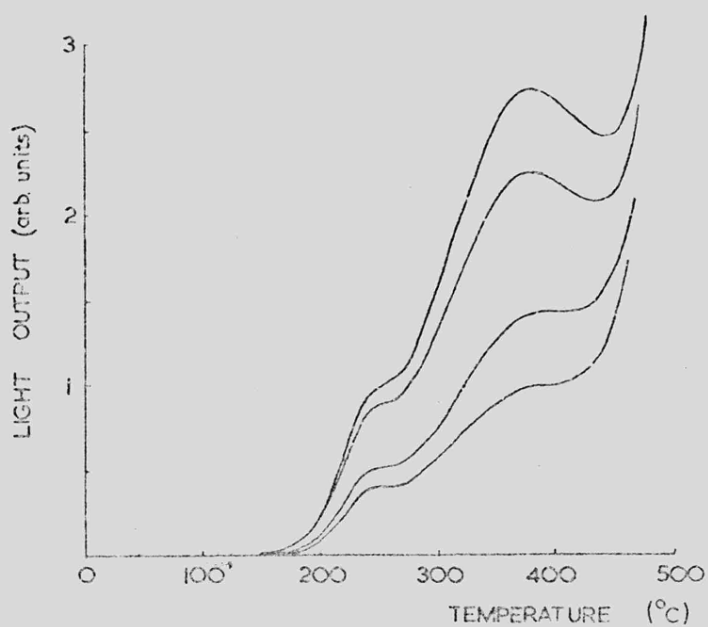
Figure VII.5 The glow curve of powder from the Estacado
meteorite showing HT of various intensities. The peak at 250 °C
becomes clearer when HT is less intense.

iii)   The 250°C peak is indigenous to the meteorite but is

drained less readily than LT and HT.

Explanations (ii) and (iii) require a suitable combination of

trap parameters such that the peak is more stable than one at

higher temperatures (case iii) or more readily filled than one at

lower temperatures (case ii).   Since this peak is never present

in unweathered meteorites in which LT has completely drained and

HT is clearly visible, the first suggestion seems the most plausible.

VII.3e   The Holbrook meteorite

A 2 mm thick slice was taken from a small (5 g) completely

encrusted stone (Leicester University Geology Department

acquisition number 24239).   The slice was too small to be cut into

bars, but instead was cut into 23   2 x 2 mm squares.   The

distribution of the natural TL, and the TL produced by irradiating

the drained powder to about 50 krad, is given in Figure VII.6.

The natural TL distribution reflects the penetration of heat into

the meteorite, plus the distribution of feldspar, while the

artificial TL reflects only the distribution of feldspar over

the slice.   The flat surface of the approximately hemi-spherical

slice appears not to have been exposed to heat and in the hand

specimen is clearly seen to be a secondary face, whereas the rest

was a primary crust.   In section the secondary crust was found

not to possess an innermost zone.
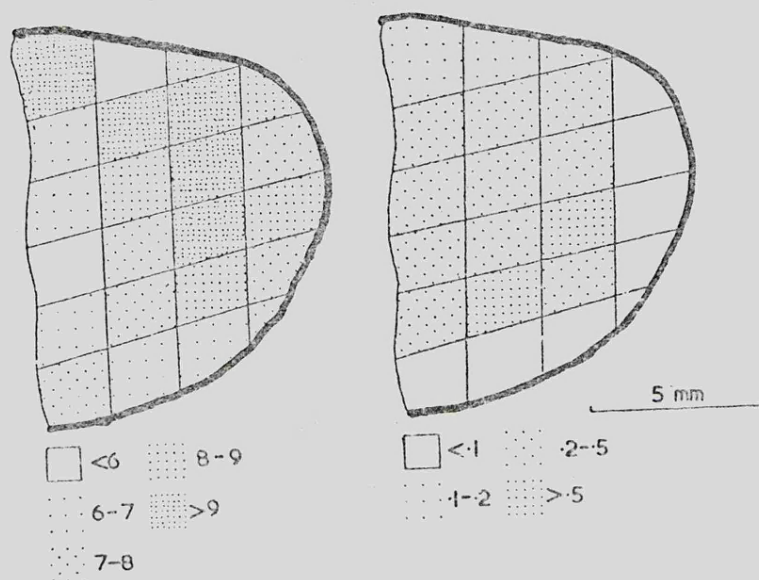
Figure VII.6a and b The distribution of thermoluminescence
across a small Holbrook stone. a (left) the intensity of the TL
produced by material that has been drained and irradiated to
about 300 krad. This reflects the feldspar distribution.
b (right) the ratio of natural to artificial TL plotted across
the slice. This describes the heat penetration. The TL has
been considerably reduced near the primary fusion crust (heavy
line) but not near the secondary crust. The TL intensity is in
arbitrary units.
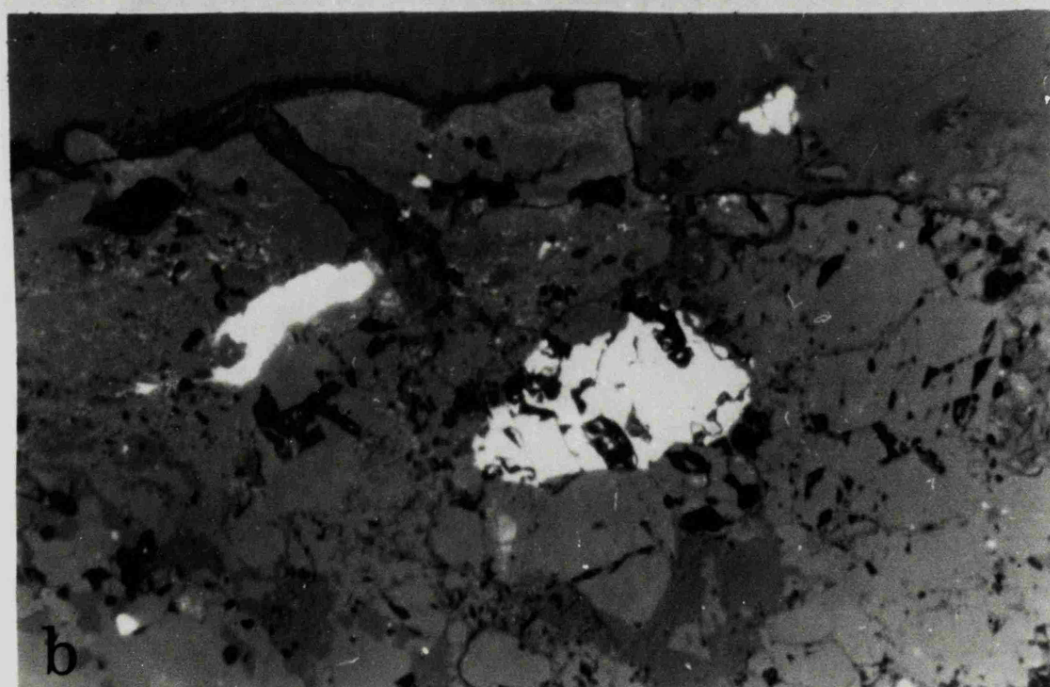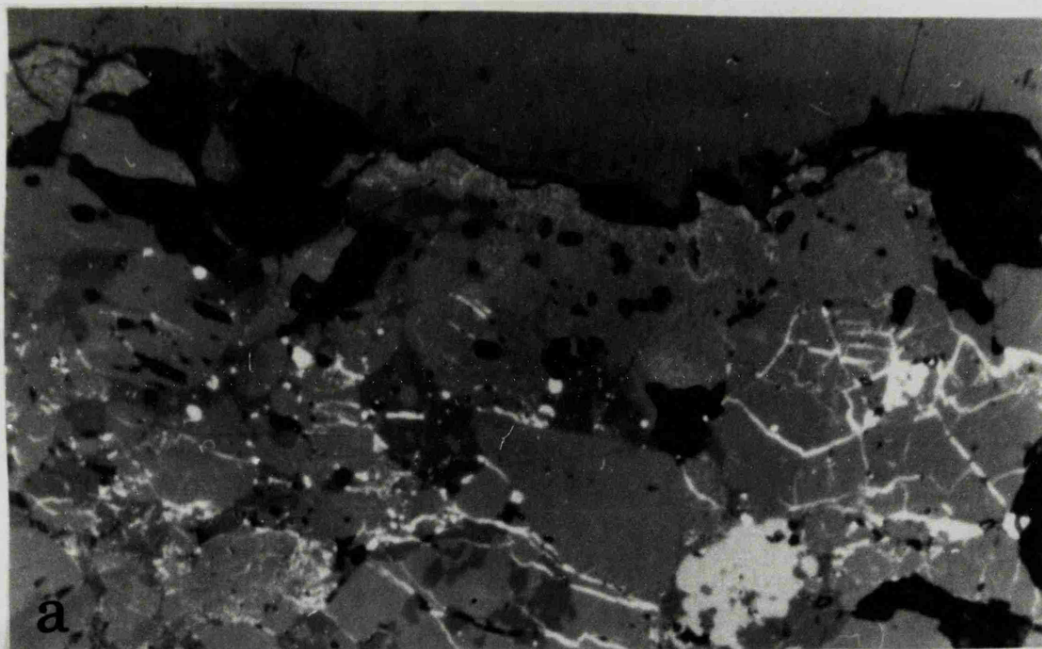
Figure VIIa and b Fusion crust specimens of the slice of the Holbrook meteorite shown in figure VII.6, as seen in reflected light. The outer 2 mm is visible. a) A well-developed primary crust showing all three zones, b) a secondary crust with no innermost zone.

VII.4 Discussion

VII.4a Theory of temperature gradients and the ablation

rates of meteorites (Carslaw and Jaeger, 1959;

Bethe and Adams, 1959; Adams, 1959).

The conductivity equation, describing the temperature T

at depth y, can be written to include a term for ablation in the

following form:

$$\frac{\partial^2 T}{\partial y^2} + \frac{v_w}{k} \frac{\partial T}{\partial y} - \frac{1}{k} \frac{\partial T}{\partial t} = 0$$

where v_w is the ablation rate, k the thermal diffusivity $(K/DC_p$,

where K is thermal conductivity, D is density and C_p is specific

heat) and t is time. The solution to this is

$$T = \frac{1}{2} T_i \left\{ \text{erfc} \left(\frac{y+v_w t}{2(kt)^{\frac{1}{2}}} \right) + \exp \left(\frac{-v_w y}{k} \right) \text{erfc} \left(\frac{y-v_w t}{2(kt)^{\frac{1}{2}}} \right) \right\}$$

where $\text{erfc } x = \frac{2}{\pi^{\frac{1}{2}}} \int_x^\infty \exp(-x^2)dx$. This requires considerable

computation but may be simplified by considering the two cases;

i) Steady state conditions ($\partial T/\partial t = 0$). Then the

temperature distribution is

$$T = T_i \exp (-v_w y/k)$$

which is the equation applicable to the fusion crust.

ii) Zero ablation, when a steady state is not established

and the temperature distribution is governed by the time during

which heat flows in. Then

$$T = T_i \ \text{erfc} \ \left(\frac{y}{2(kt)^{\frac{1}{2}}} \right) \quad *$$

The results obtained from these two equations are shown in

Figure VII.8, which also includes the results for iron meteorites

taken from Lovering et al. (1960).

VII.4b   The innermost zone of the fusion crust and the existence of TL gradients

It is now possible to understand quantitatively why the

absence of the innermost zone in the fusion crust is associated

with the absence of a temperature-induced TL gradient. In Section

VI.2 it was shown that this zone takes a period in the order of

one second to form. The temperature gradients calculated above

show that periods considerably in excess of this, say 10 to 100

seconds, are required to produce temperature gradients in the

meteorite. A useful check to make before looking for atmosphere-

induced temperature gradients in meteorites would appear to be the

existence of an innermost zone in the fusion crust.

VII.4c   Comparison of theoretical and TL-observed temperature gradients

The temperature profiles predicted by theory and those

---

*   Awebury (1949) gives a convenient expansion of this. For
an infinite plate of thickness l the temperature is given
by

$$T = T_o + \frac{T_1 - T_o}{l} y - \frac{2(T_1 - T_o)}{\pi} \sum_{p=1}^{p} \frac{(-1)^{p+1}}{p} \sin \frac{(p\pi y)}{l} \exp(\frac{-p^2 \pi kt}{l^2})$$

in which T_o and T_1 are the cold and hot face temperatures
respectively. p is an integer the maximum value of which
depends on t (usually between 5 and 10). The choice of l
is unimportant, any value in excess of 3 mm giving the same
results. 5 cm has been used here.
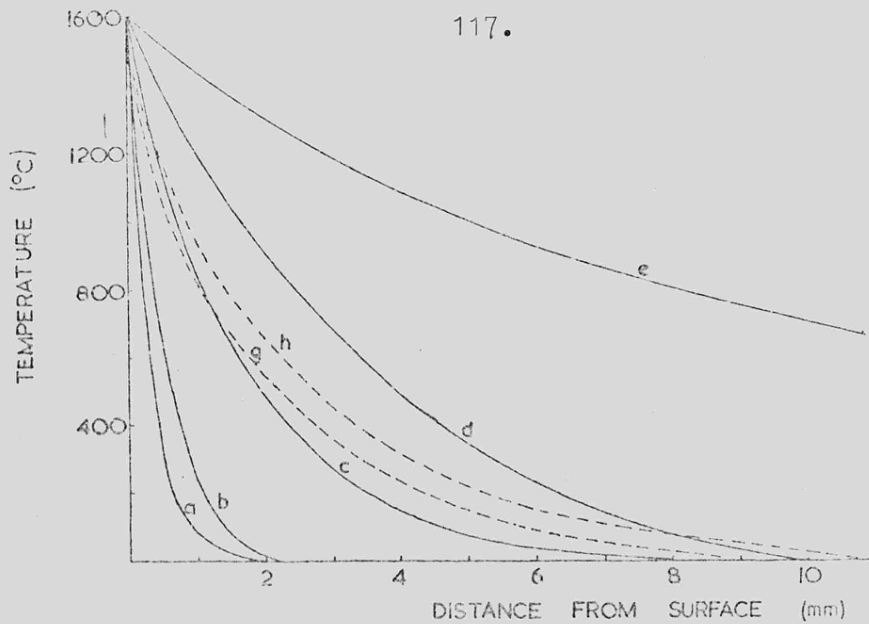
Figure VII.8 Theoretical temperature gradients in meteorites.
a. b and c are steady-state solutions assuming ablation rates of
0.25, 0.15 and 0.05 cm/sec. d and e are non-steady-state results
assuming 10 and 100 seconds luminous flight times respectively.
The dotted lines are from Lovering et al. (1960) and are appropriate
to iron meteorites; g is for a steady-state with an ablation rate
of 0.18 cm/sec and h is the non-steady -state result for a 3 second
luminous flight time.
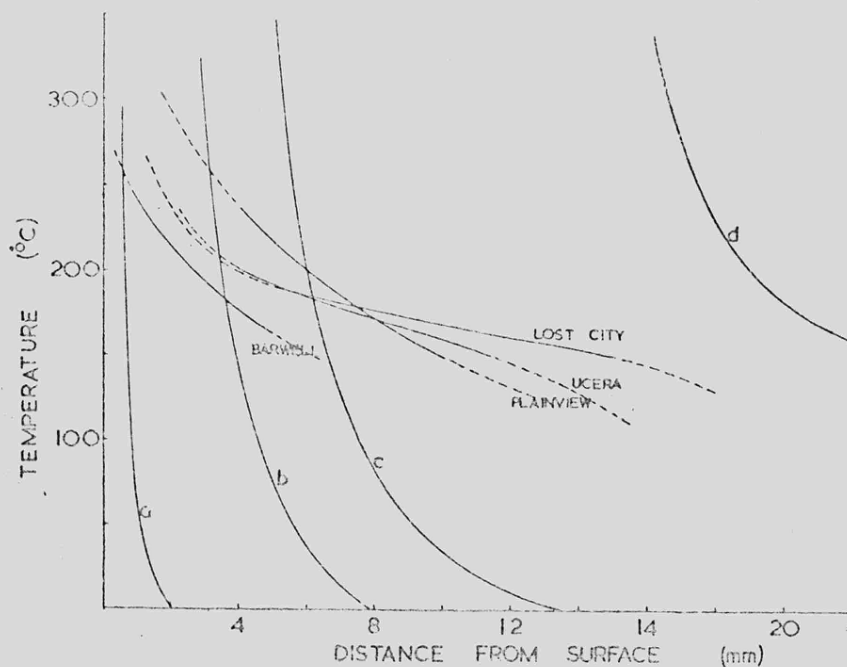
Figure VII.9 A comparison of the theoretical temperature profiles
with those obtained by TL measurement. a and b are for ablation
rates of 0.25 and 0.05 cm/sec, c and d are for zero ablation
for 10 and 100 second luminous flight times respectively. The
TL-derived gradients for Lost City and Ucera are from Vaz (1971
and 1972).

measured by TL are compared in Figure VII.9. Two main observations
may be made. Firstly that there is good agreement between theory
and experiment in the temperatures experienced at depths of 5 -
10 mm (about 200°C). From this we may conclude that steady-state
conditions do not apply to the regions in which TL gradient is
caused by atmospheric heating. Instead, the TL measurements infer
a luminous flight time in the order of 10 seconds, since 1 second
would allow a temperature of 200°C to penetrate less than a
millimeter or so, and 100 seconds would permit temperatures this
high to penetrate 20 mm. However, the Allende results show that
orientation, and so presumably ablation, is still a major factor
in controlling the temperature gradient.

Secondly, the gradients at depths of 5 - 10 mm measured
by TL are always much lower than those predicted by theory. The
TL results are 15 - 20°C/mm (Barwell), 20°C/mm (Plainview), 15 -
20°C/mm (Allende) and published values for Lost City are 25°C/mm
(Prachyabrued et al., 1971) and 15°C/mm (Vaz, 1971). The theory
predicts gradients in the order of 70°C/mm at these depths. This
is obviously an important discrepancy to explain if the atmospheric
TL gradients are to be completely understood. The major factors
in the theoretical treatment are the thermal properties, for example
a higher thermal conductivity would give a lower temperature
gradient. However, the thermal conductivity would need to be
greater than for pure iron in order to resolve the discrepancy
this way. Instead, it is necessary to examine more closely the
TL-derived temperature gradients.

VII.4d   <u>Pre-heating curve and pre-heating times</u>

The major unknown in the TL procedure for measuring

temperature gradients is the duration of pre-heating. This will

be examined in this section. From the considerations discussed

in Section I.2 it can be readily shown that the number of trapped

electrons remaining after heating for t_p seconds at a temperature

of T_p is

$$n_o = n_i \exp \left(-st_p \exp \left(-E/kT_p \right) \right)$$

where n_i and n_o are the number of trapped electrons before and

after pre-heating, s and E are the trap parameters (the "s factor"

and energy) and k is the Boltzmann constant (Garlick, 1949). Since

the intensity of the TL is proportional to the number of excited

electrons (i.e. first order decay)

$$\frac{I_p}{I} = \exp \left(-st_p \exp \left(-E/kT_p \right) \right)$$

describes the proportional drop in TL intensity after pre-heating.

s is about 10^{11} sec^{-1} (Prachyabrued et al., 1971) and E is about

1.2 eV (see Chapter IV) so that the drop in TL vs. pre-heating

temperature may be calculated (Figure VII.10). The agreement with

the experimental results is excellent, and lends support to the

theory and the E and s values used. The need to know the pre-

heating time is also emphasised by this figure. The pre-heating

time for the meteorite is probably very similar to the luminous

flight time.

A short luminous flight time would therefore increase the

temperatures that the TL would appear to be measuring. However

it would not change the value of the TL-derived temperature

gradients but merely displace them vertically (Figure VII.11),
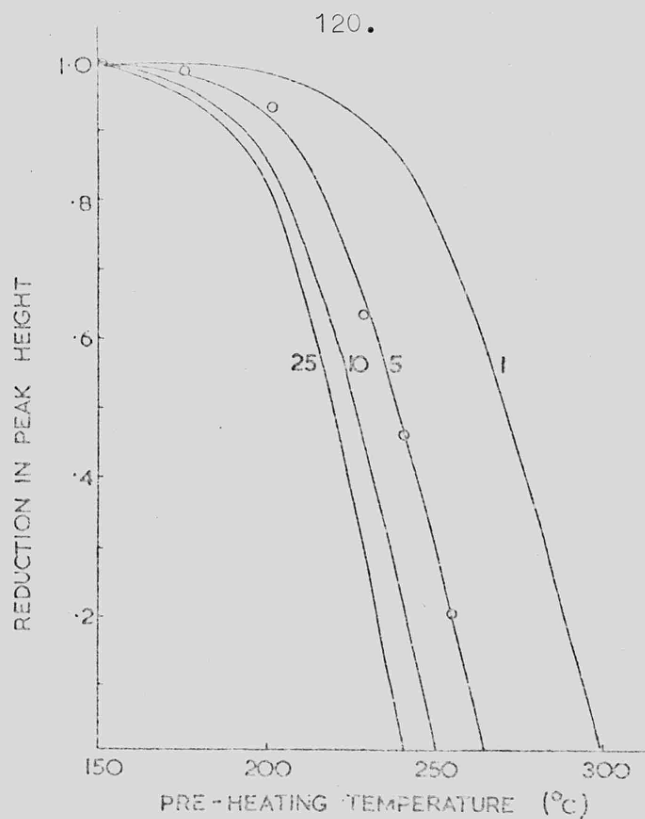
Figure VII.10 The calculated drop in LT after pre-heating to various temperatures for 1, 5, 10 and 25 seconds. The circles represent the experimental values shown in figure VII.2.
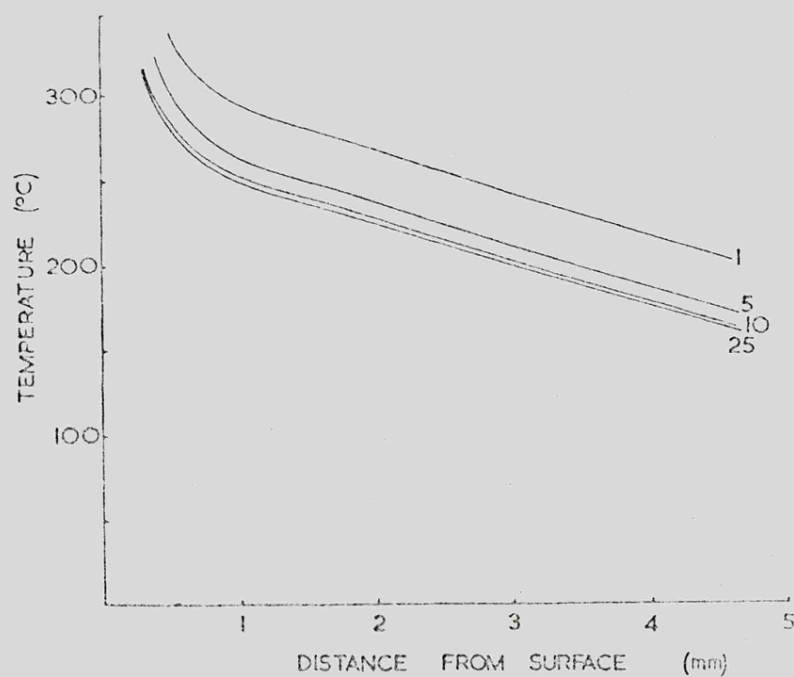
Figure VII.11 Temperature profiles for the Barwell meteorite assuming various luminous flight times and the theoretical calibration curves in figure VII.10. The time assumed changes the range of the temperatures concerned but does not change the gradient.

because the slopes of the pre-heating curves are similar for all

values of t_p.

The explanation for the difference between the theoretical

and observed temperatures gradient would appear to lie elsewhere

in the experimental procedure, possibly with the finite thickness

of the specimens cut from the bar.

VII.5 Conclusions

Although in detail there are worrying discrepancies

between the theoretical temperature gradients and those measured

by TL, in broad terms there is a measure of agreement. Temperatures

in the order of $200^{\circ}C$ have usually penetrated no further than 5 -

10 mm, which is consistent with a luminous flight time of the

order of 10 seconds. Orientation is an important factor in

determining these gradients, and they may therefore be used to

complement morphological and fusion crust studies. Since the

production of an innermost zone in the fusion crust takes a shorter

time than a measurable temperature gradient, the existence of the

former is a pre-requisite to the existence of the latter. This

may be used as a check prior to TL measurement.

CHAPTER VIII

PREATMOSPHERIC TL GRADIENTS IN METEORITES

VIII.1 Introduction

Observations on the variation in TL intensity throughout

a meteorite have been made by Lalou et al. (1970) and Vaz (1971).

The French group measured the variation along five cores taken

from the Saint-Séverin amphoterite, and Vaz measured the TL along

two bars from the much smaller Ucera bronzite. Both found

considerable depth dependence in the TL intensity. Whether TL

drops off with depth as the primary bombarbarding radiation is

attenuated, or whether it builds up with the cascade of secondary

particles is not clear from the observations. Spallogenic

nuclides show both kinds of behaviour. However, given that there

is a depth dependence of some kind, by measuring the TL intensity

across a large slice of meteorite it should be possible to build

up contours of equal TL intensity which reflect the preatmospheric

shape. This is the aim of the rest of this thesis. In this

chapter the ground-work is laid for an attempt, described in more

detail in the next chapter, to determine the preatmospheric shape

of the Estacado meteorite.

The preatmospheric TL gradients that have been discovered

are first reviewed for each meteorite separately. The nature of

cosmic ray interactions are then briefly discussed in order to

see what they lead us to expect concerning the cosmic ray produced

TL. As will be shown later, it is very probable that an

important part of the TL results from cosmic ray interactions.

Intimately associated with these considerations is the mechanism

for the production of TL and the factors controlling its

intensity. Finally the situation as far as it concerns the use

of TL to determine preatmospheric shape is reviewed.

VIII.2 Results

VIII.2a   The Allende Meteorite

The Allende, Mexico, meteorite is very large, the

recovered mass probably being about 2000 kg (Clarke et al., 1970).

It fell on the 8th February, 1969, and stones were strewn over an

area exceeding 300 km^2.

The specimen used here (NMNH 3636) was a completely

encrusted 67g stone, roughly 3 cm in diameter. A 4 mm thick

central section was removed from the stone using the Microslice II

diamond saw. From this eight bars were removed (a - h, see Figure

VIII.1). They provided 106 specimens for which both natural and

artificially induced TL was measured.

The TL of Allende is difficult to interpret for two

reasons. Firstly, Allende is an extremely heterogeneous meteorite,

with many isolated pockets of high TL. Secondly, numerous TL-

bearing minerals are present (see Section III.3). For our purposes

the most suitable TL is the 200°C peak. This TL is present in

natural samples (unlike the 140°C peak) and is more widely

distributed than the most intense TL (type 6 — see Chapter III).

Measurements referred to here are therefore restricted to the

types 3, 4 and 5 glow curves, as defined in Chapter III. Neverthe-

less, even the mineral responsible for this luminescence is

extremely heterogeneously distributed, and TL gradients cannot

reasonably be expected from the original, unmodified, natural
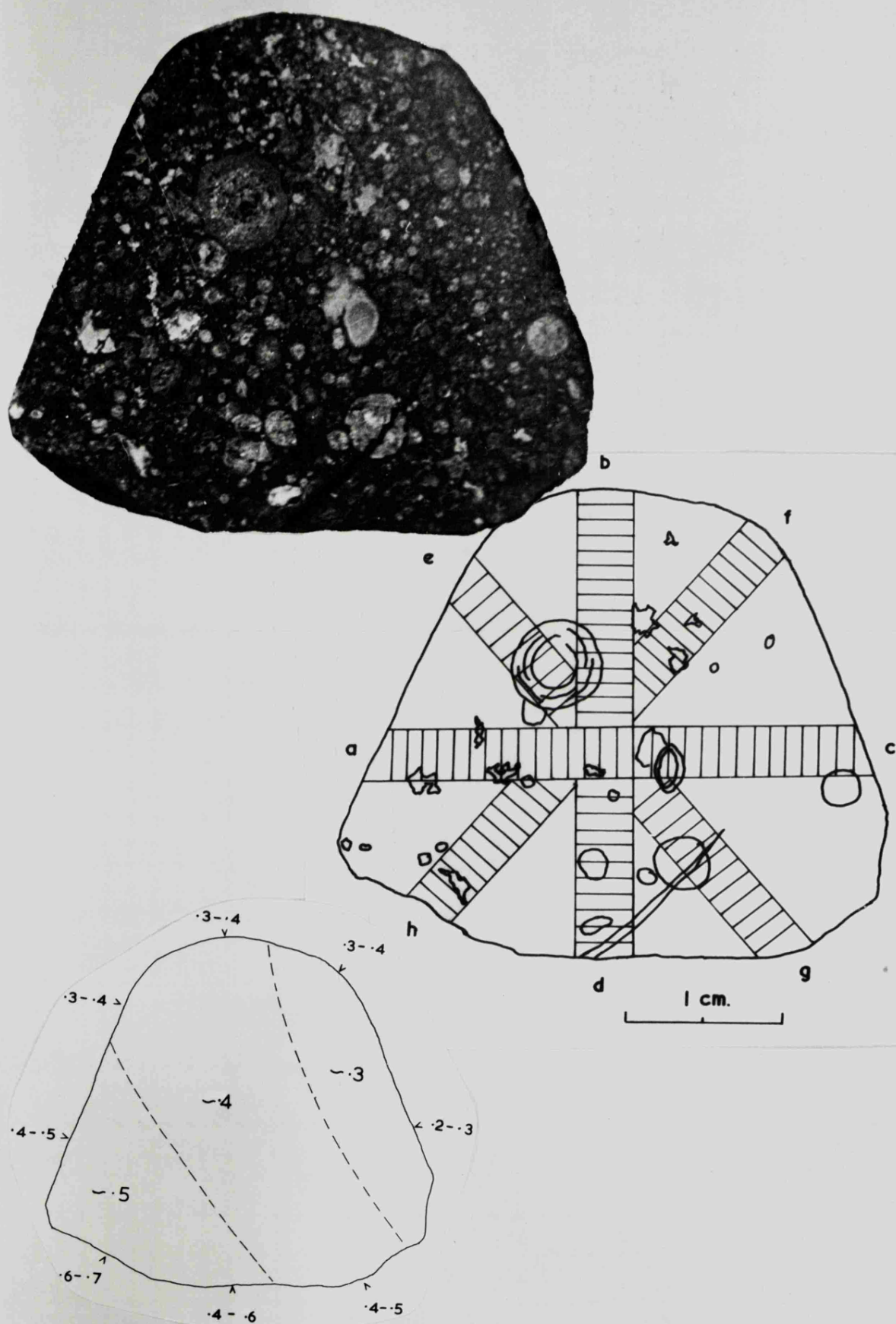
Figure VIII.1 A photograph of the slice from the Allende
meteorite used in this study, with a sketch showing the positions
of the 106 specimens cut from the slice. The bottom illustration
shows the variation of the intensity of the 200 °C peak over
the slice.
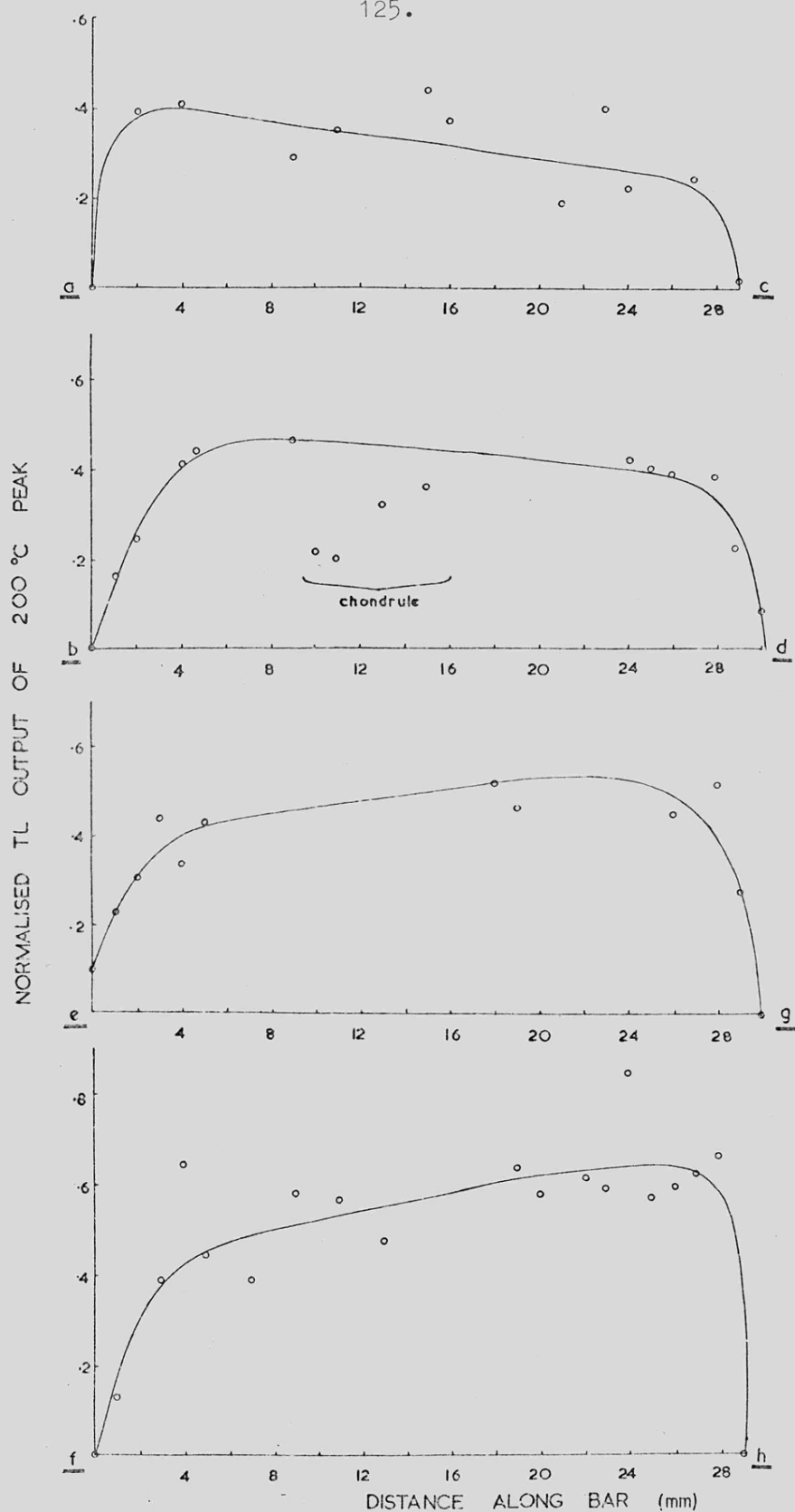
Figure VIII.2 Distribution of the TL intensity along bars ac, db, ef and hf. The area under the natural curves has been normalised to the area under the curves produced by drained powder that has been irradiated to about 50 krad by γ-radiation from a Co-60 source.

curves. In normalised curves. where the TL is expressed as the
ratio of the natural to the artificially induced TL, some
trends are discernable (Figure VIII.2). These trends can then be
transferred to the original slice as contours of equal
intensity (Figure VIII.1).

VIII.2b   The Plainview Meteorite

The Plainview meteorite is a brecciated bronzite found in
1917 (Merrill, 1917; 1918). Additional fragments were recovered
in the ninteen-thirties (Nininger and Nininger, 1950) and the
total amount of material now known is over 700 kg (Hey, 1966).
It was therefore a fall of considerable size. The piece examined
here (Figure VIII.3) is a slice taken from a completely encrusted
stone, and is that referred to in Section VII.3c. Figure VIII.3
gives the location of the two 2 x 4 mm bars along which TL
measurements were taken. The xenoliths and matrix are also shown
diagrammatically.

38 and 41 specimens were taken from the 7 and 4 cm bars
AB and CD respectively, and both the natural TL, and the TL after
irradiating the drained powder to 46 krad, was measured. The
results are presented in Figure VIII.4. In both bars the natural
TL tends to show a gradient. In the case of the shorter bar the
scatter near the centre of the slice coincides with a particular
xenolith, but otherwise the trends are not correlated with
structure and appear to be genuine. The artificial TL shows a
similar trend and this has important consequences which will be
discussed later. Finally, the ratio of natural to artificial TL,
unlike the Allende case above, shows little or no trend, with
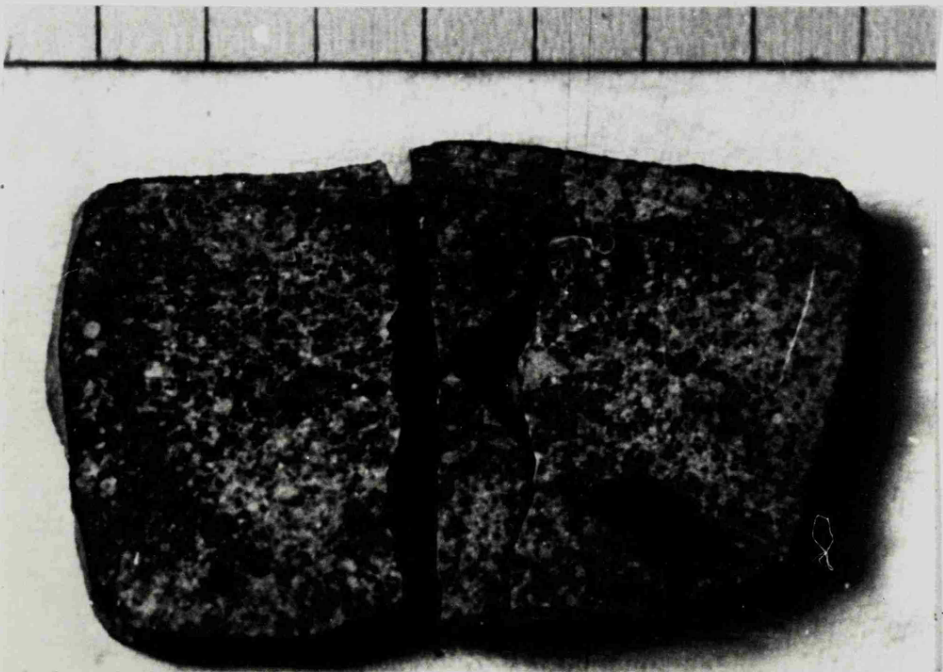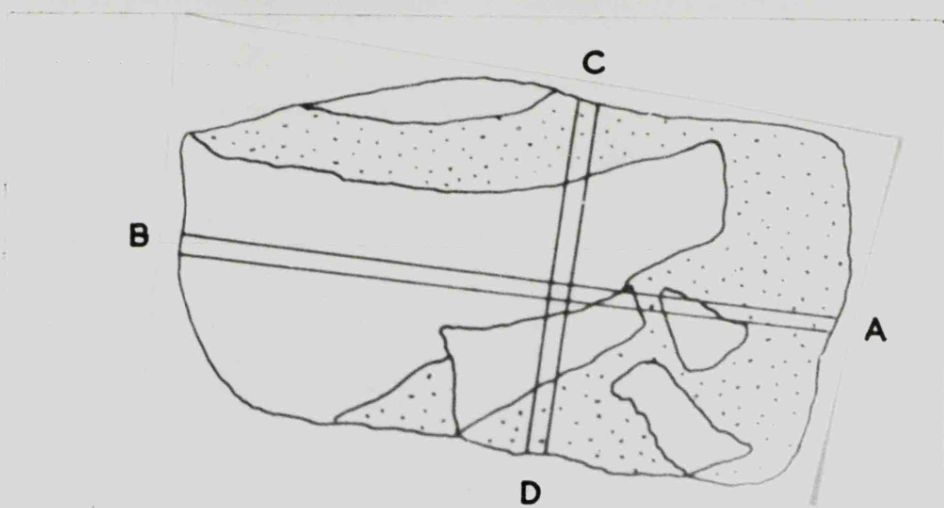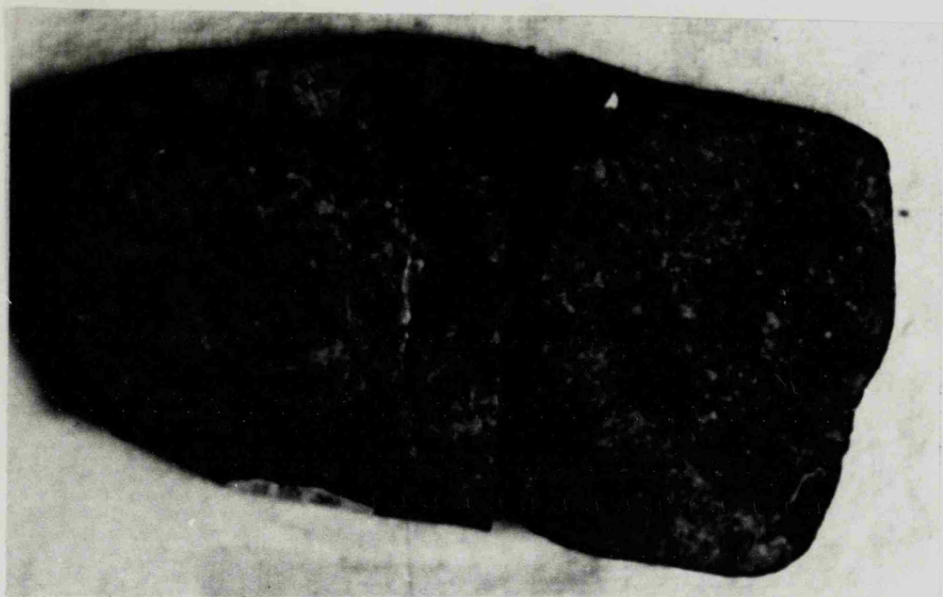
Figure VIII.3 Photographs and a sketch of the Plainview slice used in this study. The scale is marked in centimetres.
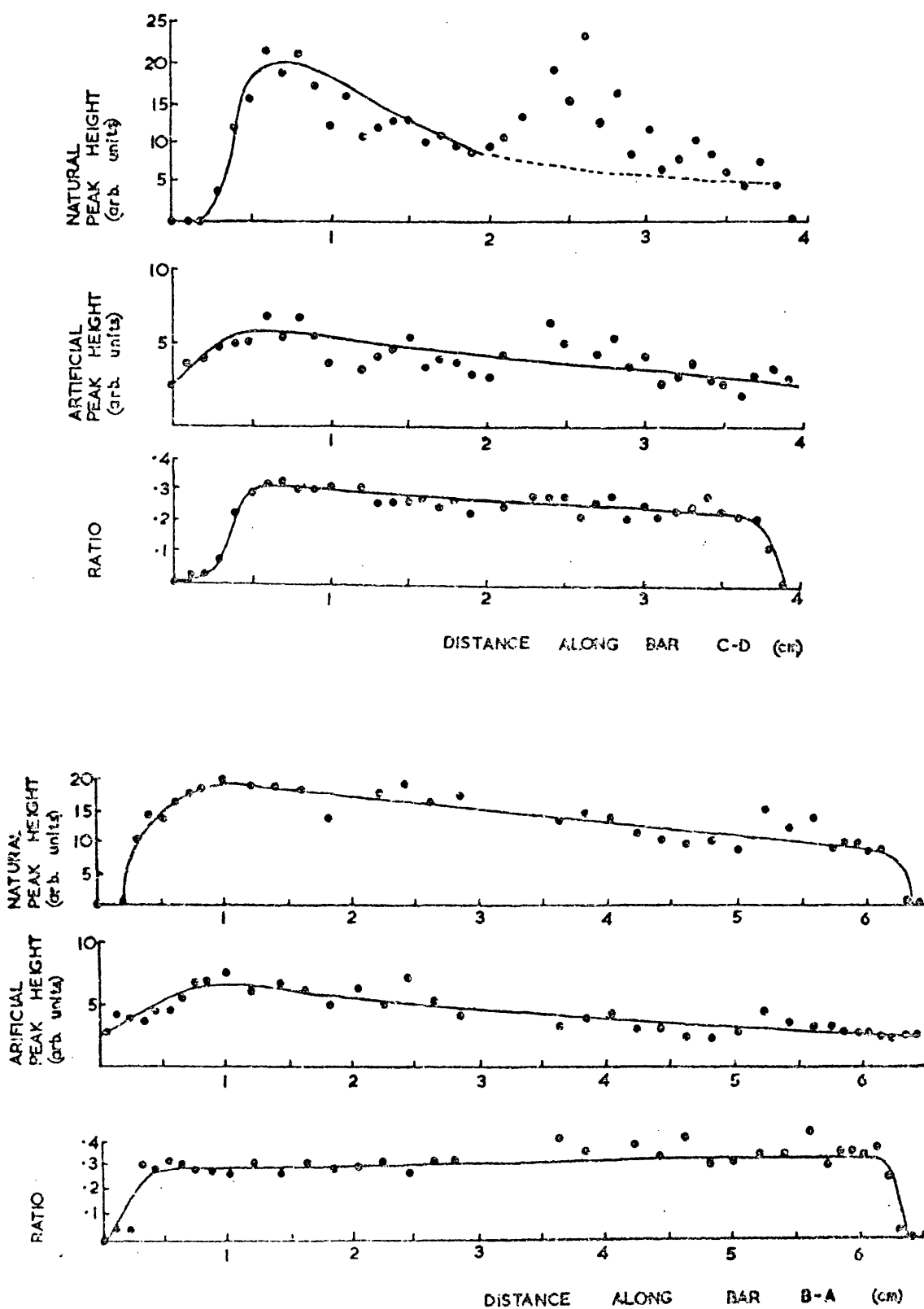
Figure VIII.4   Variation in the thermoluminescence along two bars from the Plainview slice.

considerably less scatter than the other curves because the effect of sample inhomogeneity has been removed. By way of summary the natural TL is diagrammatically superimposed on the slice and possible contours derived in Figure VIII.5. Over about 10 cm there appears to be a 60% drop in TL.

VIII.2c   The Ucera Meteorite

Vaz's results for the TL distribution along a bar from the Ucera bronzite are shown in Figure VIII.6. A drop of about 30% over 10 cm is observed in the natural TL. Also shown in this figure are the results obtained by our apparatus on material provided by Dr. Vaz. The maximum deviation between the results of the two laboratories is about 7% and the average is a few percent. Since we both claim about 5% repeatability this agreement is very good. The six samples Vaz supplied to us were drained and irradiated to about 46 krad by Co^{60} -rays. The TL after irradiation shows too much scatter to yield conclusive results concerning a trend in their intensity along the bar, but clearly they do not exclude such a possibility.

The Ucera meteorite is very small compared to the recovered mass of the preceding two meteorites: only a single 5 kg stone has been recovered.

VIII.2d   The Saint-Séverin Meteorite

Considerable effort has been put into measuring cosmic-ray interaction effects in the Saint-Séverin meteorite. Spallogenic gases were examined by Schultz et al. (1973) and charged-particle tracks by Lorin and Poupeau (1973) and Lal et al. (1969). Its
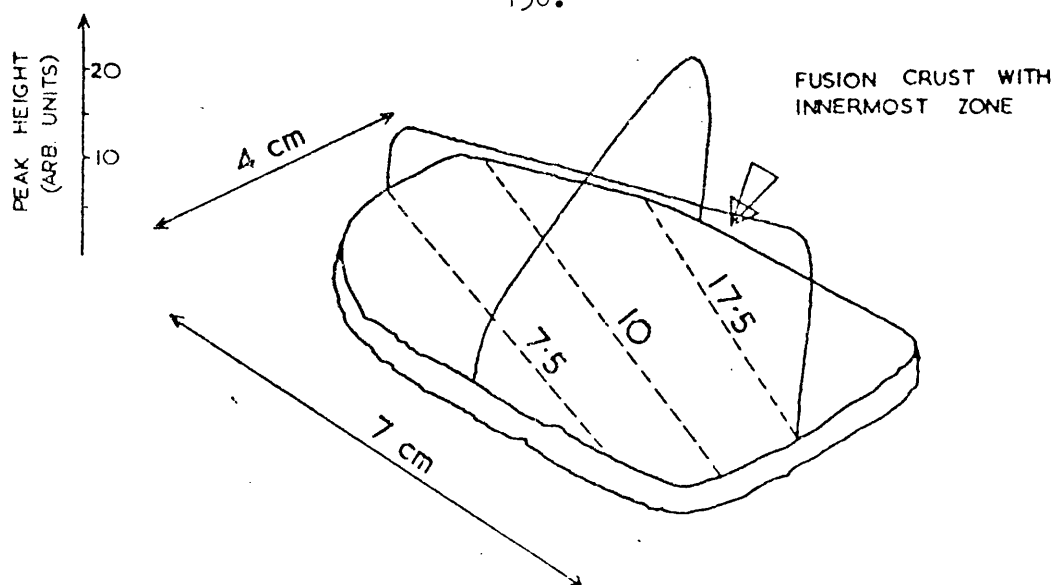
Figure VIII.5 Schematic representation of the natural TL in
the Plainview slice. The dotted lines are possible contours
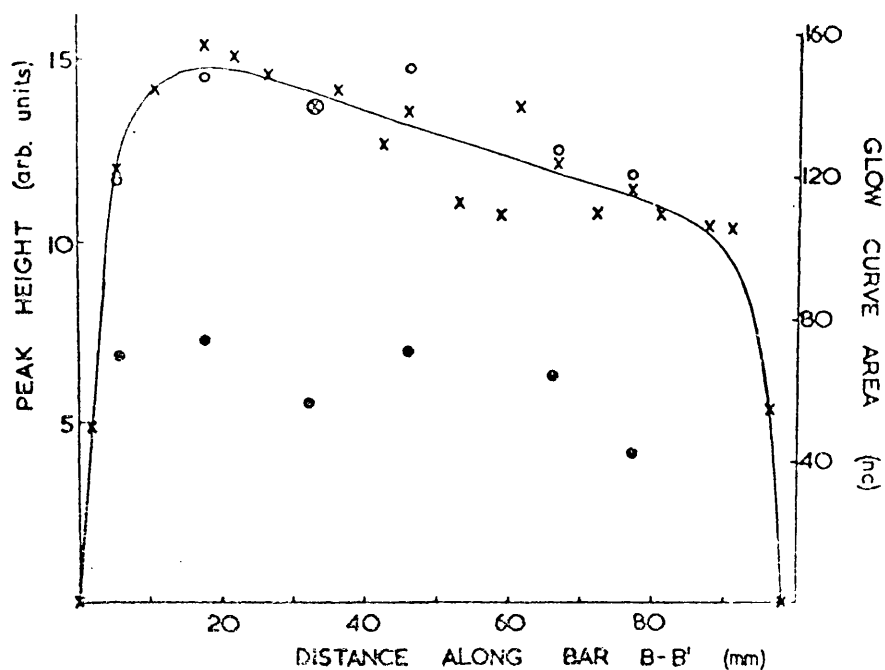
Figure VIII.6 Variation in TL along bar B-B' from the Ucera
meteorite. Crosses are point determined by Vaz (1971a) for the
natural TL, circles are values determined in this work. The
dots are values determined in this work for drained powder
irradiated to about 50 krad. (The latter have been displaced
down 5 arbitrary units for clarity). The right-hand axis applies
to Vaz's results which are expressed in nanocoulombs.
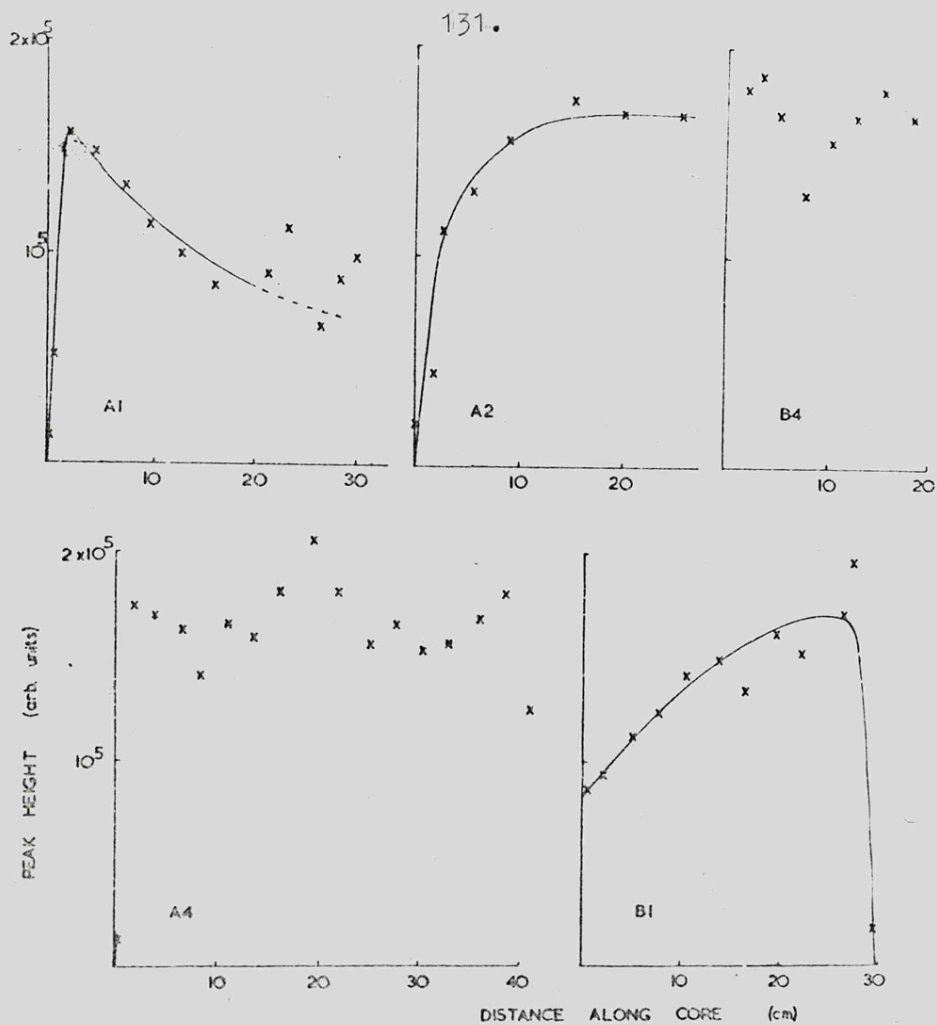
Figure VIII.7 Natural TL variation along five cores from the Saint-Séverin meteorite. (Data from Lalou et al., 1970a).
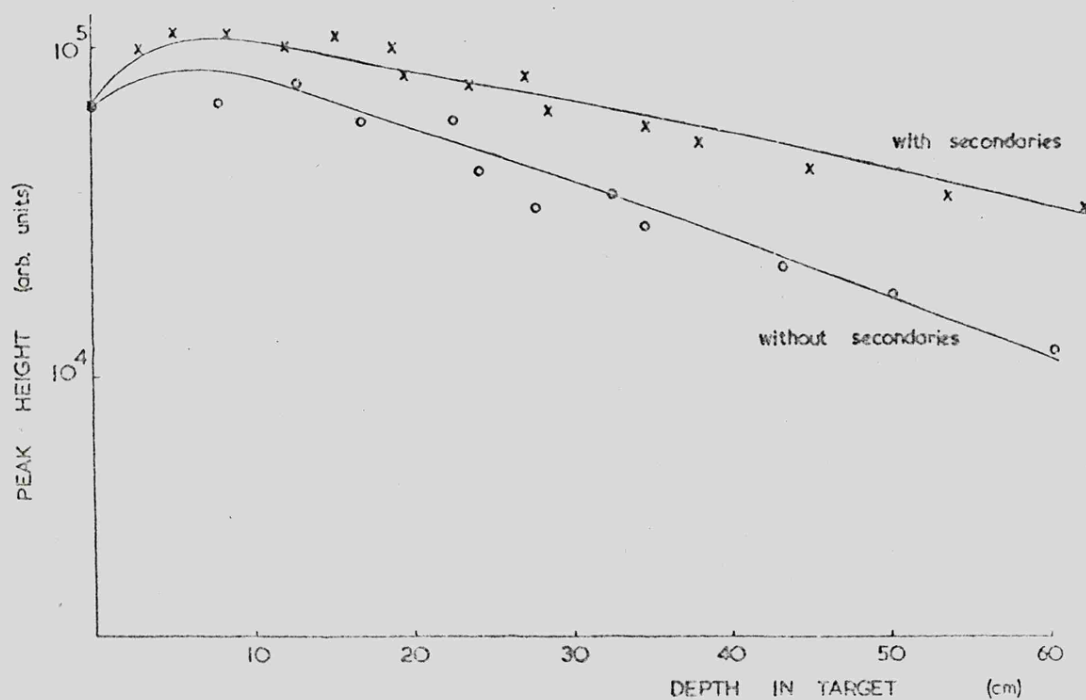
Figure VIII.8 Depth variation in the TL induced by 3 GeV proton bombardment in material from the Saint-Séverin meteorite. (After Lalou et al., 1970b).

thermoluminescence, as measured by Lalou et al. (1970a), is
shown in Figure VIII.7. Unlike the previous three specimens,
which were small wholly encrusted stones, the specimens of Saint-
Severin were both large (A, 113 kg and B 55 kg). The maximum
change in the natural TL intensity is a factor of two over about
30 cm (core Bl). No artificial TL measurements have been made on
the Saint-Séverin meteorite.

VIII.3 Discussion

      VIII.3a   Internal radioactivity and cosmic-ray bombardment

      Durrani and Christodoulides (1969) calculate that the dose
received from internal radioactivity is about 30 mrad/year. This
assumes chondritic abundances of U, Th and K and published values
of TL efficiency, and is probably accurate to within an order of
magnitude. The dose received from cosmic-ray bombardment at the
centre of a moderately sized meteorite may be estimated by the
arguments of the same authors to be in the order of a few rad/year.
However, different time-scales are involved in the two processes,
about 10^7 years for cosmic-ray bombardment compared with about
10^9 years for the lifetime of the meteorite. The total dose
received from the two sources may therefore be expected to be of
the same order of magnitude.

      The importance of cosmogenic and radiogenic TL has been
the subject of experimental investigation. A relationship between
artificial peak height and exposure age was found by Houtermans
and Liener (1966) for hypersthene chondrites. The correlation was
improved if an allowance was made for TL induced by internal
radioactivity by subtracting the TL of Farmington, which has an

exceptionally low exposure age, from the artificial TL
measurements. In such a meteorite the TL must be entirely
radiogenic. Liener and Geiss (1968) found a relationship between
artificial peak height and K/Ar age, although the correlation
was not good (about 0.6). Studies such as these, which attempt
to relate artificial TL to age, presuppose that all the traps
present result from radiation damage. It seems therefore that
both internal radioactivity and cosmic-ray bombardment may play a
significant part in determining the number of traps, and therefore
the artificial TL in meteorites.

Additional evidence for a cosmogenic origin for some of
the traps is shown by our work. The Plainview results (and
possibly the Ucera results) show that there is a gradient in the
TL artificially induced in drained material. Artificial TL is a
measure of the number of available traps, and since it varies
along the slice suggests that at least some of the traps are
the result of cosmic ray bombardment. This is contrary to a
finding of Hoyt et al. (1970) who claimed that since the number
of traps in lunar samples did not decrease after annealing at $800^{o}C$
they were not due to radiation damage. No doubt there are many
kinds of traps and luminous centres depending on the chemistry and
history of the specimen.

We feel justified in considering at least some of the TL
in meteorites to be a cosmic ray interaction product, along with
spallogenic isotopes and charged-particle tracks.

VIII.3b   Isotope gradients in meteorites

The rate of production of a given nuclide is governed by

the cosmic ray energy spectrum, because the reaction cross

section is proportional to the energy, and the rate of production

to the number, of bombarding particles. This energy spectrum is

probably the major unknown, but some success has followed from

assuming a power-law spectrum, $f(E)dE = f_o E^a dE$. From this Geiss

et al. (1962) showed that the number of nuclides produced is

$N(dA) = (dA)^{-n}$, where n, (which equals $1.5a - 0.5$) is the

irradiation hardness. dA is the mass number difference be-

tween target and product. Particle bombardments of greater energy

(hardness) therefore give products with greater dA. Since higher

energies exist nearer the surface n is a function of depth. We

can therefore predict a depth variation in the production rate

of any given isotope, and in fact the measurement of n, for

example by $^3He/^{21}Ne$ (Ebert and Wänke, 1957), is an important

means of determining preatmospheric depth (Nyquist et al., 1973,

and Table VI.4).

Isotope gradients were first measured in iron meteorites

in 1953 by Paneth et al. Since then repeated observations have

been made, and have been reviewed by Kirsten and Schaeffer (1971).

The purposes of such studies have slowly changed with time, being

aimed originally at explaining the excess helium, then at

determining preatmospheric shape and mass and now at measuring

the production rates of various nuclides in order to determine

exposure ages.

A theoretical expression for the rate of production of a

given nuclide was produced by Ebert and Wänke (1957) based on a
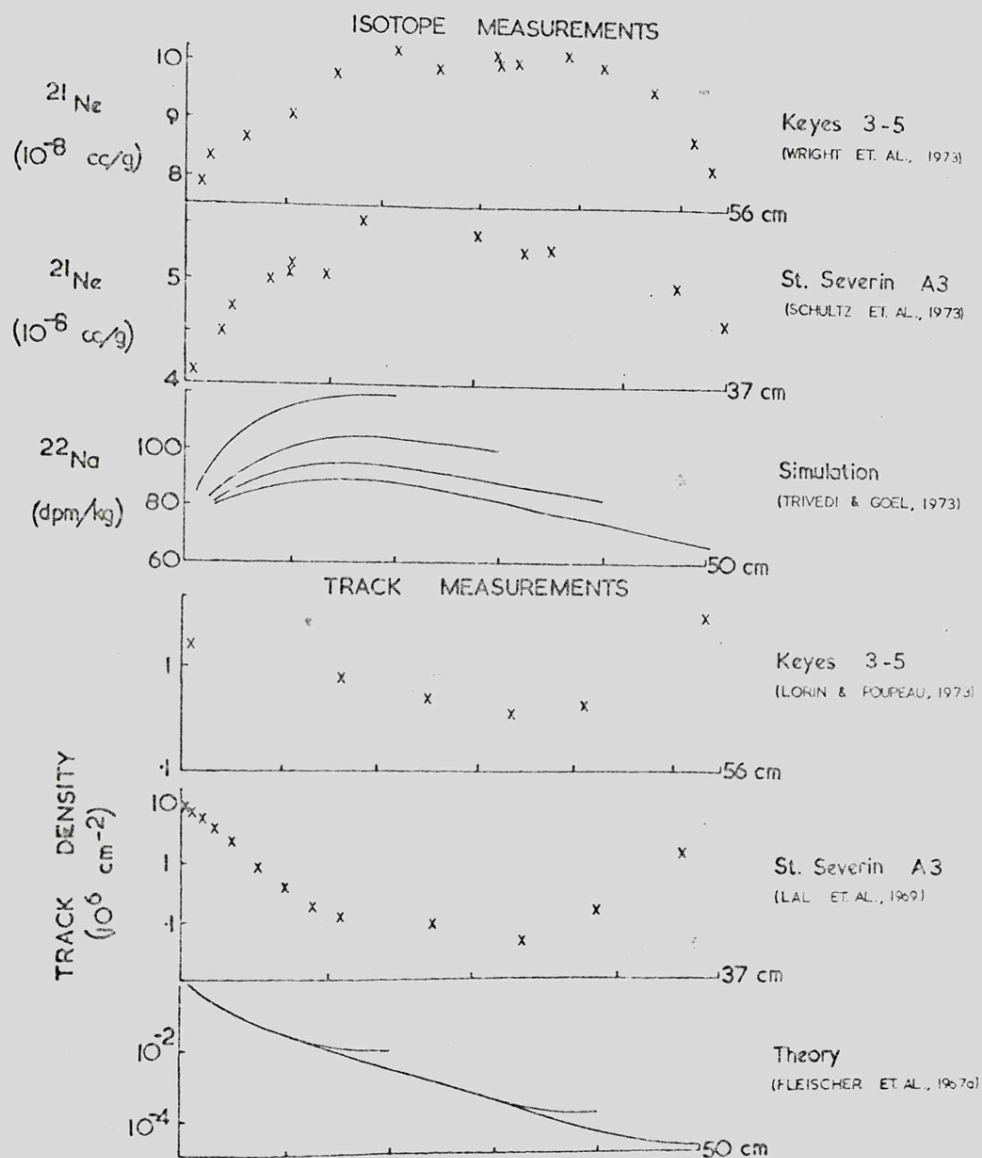
Figure VIII.9 Depth variation in spallogenic isotope content
and charged-particle track density along cores from the Keyes
and Saint-Séverin meteorites. Also given are variations in
spallogenic nuclides predicted by thick target measurements
and theoretical results for track densities. Both are calculated
for meteoroids of a variety of radii.

line of reasoning by Martin (1953). The expression has been

repeatedly used and seems a good representation of the phenomenon.

The production rate of a given nuclide, P, is given by

$$P = A \left[\int_0^{2\pi} \int_0^{\pi} e^{-k_a x} \sin \theta \, d\theta \, d\emptyset - B\left(\int_0^{2\pi} \int_0^{\pi} e^{-k_s x} \sin \theta \, d\theta \, d\emptyset \right) \right]$$

where A and B are constants (B reflecting the relative importance

of the secondaries) k_a and k_s are constants of nuclear parameters

(equal to NDs_a or $s R/M$, where N is Avagadro's number, M is the

average atomic weight, D is density, s the appropriate reaction

cross section, and R the preatmospheric radius) and x is depth/R.

The second term allows for the secondary radiation which is clearly

present. The peak in production 10 - 20 cm into the targets in

thick target measurements is interpreted as the result of the

build up of secondary radiations. More recently a semi-

theoretical formulation of Kohman and Bender has been applied to

both iron and stone targets (Kohman and Bender, 1967; Trivedi

and Goel, 1973).

Secondary radiation plays an important part in determining

the isotope gradients, and this may also be true of TL production.

Depending on the size of the body, the rate of nuclide production

may even be highest at the centre (Figure VIII.9). Fuse and

Anders (1969) suggested that ^{26}Al is constant throughout

meteorites (to within ± 15%) by observing a lack of covariation

between ^{26}Al abundance and the meteorite mass. This was confirmed

and extended to ^{53}Mn by Heimann et al. (1974). The explanation

offered is that the build-up of secondary particles almost exactly

balances the attenuation of primary radiation throughout the

meteorite. ^{26}Al and ^{53}Mn are both low energy products, having

small mass number difference from their targets. In iron

meteorites ^{3}He and ^{4}He, on the other hand, have large dA and

their abundance decreases approximately exponentially with depth

(see Signer and Nier's (1962) review for references). In fact

the only isotope gradient determinations to show a drop are those

of helium in iron meteorites. The two sets of inert gas

measurements along cores from stony meteorites show a build up

towards their centres (Figure VIII.9) even in ^{3}He since the target

mass numbers, and therefore dA, are generally lower. We may

conclude therefore that, except for helium in iron meteorites,

secondary interactions are extremely important in determining

the abundance profiles of spallogenic nuclides in meteorites.

VIII.3c   Charged-particle track gradients in meteorites

The fossil-track studies, however, show that only a very

small role is played in their genesis by secondary radiation.

Tracks are only produced by particles with an atomic number

greater than about 20 (Fleischer et al., 1967a). Galactic cosmic

rays are generally assumed to be about 85% protons, about 15% α-

particles and a few percent of heavy nuclei. At times of

maximum solar activity solar cosmic rays of 70% protons and 30% α-

particles may become important (Rancitelli et al., 1971). A

very restricted range of particles are therefore available for

producing tracks. Secondary radiation is only important when it

is capable of inducing fission in elements of small abundance in

localised patches (U, Th and K), when the fission fragments

produce characteristic v-shaped tracks on etching.

The depth dependence of track density caused by cosmic radiation is

$$\frac{dD}{dt} = 2 \times \left(\frac{dN}{dE}\right)\left(\frac{dE}{dR}\right)_{R_o} dR(z) \; F \exp\left(-\gamma R_o\right) \cos \alpha \; \sin \theta$$

where D is the track density at depth R_o, $dR(z)$ is the track length, F the fragmentation factor (which includes the effects of secondaries), ψ is the interaction probability cos α is a geometrical term (the importance of which was illustrated by Bhattacharya et al., 1973) and t is time (Fleischer et al., 1967a). dN/dE is the energy spectrum (for example the power-law used above) and dE/dR is the rate of loss of energy in the meteorite (estimated by simulation experiments). The results of these calculations and measurements in meteorites are shown in Figure VIII.9. The track density shows no tendency to build up with depth which confirms the expectation that secondary radiation is of little importance in determining the depth variation of tracks.

A number of important observations have been made by track studies on meteorites. The depth variation along cores in Saint-Séverin has been measured by Lal et al. (1969) and Amin et al. (1964) (unfortunately the cores used were not the same as those used for TL measurements) and along the Keyes cores by Lorin and Poupeau (1973). Using the depth variation equation above the burial depths have been calculated for 5 urelites (Wilkening et al., 1973), 36 chondrites (Fleischer et al., 1967b) and for Patwar and Saint-Séverin (Price et al., 1967; Cantelaube et al., 1969). In some instances space erosion rates (relevant to the low exposure ages of the stony meteorites) and preatmospheric masses have also been calculated.

VIII.3d   Comparison of TL, track and isotope gradients
in meteorites

Very few thick target measurements have been made on thermoluminescent materials. The only published results are those of Lalou et al. (1970b) which are reproduced in Figure VIII.8. The data are based on specimens of Saint-Severin placed at various intervals along a 1 m rectangular block of 9 cm^2 cross-section. The effect of secondaries was introduced by surrounding this with sand containing fragments of iron. The bombarding particles were 3 GeV protons; this energy is believed to give a good representation of total cosmic ray energies (Trivedi and Goel, 1973).

The TL reaches a peak about 10 cm into the target, as expected from the inert gas calculations and thick target measurements, but drops off more gradually for the target designed to include the effect of secondaries. These results are evidence of an important role for the secondary particles.

Since charged particle tracks are produced by a very restricted range of bombarding particles they provide little guide to the behaviour of TL, which can result from the passage of any ionising radiation. The promotion of electrons to traps is probably a favoured process energetically since it involves an energy transition of only a few eV. The most energetically favoured nuclear reactions are those involving neutron capture, dA = 1, and require particles of about 100 eV, e.g. ^{35}Cl (n,γ)^{36}Cl. One may therefore argue that since secondary radiations become more important for lower energy products, they will be of paramount importance for the production of TL.

Although the ease of trap population may be assessed by the size of the energy gap between the valence band and the conduction band there is no comparable way to evaluate the energy requirements for trap production. However, the existence of possible depth effects in the trap distribution means that the process of allowing for sample inhomogeneity by "normalising" (expressing the TL as the ratio of natural to artificial) is not always safe — sometimes one could remove a genuine depth effect. It is therefore always necessary to check artificial TL before using it to normalise. Hoyt et al. (1972) have also produced arguments against normalisation from their work on lunar samples.

The magnitude of the depth variations in TL presents an interesting case for speculation. The three small fragments, Ucera, Plainview and Allende, show large variations over very small distances (30% over 10 cm, 60% over 10 cm and 50% over 5 cm respectively) whereas the much larger Saint-Séverin meteorite varies at its steepest by 50% over 30 cm, usually much less. Cosmic ray induced variations are usually steepest at the outside of the preatmospheric body. In the case of a small meteorite, e.g. Ucera, a steep gradient is expected. However in the case of Plainview and Allende the inference is that these fragments were on the outside of the preatmospheric meteoroid.

VIII.4 Conclusions

The main conclusion to be drawn from the TL measurements through the Allende, Plainview, Ucera and Saint-Séverin meteorites is that there is a depth variation, presumably associated with cosmic ray bombardment. The Plainview data show

a gradient in the artificial TL distribution, which infers that normalisation as a means of allowing for sample inhomogeneity must be approached with some caution.

A comparison with other cosmic ray interactions leads us to expect secondary radiation to play an extremely important part in determining the nature of TL variation throughout a meteorite.

It is also noted that large variations across relatively small slices probably indicates near-surface irradiation. This being so it seems that the smallest Plainview and Allende specimens studied came from exterior faces of the preatmospheric body, and that larger fragments are interior masses.

CHAPTER IX

THE PREATMOSPHERIC SHAPE AND MASS OF THE ESTACADO METEORITE

IX.1   Introduction

In the early nineteen-sixties attempts were made to deter-
mine the preatmospheric shape of four iron meteorites from their
spallogenic gas contents. The attempts dealt mainly with the
Grant and Carbo irons, two sizeable meteorites with large cut
faces. Fireman (1958; 1959) determined contours of equal He^3
content, and by extrapolating these so as to completely enclose
the meteorites he derived minimal preatmospheric masses. Hoffman
and Nier (1958; 1959; 1960) made the same measurements, adding
He^4, but by fitting the depth-variation equation (Section VIII.3b)
were able to calculate actual preatmospheric masses. Signer and
Nier (1958) also considered Ne^{21} and Ar^{38}. These studies not only
enabled preatmospheric shapes and masses to be estimated but also
gave an indication of the various nuclear parameters (reaction
cross-sections etc.) involved in the spallation reactions, and
proved the general validity of the spallogenic production model
of Ebert and Wänke (1957).

No similar systematic measurement of the spallogenic
nuclides across a section of a stony meteorite has been made.
This is for the obvious reason that interpretation is considerably
complicated by the existence of a wide variety of target elements
in stones. However, depth variations along cores from the Saint-
Séverin and Keyes chondrites have been measured, and were
described in the previous chapter. Although they do not permit a
rigorous determination of preatmospheric shape they do allow semi-

quantitative estimates; for example the Keyes chondrite appears
to have been a 70 by 30 cm ellipsoid when it entered the
atmosphere, (Wright et al., 1973; Trivedi and Goel, 1973).
Another valuable tool for the examination of stony meteorites is
provided by charged-particle tracks, leading to estimates of the
preatmospheric shape of the Saint-Séverin meteorite (Canterlaube
et al., 1969) and the preatmospheric mass of the Patwar pallasite
(Price et al., 1967).

A third, and as yet untried, phenomenon available for
preatmospheric shape and mass determinations is thermoluminescence.
In this chapter we are concerned with an attempt to use TL to
evaluate these parameters for the Estacado meteorite. A large
(17 kg) slice of this meteorite is deposited in the British
Museum. It had previously been removed, approximately centrally,
from a 290 kg stone measuring 58.5 x 45.7 x 44.4 cm which was
found in Hale County, Texas, in 1883. The meteorite and slice
have been described by Howard and Davison (1906), and recently
the stone was analysed by Mason and Wiik (1963). It is an H6
chondrite (van Schmus and Wood, 1967). A second stone weighing
122 kg and measuring 30 x 30 x 50 cm was acquired in 1912 by the
American Museum of Natural History. The total known post-
atmospheric mass is therefore 412 kg.

IX.2   Method

A variety of meteorites with large cut faces were sampled
and their TL measured. Only the very smallest, which were recent
falls, had appreciable low temperature TL, but all displayed some
at higher temperatures (300 - 400°C). Estacado, besides

presenting the largest cut face, had by far the most intense high

temperature TL and was therefore chosen for this study.

A polythene sheet on which had been drawn a five centimeter

grid was placed over the slice. 2 - 3 mm long cores, 5 mm in

diameter, were then taken over the grid using a "Diagrit" diamond

drill operated in a hand brace and lubricated with distilled

water. The technique had previously been checked to ensure that

natural TL was not drained and that triboluminescence was not

created. 72 samples were taken in this way. Additional samples

were taken at the three fusion crust edges present on the slice

(Figure IX.2) and the results of measurements on these are

discussed in an earlier chapter (Section VII.3d). The 72 samples

were crushed and their magnetic component removed. They were

then sieved and the TL measured in the normal way, duplicate

measurements being made for all samples. Many samples had their

TL measured repeatedly to ensure constancy in the sensitivity of

the equipment. The drained material was then irradiated to about

50 krad by Co^{60} γ-rays and its "artificial TL" recorded. The

irradiated samples were allowed to decay at room temperature for

50 hours before TL measurement so that differential decay during

a run was insignificant.

IX.3   Results

Typical glow curves are presented in Figure IX.1. The

curves for the natural powder have a broad peak at about $370^{\circ}C$

and a very weak $250^{\circ}C$ peak, probably associated with weathering

(Section VII.3d). The total luminosity, i.e. the area under the

curve, was measured for each curve and the results are presented

Table IX.1

The TL intensity distribution over the Estacado slice

			1375	1190							(71, 72)
				3840							
				289							
	500	1030	1200	1470	1190						(64-69)
	3620	3960	4000	4020	3360						
	354	325	294	366	217						
1300	1260	1370	1370	1050	1430	1360	1200				(55-62)
4780	4400	4460	4040	4060	5240	442	3420				
311	282	484	332	291	364	275	226				
1160	1252	1500	900	1070	1300	1250	1170	1230			(46-54)
2840	4640	3880	2620	4860	3560	4100	4300	3960			
185	356	264	191	369	342	297	327	290			
1150	1170	1150	1210	1335	1380	1396	1156	1380	1100		(36-45)
4340	3940	3520	3600	3080	4480		3620	4000	3180		
356	270	293	270	263	410		311	311	309		
1040	1175	1300	1210	1245	1270	1280	1437	1345	1122	1150	(2535)
4100	3780	4820	4420	3640	4380	4400	3840	3940	3960	3520	
271	267	340	294	219	304	306	242	299	277	232	
1000	1180	1150	1310	1400	1270	1385	1330	1330	1120		(14-23)
3640	2980		3740	3800	3640	3240	3860	3600	3100		
274	259		336	307	291	269	377	298	259		
	900	1100	1075	1156	1250	1420	1285	1220	1370		(4-13)
	2160	3660		4200	4440	4520	3500	3960	4280		
	293	289		228	310	354	261	250	304		
						1125	1100	800			(1-3)
						4180	3620	3220			
						295	264	190			

The TL intensity is the area under the curves (i.e. total luminosity) and is expressed in arbitrary units. The numbers in parentheses are the specimen numbers allocated along the row, and for each specimen the intensities given are for the area under the natural curve (top), the area under HT (middle) and LT (bottom) in the curves of specimens that had been drained and irradiated to about 50 krad.
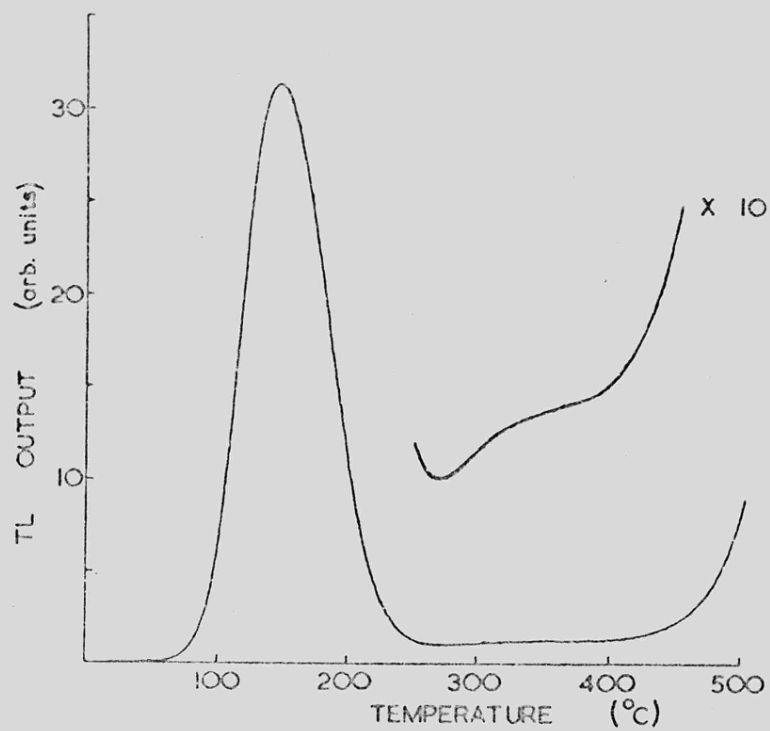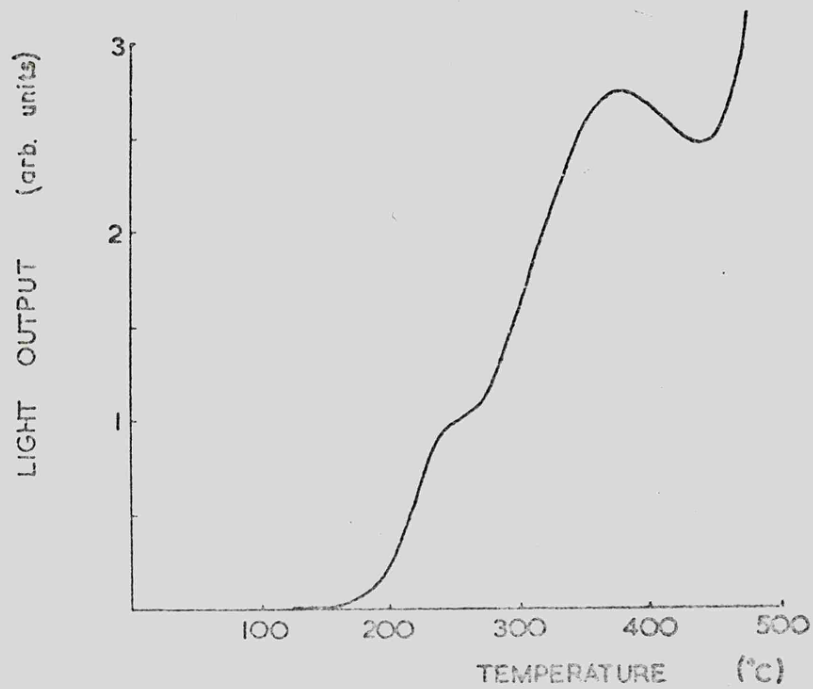
Figure IX.1 Glow curves of material from the Estacado meteorite.
Top, a curve for natural material; below, a curve for material
which has been drained of its natural TL by heating to 500 °C
and irradiated to about 50 krad by cobalt-60 γ-rays.
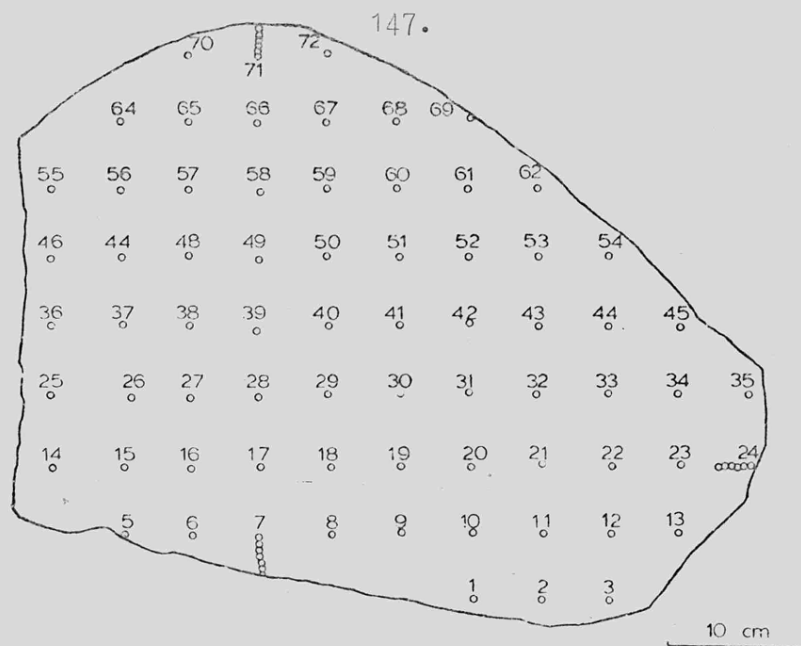
Figure IX.2 Location of the specimens over the slice.
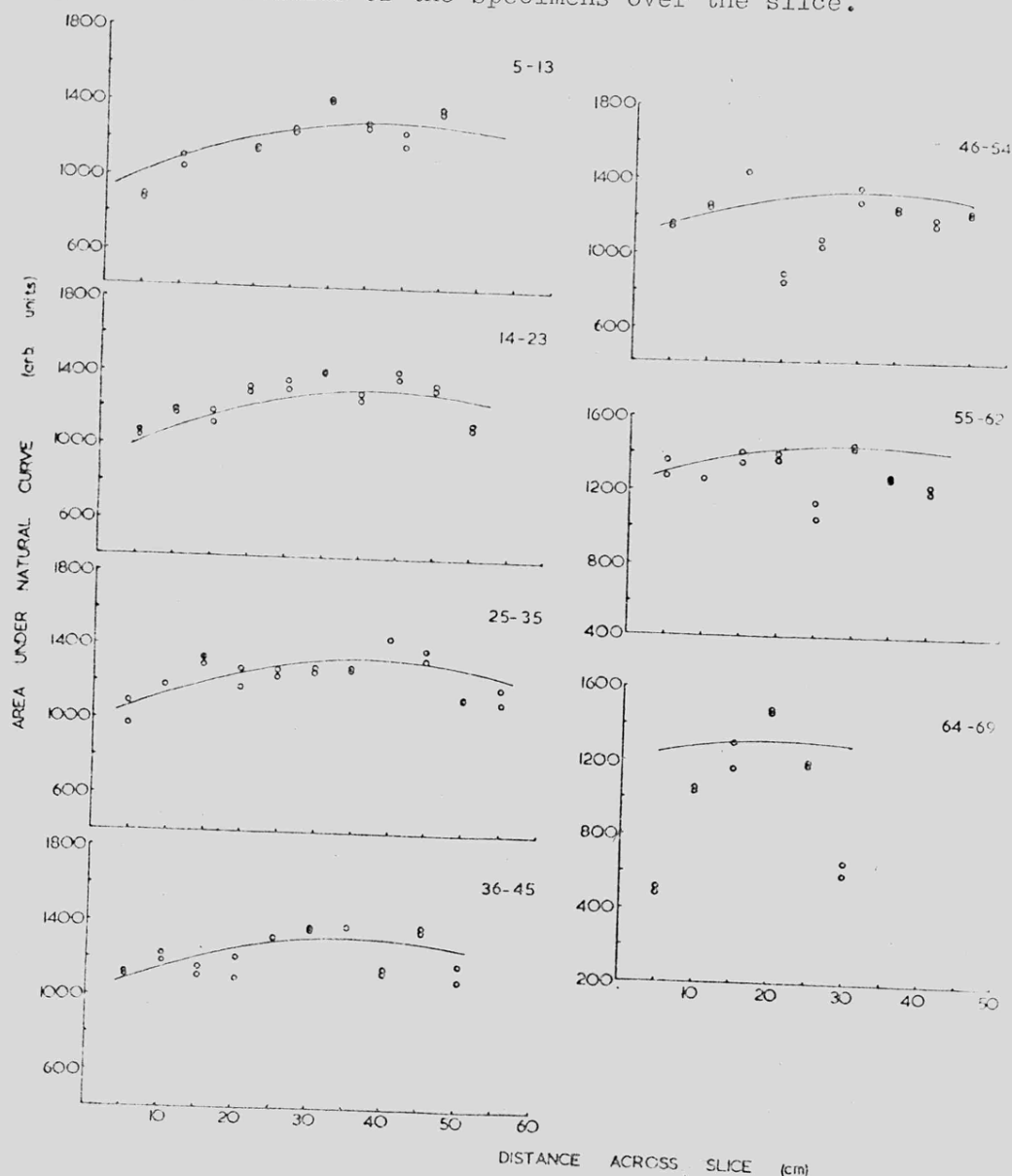
Figure IX.3 Areas under the natural glow curves as a function of distance across the slice for each row of specimens. The lines are least-squares fits of a second-order curve to all of the data. Duplicate measurements are shown for each specimen.

in Table IX.1 and in Figure IX.3. Also given in the table are the

areas under the curves obtained from specimens that had been

drained by heating to $500^\circ C$ and irradiated to about 50 krad with

Co^{60} γ-rays. The curves of irradiated specimens have a sharp

peak at $140^\circ C$ (LT) as well as some high temperature TL (HT). LT

is known to consist of two or possibly three peaks between 140

and $200^\circ C$ (Chapter III.5).

The lines in Figure IX.3 are obtained by least squares

fit to all the data — not just the row of specimens whose TL is

plotted. The data were fed into the KWIK R8 computer program

which fits a trend surface to a two-dimensional layout of data by

the method of least squares (Esher et al., 1968). The theory behind

the program has been simply but comprehensively explained by

Davis (1973) and a synopsis of it is given in Appendix : A.2

Curves described by a polynomial equation of any given order can

be fitted to the data and the standard statistical tests performed

to measure the goodness-of-fit. The test coefficient for attempts

to fit first, second, third and fourth order curves to the areas

under the natural curves, the areas under LT and HT in the

artificial curves, and the ratio of HT in the natural to HT in

the artificial curves are given in Table IX.2.

A significant fit has only been achieved for the area

under the natural curves. Davis (1973) points out that correlation

coefficients of 0.3 have been achieved with fourth-order curves

on randomly generated data. The F-test similarly indicates that

the area under the artificial curves and the artificial to natural

TL ratio do not give significant trends.

Table IX.2

Test statistics for trend surface analysis by KWIK R8

	First order		Second order		Third order		Fourth order	
	R	F-test	R	F-test	R	F-test	R	F-test
Area under natural curves	0.70	Yes	0.84	Yes	0.92	Yes	0.94	Yes
Area under LT (art)	0.29	No	0.39	No	0.46	No	0.60	No
Area under HT (art)	0.27	No	0.34	No	0.46	No	0.64	No
Ratio of area under HT (nat) to HT(art)	0.24	No	0.34	No	0.32	No	0.57	No

The correlation coefficient (R) and the results of the F-test for curves of first, second, third and fourth order fitted to the data. 'No' indicates that there is no significant trend at any level of confidence, 'Yes' indicates a significant trend at the 5% level of confidence.
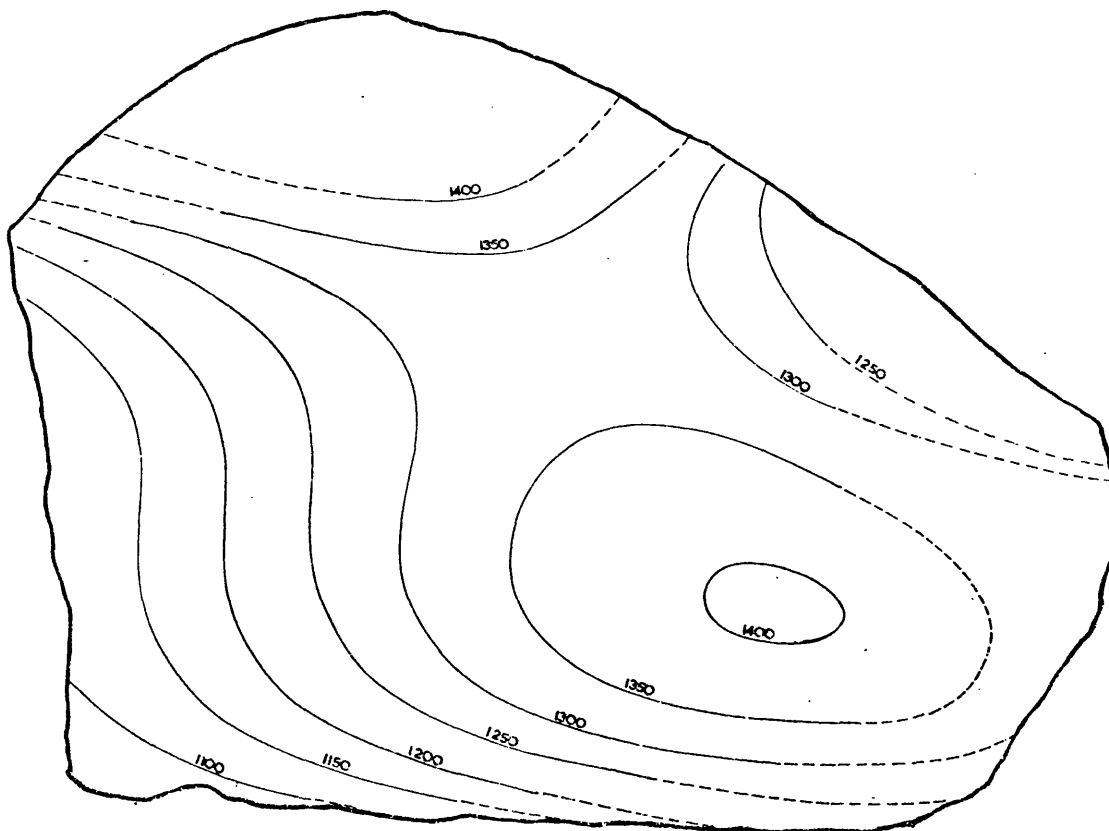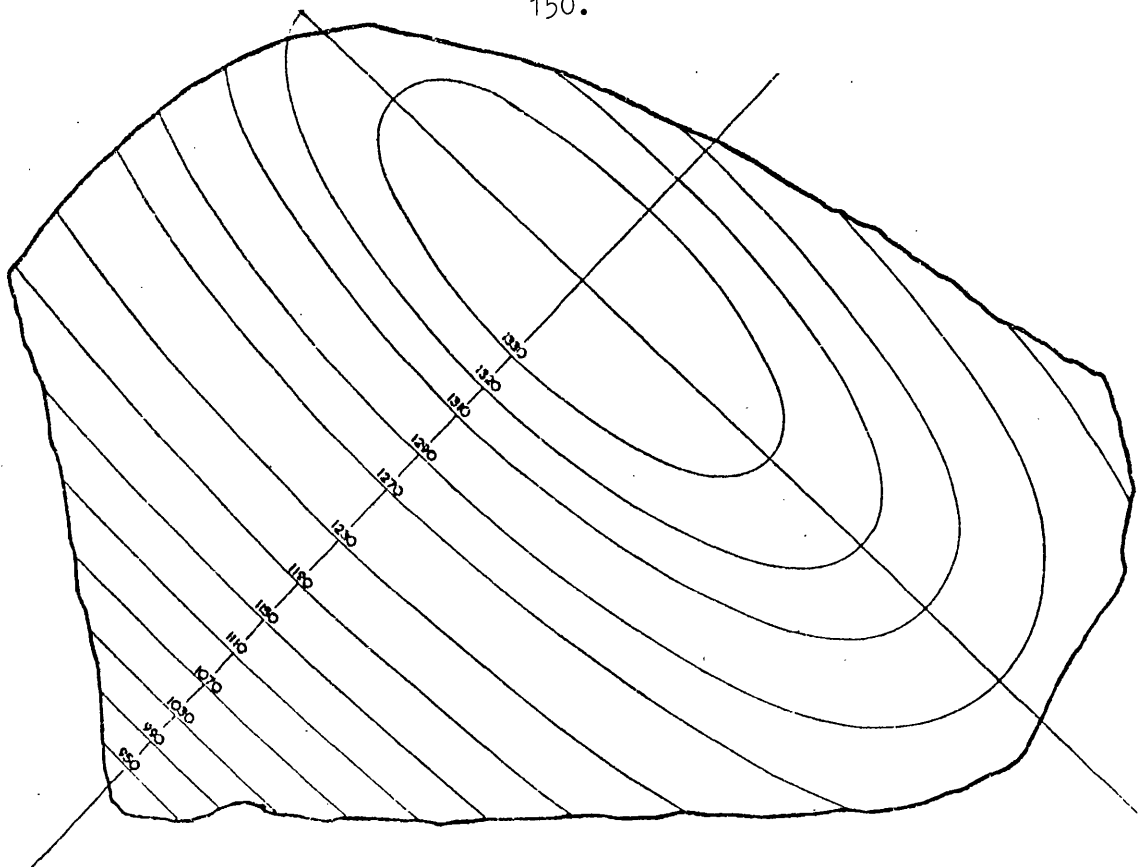
Figure IX.4 The second (top) and third-order fits to the area
under the natural glow curves. The second-order curve probably
reflects the preatmospheric shape of the meteorite.
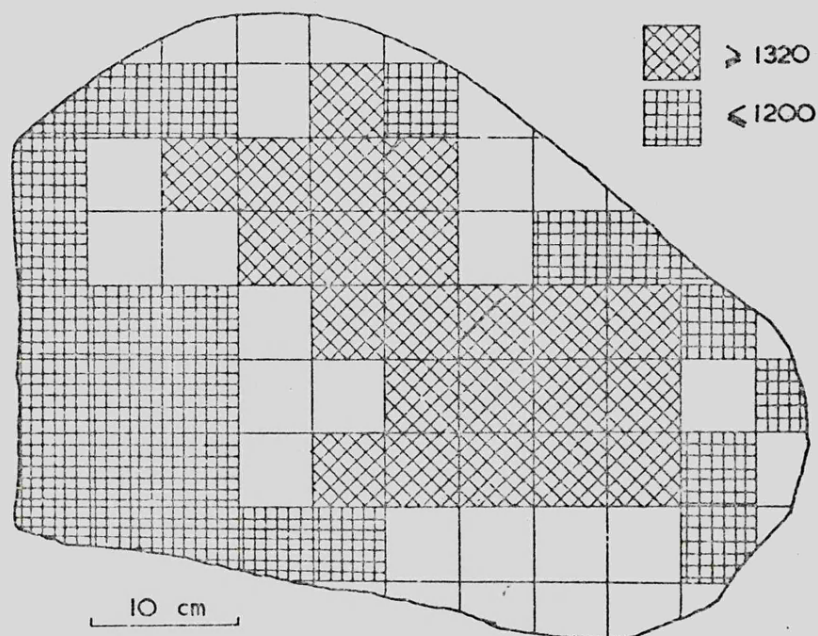
Figure IX.5 Areas under the glow curves (in arbitrary units)
as estimated from lines drawn by eye through the points in
figure IX.3 plotted across the slice.
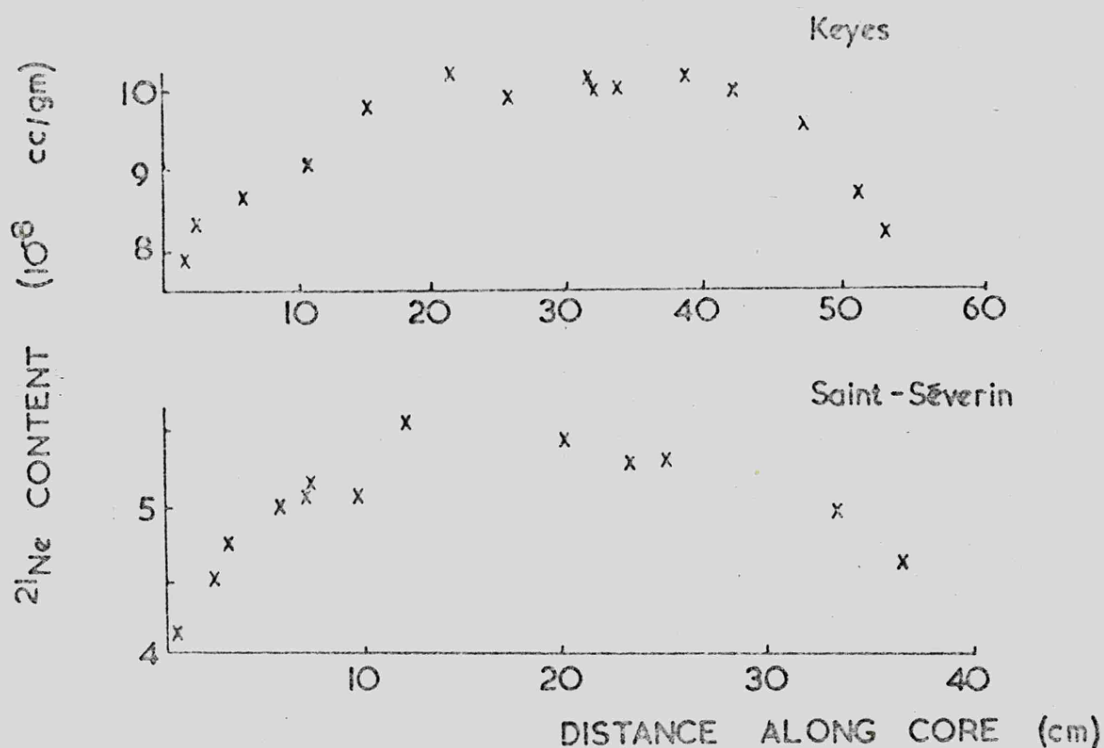
Figure IX.6 Variation in the concentration of a spallogenic
nuclide along cores from two meteorites. The profile for the
Keyes meteorite is from Wright et al. (1973) and that for
Saint-Séverin is from Schultz et al. (1973).

The area under the natural curves, however, produces fits

with good correlations with second, third or fourth order curves,

posing the question of which best reflects the overall trend in

the data and is least perturbed by spurious points. In this

instance it is clear that the third-order fit is already picking

up individual isolated high points, probably caused by a local enrichment

in the feldspar content. The best overall trend is therefore that

given by the second-order fit (Figure IX.4). Eye-estimates plotted

over the slice indicate a similar distribution and provide

confirmation of the computer-produced trend (Figure IX.5).

IX.4   Discussion

IX.4a   Preatmospheric shape

From the considerations of the previous chapter we expect

a depth-variation in TL intensity across the slice which reflects

the preatmospheric depth. The contours may therefore indicate

the preatmospheric shape of the meteorite. Similarly we expect

that secondary radiations play an important part in determining

depth variations in the TL of meteorites. The main evidence for

this was spallogenic isotope production which tends to a maximum

at the centre of the stone (Figure IX.6). From the TL results

therefore we may conclude that these predictions have been

substantiated; that secondary radiations are important for the

production of TL and that contours are present which may reflect

preatmospheric shape.

The only other factor which could be argued to be

responsible for the contours in Figure IX.4 is sample inhomogeneity.

Unfortunately, the overlap of peaks caused by the combination of

minerals in common chondrites made it impossible to measure the

feldspar distribution by X-ray diffraction. Similarly it was

impossible to assess the feldspar content chemically with the

quantities of material available. However it seems very unlikely

that a feldspar enrichment over such a large area could be the

explanation. Certainly there was no visible sign of a 10 - 20

cm xenolith in the slice. Finally, the artificially induced TL

was not higher in this region, as would be expected from a

feldspar enrichment.

The artificial results are a little disappointing in that

neither the areas under the artificial curves nor the ratio of

natural to artificial TL show a trend. The absence of a trend in

the artificial TL suggests that the trap numbers do not vary

monotonously across the slice, and that a significant number are

not cosmogenic. Alternatively, any trend in the trap numbers may

be obscured by sample inhomogeneity. If this is the case then one

may expect the ratio to show a good trend, which it does not. It

is probably the fact that the natural TL is that of HT that is

making the use of artificially irradiated materials unreliable in

this case. HT is very difficult to measure in the glow curves of

artificially irradiated specimens because of the intense LT

thermoluminescence.

We conclude, however, that the TL contours in the natural

TL are related to the meteorite's preatmospheric shape. They

suggest a non-spherical, elongated object approximating in the

plane of the slice to an ellipse with an eccentricity of about

0.8.
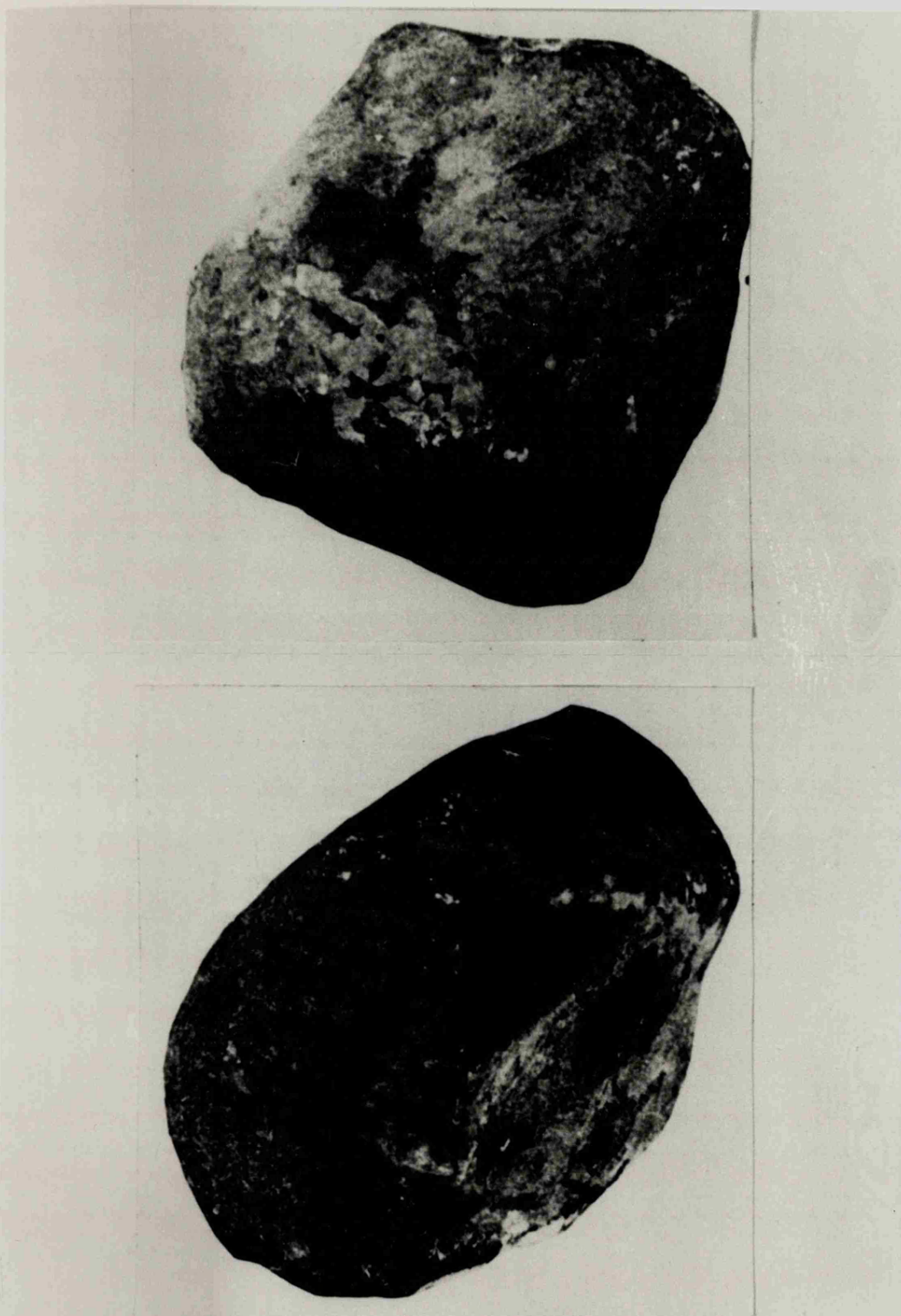
Figure IX.7 The Estacado meteorite before the slice used here
was taken (from Howard and Davison, 1906). In the top view
the plane of the slice was probably perpendicular to the plane
of the photograph, vertically down the centre of the specimen.
In the lower view the plane of the slice was probably the same
as that of the photograph.

IX.4b   <u>Minimal preatmospheric mass</u>

By extrapolating the contours so as to completely enclose
the slice we may estimate the preatmospheric mass of the Estacado
meteorite. In the plane of the slice the minimal preatmospheric
dimensions would be 130 x 70 cm. The derived preatmospheric
masses are 8 - 13 tons, depending on whether the ellipse is
rotated about its major or minor axis. A possible guide to this
is the   post-atmospheric shape (Figure IX.7). Assuming complete
recovery of the material which fell these figures correspond to
95 and 97% mass-loss. Complete recovery was almost certainly not
the case, which makes this mass-loss an overestimate. Conversely,
the fact that minimum dimensions are obtained means the values
are underestimated.

IX.4c   <u>Actual preatmospheric mass</u>

In order to follow the Hoffman-Signer-Nier approach
(described in the Introduction and Section VIII.3b) for determining
the actual preatmospheric mass, one needs a depth variation
equation for TL in meteorites. Unfortunately no such work has
been reported. However, as an initial attempt we may adapt the
Ebert and Wänke (1957) equation, stressing that its use here is
as an empirical relationship.   Then

$$\frac{TL}{TL_R} = (e^{-k_a} + B\ e^{-k_s})^{x-1}$$

where TL is the TL intensity at a fractional depth x;   B, k_a and
k_s are constants and TL_R is the TL intensity at the centre of the
preatmospheric meteoroid (x = 1). The first exponential term
represents the attenuation of primaries with depth and the second

the build-up of secondaries with depth. Fortunately, many of

the conditions assumed by Ebert and Wänke for the production of

spallogenic nuclides are also applicable to TL. For example the

exponential attenuation and build-up with no energy distribution

change, the existence of secondary radiations of lower energy than

the primaries (B $\lesssim$ 1) but which are still capable of interacting,

and the constancy of k_a and k_s. The main distinction between TL

and spallogenic nuclide production is the contribution to the TL

by internal radioactivity, and we have estimated that probably

the cosmogenic and radiogenic contributions are of equal order of

magnitude. We will therefore derive a variety of preatmospheric

masses governed by the proportion of TL ascribed to internal

radioactivity.

An exact fit between the theoretical and observational

curves is not expected because the former is the result of a

combination of exponential terms while the latter is a second

order expression. Nevertheless, a very good approximation to the

TL variation along the minor axis of the ellipse (Figure IX.8)

is obtained by putting k_a = 0.35 and k_s = 1.25 and the B values

in Table IX.3 (Figure IX.9). The same values of k_a and k_s were

found to fit the observational data regardless of the amount of TL

ascribed to internal radioactivity. This is presumably because,

as in the spallogenic nuclide case, these values are governed by

the nature of the target material. The large values of B and the

relative values of k_a and k_s are consistent with our belief in the

importance of secondary radiations in the production of TL. The

values for the preatmospheric radius obtained this way, and the

equivalent mass ranges calculated assuming an ellipsoid of
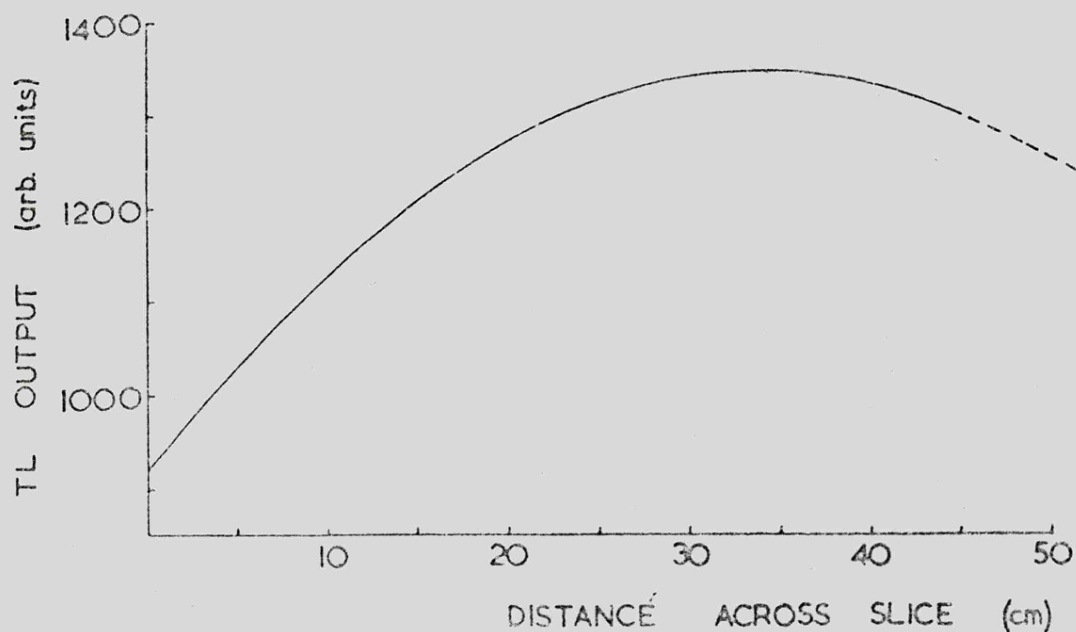
Figure IX.8   The TL profile along the minor axis of the ellipse obtained by second-order fit to the data.
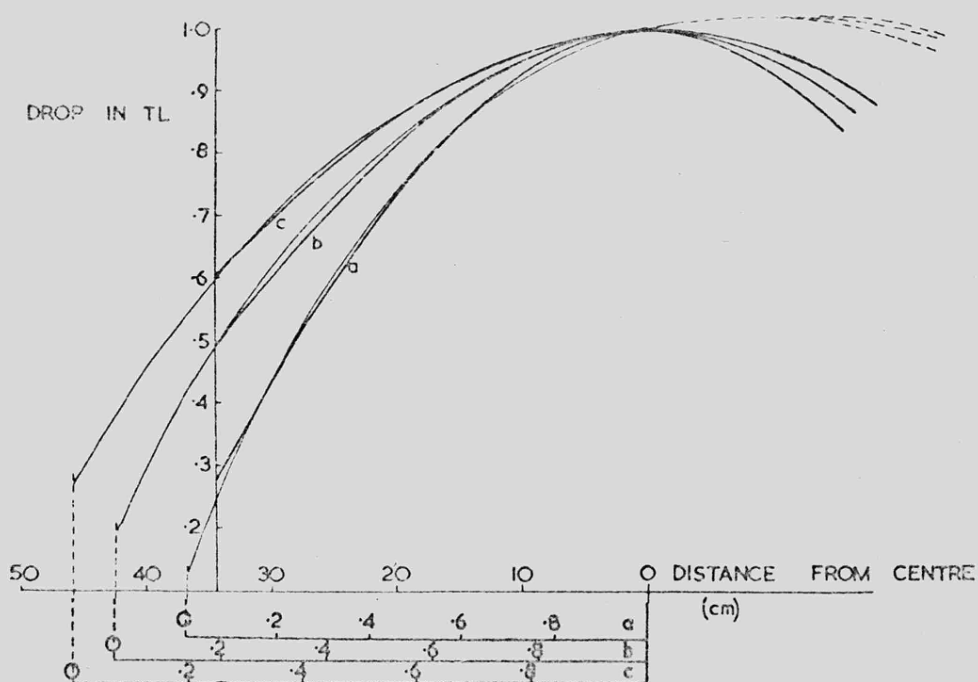
Figure IX.9   The results of fitting a theoretical expression (see text) to various TL profiles.   These have been obtained from figure IX.8 by subtracting 250, 500 and 750 arbitrary units of area under the curve (curves a, b and c) to represent various extents of contribution to the TL by internal radioactivity.

eccentricity of 0.8, are also given in Table IX.3. It is interesting to observe that an assumed radiogenic contribution to the TL in excess of about 800 arbitrary units of TL (i.e. just over half the maximum TL observed in the slice) would lead us to a preatmospheric radius less than the post-atmospheric radius. 800 therefore represents an upper limit to the amount of TL in this meteorite caused by its internal radioactivity. Because of the approximations in this technique, and the empirical nature of the expression (as used here) only a unidirectional beam of incident cosmic radiation has been considered. Integration over 4π solid angle requires an assumption to be made about the pre-atmospheric shape, and since we have some evidence concerning this, suggestions for performing the integration are made in Appendix 3.

IX.5   Conclusions

On the basis of the studies of the TL in the Estacado meteorite one may make three assertions. Firstly, that secondary radiation plays an important role in TL production; secondly, that in the plane of the slice Estacado was an elongated non-spherical shape, probably an ellipse of about 0.8 eccentricity; and finally that the preatmospheric mass was at least 8 tons and may have been up to 34 tons. The major cause of uncertainty in the latter value is the unknown extent of the contribution of radiogenic particles to the TL.

Table IX.3

Results of fitting the Ebert-Wänke equation

Assumed radiogenic contribution*	B	Preatmospheric radius (cm)	Preatmospheric mass (tons)	Mass-loss (%)
250	0.89	47	20 - 34	98 - 99
500	0.92	42	14 - 24	97 - 98
750	0.95	37	10 - 16	96 - 97

*   in arbitrary units of TL   The total (radiogenic + cosmogenic) TL is 950 - 1450.

CHAPTER X

SUMMARY, CONCLUSIONS AND SPECULATIONS

X.1   The thermoluminescence of meteorites — properties

One may describe the thermoluminescence of meteorites in

two ways; what it is like (i.e. what the glow curve is like) and

how intense it is. The shape of the glow curve is determined by

the kinds of luminescent mineral responsible; for example, the

enstatite chondrite glow curve resembles that of the enstatite

achondrites but they are quite different from common chondrite

glow curves. However, it also seems to be governed to some extent

by the radiation history of the specimen, since the glow curves

of the pyroxene-plagioclase achondrites show similarities with

those of lunar samples which they do not have with common chondrites.

This is despite their common luminescent mineral, feldspar. We

suggest here that this is because lunar samples and pyroxene-

plagioclase achondrites have a regolith history.

The intensity of the TL is governed by three factors.

The number of electron traps present, the number of electrons

excited to fill those traps and, again, the history of the

meteorite. We have three instances of the history of the

meteorite being reflected in the TL intensity; the existence of

two groups, which seems to be associated with shock, and the

thermal draining of the TL by atmospheric heating during fall and

by ambient temperatures after fall.

The number of traps is probably the result of contributions

from three sources. In all probability most are due to compositional

and structural effects produced at the time of crystallisation

(e.g. lattice defects and distortions by impurity ions). However, some are almost certainly due to radiation damage by cosmic ray bombardment (cosmogenic traps) and internal radioactive decay (radiogenic traps). The gradients in the artificial TL intensity indicate the existence of cosmogenic traps and the relationship between artificial TL and K-Ar age shows that some are radiogenic.

Finally, the intensity of the TL is governed by the extent of trap population. The traps have not only to be created, but also populated by excited electrons, and this can be achieved by any ionising radiation. One may expect that both internal radio-activity and cosmic ray bombardment could provide the few eV energy required to promote electrons to traps. The fact that this energy requirement is so low, compared to the spallogenic reactions, leads us to expect that secondary radiations will be important for the production of TL: this is confirmed by our measurements on Estacado. The existence of gradients in the natural TL intensity of specimens in which there are no artificial gradients (e.g. Estacado) provides a clear example of trap population by cosmic ray bombardment.

X.2   The thermoluminescence of Meteorites — Applications

X.2a   The glow curve (trap distribution)

This can be used to locate (and in very special circumstances identify) minerals and thereby meteorite classes. The glow curves of many minerals consist of separate low-temperature and high-temperature TL, and such an application must be regarded with caution. However, its use to infer a regolith origin for the pyroxene-plagioclase achondrites does appear to be valid, but

requires greater work on determining the identity of traps
responsible for each peak in the glow curve.

X.2b Artificial TL (trap numbers)

The examination of trap numbers may be made by draining
a specimen and artificially irradiating it until the traps are
filled. However, since so many factors are involved in trap
production TL is not really suited to the determination of
exposure age or crystallisation age. This may not be true of
studying the distribution in trap numbers over a large slice of
meteorite. If the proportion of cosmogenic traps is large, as
appears to be the case in the Plainview slice examined here, the
variation in artificial TL across a slice may reflect the pre-
atmospheric shape.

X.2c Emptying traps

Electrons leave the traps in a time and temperature
dependent fashion. This enables two applications, both of which
have been studied here. By assuming a constant temperature it is
possible to measure the terrestrial ages of meteorites that are
up to several hundred years old (but less in the case of some,
possibly shocked, meteorites which decay faster). This method
provides a useful complement to the radiocarbon method which is
not applicable to ages of less than about 2000 years.

Conversely, one may choose a situation where time is
constant and use trap drainage to measure the temperatures
experienced. This way it is possible to measure thermal gradients
set up in the meteorite by heating during its atmospheric passage.

The gradients measured are always lower than those predicted

theoretically by a factor of 3 - 5. However, temperatures

expected at a given depth are found experimentally and are

consistent with luminous flight times in the order of 10 seconds.

The fusion crust takes only one second to form, the innermost

(troilite/nickel iron flow) zone being the last to do so. It is

therefore impossible to find a temperature gradient measurable by

TL if there is no innermost zone in the fusion crust. Variations

in the temperature gradient measured by TL mirror those indicated

by the dimensions of the fusion crust which are controlled by

ablation and the orientation of the specimen. This indicates that

temperature gradients at depths measurable by TL (up to about 1 cm)

are also controlled to some extent by ablation.

X.2d   Filling traps

In this work the filling of traps by cosmic ray

bombardment has been used to measure the preatmospheric shape and

mass of the Estacado meteorite. The TL suggests an elongated, non-

spherical object approximating to an ellipse (e = 0.8). The same

build up into the specimen is observed with the spallogenic gases

in the Keyes and Saint-Séverin chondrites as is observed with TL

and it indicates an important role is being played by secondary

radiations. By extrapolating the contours of equal TL intensity

so as to enclose the specimen a minimal preatmospheric mass

estimate for Estacado of 8 - 13 tons is made. Actual estimates

for the preatmospheric mass are uncertain because the proportion

of radiogenic to cosmogenic TL is unknown and the values range

from 10 to 34 tons.

The applications of thermoluminescence and the fusion
crust studies described here have tended to be concerned with the
final stages of a meteorite's history; its shape when the
meteorite entered the atmosphere, its behaviour in the atmosphere
and its lifetime on the Earth waiting to be found. Each of these
studies has its own significance and relevance to meteoritics as
a whole and hopefully this will have emerged in the discussions.
However, we end this work by discussing a problem to which all
of the studies included here may have a bearing. This problem
is the anomaly in the flux of bright fireballs uncovered by the
Prairie camera network. The Prairie network provides most, if
not all, of the quantitative information we have about meteorite
entry into the atmosphere. Its importance is underlined by the
notorious unreliability of descriptions of falls given by eye-
witnesses.

X.3   Meteorite entry of the atmosphere

X.3a   Fall descriptions

Probably the best descriptions of what happens during a
meteorite fall are the accounts in the Meteoritical Bulletin.
These accounts are not lengthy, but provide a reasonably large
random distributed selection. Table X.1 summarises the descriptions
of twenty falls which appeared between April 1960 and November 1970.
An additional 18 falls were listed during this period but no fall
description was given. Not even an explosion is invariably
reported. To make it even more difficult to describe the "typical
meteorite fall" it is not certain that these figures give a good
indication of what actually happens. If they had been compiled

Table X.1

The Fall Descriptions of 20 Meteorites in the

Meteoritical Bulletin (April 1960 - November 1970)

Feature	Number of descriptions mentioning feature	
Explosion	17	(85 %)
Rumbling	7	(35 %)
Whistling	9	(45 %)
Impact sounds	4	(20 %)
Light	11	(55 %)
Flares	2	(10 %)
Dust trail	6	(30 %)

before 1850 an important feature would have been the smell of
sulphur (Sears, 1974c). It is possible that its absence in modern
descriptions is caused by modern enquirers not asking witnesses
if they smelled anything because the popular impression of a
meteorite fall does not include a smell. We believe that troilite
burns to evolve sulphur dioxide. The outermost zone of the
fusion crust does not contain sulphur (Brownlee and Hodge, 1973)
but at higher altitudes, when the ablation rate exceeds the rate
of troilite flow inwards (i.e. before the final second) this is
almost certainly not the case. An alternative explanation offered
by Astopovich (1958) was that electrostatic production of ozone
causes the smell. Whatever its causes it lingers with the stone
for some time after the fall (Fletcher and Milligan, 1902) which
disproves the idea that the smell was imaginary. In any event,
the discrepancy between the early and modern accounts suggests that
the subjective element has not been removed from modern meteorite
fall descriptions.

X.3b   The Prairie network and the Lost City meteorite

The Prairie network consists of 16 four-camera stations
spread out over seven states. The cameras automatically record
the trail of fireballs and various other pieces of information
needed to reduce the data (McCrosky and Boeschenstein, 1963).
After the first five years of operation (1964 - 1969) two main
results emerged; that when considered alongside the meteorite fall
statistics of Hawkins (1960) and Brown (1960)

    i)   the influx on bright fireballs is high (Figure X.1)

    ii)   the influx of meteorites is, if anything, low.

The intensity of the fireball (governed by the total mass) is
given by:

$$I = \frac{1}{2} K_o \, m \, v^3$$

where m is the meteoroid mass, v its velocity and K_o the luminosity
constant. This has been arrived at after rocket-borne simulations
and must be scaled up or down to allow for composition differences
between the actual and simulated meteoroids. The total mass of
the meteoroid producing a fireball may therefore be calculated
from its intensity. Secondly, its apparent deceleration (governed
by the leading fragment) can be determined from the classical
drag equation

$$m \, \dot{v} = \frac{1}{2} C_D \, A \, v^3 \, D$$

where C_D is the drag coefficient, A is the meteoroid's cross-
sectional area and D is atmospheric density. Because of fragment-
ation the equations give different values for the mass (for example
the Pribram meteorite had a dynamic mass of 15 tons and a
photometric mass of 50 tons).

However, the dynamic equation requires a knowledge of the
meteorite's shape $(C_D A)$ and density. Assuming a sphere, writing
A in terms of meteoroid density, and equating mass in the two
expressions, estimates of density can be made and are between
0.4 and 1.5 gm/cm^3. However the Lost City and Pribram meteorites,
the only meteorites for which this data exists, were both
recovered and found to be ordinary bronzites (with a density of
3.6 gm/cm^3). It is necessary to invoke a non-spherical shape and
for Lost City a value for $C_D A$ of 3.8 was required. This is
equivalent to a depth-to-diameter ratio of about 1 : 4. For
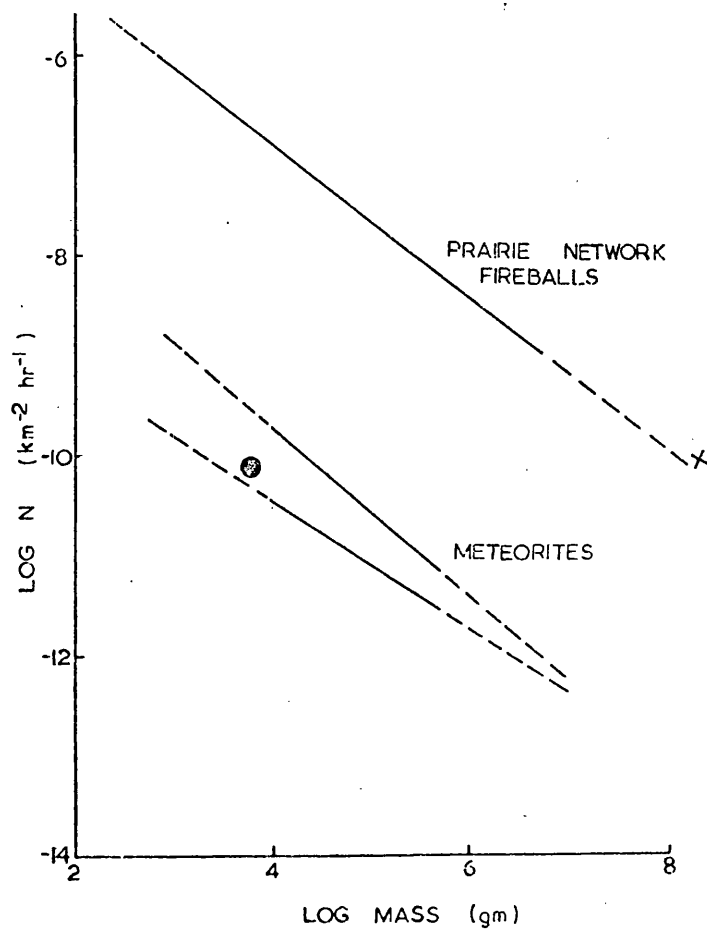plate-shaped objects the drag is higher than a sphere of equal mass.

Figure X.1   The flux of bright fireballs measured by the Prairie network compared with the observations for meteorites. The cross represents the Pribram meteoroid plotted as a fireball, and the dot as a meteorite. (From McCrosky and Ceplecha, 1968).

This explanation works only for certain fireballs since some would require a depth-to-diameter ratio of 13 and these are assumed to be friable cometary substances. There is also evidence that the faint meteors are friable objects (Verniani, 1973). For others the theoretical work of Baldwin and Sheaffer (1973) suggests a carbonaceous chondrite composition would suffice, since not only would fragmentation produce an erroneous dynamic mass but the carbon content would increase the light emitted and thus the photometric mass measured. It is these bodies that are assumed to be responsible for the high flux of bright fireballs. However, Pribram (1959) and Lost City (1970) gave anomalous results yet both are ordinary bronzites. It seems in these cases a plate-shaped preatmospheric mass is most probable.

X.3c Further information bearing on the Prairie network

results

In the work described in this thesis we have touched on many of the facts involved in this debate. Firstly, the influx of meteorites as derived from the terrestrial age of finds (Chapter V) was found to be lower than that indicated by the Hawkins (1960) and Brown (1960) fall statistics. It is therefore unlikely that these authors have overestimated the influx rate of meteorites. Secondly, simple ablation does not provide a mechanism for removing the mass difference between the photometric and recovered mass (Chapter VI). Thirdly, our preatmospheric shape determination suggests that a compact spherical shape is unlikely for the Estacado meteorite (Chapter IX). Rotating the ellipse about its minor axis produced a flattish object with a depth-to-
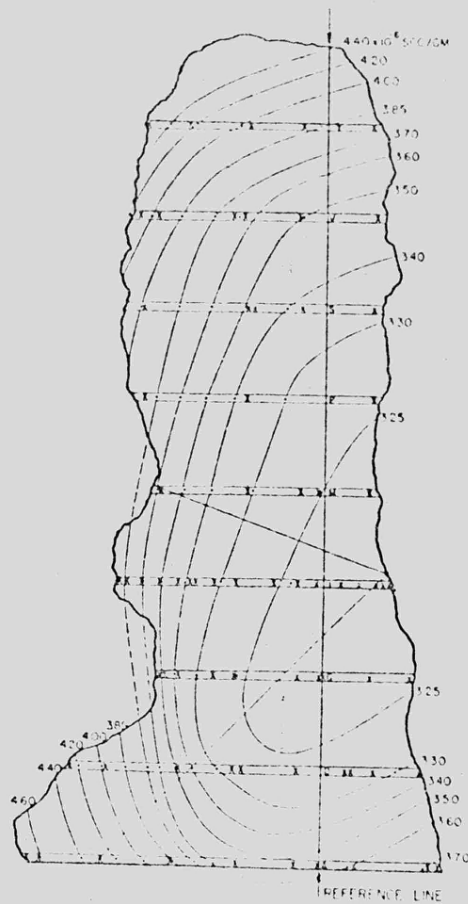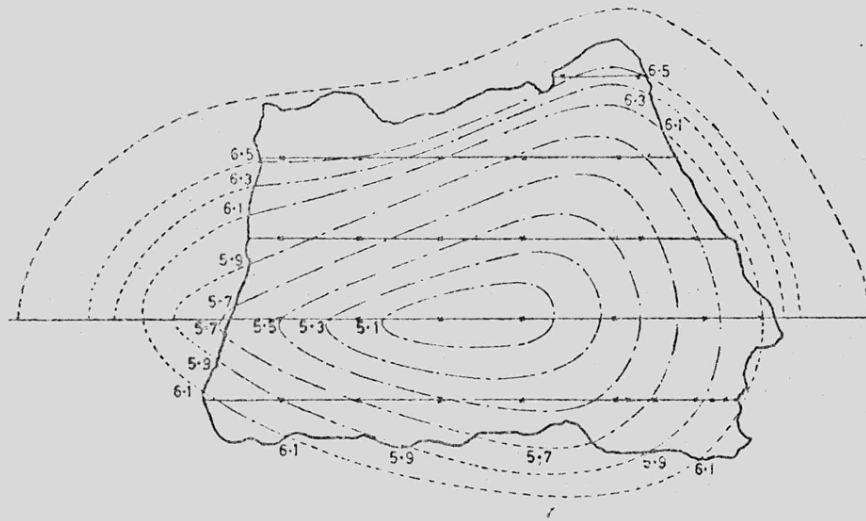
Figure X.2   Preatmospheric shape determinations for two iron
meteorites. The contour lines are for equal helium-3 content.
Top, the Grant meteorite (from Fireman, 1958); below, the
Carbo meteorite (from Hoffman and Nier, 1959). Both indicate
elongated, non-spherical bodies entered the atmosphere.

diameter ratio of about 1 : 2.5.

We now have preatmospheric shape determinations for two iron and two stony meteorites. The results for irons are shown in Figure X.2, and both have depth-to-diameter ratios of about 1 : 3. The other stony meteorite preatmospheric shape we have is for the Keyes meteorite (Trivedi and Goel, 1973; Wright et al., 1973) for which the depth-to-diameter ratio is about 1 : 2.5. While these could hardly be called plate-shaped objects they are most certainly not even approximately spherical. All of these meteorites appear to have been irregular, elongated objects when they entered the atmosphere. This may therefore go some way in explaining the discrepancy between photometric and dynamic mass observed by the Prairie network. Clearly one may expect other factors, like the presence of carbonaceous bodies and friable or cotton-wool-type objects, but we believe a significant number of ordinary chondrites entering the atmosphere to be flattish and non-spherical.

X.3d Speculations

We believe that it is not unreasonable to suggest that a large number, probably most, of the meteoroids entering the atmosphere are not the spherical bodies that simple meteor theory has always assumed. In this belief we are supported by the few observations on the shapes of asteroids (Dunlap, 1971), from which current opinion would have the meteorites coming. Although mass distribution calculations have been made, few or no calculations concern shape distribution. But the light curves of Eros, Hektor and Geographos suggest elongated non-spherical objects, and

therefore that the fragmentation process that made these, and

perhaps the meteorites, favours such shapes. It would be a little

more difficult to reconcile a preference for non-spherical

meteoroids with a cometary or lunar origin. Rocks on the Moon

which appear to have been ejected during impact are usually

blocky objects, but quantitative data is again lacking. Similarly

one usually thinks of the dust emitted by comets as micron-sized

particles which, were they to accrete to meteoroid proportions,

would adopt no particular shape. Perhaps therefore a

preponderance of bodies with a particular shape favours an

asteroidal origin.

The evidence is scanty and the conclusions are speculative.

But we can be more confident of the other conclusions to which

thermoluminescence and the fusion crust have led us, concerning

the meteorite's atmospheric passage. Edward Charles Howard, who

first observed the luminescence of meteorites, believed that it

was the answer to why a meteorite emitted so much light when it

flew through the atmosphere. It is perhaps therefore fitting that

the latter half of this final chapter be concerned with this

aspect of the study of meteorites.

APPENDICES

A.1   The Control Unit (Figure A.1)

      A.1a   The Electronic Circuit

The importance and highly satisfactory nature of the

control unit require that details should be placed on record

beyond those necessary for the main text. These details appear

in this first Appendix.

The principles of the control unit are presented as a block

diagram as Figure A.2b. The lay-out is the same as the circuit

(Figure A.2a) and the purposes of each block are described as

instructions. A linear ramp is produced (i.e. a voltage increasing

linearly with time) which is compared with the thermocouple

voltage. Any differences are compensated by increasing or

decreasing the voltage to the heavy-duty transformer which has the

heating filament connected to its secondary coil. A detailed

description of the circuitry was supplied by Mr. R. Hearsey on

which the following explanations of the instructions in Figure

A.2b are based.

"Set levelling-off temperature": The two decade switches

(labelled "Set temp" in the circuit diagram) when pre-set to the

required levelling-off temperature produce a standard voltage.

This can correspond to any temperature between ambient and $990^{\circ}C$

in steps of $10^{\circ}C$. The life-time of the filament requires that it

be as low as possible. An amplifier buffer between these controls

and the integrating comparator reduces the effect of loading.

"Check this has not been reached": Comparator 1 compares the

level of the integrator ramp at any time to that of the standard

voltage. If they are equal the integrator holds that level by a feedback loop (loop 1).

"Set heating rate and produce linear heating ramp": The ramp rate of the integrator can be set by three decade switches to give heating rates between 0.1 and $99^{\circ}C/sec.$, extending well beyond the range of heating rates previously used; $0.375^{\circ}C/sec$ (Houtermans and Liener (1966) to $30^{\circ}C/sec$ (Christodoulides et al., 1970). This not only allowed easy comparison with published results but also the determination of trap depth energy by the peak position vs. heating rate method (Braunlich, 1968). A hold facility also built into this block enabled the effects of annealing at any temperature for short durations (say a few seconds) to be investigated.

"Compare thermocouple with ramp voltage": The output of the integrator is compared in comparator 2 with the output of the thermocouple. As the thermocouple output is about 30 mv. pre-amplification is necessary before comparison. Proportional and differential feedback is used together with integral feed to make a three term controller. The output from comparator 2 is fed as a D.C. control signal to the next block, and also displayed at the "RECORDER" output of the unit from which it may be connected to the temperature axis of the X-Y recorder producing the glow curves. The signal from comparator 2 is amplified and passed to the gate pulse drive generator which produces the appropriate A.C.

"Swith off if thermocouple is damaged": If the thermocouple connection is damaged and no signal were being received by comparator 2 the unit would try to produce a signal by increasing the current to the filament. The filament would consequently

burn-out and damage would result to the unit. The safety circuit
prevents this by switching off the output in the event of a surge
of power to the primary of the heavy duty transformer.

A.1b Calibration

Both of the temperature controls and the meter have pre-
set potentiometers in their circuits to allow for zeroing and
calibration. However it was thought more accurate to produce
calibration curves than to attempt to adjust these. The
calibration charts used throughout this work are presented as
Figure A.3 and Figure A.4. The decade switch controlling the
levelling-off temperature and the meter indicating the filament
temperature agree to within $10^{\circ}C$ and indicate values approximately
three-quarters that of the true values (Figure A.4a). The heating
rate control very closely obeys the relation $B_i = 1 + 0.69\ B_t$
where B_i is the indicated and B_t the true heating rate (Figure
A.4b). $5^{\circ}C/sec$ is therefore registered as $4.4^{\circ}/sec$.

Figure A.1   The electronic heating control unit.
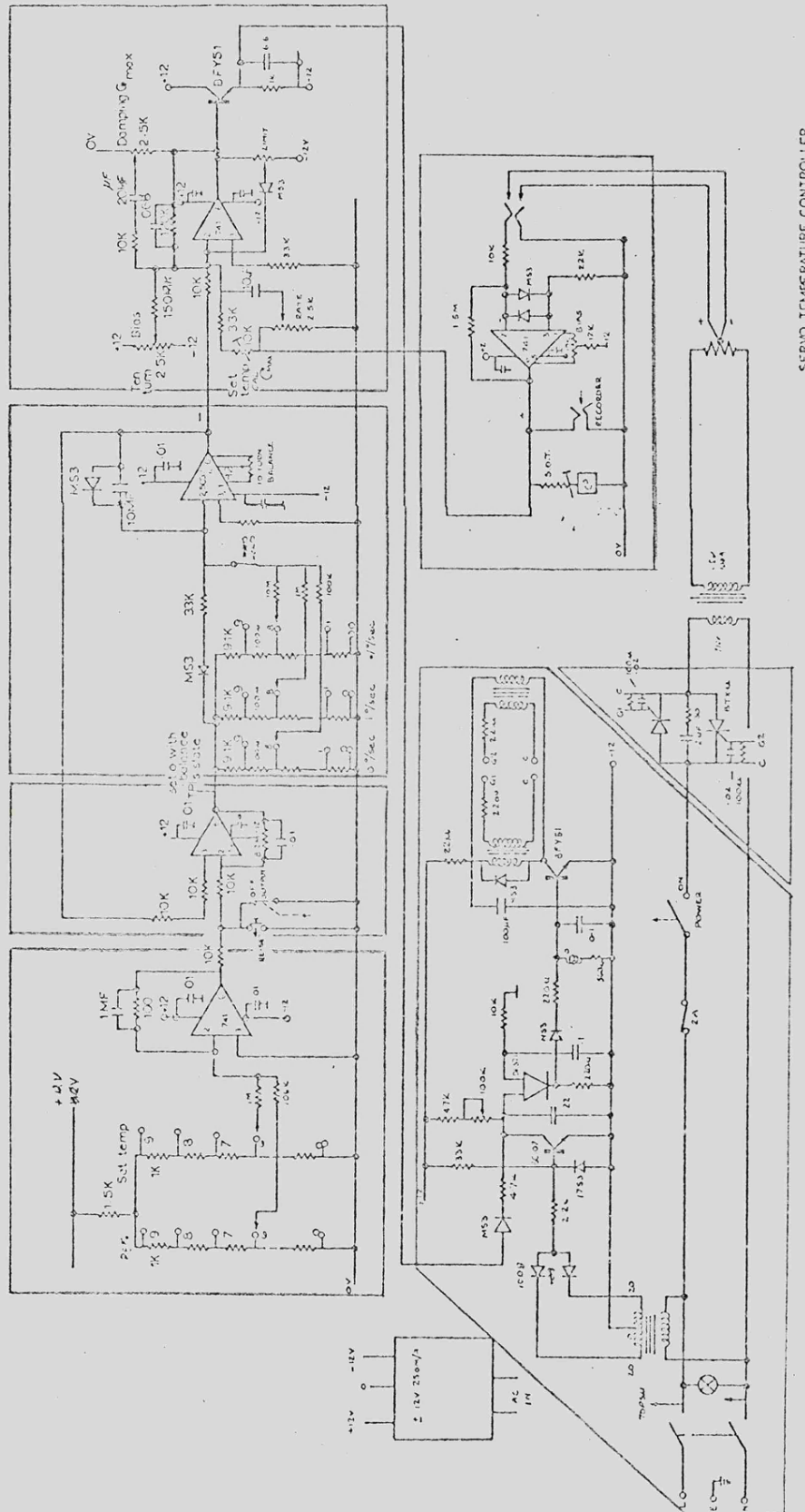
Figure A.2a   Circuit diagram for the control unit.

| Set levelling off temperature | Check this has not been reached | Set heating rate & produce linear voltage ramp | Compare thermocouple with ramp voltage |

Create A.C. to compensate for difference

Thermocouple pre-amplifier

Switch off if thermo-couple is damaged

heavy duty transformer

Thermocouple

heating filament
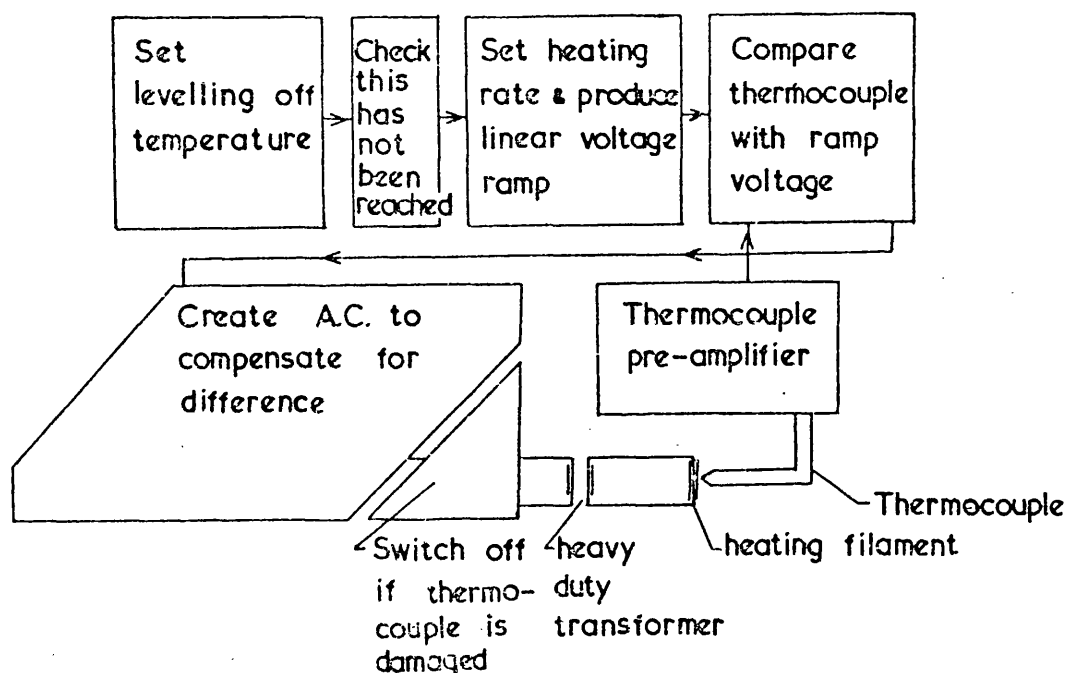
Figure A.2b   Block diagram of the circuit of the control unit laid out in the same way as figure A.2a.   The purpose of each block is shown as in instruction.
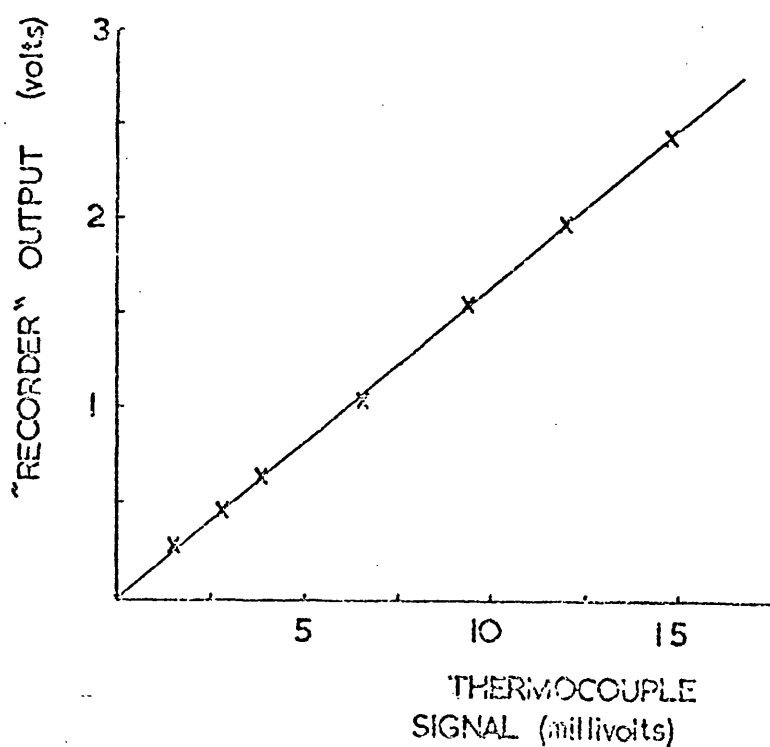
Figure A.3   Curve for the determination of the gain of the thermocouple pre-amplifier.   The signal at the "RECORDER" output is thus found to be 156 times that of the thermocouple.
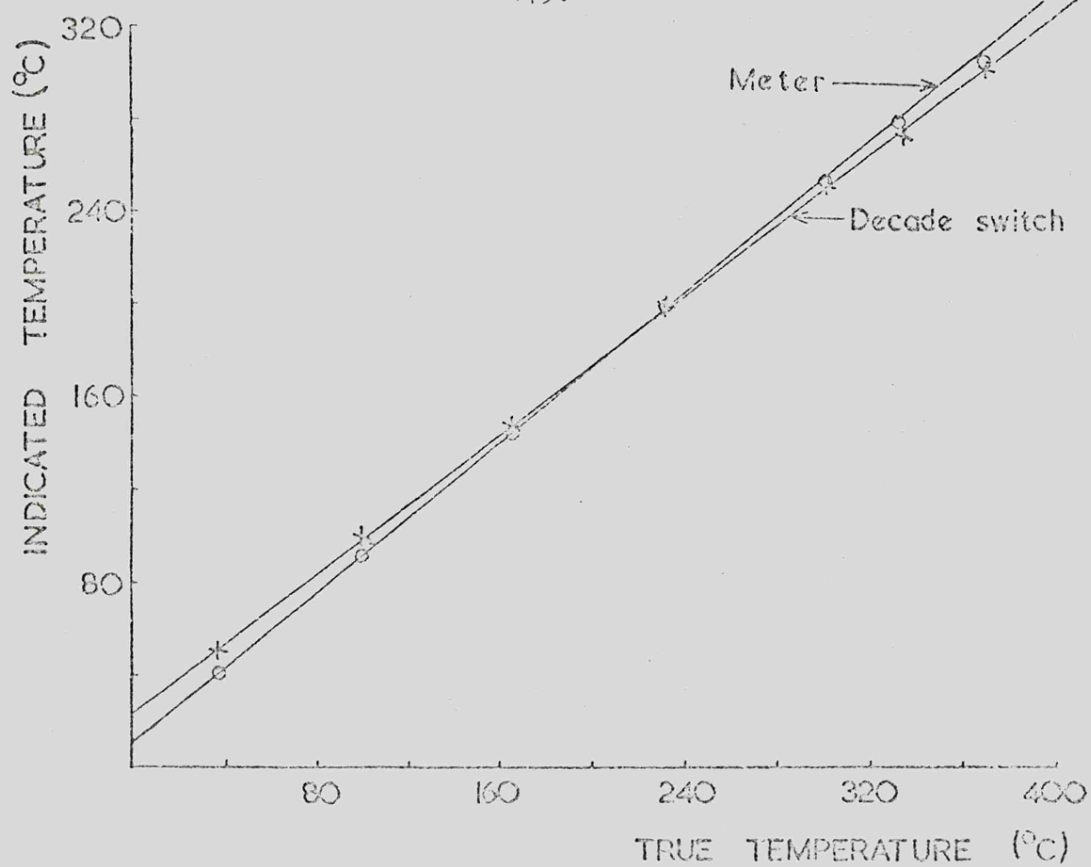
Figure A.4a Calibration curves for the meter and the decade
switch controlling the levelling-off temperature.
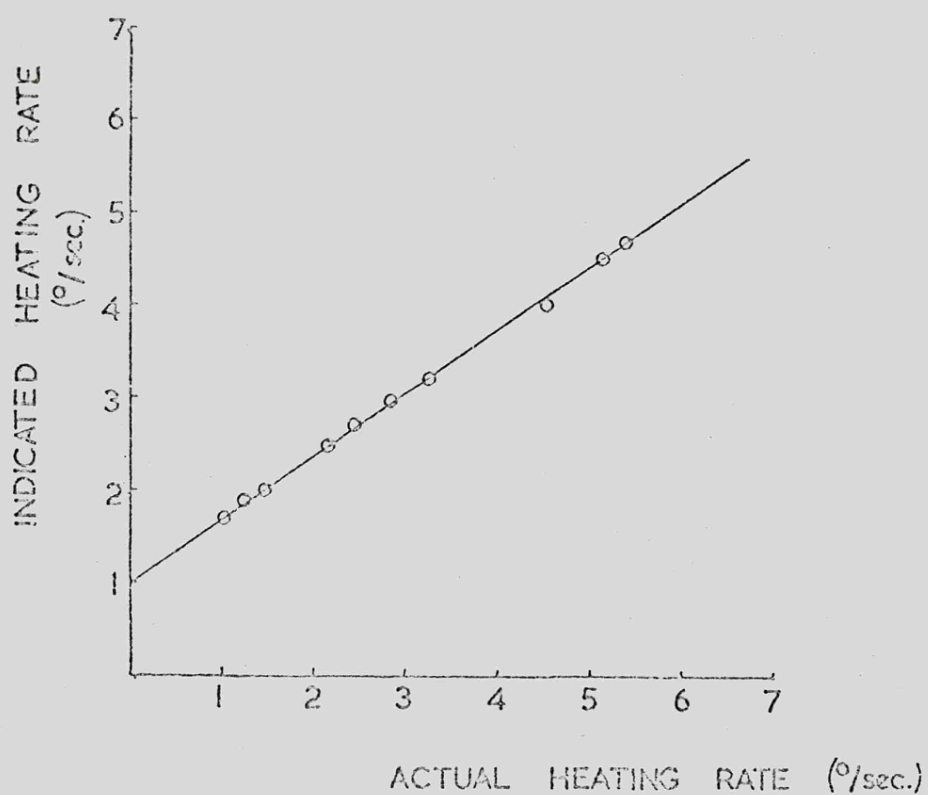
Figure A.4b Calibration curve for the decade switch
controlling the heating rate.

A.2   The curve fitting program (Davis, 1973; Esher et al., 1968)

The function which is fitted is of the form:

$$y = b_0 + b_1 x_1 + b_2 x_2 + b_3 x_1^2 + b_4 x_2^2 + b_5 x_1^3 + b_6 x_2^3 + \ldots$$

where y is the value of the TL at coordinates (x_1, x_2). The order to which it is taken is fed into the program with the data which consists of the TL values y, and their position coordinates x_1 and x_2. The coefficients are then calculated by the method of least-squares. The program consists of three parts:

i)   preparation of the necessary matrices to calculate the coefficients,

ii)   the solution of the matrices and calculation of the y corresponding to the fitted curve,

iii)   plotting the contours.

The plotting is performed on the line-printer (Figure A.5) in accordance with control cards fed in with the data. These tell the program the dimensions of the data grid, the values of the symbols it will plot between the contours and the contour interval.

Various test statistics measuring the goodness-of-fit are also given with the output; the variance, the correlation coefficient and the F-ratio (with the appropriate degrees of freedom).

A.3   Integrating the Ebert-Wänke Production Formula

(Section IX.4c)

The equation may be written (Signer and Nier, 1958)

$$P = A \left[\int_0^{2\pi} \int_0^{\pi} e^{-k_a x'} \sin\theta \, d\theta \, d\phi + B \int_0^{2\pi} \int_0^{\pi} e^{-k_s x'} \sin\theta \, d\theta \, d\phi \right]$$

where x' is the distance to the surface of the preatmospheric body

along a vector θ defined by Figure A.6. A relationship is there-

fore required relating x, the distance to the nearest preatmospheric

surface, to θ. This depends on the preatmospheric shape of the

meteoroid. Bhattacharya et al. (1973) have provided us with the

expressions for x' :

For a sphere

$$x' = -(1 - x) \cos\theta + (\cos\theta + 2x \sin^2\theta - x^2 \sin^2\theta)^{\frac{1}{2}}$$

For an ellipse

$$x' = \frac{1}{R} \frac{1}{U} \left(-v + \left[v^2 - u(w - 1) \right]^{\frac{1}{2}} \right)$$

where $u = \frac{1}{a^2} \sin^2\theta \cos^2\phi + \frac{1}{b^2} \sin^2\theta \sin^2\phi + \frac{1}{c^2} \cos^2\theta$

$v = (r_0 - x)(\frac{1}{a^2} \sin\theta \sin\eta \cos\phi \cos\delta$

$\qquad + \frac{1}{b^2} \sin\theta \sin\eta \sin\phi \sin\delta + \frac{1}{c^2} \cos\theta \cos\eta)$

$W = (r_0 - x)^2 (\frac{1}{a^2} \sin^2\eta \cos^2\delta + \frac{1}{b^2} \sin^2\eta \sin\delta + \frac{1}{c^2} \cos^2\eta$

and $r_0 = (abc)^2 (a^2b^2 \cos^2\eta + b^2c^2 \cos^2\xi \sin^2\eta$

$\qquad + c^2a^2 \sin^2\eta \sin^2\delta)^{-1}$

With either of these substituted into the production formula and

with the substitution u = cos θ (so that the limits of integration

are $\pm$ 1) the operation may be performed numerically by Gaussian

three-point integration (Kopal, 1961). It requires considerable

numerical manipulation and is therefore best considered a computer-

project.

Figure A.5 Part of the output from the KWIK R8 computer program.
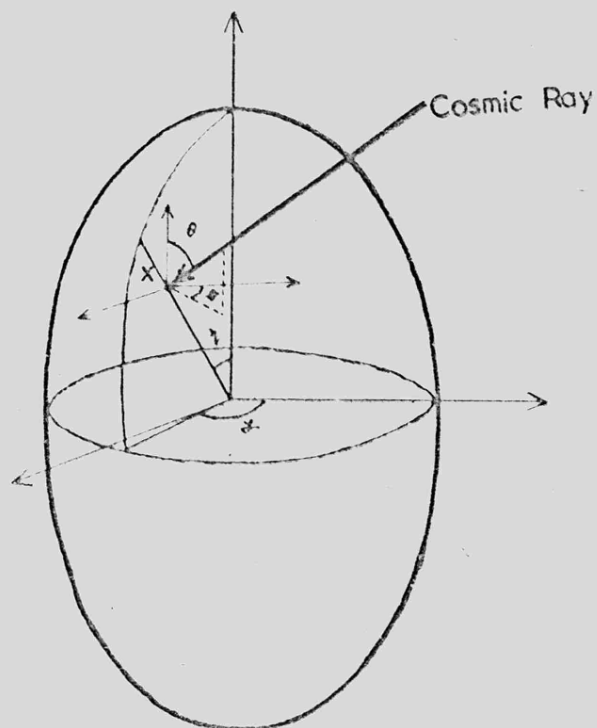
Figure A.6 Co-ordinate system for the equations related to integrating throughout an ellipse.

REFERENCES

ABELL, P.I., DRAFFAN, C.H., EGLINGTON, G., HAYES, J.R., MAXWELL, J.M. and PILLINGER, C.T. (1970) Organic analysis of the returned Apollo 11 lunar samples. Proc. Apollo 11 Lunar Sci. Conf. 2, 1757-1773.

ADAMS, M.C. (1959) Recent advances in ablation. Amer. Rocket Soc. Jour. Sept., 625-632.

AITKEN, M.J., TITE, M.S. and REID, J. (1964) Dating ancient ceramics with thermoluminescence. Nature, 202, 1032.

AITKEN, M.J., ZIMMERMAN, D.W. and FLEMING, S.J. (1968a) Thermoluminescence dating of ancient pottery. Nature, 219, 442-445.

AMIN, B.S., LAL, D., LORIN, J.D., PELLAS, P., RAJAN, R.S., TAMHANE, A.S. and VENKATAVARADAN, V.S. (1969) On the flux of low-energy particles in the Solar System during the last 10 million years. In Meteorite Research (editor P. M. Millman), pp. 316-327, D. Riedel.

ANDERS, E. (1963) Meteorite Ages. In The Solar System, Part IV. The Moon, Meteorites and Comets (editors B.M. Middlehurst and G.P. Kuiper), pp. 402-495. University of Chicago Press.

ASTOPOVICH, I'S. (1958) Meteornye larleniia V Atmosfere Zemli ("Meteoric Phenomena in the Earth's Atmosphere"). (Moscow). See also ROMIG, M.F. and LAMAR, D.L. (1963) Anomalous sounds and electromagnetic effects associated with fireball entry. Rand Corp. Mem. RM-3724 ARPA.

AWBERY, J.H. (1949) A Textbook on Heat. Longmans Green (London).

BALDWIN, B. and SHEAFFER, Y. (1971) Ablation and breakup of large meteoroids during atmospheric entry. Jour. Geophys. Res. 76, 4653-4668.

BEGEMAN, F. (1972) Argon 38/Argon 39 activity ratios in meteorites
and the spatial constancy of the cosmic radiation. Jour.
Geophys. Res. 77, 3650-3659.

BEGEMAN, F. and VILCSEK, E. (1965) Durch spallationreaktionen und
neutron-eneinfang erzeugtu ^{36}Cl in meteoriten und die
prae-atmosphaeuschi grosse von steinmeteoriten. Z. Natur-
forsch 20a, 533-540.

BEGEMAN, F. and VILCSEK, E. (1969) Chlorine-36 and argon-39
production rates in the metal of stone and stony-iron
meteorites. In Meteorite Research (editor P. Millman), pp.
355-363, D. Riedel.

BETHE, H. and ADAMS, M.C. (1959) Theory for the ablation of glassy
materials. Jour. Aero/Space Sci. 26, 321-328, 350.

BHATTACHARYA, S.K., GOSWAMI, J.N., GUPTA, S.K. and LAL, D. (1973)
Cosmic ray effects induced in a rock exposed on the Moon
or in free space: Contrast in patterns for 'tracks' and
'isotopes'. The Moon 8, 532-286.

BLANCHARD, M.B. (1972) Artificial meteor ablation studies: iron
oxides. Jour. Geophys. Res. 77, 2442-2455.

BOECKL, R. (1972) The terrestrial ages of 19 stony meteorites
derived from their radiocarbon contents. Nature, 236, 25-26.

BONFIGLIOLI, G. (1968) Criteria for the design of thermoluminescence
apparatus. In Thermoluminescence of Geological Materials
(editor D. J. Macdougal), pp. 559-568. Academic Press.

BORGSTROM, H.L. (1912)
Bull. Comm. Geol. Finlande 34, 22.

BRÄUNLICH, P. (1968) Thermoluminescence and thermally stimulated

current — tools for the determination of trapping

parameters. In Thermoluminescence of Geological Materials

(editor D. J. MacDougall), pp. 61-90. Academic Press.

BRONSHTEN, V.A., BUEVICH, Yu.A., EGOROV, O.K., PORTNYAGIN, Tu.I.

and YAKUSHIN, M.I. (1968) Experimental study of the ablation

of meteorites. Solar System Res. 2, 120-129. (Translation

of Astronomicheskii Vestnik 2 (3), 139-152.)

BROWN, H. (1960) The density and mass distribution of meteoritic

bodies in the neighbourhood of the Earth's orbit. Jour.

Geophys. Res. 65, 1679-1683.

BROWNLEE, D.E. and HODGE, P.W. (1973) Ablation debris and primary

micrometeoroids in the stratosphere. Space Research XIII,

1139-1151.

BROWNLEE, D.E. and RAHAN, R.S. (1973) Micrometeorite craters

discovered on chondrule-like objects from Kapoeta meteorite.

Science 182, 1341-1344.

BUCHWALD, V. (1961) The iron meteorite "Thule", North Greenland.

Geochim. Cosmochim. Acta. 25, 95-98.

BUCHWALD, V.F. (1967) The iron meteorite Föllinge, Sweden.

Geochim Cosmochim. Acta. 31, 1559-1567.

CANTELAUBE, Y., PELLAS, P., NORDEMANN, D. and TOBAILEM, J. (1969)

Reconstitution de la météorite Saint-Séverin dans l'espace.

In Meteorite Research (editor P. Millman), pp. 705-713.

D. Riedel.

CARR, M.H. (1970) Atmospheric collection of debris from the

Revelstoke and Allende Fireballs. Geochim. Cosmochim.

Acta. 34, 689-700.

CARSLAW, H.S. and JAEGER, J.C. (1959) Conduction of Heat in Solids.
Clarendon Press (Oxford).

CHANG, C. and WÄNKE, H. (1969) Beryllium-10 in iron meteorites,
their cosmic ray ages and terrestrial age. In Meteorite
Research (editor P. Millman), pp. 397-407. D. Riedel.

CHRISTODOULIDES, C., DURRANI, S.A. and ETTINGER, K.V. (1970)
Study of the thermoluminescence in stony meteorites.
Modern Geology 1, 247-259.

CLARKE, R.S., JAROSEWICH, E., MASON, B., NELEN, J., GOMEZ, M. and
HYDE, J.R. (1970) The Allende, Mexico, Meteorite Shower.
Smithsonian Contributions to Earth Science (5).

CROZAZ, G., MAACK, U., HAIR, M., MAURETTE, M., WALKER, R. and
WOOLUM, D. (1970) Nuclear track studies of ancient solar
radiations and dynamic lunar surface processes. Proc.
Apollo 11 Lunar Sci. Conf. 3, 2051-2080.

DANIELS, F., BOYD, C.H. and SAUNDERS, D.F. (1953) Thermoluminescence
as a research tool. Science 117, 343-349.

DAS GUPTA, D.C., VISWANATHAN, T.V., SEN GUTA, N.R. and BANERJEE, S.
(1969) Muzzaffarpur meteorite. Geochim. Cosmochim. Acta.
33, 1298-1302.

DAVIS, J.C. (1973) Statistics and Data Analysis in Geology.
J. Wiley & Sons.

DEWAR, J. and ANSDELL, G. (1886) Recent researches on meteorites.
Proc. Roy. Inst. 11, 541-552.

DUNLAP, J.L. (1971) Laboratory work on the shapes of asteroids.
In Physical Studies of the Minor Planets (editor T. Gehrels)
NASA spec. rep. SP-267.

DURRANI, S.A. (1972) Refrigeration of lunar samples destined for

thermoluminescence studies. Nature 240, 96-97.

DURRANI, S.A. and CHRISTODOULIDES, C. (1969) Allende meteorite:

Age determination by thermoluminescence. Nature 223,

1219-1221.

EBERT, K.H. and WÄNKE, H. (1957) Über die einwirking der

höhenstrahlung auf eisenmeteoriten. Z. Naturforsch 12a,

766-773.

EL GORESY, A. and FECHTIG, H. (1967) Fusion crust of iron meteorites

and mesosiderites and production of cosmic spherules.

Smithsonian Contributions to Astrophysics 11, 391-397.

ESHER, J.E., SMITH, P.F. and DAVIS, J.C. (1968) KWIK R8, a FORTRAN

IV program for multiple regression and geolic trend

analysis. Kansas Geol. Surv. Computer Contrib. 28, 31 pp.

EUGSTER, O., EBERHARDT, P. and GEISS, J. (1969) Isotopic analysis

of krypton and xenon in 14 stone meteorites. Jour. Geophys.

Res. 74, 3874-3896.

FARRINGTON, O.C., (1910)

Publications of the Field Museum, Geol. Ser. iii, 176.

FARRINGTON, O.C. (1915) Meteorites. Publ. by author in Chicago.

FECHTIG, H. and UTECH, K. (1964) On the presence or absence of

nickel in dark magnetic cosmic spherules and their

mechanisms of origin. Ann. New York Acad. Sci. 119, 243-249.

FIREMAN, E.L. (1958) Distribution of ^{3}He in the Carbo meteorite.

Nature 181, 1725.

FIREMAN, E.L. (1959) The distribution of helium-3 in the Grant

meteorite. Plan. Space Sci. 1, 66-70.

FLEISCHER, R.L., PRICE, P.B., WALKER, R.M. and WALKER, M. (1967a)

 Origins of fossil charged-particle tracks in meteorites.

 Jour. Geophys. Res. 72, 331-353.

FLEISCHER, R.L., PRICE, P.B., WALKER, R.M., MAURETTE, M. and

 MORGAN, G. (1967b) Tracks of heavy primary cosmic rays in

 meteorites. Jour. Geophys. Res. 72, 355-366.

FLETCHER, L. (1889) On the meteorites which have been found in

 the Desert of Atacama and its neighbourhood. Min. Mag. 8,

 223-264.

FLETCHER, L. and MILLIGAN, W.H. (1902) Fall of a meteoric stone

 near Crumlin (Co. Antrim) September 13. Nature 66, 577-579.

FOLINSBEE, R.E., BAYROCK, L.A., CUMMING, G.L. and SMITH, D.G.W.

 (1969) Vilna meteorite-camera, visual, seismic and analytic

 records. Roy. Astron. Soc. Canada Jour. 63, 61-86.

FUSE, K. and ANDERS, E. (1969) Aluminium-26 in meteorites — VI.

 Achondrites. Geochim. Cosmochim. Acta. 33, 653-670.

GARLICK, G.F.J. (1949) Luminescent Materials. Clarendon Press.

GARLICK, G.F.J. and GIBSON, A.F. (1948) The electron trap mechanism

 of luminescence in sulphide and silicate phosphors. Proc.

 Phys. Soc. (London) 60, 574-590.

GARLICK, G.F.J., LAMB, W.E., STEIGMANN, G.S. and GEAKE, J.E. (1971)

 Thermoluminescence of lunar samples and terrestrial

 plagioclases. Proc. Second Lunar Sci. Conf. 3, 2277-2283.

GEAKE, J.E. and WALKER, G. (1966) The luminescence spectra of

 meteorites. Geochim. Cosmochim. Acta. 30, 927-937.

GEISS, J., OESCHGER, H. and SCHWARZ, V. (1962) The history of

 cosmic radiation as revealed by isotopic changes in the

 meteorite and on the Earth. Space Sci. Rev. 1, 197-223.

GOEL, P.S. and KOHMAN, T.P. (1962) Cosmogenic carbon-14 in

meteorites and terrestrial ages of "finds" and "craters".

Science 136, 875-876.

GRÖGLER, N. and LIENER, A. (1968) Cathodoluminescence and

thermoluminescence observations of aubrites. In

Thermoluminescence of Geological Materials. (editor D. J.

Macdougall), pp. 569-578. Academic Press.

HARVEY, E.N. (1957) A History of Luminescence - From Earliest

Times until 1900. Chapter IX. Amer. Phil. Soc.

HERSCHEL, A.S. (1899) Triboluminescence. Nature 60, 29.

HAWKINS, G.S. (1960) Asteroidal Fragments. Astron. Jour. 65,

318-322.

HEIMANN, M., PAREKH, P. P. and HERR, W. (1974) A comparative study

on ^{26}Al and ^{53}Mn in eighteen chondrites. Geochim. Cosmochim.

Acta. 38, 217-234.

HEINZINGER, K., JUNGE, C. and SCHIDLOWSKI, M. (1971) Oxygen

isotope ratios in the crust of iron meteorites. Z. Natur-

forsch. 26a, 1485-1490.

HENDERSON, E.P. and DAVIS, H.T. (1936) Moore County, North Carolina,

Meteorite - a new eucrite. Amer. Min. 21, 215-229.

HENDERSON, E.P. (1941) Chilean hexahedrites and the composition

of all hexahedrites. Amer. Min. 26, 546-550.

HEY, M.A. (1966) Catalogue of Meteorites. Trustees of the British

Museum. (London).

HODGE, P.W. and WRIGHT, F.W. (1964) Studies of particles for

extraterrestrial origin 2. A comparison of microscopic

spherules of meteoritic and volcanic origin. Jour.

Geophys. Res. 69, 2449-2454.

HODGE, P.W. and WRIGHT, F.W. (1968) Studies of particles for

extraterrestrial origin 6. Comparisons of previous influx

estimates and present satellite flux data. Jour. Geophys.

Res. 73, 7589-7592.

HODGE, P.W. and WRIGHT, F.W. (1969) Semi-empirical estimate of

the micrometeorite flux at the Earth's surface and its

implications. Icarus 10, 214-219.

HODGE, P.W., WRIGHT, F.W. and LANGWAY, C.C. (1964) Studies of

particles for extraterrestrial origin 3. Analysis of dust

particles from polar ice deposits. Jour. Geophys. Res.

69, 2919-2931.

HODGE, P.W., WRIGHT, F.W. and LANGWAY, C.C. (1967) Studies of

particles for extraterrestrial origin 5. Compositions of

the interiors of spherules from Arctic ice deposits.

Jour. Geophys. Res. 72, 1404-1406.

HOFFMAN, J.H. and NIER, A.O. (1958) Production of helium in iron

meteorites by the action of cosmic rays. Phys. Rev. 112,

2112-2117.

HOFFMAN, J.H. and NIER, O.A. (1959) The cosmogenic He^3 and He^4

distribution in the meteorite Carbo. Geochim. Cosmochim.

Acta. 17, 32-36.

HOFFMAN, J.H. and NIER, A.O. (1960) Cosmic-ray-produced helium

in the Keen Mountain and Casas Grandes meteorites. Jour.

Geophys. Res. 65, 1063-1068.

HOUTERMANS, F.G. and LIENER, H. (1968) Thermoluminescence of

meteorites. Jour. Geophys. Res. 71, 3387-3396.

HOWARD, E.C. (1802) Experiments and observations on certain

    stony and metalline substances, which at different times

    are said to have fallen on the Earth; also on various

    kinds of native iron. Phil. Trans. Roy. Soc. 92, 168-212.

HOWARD, K.S. and DAVISON, J.M. (1906) The Estacado Aerolite.

    Amer. Jour. Sci. 22, 55-60.

HOYT, H.P., WALKER, R.M., ZIMMERMAN, D.W. and ZIMMERMAN, J. (1972)

    Thermoluminescence of individual grains and bulk samples

    of lunar fines. Proc. Third Lunar Sci. Conf. 3, 2997-3007.

HOYT, H.P., KARDOS, J.L., MIYAJIMA, M., SEITZ, SUNN, S.S.

    WALKER, R.M. and WITTEL, M.C. (1970) Thermoluminescence,

    X-ray and stored energy measurements on Apollo 11 samples.

    Proc. Apollo 11 Lunar Sci. Conf. 3, 2269-2287.

HUSS, G.I. and WILSON, I.E. (1973) A census of the meteorites of

    Roosevelt County, New Mexico. Meteoritics 8, 287-290.

HWANG, F.S.W. (1973) Fading of thermoluminescence induces in

    lunar fines. Nature 245, 41-43.

IUDIN, I.A. (1955) Meteoritika 13, 143 ff.

IUDIN, I.A., DUZMANOV, Iu.D. and REMENNIKOVA, M.M. (1968)

    Investigation of the minerals in the ablated crust of

    the Saratov meteorite. Meteoritika 28, 156-157. (Int.

    Aerospace Abs. 9, 160; 1969).

IVANOV, A.V. and FLORENSKI, K.P. (1968) Finely dispersed cosmic

    matter on the Earth. Solar System Res. 5, 4-11.

JAMES, J.F. and STERNBERG, R.S. (1969) Design of Optical

    Spectrometers. Chapman and Hall (London).

JOHNSON, R.P. (1939) Jour. Opt. Soc. Amer. 29, 387.

KEIL, K., BUNCH, T.E. and PRINZ, M. (1970) Mineralogy and
composition of Apollo 11 lunar samples. Proc. Apollo 11
Lunar Sci. Conf, 1, 561-598.

KELLERUD, G. and YODER, H.S. (1959) Pyrite stability relations
in the Fe-S system. Econ. Geol. 54, 533-572.

KIEL, K. and FUCHS, L.H. (1971) Hibonite $(Ca_2(Al,Ti)_{24}O_{38})$ from
the Leoville and Allende chondritic meteorites. Earth
Planet. Sci. Letters 12, 184-190.

KIRSTEN, T.A. and SCHAEFFER, O.A. (1971) High energy interactions
in space. In Elementary Particles (editor L.C.L. Yuan)
pp. 75-157. Academic Press.

KOHMAN, T.P. and BENDER, M.L. (1967) Nuclide production by cosmic
rays in meteorites and on the Moon. In High-Energy
Nuclear Reactions in Astrophysics (editor B.S.P. Shen),
pp. 169-245.

KOLOMENSKY, V.D. and IUDIN, I.A. (1958) Mineral composition of
the fusion crust of the Sikhote Alin meteorite and
meteoritic and meteoric dust. Meteoritika 16, 59-66.

KOPAL, Z. (1961) Numerical Analysis. Chapman and Hall (London).

KRACEK, F.C. and CLARK, S.P. (1966) Melting and transformation
points in oxide and silicate systems at low pressure.
In Handbook of Physical Constants (Geol. Soc. Amer.,
Memoir 97) (editor S. P. Clark).

KRINOV, E.L. (1960) Principles of Meteoritics. Pergamon.

LABYRIE, J., LALOU, C. and NORDEMANN, D. (1968) A high sensitivity
apparatus to detect thermoluminescence induced by very
weak radiations. In Thermoluminescence of Geological
Materials (editor D.J. Macdougall), pp. 175-182. Academic
Press.

LAL, D., LORIN, C., PELLAS, P., RAJAN, R.S. and TAMHANE, A.S.
(1969) On the energy spectrum of iron-group nuclei as
deduced from fossil-track studies on meteoritic minerals.
In Meteorite Research (editor P. Millman), pp. 275-285.
D. Riedel.

LALOU, C., NORDEMANN, D. and LABYRIE, J. (1970a) Etude Préliminaire
de la thermoluminescence de la météorite Saint-Séverin.
Comptes Rendus Acad. Sci. (Paris) Serie D, 270, 2401-2404.

LALOU, C., BRITO, U., NORDEMANN, D. and MARY, M. (1970b) TL
induite dans des cibles epaises par des protons de 3 GeV.
Comptes Rendus Acad. Sci. (Paris) Serie D, 270, 1706-1708.

LALOU, C., VALLADAS, G., BRITO, U., MENNI, A., CAVA, T. and
VISOCEKAS, R. (1972) Spectral emission of natural and
artificially induced TL in Apollo 14 lunar sample 14163,
147. Proc. Third Lunar Sci. Conf. 3, 3009-3020.

LIENER, H. and GEISS, J. (1968) Thermoluminescence measurements
on chondritic meteorites. In Thermoluminescence of
Geological Materials (editor D. J. Macdougall), pp. 559-568.
Academic Press.

LORIN, J.C. and POUPEAU, G. (1973) Track studies in Keyes and
Saint-Severin chondrites. Meteoritics 8, 410-411 (Abstract
only).

LOVERING, J.F., PARRY, L.G. and JAEGER, J.C. (1960) Temperatures
and man losses in iron meteorites during ablation in the
earth's atmosphere. Geochim. Cosmochim. Acta. 19, 156-167.

MARINGER, R.E. and MANNING, G.K. (1960) Aerodynamic heating of
the Grant meteorite. Geochim. Cosmochim. Acta. 18, 157-161.

MARTI, K., EBERHARDT, P. and GEISS, J. (1966) Spallation, fission and neutron capture anomalies in meteoritic krypton and xenon. Z. Naturforsch 21a, 398-413.

MARTIN, G.R. (1953) Recent studies on iron meteorites IV: The origin of meteoritic helium and the age of meteorites. Geochim. Cosmochim. Acta. 3, 288-309.

MARVIN, U.B., WOOD, J.A. and DICKEY, J.S. (1970) Ca-Al rich phases in the Allende Meteorite. Earth Planet. Sci. Letters 7, 346-350.

MARVIN, U.B. (1963) Mineralogy of the oxidation products of the Sputnik 4 fragment and of iron meteorites. Jour. Geophys. Res. 68, 5059-5068.

MASON, B. (1962) Meteorites. J. Wiley.

MASON, B. (1967) The Bununu meteorite, and a discussion of the pyroxene-plagioclase achondrites. Geochim. Cosmochim. Acta. 31, 107-115.

MASON, B. and WIIK, H.B. (1963) The composition of the Richardton, Estacado and Knyahinya meteorites. Amer. Mus. Novitates No. 2154.

McCROSKY, R.E. and BOESCHENSTEIN, H. (1963) The Prairie Meteorite Network. Smithsonian Astrophys. Obs. Spec. Rep. 173. 23 pp. Also in Jour. Soc. Photo-Opt. Instr. Eng. 3, 127 (1965).

McCROSKY, R.E. and CEPLECHA, Z. (1968) Photographic networks for fireballs. Smithsonian Astrophys. Obs. Spec. Rep. 288. Also in Meteorite Research (editor P. Millman), pp. 600-612. D. Riedel.

McCROSKY, R.E., POSEN, A., SCHWARTZ, G. and SHAO, C.-Y. (1971)
Lost City meteorite - its recovery and a comparison with
other fireballs. Jour. Geophys. Res. 76, 4090-4108.

MEDLIN, W.L. (1968) The nature of traps and emission centres in
thermoluminescent rock materials. In Thermoluminescence
of Geological Materials (editor D. J. Macdougall), pp. 193-
223. Academic Press.

MERRIL, G.P. (1917) Proc. U.S. Nat. Mus. Washington 52, 419, and
ibid (1918) 54, 503.

MUTCH, T.A. (1964) Extraterrestrial particles in Paleozoic salts.
Ann. New York Acad. Sci. 119, 166 ff.

NININGER, H.H. (1952) Out of the Sky. Dover Books.

NININGER, H.H. (1935a) The surface features of meteorites. Pop.
Astron. 42, 121-126.

NININGER, H.H. (1935b) The Lafayette meteorite. Pop. Astron. 43,
(7).

NININGER, H.H. (1936a) The Pasamonte, New Mexico, Meteorite. Pop.
Astron. 54, 6-7.

NININGER, H.H. (1936b) Further studies on the surface features of
meteorites. Amer. Jour. Sci. 32, 1-20.

NININGER, H.H. (1936c) The Bruno meteorite. Amer. Jour. Sci. 31,
209-222.

NININGER, H.H. and NININGER, A.D. (1950) The Nininger Collection
of Meteorites.

NYQUIST, L., FUNK, H., SCHULTZ, L. and SIGNER, P. (1973) He, Ne,
and Ar in chondritic nickel iron as irradiation hardness
sensors. Geochim. Cosmochim. Acta. 37, 1655-1686.

ÖPIK, E. (1958) Physics of Meteor Flight in the Atmosphere.

Interscience (New York).

PANETH, F.A., PEASBECK, P. and MAYNE, K.I. (1953) Production by

cosmic rays of helium-3 in meteorites. Nature 172, 200.

PRACHYABRUED, W., DURRANI, S.A. and FREMLIN, J.H. (1971) Thermo-

luminescence of the Lost City meteorite. Meteoritics 6,

300-301 (Abstract only).

PRICE, P.B., RAJAN, R.S. and TAMHANE, A.S. (1967) On the pre-

atmospheric size and maximum space erosion rate of the

Patwar stony-iron meteorite. Jour. Geophys. Res. 72,

1377-1388.

RAMDOHR, P. (1967) Die schmelzkruste der meteoriten. Earth Planet.

Sci. Letters 2, 197-209.

RAMDOHR, P. (1972) The highly reflecting and opaque components in

the mineral content of the Havero meteorite. Meteoritics

7, 565-578.

RANCITELLI, L.A., PERKINS, R.W., FELIX, W.D. and WOGMAN, N.A. (1971)

Cosmogenic and primordial radionuclide measurements in

Apollo 12 lunar samples by nondestructive analysis. Proc.

Second Lunar Sci. Conf. 2, 1757-1772.

RANDALL, J.T. and WILKINS, M.F.H. (1945) Phosphorescence and

electron traps. Proc. Roy. Soc. (London) A, 184, 366-407.

REED, S.J. (1972) The Oktibbeha County iron meteorite. Min. Mag.,

38, 623-626.

REID, A.M. and COHEN, A.J. (1967) Some characteristics of

enstatite from enstatite achondrites. Geochim. Cosmochim.

Acta. 31, 661-672.

SCHULTZ, L., PHINNEY, D. and SIGNER, P. (1973) Depth dependence

of spallogenic noble gases in the St. Séverin chondrite.

Meteoritics 8, 435-436. (Abstract only).

SEARS, D.W. (1974a) Interplanetary dust on the Earth's surface.

Jour. Brit. Astron. Ass. In press.

SEARS, D.W. (1974b) Edward Charles Howard and an early contribution

to meteoritics. Jour. Brit. Astron. Ass. In Press.

SEARS, D.W. (1974c) Why did meteorites lose their smell? Jour.

Brit. Astron. Ass. 84, 299-300.

SEARS, D.W. and MILLS, A.A. (1973) Temperature gradients and

atmospheric ablation rates for the Barwell meteorite.

Nature Physical Science 242, 25-26.

SEARS, D.W. and MILLS, A.A. (1974a) Thermoluminescence and the

terrestrial age of meteorites. Meteoritics 9, 47-68.

SEARS, D.W. and MILLS, A.A. (1974b) Existence of two groups in

the thermoluminescence of meteorites. Nature 249, 234-235.

SEARS, D.W. and MILLS, A.A. (1974c) Thermoluminescence studies of

the Allende meteorite. Earth Planet. Sci. Letters 22, 391-396.

SIGNER, P. and NIER, A.O. (1960) The distribution of cosmic-ray-

produced rare gases in iron meteorites. Jour. Geophys.

Res. 65, 2947-2964.

SIGNER, P. and NIER, O.A. (1962) The measurement and interpretation

of rare gas concentrations in iron meteorites. In

Researches on Meteorites (editor C.B. Moore), pp. 7-35.

J. Wiley.

SMITH, F.G. (1963) Physical Geochemistry. Addison-Wesley (London).

SUESS, H.R. and WÄNKE, H. (1962) Radiocarbon content and

    terrestrial age of twelve stony meteorites and one iron

    meteorite. Geochim. Cosmochim. Acta. 26, 475-488.

SUN, K.H. and GONZALES, J.L. (1966) Thermoluminescence of the

    Moon. Nature 212, 23-25.

TRIVEDI, B.M. and GOEL, P.S. (1973) Nuclide production rates in

    stone meteorites and lunar samples by galactic cosmic

    radiation. Jour. Geophys. Res. 78, 4885-4900.

TSCHERMAK, G. (1885) Die Mikroskopische Beschaffenheit der

    Meteoriten (Stuttgart) translated and reprinted as Micro-

    scopic Properties of Meteorites. Smithsonian Contrib.

    Astrophys. 4, 138-239 (1964).

VALLADAS, G. and LALOU, C. (1973) Etude de la thermoluminescence

    de la meteorite Saint Severin. Earth Planet. Sci. Letters

    18, 168-171.

VAN SCHMUS, W.R. and RIBBE, P.H. (1968) The composition and

    structural state of feldspar from chondritic meteorites.

    Geochim. Cosmochim. Acta. 32, 1327-1342.

VAN SCHMUS, W.R. and WOOD, J.A. (1967) A chemical-petrologic

    classification for the chondritic meteorites. Geochim.

    Cosmochim. Acta. 31, 747-765.

VAZ, J.E. (1971a) Asymmetric distribution of thermoluminescence

    in the Ucera meteorite. Nature Physical Science 230, 23-24.

VAZ, J.E. (1971b) Lost City meteorite: Determination of the

    temperature gradient induced by atmospheric friction

    using thermoluminescence. Meteoritics 6, 207-216.

VAZ, J.E. (1972) Ucera meteorite: Determination of differential

    atmospheric heating using its natural thermoluminescence.

    Meteoritics 7, 77-86.

VAZ, E. and ZELLER, A.N. (1966)   Thermoluminescence of calcite from high gamma radiation doses. Amer. Mineral. 51, 1156-1166.

VERNIANI, F. (1973) An analysis of the physical parameters of 5759 faint radio meteors. Jour. Geophys. Res. 78, 8429-8462. See also the news report in Nature 248, 99 (1974).

WASSON, J.T. and GOLDSTEIN, J.I. (1968) The north Chilean hexa-hedrites: Variations in composition and structure. Geochim. Cosmochim. Acta. 32, 329-339.

WILKENING, L.L., HERMAN, G.F. and ANDERS, E. (1973) Aluminium-26 in meteorites - VII. Ureilites, their unique radiation history. Geochim. Cosmochim. Acta. 37, 1803-1810.

WLOTZKA, F. (1972) Havero urielite: Evidence for recrystallisation and partial reduction. Meteoritics 7, 591-600.

WRIGHT, A.W. (1875) Spectroscopic Examination of gases from meteoric iron. Amer. Jour. Sci. 9, 294-302.

WRIGHT, F.W. and HODGE, P.W. (1965a) Analysis of artificial meteoritic spherules. Smithsonian Astrophys. Obs. Spec. Rep. 192. 10 pp.

WRIGHT, F.W. and HODGE, P.W. (1965b) Studies of particles for extraterrestrial origin 4. Spherules from Volcanic eruptions. Jour. Geophys. Res. 70, 3889-3898.

WRIGHT, F.W., HODGE, P.W. and LANGWAY, C.C. (1963) Studies of particles for extraterrestrial origin. 1. Chemical analyses of 118 particles. Jour. Geophys. Res. 68, 5575-5587.

WRIGHT, F.W., HODGE, P.W. and LANGWAY, C.C. (1969) Further measurements of the composition of dust particles. Smithsonian Astrophys. Obs. Spec. Rep. 297, 19 pp.

WRIGHT, R.J., SIMMS, L.A., REYNOLDS, M.A. and BOGARD, D.D. (1973) Depth variation of cosmogenic noble gases in the 120 kg Keyes chondrite. Jour. Geophys. Res. 78, 1308-1318.

PUBLICATIONS

Temperature Gradients and Atmospheric Ablation Rates for the Barwell Meteorite

WE have been studying the fusion crust of the Barwell meteorite (an olivine-hypersthene chondrite[1]) in order to quantify the way meteorites behave in the atmosphere. We have found that systematic differences occur in the temperature gradients associated with specimens derived from various faces of the original stone. We have also determined the corresponding ablation rates (which seem to be the first to be reported for any stony meteorite), the mass loss and the effective heating time for this meteorite.

Tschermak[2] described the fusion crust as consisting of zones of fusion, absorption and impregnation. The third zone was said by Borgstrom[3] to be troilite-rich. We have confirmed this for Barwell by point counting: four specimens of fusion crust showed an average volume % of non-stoichiometric FeS and non-stoichiometric FeS/Ni-Fe eutectic near 25%, compared with 5% for the bulk matrix. Departures from stoichiometry in the FeS are being investigated with the electron probe.

More recently, Ramdohr[4] has studied the mineralogical changes that occur in the fusion crust. From these he was able to define six zones and estimate the temperatures at four of the zone boundaries (Fig. 1). The outer zone contains two phases—skeletal magnetite in a black opaque glass. All surface morphology occurs in this zone and it is assumed to have been wholly molten and isothermal. It ends abruptly at boundary a, after which a zone of opaque glass with no inclusions occurs. At boundary b there begins a zone of fragmented crystals which have melted around the edges and are surrounded by darker glass. Boundary c marks the start of a zone of unaltered material into which the metal and sulphide has flowed, and finally the original matrix of the meteorite is reached at d.

Table 1 Parameters of Heat Flow in Barwell Meteorite

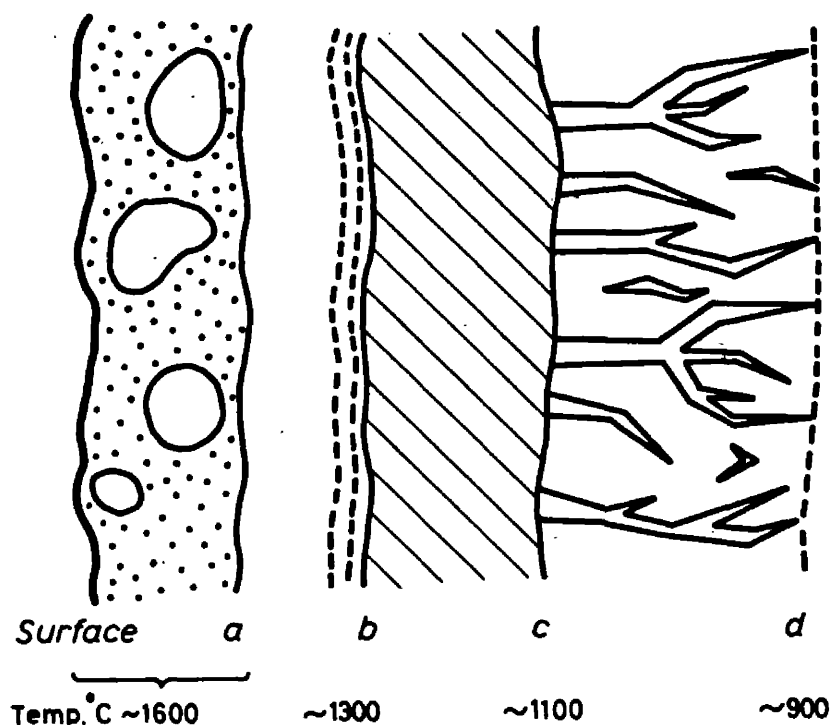| Specimen	Face type	Temp. gradient at boundary c (°C/μm)		Ablation rate (cm s⁻¹)
		From ablation theory	From Fig. 2	
BM 1966, 59	Front, close	12	5.0	0.35
BM 1966, 65	Front/side, close	7.6	3.9	0.27
BM 1966, 57	Lateral, striated	6.1	3.3	0.22
BM 1966, 57	Rear, warty	3.5	2.3	0.18

Fig. 1 Schematic representation of the fusion crust. The total depth represented would be about 0.4–0.8 mm, depending on orientation of the face.

We have examined the surface morphology of specimens of the Barwell meteorite and assigned face-type classifications as defined by Krinov[5]. This is a descriptive classification relating flow structures to the orientation of the face from which the specimen came (for example, front, lateral or rear). The Barwell fall was chosen because it is plentiful and contains representatives of all face-types found on stony meteorites. Polished sections were prepared of chips taken from faces of assigned type, and the distances of all four boundaries from the outer surface measured ten times at representative locations. Local differences were numerous but readily identified. The percentage standard deviations were: a, 75%; b, 29%; c, 20%; and d, 22%. Except for boundary a these values reflect the relative clarity of the boundary. Boundary a is very distinct, and the high standard deviation arises because the outer surface from which it is measured is very uneven the irregularities often representing a major proportion of this first zone. The value for boundary d is the least meaningful, because it depends as much on the amount of metal and sulphide initially present as on the temperature gradient. Temperatures associated with these boundaries are plotted against distance from the molten-solid boundary a in Fig. 2.

It is possible to determine the temperature gradient at any point in the fusion crust from these curves. Unfortunately

2

the errors in such values may be considerable, arising chiefly from the assigned temperatures. An alternative approach involves taking the most reliable temperature/distance data— those for non-stoichiometric FeS melting at boundary c—and applying the theory of Bethe and Adams[6] for the ablation of glassy materials. In that case the ablation rate (v_w cm s^{-1}) is given by

$$v_w = -(k/y)\ln(T/T_1)$$

where k is the thermal diffusivity (a typical stony meteorite value is 8.4×10^{-3} cm^2 s^{-1}), T_1 is the temperature at the surface (1,600° C assumed), and T is the temperature at distance y from that surface. With the ablation rate determined, the temperature gradient can then be found from

$$\partial T/\partial y = v_w T_1 k^{-1} \exp(-y v_w k^{-1})$$

Values obtained by this method for the ablation rate and the thermal gradient across boundary c are given in Table 1. Eye-estimates of the gradient from Fig. 2 are also given for comparison.

Because the temperature gradients across the fusion crust of a meteorite are controlled by ablation, we expect them to be greater where the rate of ablation is greater. All the thermal gradients determined here show this trend. We believe this is
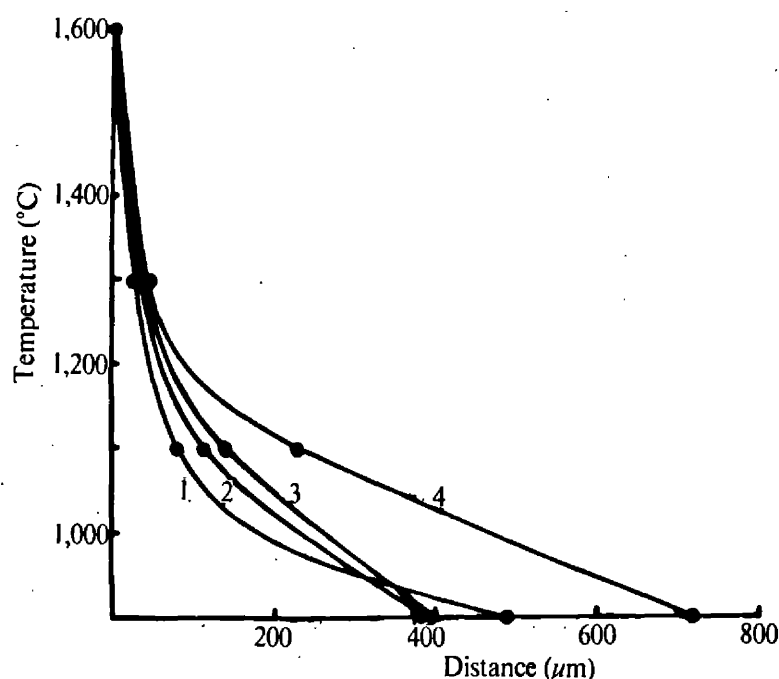

Fig. 2 Temperature as a function of distance from boundary a for four types of surface on the Barwell meteorite. 1, Front, BM 1966, 59; 2, front/side, BM 1966, 65; 3 (side) and 4 (rear), BM 1966, 57.

the first instance of stony meteorite ablation rates being determined: irons have already received some attention because of the more readily applicable metallurgical techniques. Their ablation rates are typically about 0.2 cm s^{-1} (ref. 7) which is surprisingly similar to the figures obtained here. It seems that a lower melting point is balanced by a higher thermal conductivity.

The mass loss experienced by the Barwell meteoroid may be estimated by taking the mean ablation rate of 0.25 cm s^{-1} and assuming this was sustained throughout a luminous flight time of 10 s, thereby removing 2.5 cm of material. No direct observation of the luminous flight time of Barwell is available, so we have been guided chiefly by the figure of 9 s quoted for the Lost City meteorite[8]. The ground track and beginning height of the latter are very similar to those of Barwell[9], although the velocity may well have been different. Total reconstruction of the Barwell meteorite from the 47 kg of fragments was not possible, and it is thought that only about one half has been recovered. The actual mass of about 100 kg would be equivalent to a spherical body of radius 19.0 cm. Replacing the material removed by ablation gives an original radius of 21.5 cm and a mass loss of 31%. This is an underestimate, because ablation is greater at altitudes higher than that at which the terminal fusion crust was formed. This figure may be compared with a fossil track estimate of 25% mass loss for the St Severin meteorite[10].

The "effective heating time" of any meteorite may be defined as the period required to form the terminal fusion crust and observable thermal gradients. Both Nininger[11] and Krinov[5] arrive at periods of the order of one second for this parameter. The method we explored to find this figure required measuring the enrichment of "troilite" in the innermost zone by point counting, and applying a knowledge of its rate of flow into this zone. When the latter was assigned a maximum value equal to the ablation rate, our result also was close to one second. It seems that only at the very end of luminous flight does the heat wave penetrate a meteorite to a depth greater than a few tens of micrometres: prior to that ablation must remove material faster than heat penetrates. It also seems that during this final second the Barwell meteorite did not significantly alter its orientation; if it had done so the observed differences would have been smoothed out.

We thank Dr R. Hutchison (British Museum, Natural History) and the Leicester Museums for the donation of specimens.

D. W. SEARS
A. A. MILLS

Departments of Astronomy and Geology,
University of Leicester

4

[1] Jobbins, E. A., Dimes, F. G., Binns, R. A., Hey, M. H., and Reed, S. J., *Min. Mag.*, 35, 881 (1966).

[2] Tschermak, G., *Die Mikroskopische Beschaffenheit der Meteoriten* (Stuttgart, 1885); reprinted as *Smithsonian Contrib. Astrophys.*, 4 (6), 138 (1964).

[3] Borgstrom, H. L., *Bull. Comm. Geol. Finlande*, 34, 22 (1912).

[4] Ramdohr, P., *Earth Planet. Sci. Lett.*, 2, 197 (1967).

[5] Krinov, E. L., *Principles of Meteoritics*, 264 (Pergamon, 1960).

[6] Bethe, H. A., and Adams, M. C., *J. Aero/Space Sci.*, 26, 321 (1959).

[7] Anders, E., *Meteorite Ages* in *The Moon, Meteorites and Comets* (edit. by Middlehurst, B. M., and Kuiper, G.) (Univ. Chicago Press, 1963).

[8] McCrosky, R. E., Posen, A., Schwartz, G., and Shao, C.-Y., *J. Geophys. Res.*, 76, 4090 (1971).

[9] Miles, H. G., and Meadows, A. J., *Nature*, 210, 83 (1966).

[10] Cantelaube, Y., Pellas, P., Nordemann, D., and Tobailem, J., in *Meteorite Research* (edit. by Millman, P.), 705 (Riedel, 1969).

[11] Nininger, H. H., *Pop. Astron.*, 42, 121 (1935) .

Existence of two groups in thermoluminescence of meteorites

THE thermoluminescence (TL) properties of meteorites[1-4] may be applicable to the determination of exposure age, terrestrial age, thermal gradients, radiation history and preatmospheric shape. In an attempt to apply TL to the determination of terrestrial age we have discovered that meteorites can be divided into two groups, the existence of which is relevant to several of the applications.

Our apparatus consists of a molybdenum strip heated electrically at $5 \pm 0.05° C\ s^{-1}$ by an electronic control unit. The light emitted by 10 mg of 50 μm sieved powder placed on a defined area of the strip is measured by a cooled and shielded 9635B EMI photomultiplier tube. The amplified signal is plotted automatically against temperature. The resulting 'glow curve' has two peaks, one at about 200° C (LT) and one at about 350° C (HT).

Table 1	Details of meteorites of known terrestrial age			
Meteorite	Terrestrial age (yr)	BM no. (if applicable)	Class	Thermolumin-escence group
Barwell	8		L6	Low
Bruderheim	13		L6	Low
Khanpur	21		LL5	Low
Mangwendi	39		LL6	Low
Olivenza	49		LL5	Low
Saratov	55	BM1956, 169	L4	High
Crumlin	71	BM86115	L5	Low
Gambat	76	BM83864	L6	Low
Jelica	83		LL6	Low
Soko Banja	96		LL4	High
Tennasilm	101	BM1913, 218	L4	High
Butsura	112	BM34795	H6	High
Dhurmsala	113		LL6	Low
Aldsworth	138	BM61308	LL5	Low
Durala	158	BM32097	L6	High
Limerick	160		H5	Low
Wold Cottage	178	BM1073	L6	High
Mauerkirchen	205	BM19967	L6	High
Ogi	232	BM55256	H6	High

We recorded the glow curves of nineteen meteorites that were seen to fall and are therefore of accurately known terrestrial age (Table 1). Two groups were immediately apparent; one in which LT falls below HT in about 100 yr after fall, and one in which it takes several hundred years for this to occur. Although the two groups are evident by visual inspection of the glow curves they are more obvious in Fig. 1, a plot of $\log_e$ (peak height ratio, LT/HT) against the terrestrial age of the meteorite. The low retentivity group, in which LT is fading fastest, shows much scatter from the line but the high group shows surprisingly little. The cause of the scatter is probably small initial differences in the TL of the meteorites, different thermal histories since the decay is temperature sensitive and, in the case of the low group, varying degrees of shock.
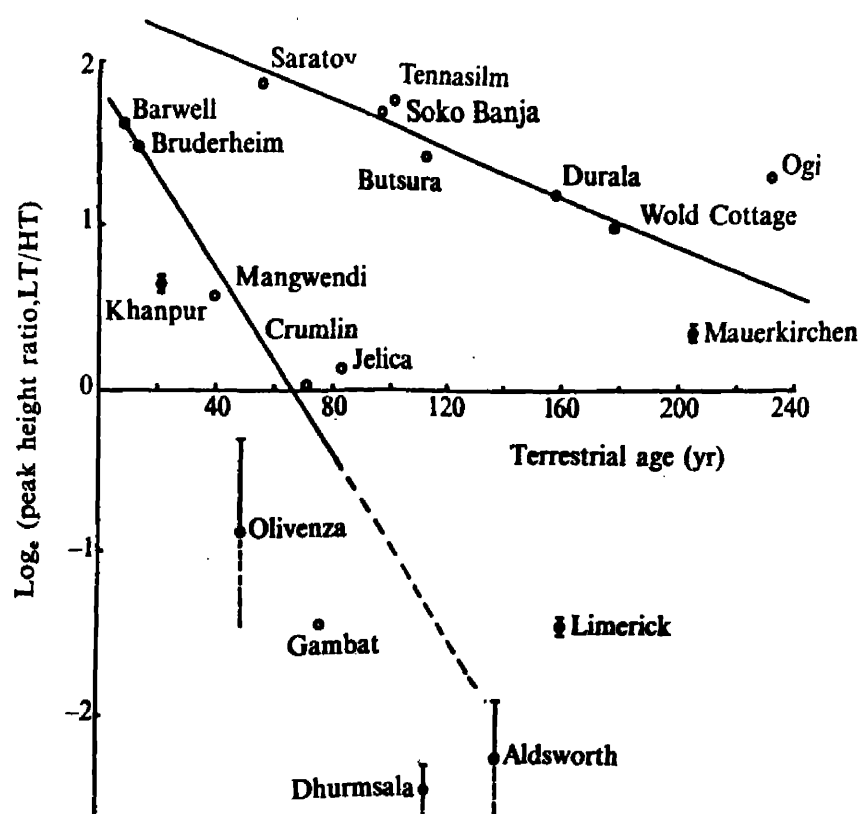

Fig. 1 Natural logarithm of the peak height ratio (LT/HT) as a function of terrestrial age, for meteorites of known terrestrial age.

To confirm that meteorites in the low retentivity group are fading faster than meteorites in the high retentivity group, the mean life (time to fall to 1/e) of LT in six meteorites was determined. We heated powder from three high and three low group meteorites in the dark at 120° C for various periods up to 70 h. Heating was done in an Abderhalden drying pistol surrounded by refluxing tetrachloroethylene. The results are shown in Fig. 2. Although the curves are not exponential, and

the results must be treated as approximate, it is clear that the two groups are due to different mean lives of LT in the luminescent material. The mean life, τ, at room temperature can be calculated from

$$\tau\,(300\text{K}) \;=\; \tau(393\text{K})\exp\left[(E/k300) - (E/k393)\right]$$

where E, the energy of the peak, can be found by the initial rise method and k is the Boltzman constant[5]. For the low retentivity group the mean life at room temperature is 6–8 yr and for the high group 45–55 yr.

We have not been able to determine with certainty the reason for the two groups but suspect that it is related to shock. Both metamorphism and shock change the nature of the luminescent feldspar, shock producing maskelynite and metamorphism causing recrystallisation. Chemical–petrological groups assigned on the extent of metamorphism[6] show no correlation
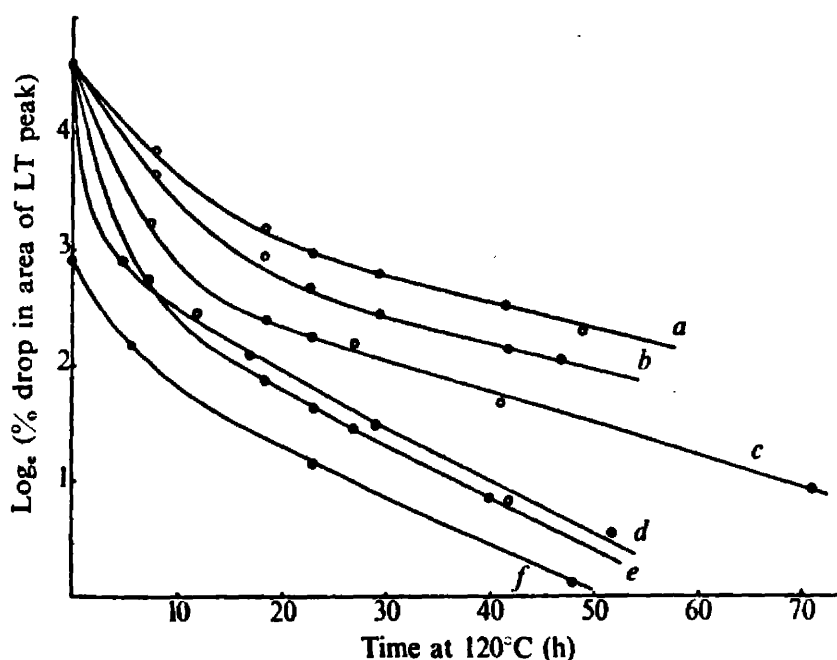

Fig. 2 Isothermal annealing curves for three high and three low retentivity meteorites. The ordinate is the natural logarithm of the percentage drop in the area under LT. Overlap has been allowed for where necessary and the curve for Jelica has been displaced vertically downwards for clarity. *a*, Wold Cottage (50–54 h); *b*, Saratov (50–55 h); *c*, Tennasilm (50–55 h); *d* Barwell (28–34 h); *e*, Bruderheim (26–34 h); *f*, Jelica (28–34 h). The numerical values are estimated for the mean lives at 120°C.

with the TL groups of the meteorites, inferring that metamorphism does not govern TL group membership. Shock is known to reduce TL intensity, however, and we have reason to believe that it also reduces the mean life of LT. Most of the members of the low group have been shocked or are breccias (R. Hutchison, personal communication). Olivenza and Barwell are anomalous in this respect, as is Soko Banja which is in the high group but is a breccia. Shock may also explain the scatter in the low group line in Fig. 1 since it can occur with various degrees of severity.

We thank Mr W. Prachyabrued (University of Birmingham) and Dr R. Hutchison (British Museum, Natural History) for discussions and the latter for supplying the ten BM specimens.

D. W. SEARS
A. A. MILLS

Departments of Astronomy and Geology,
University of Leicester, UK.

[1] Houtermans, F. G., and Liener, A., *J. geophys. Res.*, **71**, 3387 (1966).
[2] Lalou, C., Nordemann, D., and Labeyrie, J., *C. r. hebd. Séanc. Acad. Sci., Paris*, Serie D, **270**, 2401 (1970).
[3] Chrostodoulides, C., Durrani, S.A., and Ettinger, K. V., *Modern Geology*, **1**, 247 (1970).
[4] Vaz, E.., *Meteoritics*, **6**, 207 (1971).
[5] Garlick, G. F. J., *Luminescent Materials* (Clarendon Press, Oxford, 1949).
[6] Van Schmus, W. R., and Wood, J. A., *Geochim. cosmochim. Acta.*, **31**, 747 (1967).

1

THERMOLUMINESCENCE AND
THE TERRESTRIAL AGE OF METEORITES

D. W. Sears and A. A. Mills

The University of Leicester, England

The use of thermoluminescence (TL) to determine the terrestrial age of meteorites is investigated. It is found that meteorites can be divided into two groups. One group, in which members lose their low temperature TL rather rapidly (the "low retentivity" group), may be dated up to about 100 years after fall, although with little accuracy. The other (the "high" group) is more retentive, and may still be dated several hundred years after fall. A meteorite of unknown date of fall may be assigned to the high or low group by laboratory determination of the rate of decay of the low temperature TL.

Weathering coats the grains with limonite and lowers the intensity of the TL. The percentage reduction is constant for various intensities, but the peak height ratio is changed. Therefore, for weathered specimens, a method which examines the decrease in the intensity of a single peak is preferred to one which depends upon peak height ratios: this is made possible by artificially irradiating the meteorites. The following terrestrial ages for finds were obtained: Plainview 225-300 years; Dimmitt 280-330 years; Calliham 350-400 years. Bluff, Etter, Potter, Shields and Wellman (c) proved to be too old to be dated by our methods ($\gtrsim 500$ years). None of the low group finds available to us proved to be young enough to be dated precisely. Terrestrial ages indicate an extremely low efficiency of recovery ($\lesssim 1\%$) for meteorites that are not seen to fall.

Artificially irradiating the meteorites also revealed the fact that 9 of our 19 meteorites were saturated with respect to thermoluminescence when they entered the atmosphere, and therefore that a technique based on this phenomenon would not be applicable to such specimens to obtain their cosmic ray exposure age.

INTRODUCTION

The 'terrestrial age' of a meteorite is that period which has elapsed since it fell to Earth. The terrestrial ages of most meteorites are not known directly since the majority in collections are 'finds' rather than observed 'falls.' The methods so far used to determine this age (Anders, 1963; Boeckl, 1972;

Begemann and Vilcsek, 1969; Chang and Wänke, 1969) employ the decay of spallation-produced radioactive isotopes, and depend on knowing an original value for the decaying isotope. This is determined from falls of known age and assumed constant for all meteorites.

Thermoluminescence (TL) is the luminescence produced on heating a specimen. The thermal energy dislodges electrons which have been excited to "traps" in the crystal lattice by ionising radiation. The electrons drop to the ground state via a luminescent centre and in doing so emit light. TL is therefore a function of the ionising radiation received and the thermal history of the specimen (Randall and Wilkins, 1945). Groups in Berne, Paris and Birmingham (e.g. Houtermans and Liener, 1966; Lalou et al., 1970; Christo-doulides et al., 1970) have studied the thermoluminescence of meteorites. The latter suggested its use for determining terrestrial age, but no rigorous examination of the possibility appears to have been made. This is the aim of the present paper.

APPARATUS AND TECHNIQUE

Our equipment is shown diagrammatically in Fig. 1. The specimen (10 mg of 50 micron sieved powder from which any magnetic fraction has been removed) is placed on a defined area of a molybdenum strip, and heated by a high-amperage electric current at a linear heating rate of $5\pm0.05°$/sec. It is important that the heating rate is strictly linear because any slight deviation can produce perfectly reproducible but nevertheless spurious "peaks" (see Fig. 2 in Houtermans and Liener, 1966). Lower heating rates improved the resolution at the expense of intensity, and $5°$/sec was a good compromise. The emitted light was recorded with a 9635B EMI photomultiplier tube having a peak sensitivity between 3000 and 5000 Å. It was checked to give a
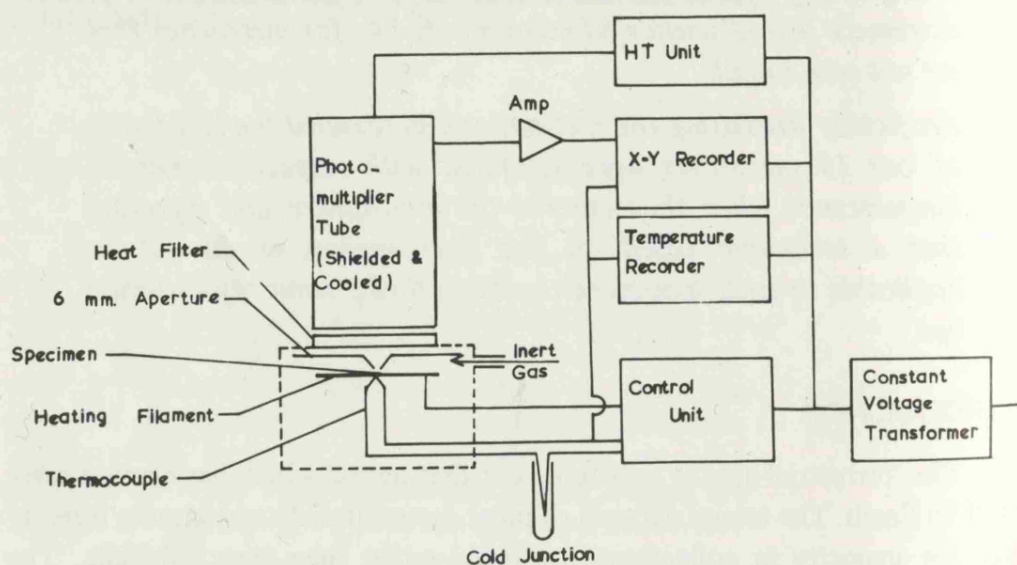

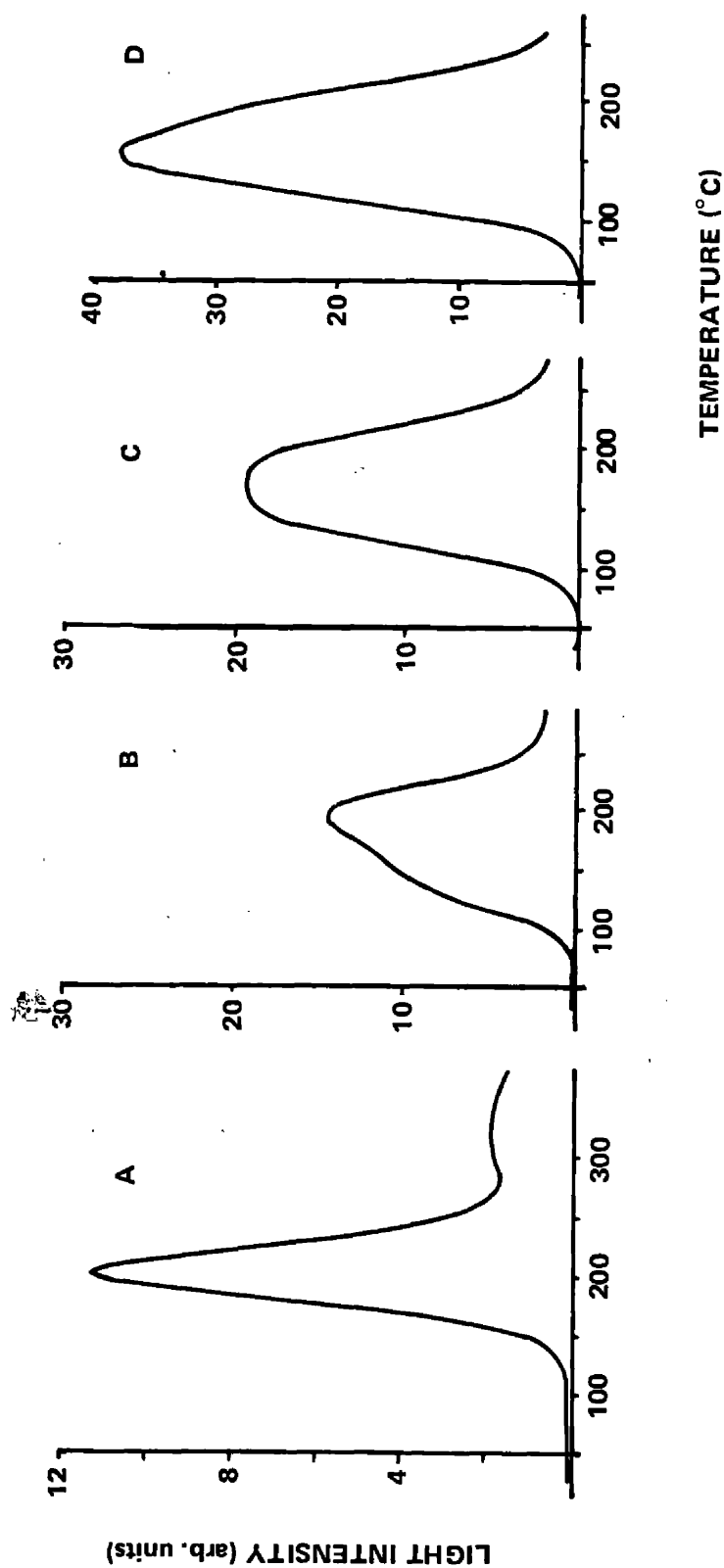Fig. 1   Schematic diagram of the thermoluminescence apparatus.

48

Fig. 2   The low temperature region of the Tennasilm meteorite glow curves. A) natural, B) natural + 23 krad, C) natural + 46 krad, D) natural + 69 krad. Thereafter the TL is saturated and the form of the glow curve changes little. The doses of γ-rays from ^{60}Co bomb are accurate to ±2 krad.

49

linear response at the light levels concerned. A Chance HA3 heat filter was placed between the photomultiplier tube and the specimen. The results are plotted automatically on an x-y recorder as light intensity *vs.* temperature to produce the "glow curve". A standard lamp (a Saunders-Roe "Betalight") is used before each set of runs to check that the sensitivity is constant. Results that are to be compared directly are obtained at one session, duplicating occasionally to ensure constancy. Irradiation is performed with a ^{60}Co source delivering γ-rays at about 700 krad/hour, and irradiated specimens are allowed to decay at room temperature for about 30 hours. This ensures that decay during a run is minimal, as it is only relative differences in decay which will affect the results used here. Figure 2 illustrates the importance of using low doses when examining the shape of the glow curve. Irradiation to high doses enhances the lowest peak considerably more than the others until it eventually dominates the glow curve. We do not work in red light since we have failed, using both irradiated and natural meteorite powder, to detect any draining by our laboratory fluorescent lights. Where possible, specimens were taken at least two centimetres from the fusion crust to exclude material that might have experienced atmospheric heating and be already partially drained. We have checked for possible tribo-thermoluminescence induced by the mild grinding procedure, but have not found any.

RESULTS

Natural thermoluminescence

The TL of common chondrites has been shown to be due to feldspar (Lalou *et al.*, 1970). The TL occurs in two temperature regions, one at about 200 °C, *LT*, and one at about 360 °C, *HT*. The peaks vary slightly in position depending on the amount of overlap between them.

Figure 3 shows the natural glow curves of the 19 specimens of known terrestrial age used in this study. They appear to fall into at least two main groups: one in which *LT* falls below *HT* in less than 100 years, and one in which *LT* is still much stronger than *HT* after 200 years. These differences are perhaps more noticeable in Fig. 4, a plot of $\log_e$ peak height ratio *vs.* terrestrial age. The 'high retentivity' group lies close to a straight line, whereas the 'low' group shows considerable scatter.

Artificial thermoluminescence

Christodoulides *et al.* (1970) suggested a way of determining the initial glow curve. Assuming *HT* has not faded (its half-life is considerably greater than *LT*) the radiation dose that is equivalent to the present TL of a specimen can be determined. If this is then given to drained material its luminosity will be restored to the initial level. However, using the following technique, these

Low Retentivity Group
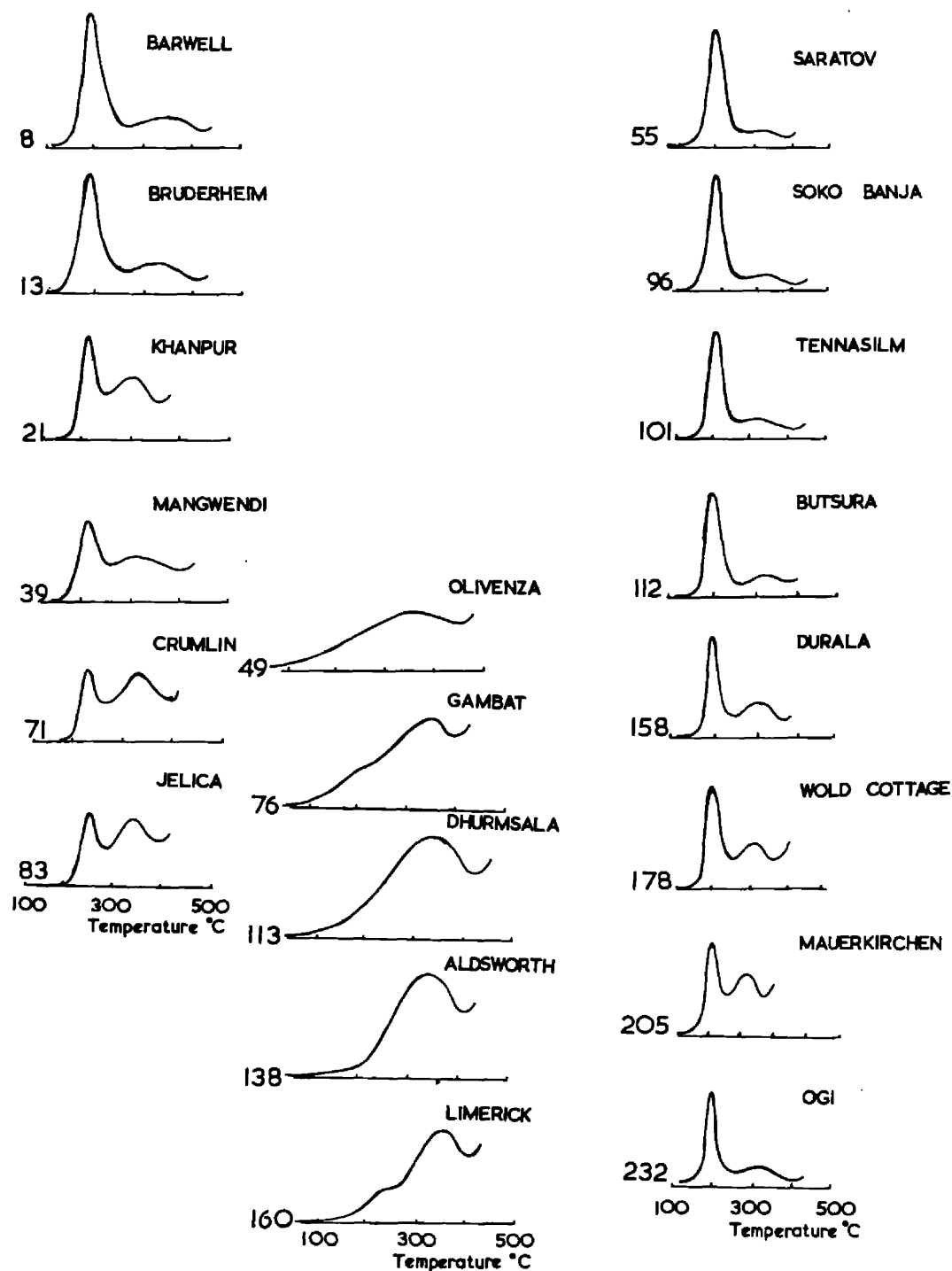
High Retentivity Group

Fig. 3 Sketches of the glow curves of 19 meteorites of known terrestrial age. The numbers denote this age in years. Details of the meteorites, peak positions and intensities are listed in Table 1. The vertical axis changes slightly, the height of *HT* is approximately constant. The curves turn up at the right with the onset of black-body radiation.
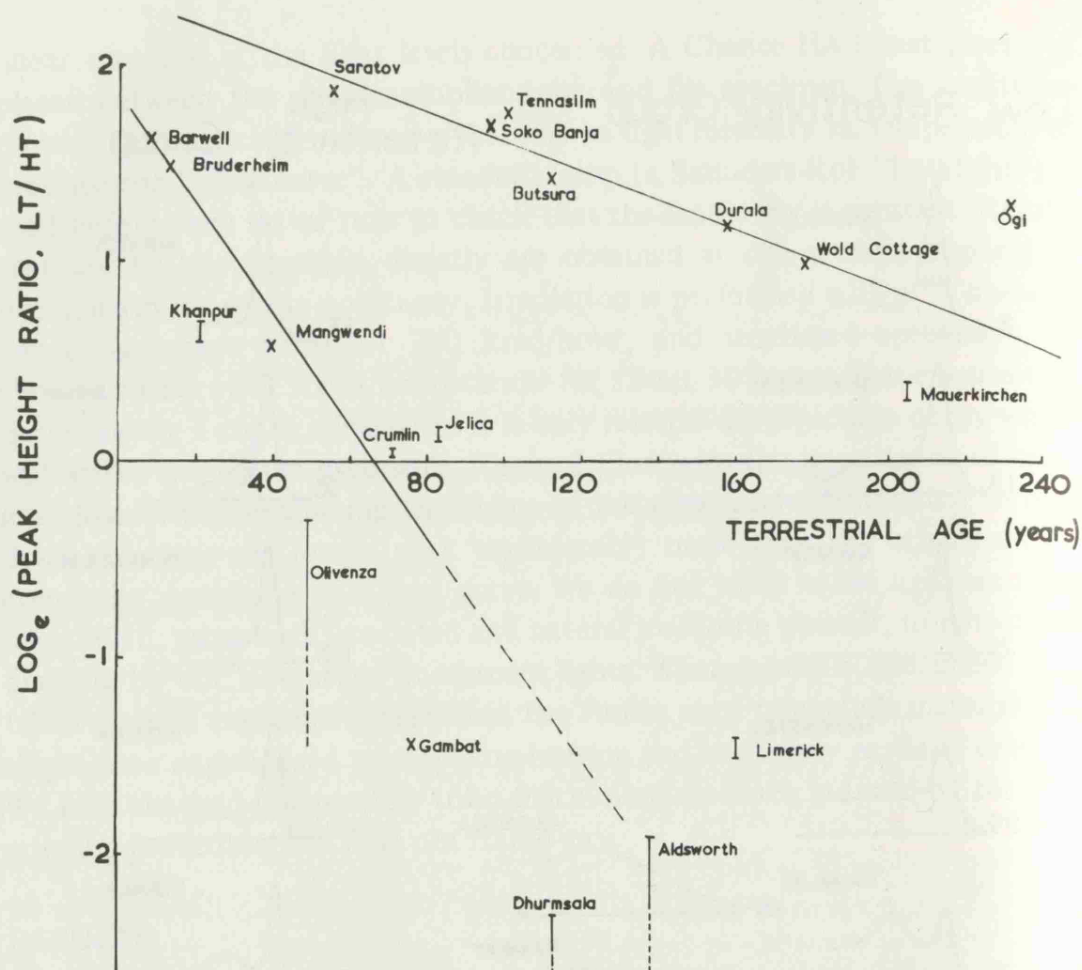
Fig. 4 Natural logarithm of the peak height ratio (LT/HT) as a function of terrestrial age for the meteorites of known terrestrial age.

two operations can be performed at the same time and the use of previously drained material avoided, since this introduces poorly understood complications. Various doses of radiation are given to the meteorite and curves of luminosity against superimposed dose produced for each of the two peaks (Fig. 5). By extrapolating the HT line back to zero TL the initial dose may be found. The intercept of the HT line and the dose axis is assumed to equal the natural equivalent dose D. The height of LT equivalent to this dose, ℓ_0, may then be determined from the LT line.

The main problem of this technique for determining D is that irradiation appears to broaden the peak and move it to lower temperatures, inferring that more than simple enhancement is occurring. This effect was explained by Liener and Geiss (1968) as being due to the irradiation times in the laboratory being so much shorter than those in space, resulting in an extra peak below 200 °C. The contribution from this extra peak was minimised by measuring height rather than the theoretically more meaningful area, since the extra peak appears to broaden LT to a greater extent than it adds height.

Figure 6 shows a plot of $\log_e [\ell_0/\ell_{LT}]$ vs. terrestrial age. Certain meteorites (Olivenza, Dhurmsala, Aldsworth) show a very large ℓ_0/ℓ_{LT} ratio,
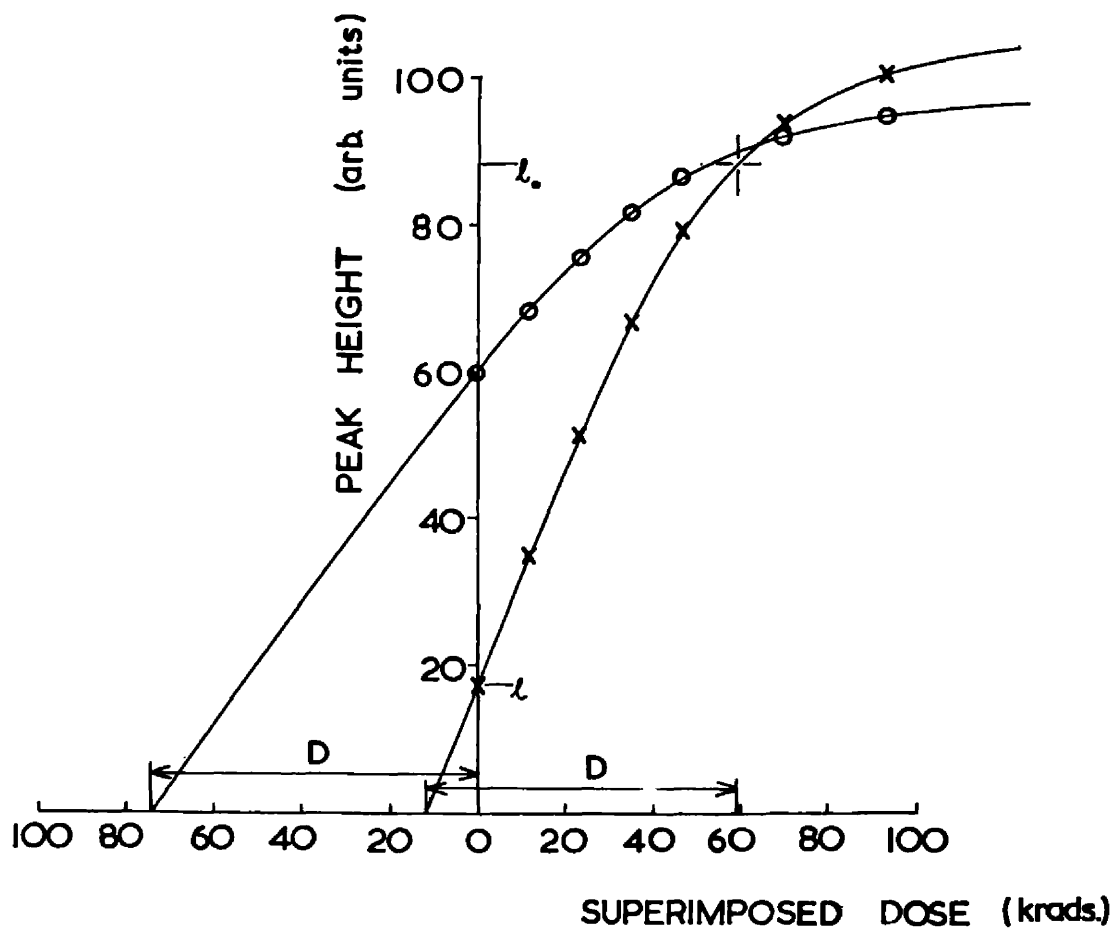
Fig. 5   Dose curves, peak height *vs.* superimposed dose, for the Soko Banja meteorite. Crosses denote heights of LT, circles represent heights of HT times twenty.
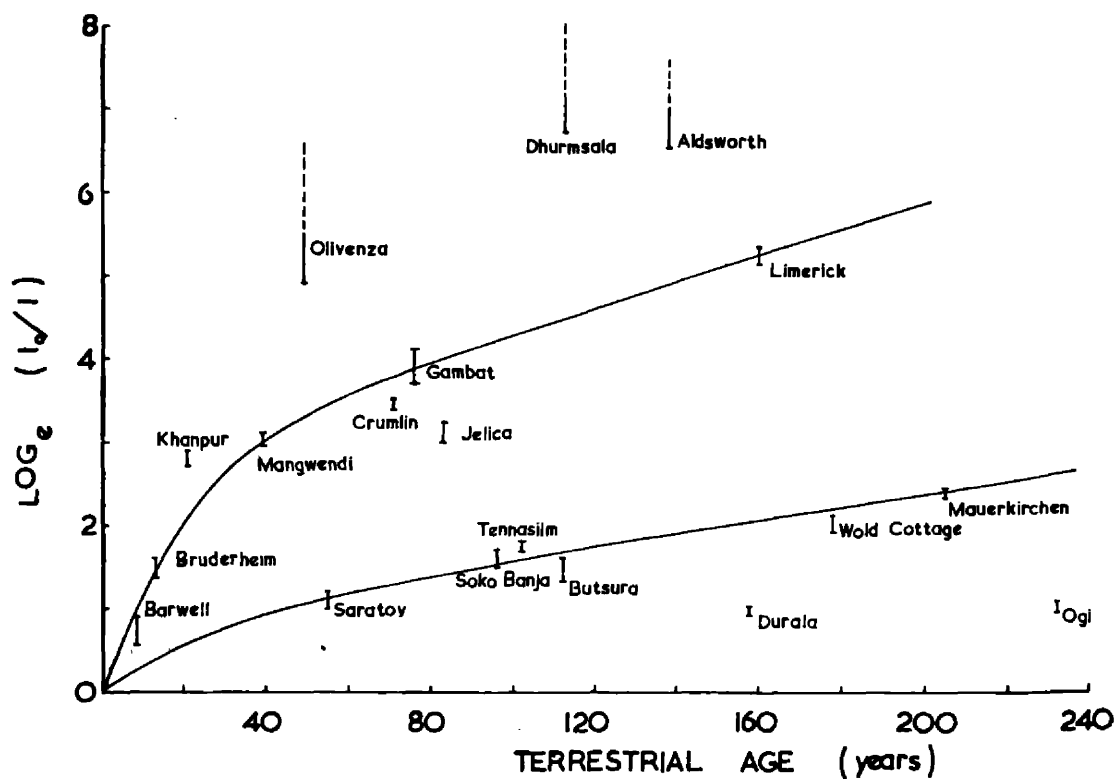

Fig. 6   Natural log of ℓ_0/ℓ_{LT} as a function of terrestrial age.

which together with the natural curves, Fig. 3, hints at a third group of meteorites.

It is interesting to note that many of the meteorites examined here had saturated TL when they entered the atmosphere; that is, the natural dose is on the plateau of the peak height *vs.* dose curve, Fig. 5, Table 1. This increases the accuracy with which ℓ_0 can be measured by decreasing its dependence on dose. Valladas and Lalou (1973) pointed out that it also means that these meteorites cannot be used to determine cosmic ray exposure age.

Determination of terrestrial age

The next step is to determine how a find can be assigned to one or other of the main groups, so that its terrestrial age can be found. No difference, within our experimental limits, was apparent in *LT* position for high or low group meteorites, or in the energy of the peak as determined by the initial rise method, Table 1 (Garlick and Gibson, 1948). However, the experimentally determined τ (the mean-life, time to fall 1/e) appeared to be different for meteorites in the high and low retentivity groups, Fig. 7. Using three meteorites from each group, τ at 120 °C was determined by annealing the powder in the dark for up to 70 hours in an Abderhalden drying pistol surrounded by refluxing tetrachloroethylene. A temperature of 120 °C was chosen because it should readily disclose if the main difference in Fig. 6 was due to different mean-lives. The values of τ at 120 °C are given in Table 1 and indicate room temperature mean-lives of 6-10 years for the low group and about 50 years for the high group. These results suggested it was possible to assign a meteorite to one of the two groups on the basis of the mean-life of its low-temperature TL peak.

The cause of the two groups is uncertain. However, the low group contains many meteorites which are breccias or have been shocked, and this suggests that shock may be responsible for the division (Sears and Mills, 1974).

Several finds were then examined, their descriptions and mean-lives being given in Fig. 8 and Table 2. It is apparent that Plainview, Calliham and Dimmitt are very young since they still retain a high peak height ratio `LT/HT`. In Table 3 those in the high group are given an age from their peak height ratio using Fig. 4. We also present their $\log_e [\ell_0/\ell_{LT}]$ terrestrial age values. The disagreement between the ages found by each method is at first sight unexpected. However, the possibility that it was associated with the degree of weathering the finds had received was examined in the following way. We placed a piece of the Barwell meteorite on damp filter paper for two weeks. After this treatment it had acquired localised rusting but not an overall brown coloration. This sample, and a piece that had been kept dry, were prepared in the same manner for TL measurement, irradiated, and the dose curves produced, Fig. 9. As expected, the TL from the rusted specimen had

WOLD COTTAGE (50-54 hr)

SARATOV (50-55 hr)

TENNASILM (50-55 hr)

BARWELL (28-34 hr)

BRUDERHEIM (26-34 hr)

JELICA (28-34 hr)

TIME AT 120 °C (HOURS)
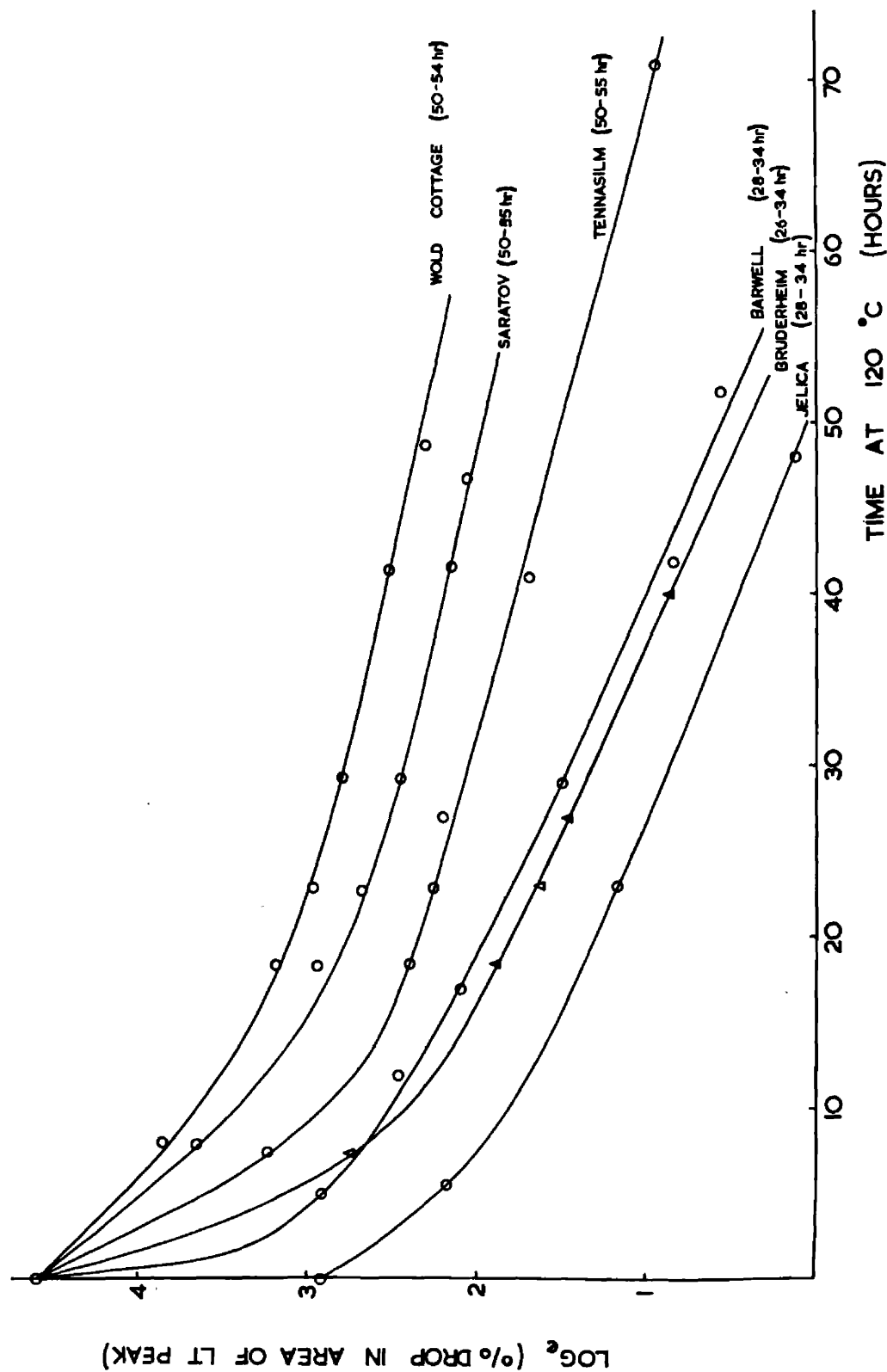
LOG_e (% DROP IN AREA OF LT PEAK)

Fig. 7   Isothermal annealing curves for three high and three low group meteorites. The abscissa is the natural log of the percentage drop in the area under half LT. Overlap with HT has been allowed for where necessary. The curve for Jelica has been displaced vertically for clarity.

55

Table 1
Details of the thermoluminescence of meteorites of known terrestrial age

	Group[1]	Terrestrial Age in years	Natural Peak Height Ratio	Natural Curve Peak Temperatures, °C ±5°C LT	HT	$E_{LT}^{(2)}$ (eV)	Mean-Life at 120°C in hours	Natural equivalent dose in krad	$\ell_0^{(3)}$ in arbitrary units
Saratov	L4	55	6.14	200	320	1.4-1.2[4]	50-55	46-49	25-28
Soko Banja	LL4	96	5.5-5.3	190	320	1.13		70-81	80-88
Tennasilm	L4	101	5.85-5.7	205	330	1.16	50-55	134-145	65-70 sat.[5]
Butsura	H6	112	4.17	190	235			52-120	45-58 sat.
Durala	L6	158	3.3-3.26	180	320			81-105	84-86 sat.
Wold Cottage	L6	178	2.78-2.72	205	345	1.09	50-54	58-250	87-97 sat.
Mauerkirchen	L6	205	1.37-1.54	220	365	1.06		75-230	96-98 sat.
Ogi	H6	232	3.67-3.63	200	345			81-105	57-61 sat.

Barwell	L6	8	5.12	200	360	1.24	28-34	15-27	40-60
Bruderheim	• L6	13	4.44	190	335	1.18	26-34	70-75	50-60
Khanpur	LL5	21	2.0-1.8	205	330			105-116	108-112
Mangwendi	LL6	39	1.78	210	335			116-140	110-130
Olivenza	LL5	49	≤0.74	(225)[6]	375			96-116	102-104 sat.
Crumlin	L5	71	1.06-1.02	225	350	0.86		145-155	92-95 sat.
Gambat	L6	76	0.237	220	320			35-46	9-12
Jelica	LL6	83	1.19-1.12	230	395	1.42	28-34	38-42	75-85
Dhurmsala	LL6	113	0.1-0.0	(225)	345			52-150	80-130
Aldsworth	LL5	138	0.15-0.0	(225)	340			170-180	105-115
Limerick	H5	160	0.26-0.24	235	345			43-49	43-48 sat.

Footnotes:
(1) As defined by Van Schmus and Wood (1967).
(2) As determined by Initial Rise Method (Garlick and Gibson, 1948).
(3) See text for definition.
(4) Two determinations using different curves.
(5) These meteorites are saturated at the natural equivalent dose, *i.e.*, additional dose makes no difference to ℓ.
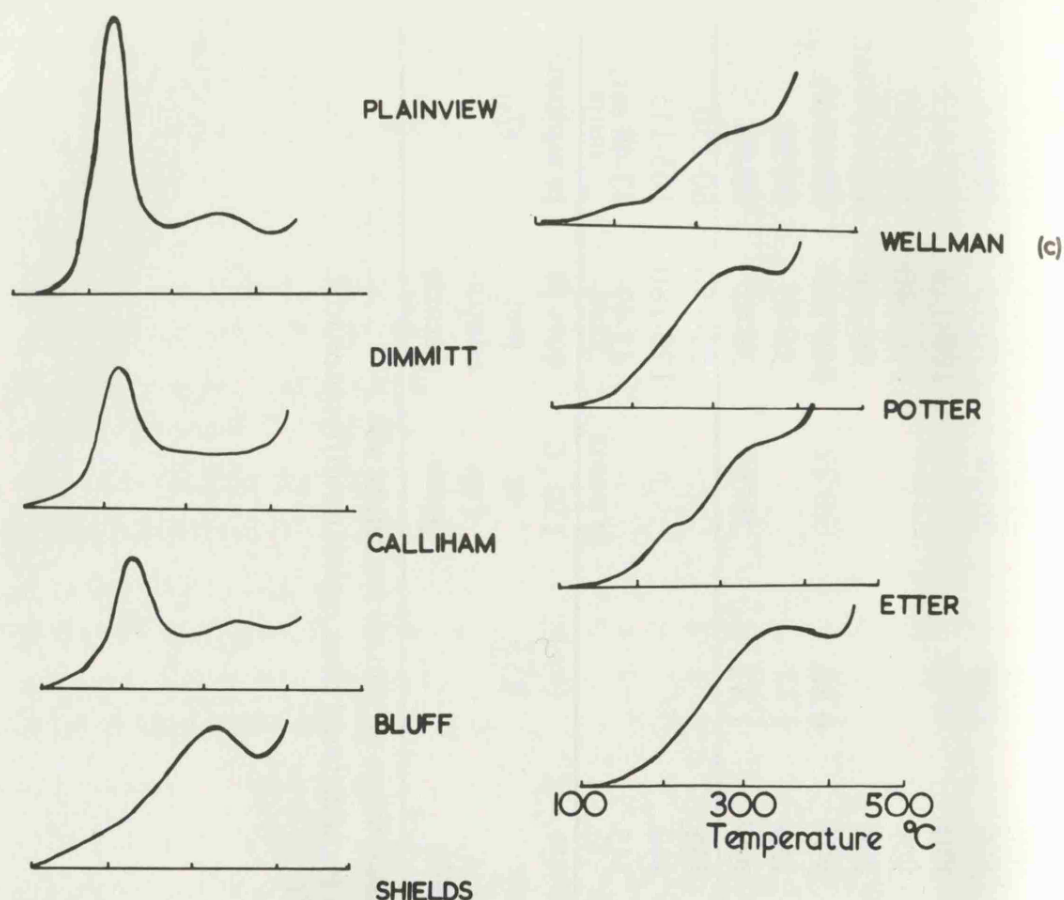(6) Where no peak is obvious, intensity of LT is measured at 225 °C.

Fig. 8   Sketches of the glow curves of several finds. Details of the meteorites, peak positions and intensities are given in Table 2. The curves turn up at the right with the onset of black body radiation.

dropped. The percentage reduction was the same for specimens which had received various doses, the intensity of the rusted specimen being always about one-third that of the fresh specimen. However, the peak height ratios were clearly different, being 24, 31 and 39 for rusted specimens after 23, 46, 69 krad of γ-radiation compared with 16, 27 and 31 for fresh specimens. That is, the meteorite that had been allowed to rust appeared younger on the basis of its peak height ratio. Rusting has little effect on the ℓ_0/ℓ_{LT} values since the drop due to obscuration appears to be approximately constant at all intensities. The obscuration seems to be a selective filtering effect, varying with wavelength of the TL peak. Valladas and Lalou (1973) have recently shown that LT and HT have different coloured luminescence. Therefore, the first column in Table 3, where the peak height ratio is employed to date the meteorites, is not considered reliable. We prefer the results determined by ℓ_0/ℓ_{LT} and use them in Table 4.

ACCURACY AND SOURCES OF ERROR

The measurement of peak heights is complicated by the fact that many peaks are present and these usually overlap. The presence of peaks below

58

Table 2
Details of the thermoluminescence of meteorites of unknown terrestrial age

|	Group	Year found	Natural Peak Height Ratio	Natural Curve Peak Temperatures, °C ±5 °C LT	HT	Mean-Life at 120 °C in hours	Natural equivalent dose in krad	$\ell_0^{(3)}$ in arbitrary units
Plainview	H5	1917	3.7	220	365	39-52	55-65	31-35
Calliham		1958	2.95-2.35	210	350	40-60	145-165	7.5-8.5
Etter			0.25	(225)	330	45-55	20-24	3.2-3.8
Potter	L6	1941	0.48-0.40	250	365	20-28	26-30	6.6-7.7
Bluff	L5	1878	0.05-0.15	(225)	335	22-30	22-26	4.0-5.0
Dimmitt	H3,4	1947	3.5-3.0	220	315-340	45-55	86-100	5.0-6.0
Shields			0.13-0.28	225	345	50-54	36-40	8.0-8.5
Wellman(c)			0.43-0.17	(225)	310	40-50	9-20	4.0-9.0

See Table 1 for footnotes.
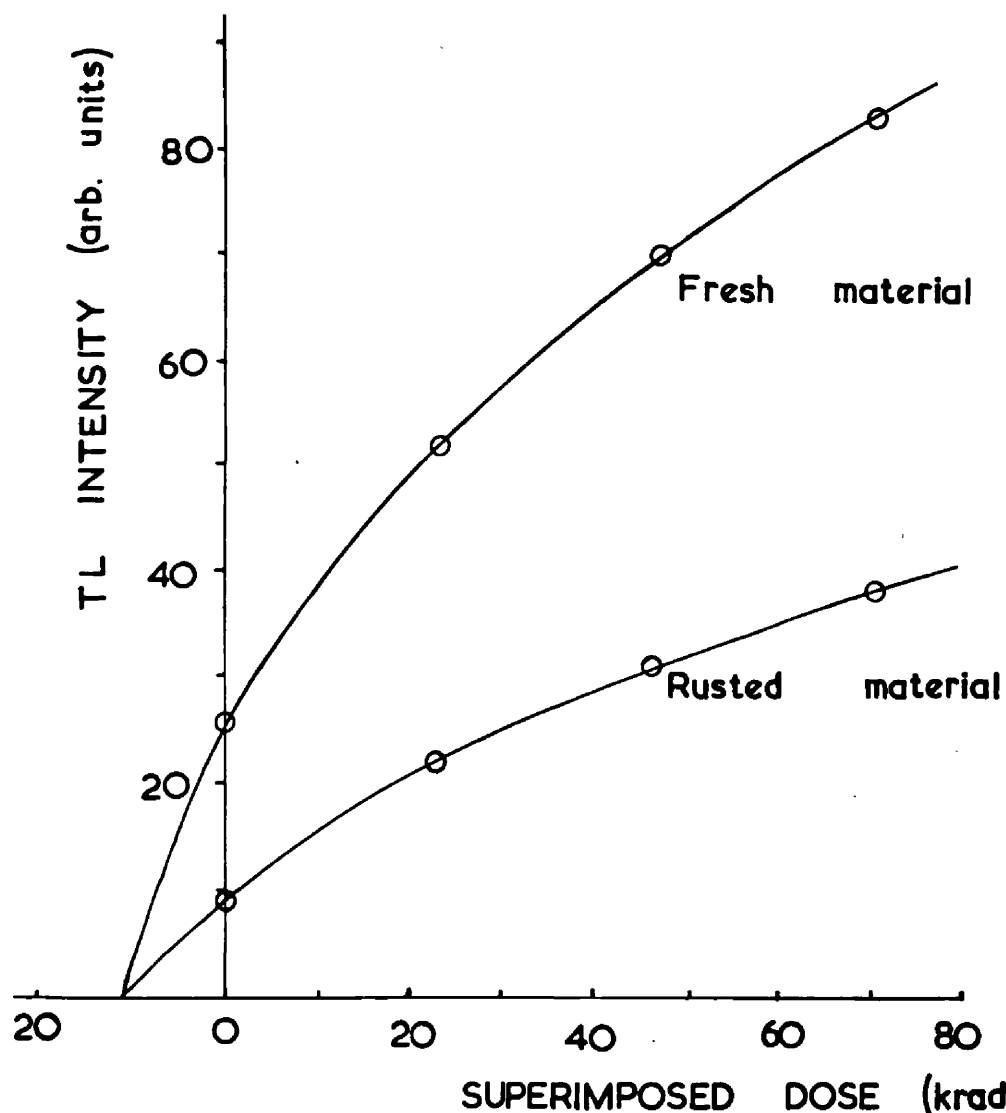
Fig. 9   The effect of rusting on the dose curve. Both curves are for the Barwell meteorite. The rusted specimen was produced by being left on wet filter paper for two weeks.

Table 3

The terrestrial ages of stony meteorites in
Table 2 as determined by two thermoluminescence methods

Meteorite	From peak height ratio and Fig. 3	From $\log_e(\ell_0/\ell_{LT})$ and Fig. 8
Plainview	135-145	225-300
Calliham	170-210	350-400
Etter	$\geqslant$ 300	$\geqslant$ 350
Potter	—	$\geqslant$ 300
Bluff	—	$\geqslant$ 200
Dimmitt	140-170	280-330
Shields	$\geqslant$ 300	$\geqslant$ 500
Wellman (c)	$\geqslant$ 300	$\geqslant$ 350

60

Table 4
Thermoluminescence ages of stony meteorites compared with radiocarbon ages

Meteorite	TL age in years	Radiocarbon age in years	Ref.
Plainview	225-300	$\leqslant 2000$	a
		$\leqslant 3800$	b
Calliham	350-400	—	
Etter	$\geqslant 350$	—	
Potter	$\geqslant 300$	$\geqslant 20,000$	a
		$\geqslant 21,000$	
Bluff	$\geqslant 200$	1300-6500	c
Dimmitt	280-300	0-4000	a
		1200-6400	c
Shields	$\geqslant 500$	—	
Wellman (c)	$\geqslant 350$	—	

References: a. Suess and Wänke (1962)
               b. Goel and Kohman (1962)
               c. Boeckl (1972)

200 °C is evident in three ways: i) the dose curves are occasionally supralinear, Fig. 10; ii) the shape of some glow curves clearly show its presence, Fig. 2; iii) there is a shift in the low temperature peak height vs. peak temperature, Fig. 10. Hwang (1973) has argued for the existence of two peaks below LT in lunar samples using completely different evidence. However, these low-temperature peaks should not affect the results because they are caused by the same mineral as the 200 °C peak and are present in both falls and finds. The curves derived from falls therefore include any effects from these extra peaks. However, this may not be true of extra peaks at higher temperatures than LT. In achondrites, Fig. 12, and lunar samples (see, for example, Hoyt et al., 1970) there is a peak at 260 °C which may be confused with LT when it occurs in chondrites. Only one of our 28 samples has a peak at 260 °C; namely Potter, which is also the most highly weathered meteorite. Overlap may move LT from 200 °C, e.g. Barwell, to 235 °C, e.g. Limerick, as illustrated in Fig. 10. However, confusion with a possible peak at 260 °C may be avoided by careful observation of the temperature of LT.

The error bars on the ℓ_0/ℓ_{LT} values in Fig. 6 are determined from the measurement of ℓ_0 and ℓ_{LT}. The error in ℓ_{LT} is determined from duplicate curves, where the repeatability was about 5%. ℓ_0 usually contains greater error and is determined from the dose curves, Fig. 5. It is governed by the accuracy by which the lines may be extrapolated to zero height to find the natural
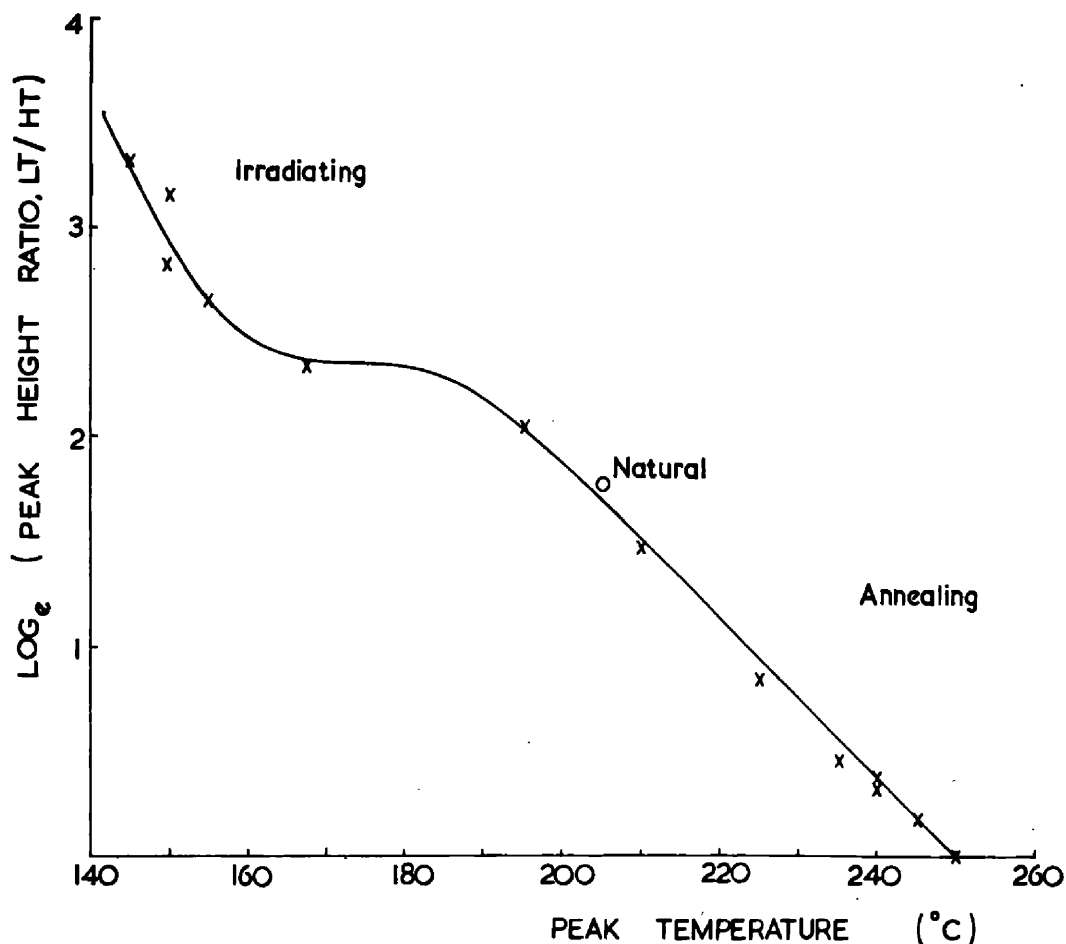
Fig. 10 Natural log of the peak height ratio *vs.* the position of the peak of *LT*. The movement of the peak due to overlap with *HT* is monotonous. The discontinuity at 170 °C is caused by the appearance after irradiation of a discrete second peak at lower temperatures.

dose. For saturated meteorites, where the natural dose was on the plateau of the peak height *vs.* dose curve, Fig. 5, ℓ_0 may be determined very accurately.

The error bars have been slightly underestimated since there is another source of error which cannot be determined, namely the different terrestrial histories of the meteorites. This is mainly the temperature at which the meteorites have been kept, since the decay rate is temperature sensitive. The effect is probably less for meteorites in the high group because of their longer mean-lives. Six of the eight high group meteorites fall on or very near the line and we think, therefore, that this line is reasonable. Ogi displays anomalously high present TL in both Fig. 6 and Fig. 8. Abnormal histories, *e.g.* heating on a hot-plate after cutting, probably account for the remaining discrepancies. The scatter of the low group may be caused by additional factors, but clearly the use of TL to determine accurately the ages in this group will be difficult. To allow for finds that have suffered appreciably different temperatures we have made a generous allowance for the scatter on the curves in determining the age ranges in our results (Table 4).
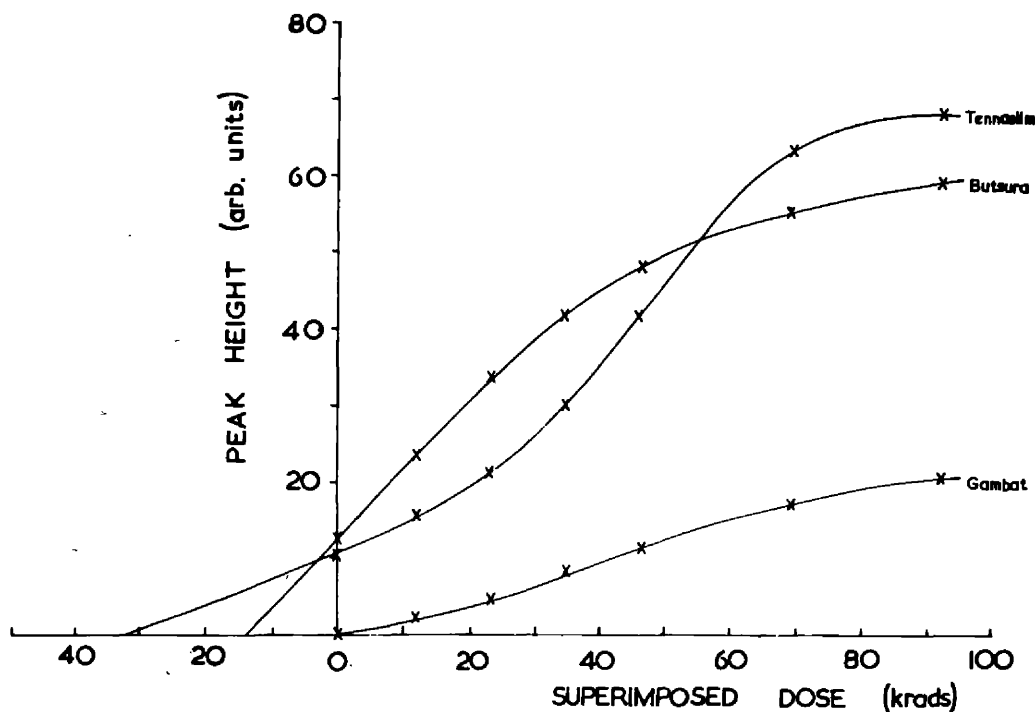
62

Fig. 11   Dose curves, peak height *vs.* superimposed dose, for *LT* for meteorites. Tennasilm shows abnormally bad supralinearity, a few have slight supralinearity like Gambat, but most have curves in which the slope is initially linear like Butsura.
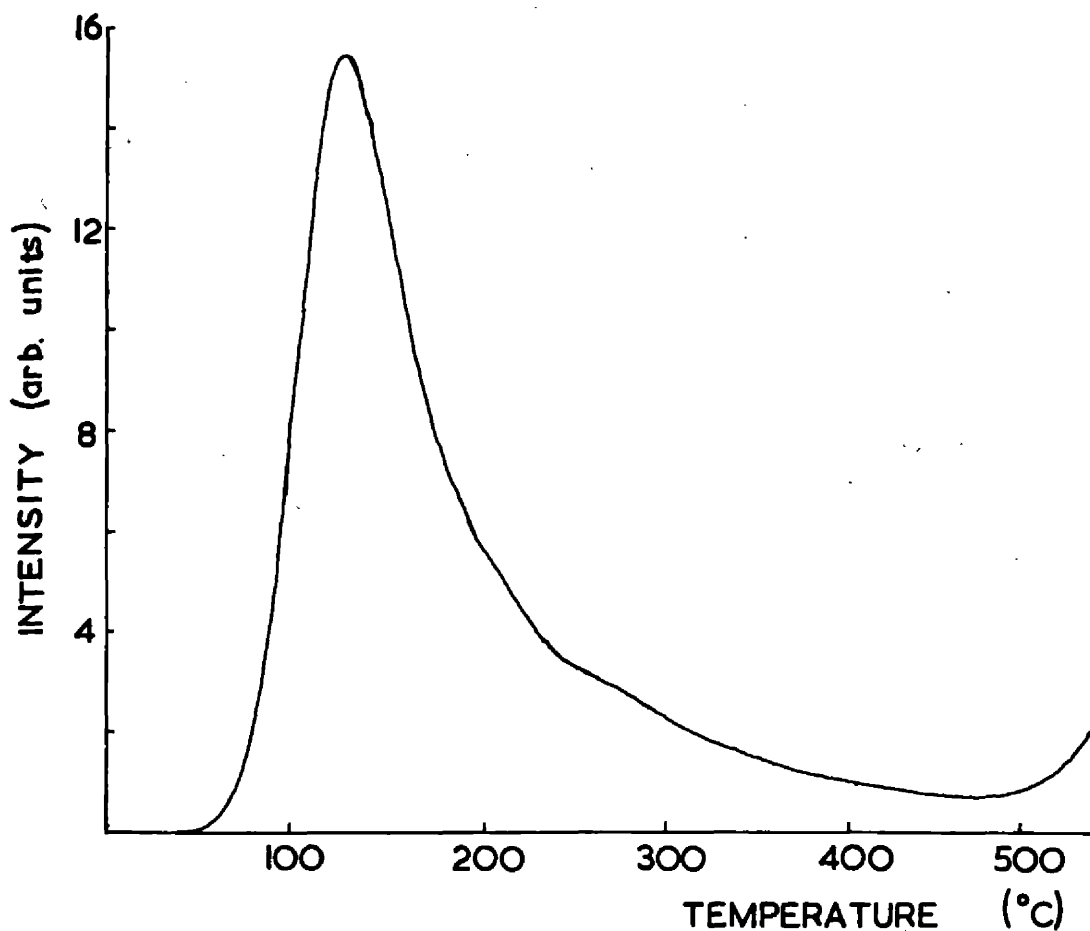

Fig. 12   Glow curve for the Kapoeta pyroxene-plagioclase anchondrite.

DISCUSSION AND CONCLUSIONS

The only method for determining the terrestrial age of stony meteorites, prior to that investigated here, utilises the decay of carbon-14. It is applicable only to ages exceeding a few thousand years, because the half-life of carbon-14 is 5760 years and the initial value for the abundance of the isotope is not known directly. TL makes available a method for the few-hundred-year range for certain meteorites and enables a lower limit to be established for others.

Dimmitt, Plainview, Potter and Bluff have been dated by the carbon-14 method, and the values so obtained are compared with those from TL in Table 4. Plainview is an interesting case since a fireball was seen and a stone recovered in 1902/1903 (Nininger, 1952). However, at least two more finds have been made in the Plainview area, and it is not certain which belongs to the observed fireball. Our result suggests that the Plainview meteorite we examined (Plainview 1917) was not associated with the 1902/1903 fireball.

The carbon-14 method has produced two surprising results of terrestrial ages in excess of 10,000 years, *viz.*, Potter and Woodward County (Suess and Wänke, 1962; Goel and Kohman, 1962). Boeckl (1973) found the average results for 19 terrestrial age determinations to be about 5000 years. The results presented here show that, although terrestrial ages of the order of a few thousand years may be common, a significant number may fall in the few hundred year range.

From these results we may estimate the efficiency of recovery of finds, assuming the meteorite influx derived from observed falls is correct (Hawkins, 1960; Brown, 1960). The surface density of finds can be calculated for the Prairie states from, for example, the compilation in Mason's (1962) book. Hawkins meteorite flux equation

$$N = N_0 - \log m$$

where N is the number of meteorites falling per unit area per unit time of mass equal to or greater than m, and N_0 is a constant, can be written

$$\frac{n}{A\beta T} = N_0 - \log m$$

where n is the total number of stony meteorites actually found in the Prairie states (76), A is the land area concerned, β the efficiency of recovery, and T the typical terrestrial age. Numerous factors control β; the population, soil colour, land use, climate and history of the region for example. The rate of recovery (and therefore β) is probably higher in the Prairie states than anywhere else in the world. Consequently, most of the stones for which we

have terrestrial ages were found in the Prairie states. Accepting typical terrestrial ages for stones from this area as a few thousand years we find β to be $\lesssim 1\%$ (Table 5). A similarly low β is found for irons, but we will here restrict ourselves to a discussion of stones. Brown's results give a slightly lower meteorite flux but make no significant change to the β estimated here. This figure may be underestimated if the influx rate is lower than the flux equation predicts. That this is so is suggested by the meteor camera network operated in the Prairie states. After eight years' operation the Prairie Network had witnessed only five meteorite-sized objects, whereas 1.5 per year were predicted by the influx statistics (McCrosky et al., 1971). The true influx of meteorites would therefore seem to be lower than the presently accepted statistics suggest.

ACKNOWLEDGEMENTS

Table 5
Terrestrial ages expected from the observed
surface density and fall rate of meteorites

Percent Recovered	Stones Estimated age in years	Irons Estimated age in years
.5	2,600	22,900
1	1,320	11,500
2	661	5,740
5	265	2,270
10	105	1,140
15	88.3	760
20	53.8	570

REFERENCES

Anders, E., 1963. Meteorite Ages. In *The Solar System, Part IV. The Moon, Meteorites and Comets*, B. M. Middlehurst and G. P. Kuiper, eds., University of Chicago Press, 402-495.

Begemann, F. and Vilcsek, E. 1969. Chlorine-36 and argon-39 production rates in the metal of stone and stony-iron meteorites. In *Meteorite Research*, P. M. Millman, ed., D. Riedel. Dordrecht, Holland, 355-363.

Boeckl, R., 1972. The terrestrial ages of 19 stony meteorites derived from their radiocarbon contents *Nature* **236**, 25-26.

Brown, H., 1960. The density and mass distribution of meteoritic bodies in the neighbourhood of the earth's orbit. *J. Geophys. Res.* **65**, 1679-1683.

Chang, C. and Wänke, H., 1969. Beryllium-10 in iron meteorites, their cosmic ray exposure ages and terrestrial age. In *Meteorite Research*, P. M. Millman, ed., D. Riedel, Dordrecht, Holland, 397-467.

Christodoulides, C., Durrani, S. A. and Ettinger, K. V., 1970. Study of the thermoluminescence in some stony meteorites. *Modern Geology* **1**, 247-259.

Garlick, G. F. J. and Gibson, A. F., 1948. The electron trap mechanism of luminescence in sulphide and silicate phosphors. *Proc. Phys. Soc. (London)* **A60**, 547-590.

Hawkins, G. S., 1960. Asteroidal fragments. *Astron. Jour.* **65**, 318-322.

Houtermans, F. G. and Liener, H., 1966. Thermoluminescence of meteorites. *Jour. Geophys. Res.* **71**, 3387-3396,

Goel, P. S. and Kohman, T. P., 1962. Cosmogenic carbon-14 in meteorites and terrestrial ages of "finds" and craters. *Science* **136**, 875-876.

Hoyt, H. P., Karlos, J. L., Miyajima, M., Seitz, R. C., Sun, S. S., Walker, R. M. and Wittels, M. C., 1970. Thermoluminescence, X-ray and stored energy measurements on Apollo 11 samples. In *Proc. Apollo 11 Lunar Sci. Conf., Geochim. Cosmochim. Acta* Suppl. 1, Vol. 3, 2269-2287. Pergamon.

Hwang, F. S. W., 1973. Fading of thermoluminescence induced in lunar fines. *Nature* **245**, 41-43.

Lalou, C., Nordemann, D. and Labeyrie, J., 1970. Etude préliminaire de la thermoluminescence de la météorite Saint-Séverin. *Comptes Rendus Acad. Sci.* (Paris) Serie D **270**, 2401-2404.

Liener, H. and Geiss, J., 1968. Thermoluminescence measurements on chondritic meteorites. In *Thermoluminescence of Geological Materials*, D. J. Macdougal, ed., Academic Press, New york, 559-568.

Mason, B., 1962. *Meteorites*, J. Wiley & Sons, New York.

McCrosky, R. E., Posen, A., Schwartz, G. and Shao, C.-Y., 1971. Lost City Meteorite – the recovery and a comparison with other fireballs. *J. Geophys. Res.* **76**, 4090-4180.

Nininger, H. H., 1952. *Out of the Sky*, Dover Books, New York.

Randall, J. T. and Wilkins, M. F. H., 1945. Phosphorescence and electron traps. *Proc. Roy. Soc. (London)* **A184**, 366-407.

Sears, D. W. and Mills, A. A., 1974. Thermoluminescence of Meteorites: Existence of two groups. *Nature*, in press.

Suess, H. E. and Wänke, H., 1962. Radiocarbon content and terrestrial age of twelve stony meteorites and one iron meteorite. *Geochim. Cosmochim. Acta* **26**, 475-480.

van Schmus, W. R. and Wood, J. A., 1967. A chemical-petrologic classification for the chondritic meteorites. *Geochim. Cosmochim. Acta* **31**, 747-765.

Valladas, G. and Lalou, C., 1973. Etude de la thermoluminescence de la météorite Saint Séverin. *Earth Planet. Sci. Letters* **18**, 168-171.

THERMOLUMINESCENCE STUDIES OF THE ALLENDE METEORITE

D.W. SEARS and A.A. MILLS

Departments of Astronomy and Geology, University of Leicester, Leicester (Great Britain)

The Allende meteorite has been examined with a view to applying thermoluminescence (TL) to the study of a meteorite's passage through the atmosphere. At least three kinds of TL-bearing minerals are present. A strong peak at 140°C is due to forsterite, and one at 200°C is probably caused by cordierite. By far the most intense TL comes from an alteration product associated with gehlenite.

In the 4-cm diameter meteorite examined the 200°C TL varied in intensity across the stone, showing it to be produced by fragmentation. Temperature gradients induced by atmospheric heating can also be derived, and indicate the orientation of the meteorite. Together with fusion crust measurements these results enable the final phase of the meteorite's passage through the atmosphere to be delineated.

1. Introduction

The Allende meteorite fell on 8th February 1969, the explosion leaving thousands of stones strewn over an area exceeding 300 km^2. It is a Type III carbonaceous chondrite. The morphology and fusion crust of many specimens has been reported by Clarke et al. [1]. The size and the great general interest in Allende led us to attempt a study of the atmospheric passage of this meteorite. The specimen used here (NMNH 3636) was a completely encrusted 67-g stone, roughly 4 cm in diameter.

In this report we describe thermoluminescence (TL) measurements. TL is the luminescence produced on releasing electrons from traps (lattice defects, etc.) by thermal excitation. They drop to the valence band via a luminescent centre and in doing so emit light.

Durrani and Christodoulides [2] explored the use of TL for determining the exposure age of Allende, whilst Keil and Fuchs [3] have described an electroluminescent mineral, hibonite. One may expect many luminescent species to be present because Allende is an extremely heterogeneous meteorite containing many Ca–Al-rich aggregates. The mineralogy of Allende has been described by Clarke et al. [1] and the Ca–Al-rich aggregates discussed by Marvin et al. [4].

2. Method

We removed a 4 mm thick central section from the stone using a Metals Research Ltd. Microtome II diamond saw. From this we cut eight bars (*a–h*, see Fig. 1.), and from these obtained 106 4 X 4 X 1 mm slices. The slices were powdered and passed through a 50-μm sieve. A glow curve (light emitted vs. temperature) was recorded for each slice, using both powder in its natural state and powder that had been drained of its TL by heating to 500°C and given a standard dose of about 50 krad from a ^{60}Co γ-ray source. The light emitted was measured by an EMI 9635B photomultiplier tube at a heating rate of 5 ± 0.05°/sec. A chance HA3 heat filter was inserted between a 6-mm aperture and the photomultiplier tube. A standard lamp was used to check constancy of sensitivity and a device based on integrating spheres was used to prove linearity of response of the photomultiplier to light.

Examination of electroluminescence was performed using both a luminescence microscope of our own construction [5] in which the luminescence is excited by 6 keV electrons, and a Cambridge Microscan 5 electron-probe operated at 20 kV accelerating voltage. Some minerals appeared to have different colours in the two instruments, presumably because additional or dif-
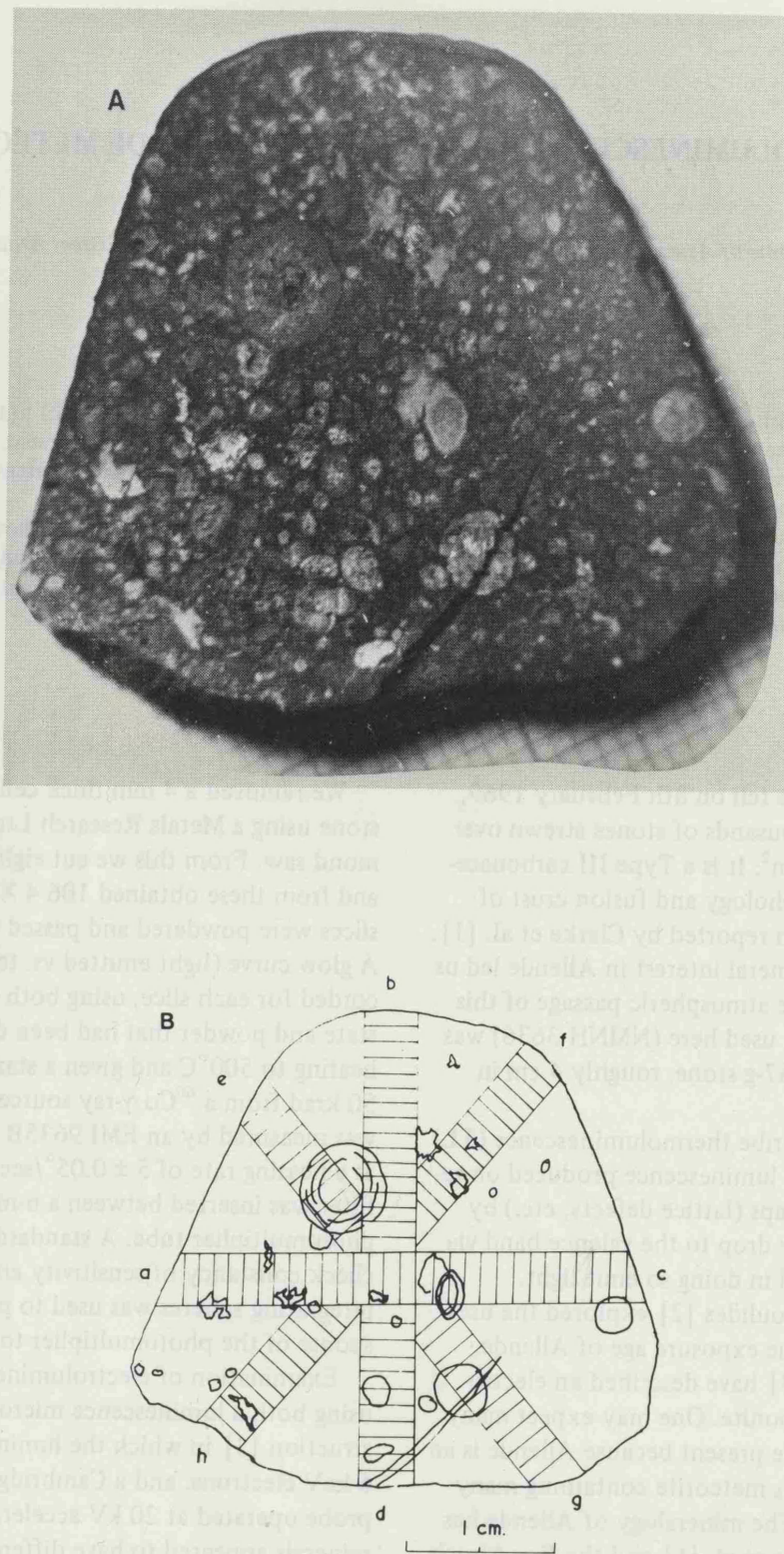
Fig. 1. Photograph (A) and sketch (B) of the slice of Allende used for thermoluminescence measurements. The locations of the 106 slices are marked on the sketch.
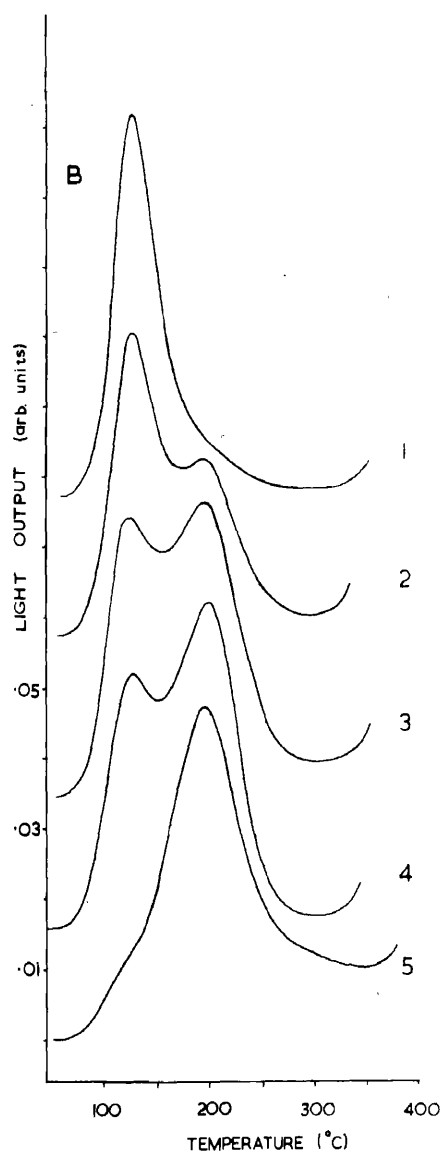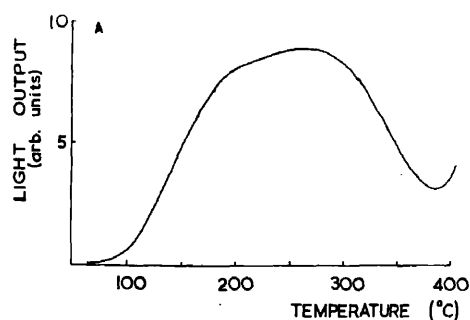
Fig. 2. The three types of artificial glow curve found in the Allende meteorite: (A) types 1 and 5, with intermediate groups resulting from various combinations; (B) type 6 glow curves.

ferent peaks were being excited. The colours mentioned here refer to those seen with the electroluminescence microscope.

3. Results

3.1. Types of glow curve

Three basic kinds of glow curve were obtained from the 106 specimens. These are shown in Fig. 2. Type 1, in which a peak at 140°C dominates the glow curve (this was only present in specimens that had been irradiated); type 5, in which a peak at 200°C dominates; and finally type 6 in which an extremely broad band of luminosity occurs with a peak at about 270°C. All combinations of types 1 and 5 were possible; these combinations are called 2, 3, and 4, where 3 has peaks at 140° and 200°C of similar intensity. These peaks are known to be due to different minerals since their intensities vary independently over extremely short distances. For types 1, 5 and 6 the relative intensities are 0.05, 0.05 and 10 respectively. For comparison, ordinary chondrites are about 30 and enstatite achondrites (the most luminous meteorites) are about 100 on the same arbitrary scale.

TABLE 1

Quantitative electron microprobe analyses of the main thermoluminescent minerals in the Allende meteorite*

	A	B		C	D
CaO	0.5	10.6	(3.1–20.9)	39.2	30.0
SiO_2	38.5	39.7	(36.4–42.1)	22.7	37.2
Al_2O_3	0.5	22.3	(10.8–33.8)	33.2	30.2
FeO	0.5	6.4	(1.5– 7.6)	0.2	1.7
MgO	57.4	20.5	(7.0–32.3)	2.4	1.8
TiO_2	0.1	n.d.		n.d.	n.d.
Total	97.5	99.5		97.7	100.9
Number of points	3	6		6	3

* Oxides calculated by stoichiometry; n.d. = not detectable.
A: Forsterite giving the 140°C thermoluminescent peak.
B: Blue electroluminescent grains in white aggregates, probably cordierite, responsible for the 200°C peak.
C: Gehlenite.
D: Luminescent bands, associated with gehlenite, responsible for the strong thermoluminescence between 200 and 400°C. Analyses for A, C and D are accurate to about 10% of the value for the element.

3.2. Distribution of glow curve types

By examining the distribution of glow curve types over the specimen it is possible to relate certain types with structures, and thereby suggest the minerals responsible for the glow curves. Type 6 is associated with Ca—Al-rich white aggregates and type 1 with chondrules. The chondrules in Allende are mainly forsteritic olivine.

3.3. The luminescent minerals in Allende

The residual powders and a slice from a region giving type 6 glow curves were investigated by X-ray diffraction, electroluminescence and electron-microprobe analyses. X-ray diffraction showed the type 1 material to be rich in forsteritic olivine. The electroluminescence of this type was red, and in polished section forsterite was found to give a red electroluminescence.

The type 5 powder showed blue electroluminescence. In polished sections the blue grains most frequently appeared as micron or submicron grains in white aggregates. They were difficult to electron-probe, because when the beam size was small enough to cover only the grain its luminescence could not be seen. An average of 6 analyses of blue grains in white aggregates (Table 1) suggests that cordierite ($Mg_2Al_4Si_5O_{18}$) is responsible. Our calcium value is probably almost entirely due to the beam extending beyond the grain and on to the Ca-rich matrix of the aggregate. Keil and Fuchs [3] have shown that hibonite can have these luminescence properties, but it then contains appreciable titanium.

The most intense luminescence in the slice from the type 6 region came from an orange-pink electroluminescent material. Closer inspection showed the the electroluminescence was associated with alteration bands, usually of a brownish tinge. The host mineral is gehlenite ($Ca_2Al_2SiO_7$) but the luminescent band had an appreciably different composition (Table 1).

3.4. Distribution of TL intensity

Since the 140°C peak was absent in the natural specimen it is of no use in determining either TL shape contours or atmospheric heating effects. For these the 200°C peak must be employed. Being an extremely heterogeneous meteorite the amount of the originating mineral in any one particular slice is highly variable. To some extent this will be allowed for by expressing the natural TL relative to the TL of the same specimen when drained and given a standard dose of radiation.
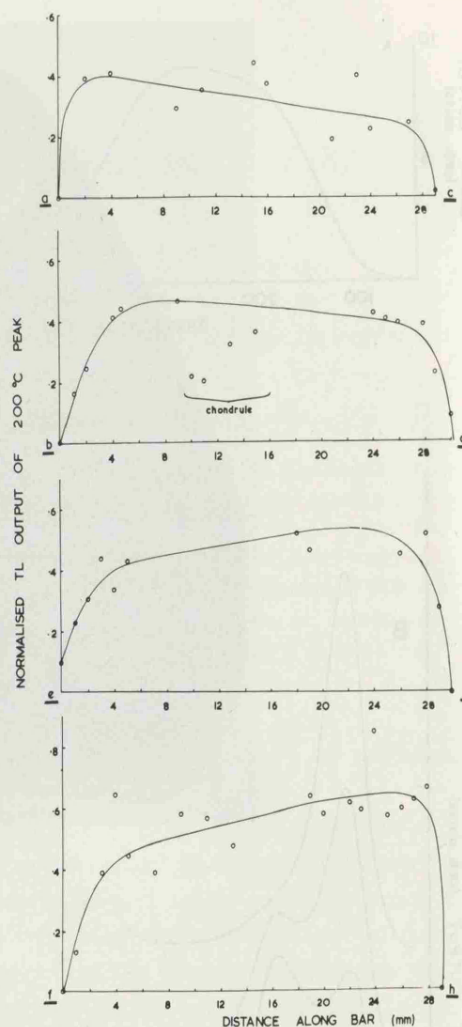

Fig. 3. Distribution of thermoluminescence intensity along bars *ac, db, ef* and *hf*. The area of the natural curves has been normalised to the area under the curves produced by drained powder that has been given 50 krad of γ-radiation from a ^{60}Co source.

Fig. 3 presents plots of normalised TL output vs. distance along bars *ac, bd, ef* and *gh*. The area of the 140°C peak had to be subtracted from the area of the artificial glow curves and this may introduce some error. Glow curves of types 1 and 6 have been omitted from Fig. 3 since the 200°C peak cannot be measured in these. As expected from a meteorite of the heterogeneity of Allende the scatter is considerable. However, it is possible to discern some trends, and these are presented on the original section across the stone in Fig. 4. It can be seen that there appears to be a variation in the intensity of the 200°C peak across the meteorite. This is ascribed to cosmic ray bombardment in space whilst part of a larger body.
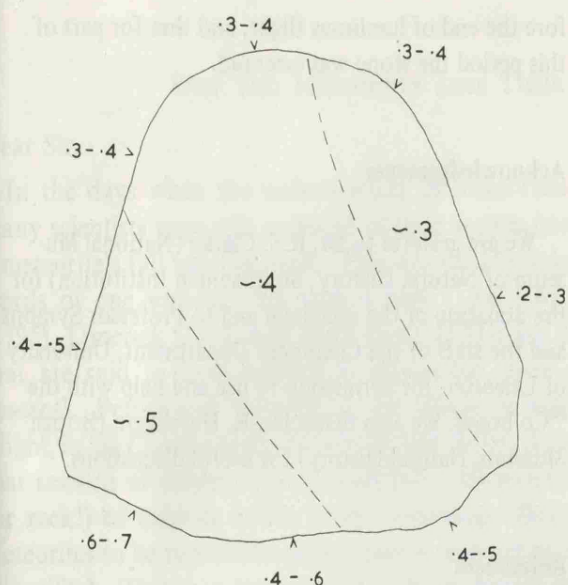
Fig. 4. Variation of the intensity of the 200°C peak over the slice.

3.5. Temperature gradients

At the eight points at which a bar intercepts the fusion crust it should be possible to determine a temperature gradient using the method of Vaz [6]. Four of our bars show reasonable gradients (Fig. 5), heterogeneity obscuring the gradient in the other four locations. The reduction in TL due to atmospheric heating may be expressed in terms of temperature by a calibration curve.

This is obtained by annealing some natural powder at various temperatures prior to determining the glow curves. The percentage drop in the TL is then expressed as a function of the annealing temperature to obtain the calibration curve. The period of annealing was found to be of minor importance, similar results being found for 1 and 10 sec. It is thus possible to assign approximate temperatures to the observed gradients. From Fig. 5 it is apparent that face d has a steeper gradient due to atmospheric heating than the others, especially b. From this we conclude d to be the front and b the rear of the stone when the meteorite was near the end of its luminous flight. The temperature gradient may also be determined from the dimensions of certain zones in the fusion crust [7]. The values so obtained have the same relative values; face d has a temperature gradient of $5°C/\mu m$ (for an ablation rate of 0.39 cm/sec) and face b a value of $4.1°C/\mu m$ (for an ablation rate of 0.31 cm/sec). These values are much greater than the values indicated by the TL measurement since they apply to much hotter regions, namely to a boundary about 200 μm from the surface, and the temperature drops off approximately exponentially with distance.

4. Discussion and conclusions

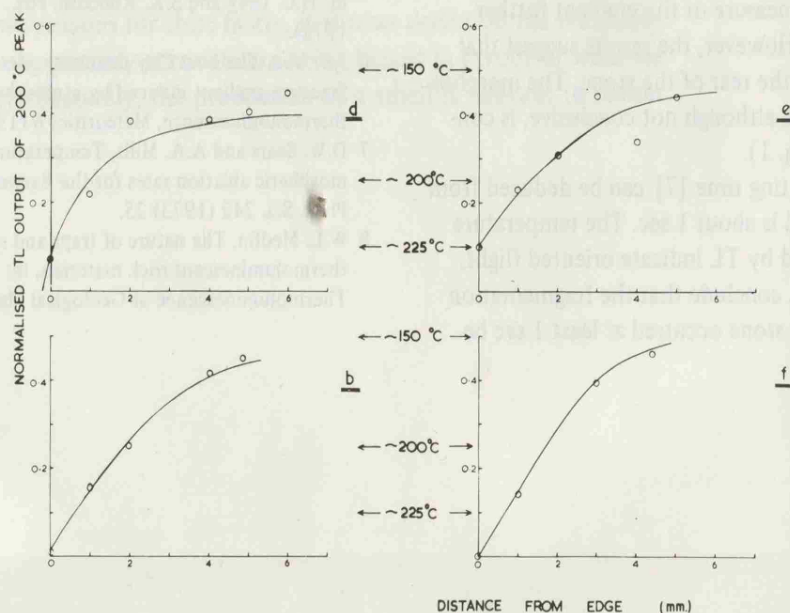As one would expect from the complexity and var-

Fig. 5. Drop in thermoluminescence at the edge of the slice, due to atmospheric heating.

ied nature of the mineralogy of Allende, the lumines-
cent properties are very complicated. The TL indicates
that at least three kinds of material are responsible,
while electroluminescence appears in at least three co-
lours. When structures and associations are taken into
account the number of types of electroluminescence
rises to at least six.

We believe that the 140°C peak is due to forsterite.
The peak at 200°C is very probably caused by cordie-
rite, whilst the most intense luminosity, occupying a
range of temperatures between 200 and 500°C, is due
to an alteration product of gehlenite. Gehlenite occurs
in the aggregates and in a few chondrules. The nature
of the alteration is unclear. The luminous material can
occur in lines across the gehlenite, as if caused by
shock, and around the edges in a way suggestive of re-
action with the matrix. Structural changes are probably
responsible for the TL in this material since the com-
position gives no clear indication of a chemical cause.
In Ca-bearing minerals it is usually considered that Mn
substitution for Ca produces the luminescence [8].

Heterogeneity makes it difficult to determine shape-
contours and atmospheric heating gradients for Allende.
It has been shown that the 200°C peak tends to more
intense on one side of the specimen, which is consis-
tent with the meteoroid fragmenting in the atmosphere
rather than the stone being part of a shower before en-
try. The temperature gradients determined by TL are
lower than the values indicated by the fusion crust meth-
od since they are a measure of the gradient further
into the meteorite. However, the results suggest that
d is the front and b the rear of the stone. The morphol-
ogy of the specimen, although not conclusive, is con-
sistent with this (Fig. 1).

The effective heating time [7] can be deduced from
the fusion crust, and is about 1 sec. The temperature
gradients determined by TL indicate oriented flight.
One may, therefore, conclude that the fragmentation
which produced the stone occurred at least 1 sec be-
fore the end of luminous flight, and that for part of
this period the stone was oriented.

Acknowledgements

References

1 R.S. Clarke, E. Jarosewich, B. Mason, J. Nelen, M. Gomez
   and J.R. Hyde, The Allende, Mexico, meteorite shower,
   Smithsonian Contrib. Earth Sci. 5 (1970).
2 S.A. Durrani and C. Christodoulides, Allende meteorite:
   age determination by thermoluminescence, Nature 223
   (1969) 1219.
3 K.Keil and L.H. Fuchs, Hibonite [$Ca_2(Al, Ti)_{24}O_{38}$] from
   the Leoville and Allende chondritic meteorites, Earth Planet.
   Sci. Lett. 12 (1971) 184.
4 M.B. Marvin, J.A. Wood and J.S. Dickey, Ca–Al-rich phases
   in the Allende meteorite, Earth Planet. Sci. Lett. 7
   (1970) 346.
5 J.E. Geake, G. Walker and A.A. Mills, Luminescence exci-
   tation by protons and electrons, applied to lunar samples,
   in: H.C. Urey and S.K. Runcorn, eds., The Moon (IAU,
   1972).
6 J.E. Vaz, The Lost City meteorite: determination of tem-
   perature gradient induced by atmospheric friction using
   thermoluminescence, Meteoritics 6 (1971) 207.
7 D.W. Sears and A.A. Mills, Temperature gradients and at-
   mospheric ablation rates for the Barwell meteorite, Nature
   Phys. Sci. 242 (1973) 25.
8 W.L. Medlin, The nature of traps and emission centres in
   thermoluminescent rock materials, in: D.J. McDougall, ed.,
   Thermoluminescence of Geological Materials (1968) 193.

Why Did Meteorites Lose Their Smell?

Dear Sir,

In the days when the serious study of meteorites was just beginning, and many scientists were still sceptical of their very existence, a frequent feature of a meteorite's fall was the smell. This was usually sulphurous, producing, in the words of one witness, "oh such a reek". Pettiswood (1779), Wold Cottage (1795), Limerick (1813) and High Possil (1804) are all early British meteorites that are said to have emitted a sulphurous smell during their atmospheric descent[1]. Pettiswood "enveloped the village in sulphur fumes". Dr Walter Flight, in his *Chapter in the History of Meteorites*, described two early meteorites that smelled of sulphur during their fall[2]. However, the presence of the smell (or reek!) of sulphur is not really surprising. One of the first properties of meteorites to be recorded was that they contained an iron sulphide (now known as troilite). This may be expected to burn during the atmospheric descent to produce iron oxides and sulphur dioxide, the latter having a pungent and acrid smell.

Why then is a smell never mentioned in modern descriptions? For example, *The Meteoritical Bulletin*, which publishes details of new falls and finds, lists the fall of 38 stony meteorites between November 1960 and April 1970[3]. The fall is described for 20 of them, but no mention is made of a smell. A strange and perhaps slightly puzzling discrepancy. Perhaps in an earlier, less enlightened age, the observers were more inclined to imagine the smell (reminiscent of fire and brimstone!). Alternatively, and more likely, modern enquirers do not ask witnesses if they smelled anything because the popular impression of a meteorite fall does not include a smell.

Unfortunately, as amusing as it is, the discrepancy may not be as trivial as it seems. There are two reasons for this; firstly, it throws doubt on the reliability of the reports we have, possibly accounts are being biased in favour of what we have come to expect. Secondly, the production of a smell is relevant to fusion

crust studies, as it would give an indication as to whether much of the troilite is burned or not.

I would be interested to hear from any witnesses of the two most recent British meteorite falls, Barwell (1965) and Bovedy (1969), concerning the existence of a smell during their fall.

<div align="center">Yours faithfully,</div>

DEREK SEARS,

Department of Astronomy and
History of Science, University of
Leicester, University Road,
Leicester LE1 7RH.

POSTSCRIPT

Immediately after the sonic and visual effects observed over North Wales in 1974 January one witness reported the smell of sulphur. Further investigation showed that the inhabitants of two other farms noticed a similar smell. An examination of the area has so far failed to locate any signs of meteorite fall.

<div align="center">*References*</div>

1 References to the accounts of these falls can be found in Hey, M., *Catalogue of Meteorites*, London, 1966.
2 Flight, W., *Chapter in the History of Meteorites*, London, 1887.
3 Krinov, E. L. (Ed.), *The Meteoritical Bulletin*, Moscow, 1960–70.

ABSTRACT

The thermoluminescence (TL) of meteorites has been
examined with apparatus designed with emphasis on linear
heating of the sample. The type of TL (i.e. the glow curve)
depends on the minerals producing it and on the history of the
specimen.

The applications that have been made concern three
phases of a meteorite's arrival on Earth; its preatmospheric
shape, the temperature gradients produced by heating during
atmospheric passage, and the terrestrial age of meteorites for
which the fall was not observed. It has been found possible to
measure terrestrial ages for some meteorites that have been on
the Earth several hundred years. It appears probable that shock
considerably increases the rate of decay of TL.

The extent to which high temperatures experienced by the
surface of the meteorite during its atmospheric passage have
penetrated into the matrix suggests luminous flight times in the
order of 10 seconds, but the gradients tend to be 3 - 5 times
less than those predicted theoretically. They appear to have the
same dependence on the orientation of the meteorite as the
temperature gradients determined from the fusion crust; the
steepest gradients being experienced at the front of the
meteorite. The fusion crust, besides enabling much of the
atmospheric behaviour to be determined, provides a useful source
of information complementary to TL work. For example, TL
gradients produced by atmospheric heating will only be found
when the fusion crust contains an innermost zone.

The preatmospheric TL gradients measured in many
meteorites suggest that cosmic ray bombardment produces a
significant amount of TL, and therefore that TL can be used to
measure preatmospheric shape. A comparison with spallogenic
nuclide profiles in meteorites suggests that secondary particles
play an important part in determining TL. Studies of the
Estacado meteorite confirm this expectation and suggest an
elongated preatmospheric shape, approximating to an ellipse of
eccentricity 0.8. From this it is calculated that the pre-
atmospheric mass of Estacado exceeded 8 tons.